

# Metabolic regulation during early embryo development

Paul Joseph McKeegan, BSc (Hons), PGCE

A thesis submitted for the degree of PhD

The University of Hull and the University of York

Hull York Medical School

January 2015

# Abstract

The preimplantation embryo must satisfy dynamic changes in energy demand during development to the blastocyst stage. Energy is provided through regulated metabolic pathways including glycolysis,  $\beta$ -oxidation and oxidative phosphorylation. Oxygen consumption rate (OCR), representing overall oxidative metabolism, has been reported in several species but few studies have examined the bioenergetics of embryo development.

Several methods were optimised to measure components of OCR by individual embryos. On average, 66% of blastocyst OCR was coupled to ATP synthesis, the majority being complex I-dependent. A further 13% was of non-mitochondrial origin, while maximal OCR was 189% of basal, providing a spare respiratory capacity of +89%. This profile allows re-interpretation of existing data to estimate ATP production by the bovine embryo.

The endogenous triglyceride store of the oocyte is increasingly considered a vital energy source in preimplantation development. In the present study,  $\beta$ -oxidation was manipulated during embryo culture. Inhibition of  $\beta$ -oxidation led to i) increased OCR ii) increased lipid content, iii) increased pyruvate uptake and iv) decreased lactate release at the blastocyst stage. Enhancing  $\beta$ -oxidation caused i) OCR at blastocyst stage to fall, ii) decreased lipid content during early cleavage, iii) decreased pyruvate consumption and iv) increased lactate release. Neither treatment affected blastocyst development rate or differential cell count, while both led to mitochondrial depolarisation.

These metabolic observations were hypothesised to have legacy effects on gene expression. Groups of 10 blastocysts with similar metabolic profiles were analysed using transcription and DNA methylation microarray platforms. Following manipulation of  $\beta$ -oxidation, gene transcripts involved in mitochondrial function, metabolism, key signalling cascades, recognition of pregnancy, stress response, protein modification and transcription were differentially expressed. Genes involved in transcription, protein modification, key signalling cascades and disease were differentially methylated, potentially linking dysregulated  $\beta$ -oxidation to deleterious conditions in later development.

These data highlight the plasticity of metabolic regulation in the embryo, allowing successful preimplantation development despite an apparently deleterious phenotype, yet indicate that metabolic activity has subtle effects on development.

# Contents

Abstract.....	ii
Contents.....	iii
List of tables.....	xi
List of figures.....	xiii
List of abbreviations.....	xvii
Acknowledgements.....	xxv
Author's declaration .....	xxvi
<b>1</b> Introduction .....	<b>1</b>
1.1 Bovine oocyte and embryo development.....	2
1.1.1 <i>In vivo</i> oocyte development.....	2
1.1.2 The ovarian cycle.....	3
1.1.3 Follicle development.....	5
1.1.4 Oocyte maturation.....	6
1.1.5 Fertilisation .....	8
1.1.6 Pre-implantation embryo development .....	9
1.1.7 Predicting oocyte and embryo viability .....	10
1.2 Eukaryotic energy metabolism .....	12
1.2.1 Glycolysis.....	12
1.2.2 Fatty acid metabolism.....	14
1.2.3 Tricarboxylic acid cycle.....	14
1.2.4 Oxidative phosphorylation.....	17
1.2.5 Productive and non-productive oxygen consumption .....	18
1.2.6 Mitochondrial function .....	18

1.3	Bovine oocyte and embryo metabolism .....	20
1.3.1	Glucose, pyruvate and lactate .....	22
1.3.2	Fatty acids .....	24
1.3.3	Amino acids .....	25
1.3.4	Oxygen consumption .....	26
1.3.5	Oxidative damage .....	29
1.4	Aims.....	31
<b>2</b>	<b>General materials and methods .....</b>	<b>32</b>
2.1	Bovine embryo <i>In Vitro</i> Production (IVP).....	33
2.1.1	Source of reagents .....	33
2.1.2	Preparation of glassware and consumables for embryo culture.....	33
2.1.3	Preparation of IVP media.....	33
2.1.4	Holding medium stocks.....	35
2.1.5	FSH:LH stock.....	35
2.1.6	EGF:FGF stock.....	36
2.1.7	Maturation additives.....	36
2.1.8	Preparation of holding and bovine maturation media .....	37
2.1.9	Preparation of <i>in-vitro</i> fertilisation media .....	38
2.1.10	Preparation of Percoll® gradient.....	40
2.1.11	Preparation of <i>in vitro</i> embryo culture media .....	42
2.1.12	Preparation of amino acid supplement .....	44
2.1.13	Collection and <i>In Vitro Maturation</i> (IVM) of bovine oocytes. ....	45
2.1.14	<i>In Vitro</i> Fertilisation (IVF) .....	46
2.1.15	<i>In Vitro</i> Culture (IVC) .....	46
2.2	Measurement of Oxygen Consumption Rate (OCR) .....	48
2.2.1	Measurement of OCR by the Becton-Dickinson Oxygen Biosensor System .....	48
2.2.2	Measurement of OCR by nanorespirometry.....	49

2.3	Energy substrate assays .....	51
2.3.1	Pyruvate .....	54
2.3.2	Glucose.....	55
2.3.3	Lactate.....	56
2.4	L-carnitine assay.....	57
2.5	Time-lapse imaging of embryo development using the Primo Vision system.....	58
2.6	Cell allocation ratios.....	59
<b>3</b>	<b>Bovine embryo bioenergetics .....</b>	<b>60</b>
3.1	Introduction .....	61
3.1.1	Metabolic profiling of pre-implantation embryos .....	61
3.1.2	Oxygen consumption .....	62
3.1.3	Embryo mitochondria .....	63
3.1.4	Oxidative phosphorylation.....	64
3.1.5	Classification of respiration.....	66
3.1.6	Uncoupled respiration .....	67
3.1.7	Oxygen profiling methods in oocytes and embryos .....	68
3.1.8	Nanorespirometry.....	71
3.1.9	Fluorometric techniques.....	73
3.2	Aims.....	74
3.3	Materials and methods .....	75
3.3.1	Linearity of the BD Oxygen Biosensor System .....	75
3.3.2	Validation of the BD Oxygen Biosensor System.....	75
3.3.3	Comparison of the BD Oxygen Biosensor System and Nanorespirometer oxygen profiling methods.....	75
3.3.4	Optimisation of solvent.....	76
3.3.5	Inhibitor preparation. ....	76
3.3.6	Coupled oxygen consumption .....	77

3.3.7	Non-mitochondrial oxygen consumption .....	77
3.3.8	Maximal rate and spare respiratory capacity .....	78
3.3.9	NADH and FADH <sub>2</sub> -dependent OCR.....	78
3.3.10	Statistical analyses .....	79
3.4	Results.....	80
3.4.1	Linearity of the BD Oxygen Biosensor System .....	80
3.4.2	Validation of the BD OBS system with OCCs.....	81
3.4.3	Comparison of blastocyst OCR profiles by nanorespirometry and BD OBS.....	82
3.4.4	Optimisation of solvent for respiratory inhibitor experiments .....	83
3.4.5	Non-mitochondrial oxygen consumption rate.....	84
3.4.6	Coupled oxygen consumption .....	86
3.4.7	Maximal rate and spare respiratory capacity .....	87
3.4.8	NADH and FADH <sub>2</sub> -dependent OCR.....	88
3.5	Discussion.....	89
3.5.1	Overview .....	89
3.5.2	Bioenergetic profile of bovine blastocysts.....	90
3.5.3	Linearity of the BD Oxygen Biosensor System .....	91
3.5.4	Validation of the BD Oxygen Biosensor System.....	91
3.5.5	Comparison of techniques .....	92
3.5.6	Optimisation of solvent for respiratory inhibitor experiments .....	92
3.5.7	The non-mitochondrial OCR of bovine blastocysts.....	93
3.5.8	Coupled OCR of bovine blastocysts .....	95
3.5.9	Maximal rate and spare respiratory capacity .....	96
3.5.10	NADH and FADH <sub>2</sub> -dependent OCR.....	98
3.5.11	Linking components of oxygen consumption to ATP supply .....	98
3.5.12	Evaluation of methodology.....	99
3.5.13	Strengths and limitations .....	99

3.5.14	Conclusion.....	100
<b>4</b>	<b>The effects of manipulating bovine embryo lipid metabolism.....</b>	<b>101</b>
4.1	Introduction.....	102
4.1.1	Fatty acid metabolism.....	102
4.1.2	Diet and fatty acid composition.....	104
4.1.3	Lipids in the oviduct and uterus.....	105
4.1.4	Lipid metabolism and mitochondria.....	106
4.1.5	The role of L-carnitine in fatty acid metabolism.....	106
4.1.6	Inhibition of fatty acid $\beta$ -oxidation.....	108
4.2	Aims.....	110
4.3	Methods.....	111
4.3.1	The effect of acute BMA treatment on bovine blastocyst oxygen consumption measured by nanorespirometry.....	111
4.3.2	Measurement of the effect of chronic BMA treatment on bovine blastocyst oxygen consumption by nanorespirometry.....	111
4.3.3	The effect of enhanced $\beta$ -oxidation on OCR.....	112
4.3.4	Determination of follicle L-carnitine.....	112
4.3.5	Assessment of embryonic lipid content by confocal microscopy.....	113
4.3.6	Assessment of mitochondrial polarity by confocal microscopy.....	115
4.3.7	Statistical analyses.....	117
4.4	Results.....	118
4.4.1	Inhibiting FAO during embryo development increases OCR.....	118
4.4.2	Acute BMA treatment increases OCR of blastocysts dependent on FCS supplementation.....	120
4.4.3	Manipulating fatty acid $\beta$ -oxidation significantly alters OCR.....	121
4.4.4	Manipulating fatty acid $\beta$ -oxidation alters carbohydrate metabolism.....	122
4.4.5	L-carnitine is present in follicular fluid and FCS.....	124
4.4.6	FCS supplementation increases lipid content in day 2-3 embryos.....	125

4.4.7	Increasing FCS concentration correlates with decreased mitochondrial polarisation of day 2-3 embryos .....	126
4.4.8	Manipulating $\beta$ -oxidation of endogenous stores significantly alters lipid droplet staining.....	127
4.4.9	Manipulating FAO without FCS significantly decreases mitochondrial polarisation ratio during early cleavage.....	128
4.4.10	Manipulating FAO does not affect blastocyst polarisation ratio with or without FCS .....	129
4.4.11	Treatment with BMA, Etomoxir or L-carnitine does not alter development rate or blastocyst cell allocation. ....	130
4.4.12	Treatment with L-carnitine may accelerate blastocyst development .....	131
4.5	Discussion.....	132
4.5.1	Inhibiting $\beta$ -oxidation during embryo development increases OCR.....	132
4.5.2	Manipulating fatty acid $\beta$ -oxidation significantly alters OCR.....	133
4.5.3	Manipulating fatty acid $\beta$ -oxidation alters carbohydrate metabolism.....	133
4.5.4	L-carnitine is present in the follicular environment and consumed by early cleavage stage embryos .....	135
4.5.5	FCS supplementation increases lipid content in day 2-3 embryos .....	136
4.5.6	Increasing FCS concentration correlates with decreased mitochondrial polarisation of day 2-3 embryos .....	137
4.5.7	Manipulating $\beta$ -oxidation of endogenous stores significantly alters lipid droplet staining.....	137
4.5.8	Manipulating FAO without FCS significantly decreases mitochondrial polarisation ratio in day 2-3 embryos .....	139
4.5.9	Manipulating FAO does not significantly affect blastocyst polarisation ratio with or without FCS .....	140
4.5.10	Treatment with BMA, Etomoxir or L-carnitine does not alter cell allocation ratio	140
4.5.11	Treatment with L-carnitine may accelerate blastocyst development .....	141
4.5.12	Strengths and limitations .....	142
4.5.13	Conclusions .....	142
5	The effects of manipulating bovine embryo lipid metabolism on gene expression and methylation.....	144

5.1	Introduction .....	145
5.1.1	Gene expression in mammalian embryos.....	145
5.1.2	Epigenetics and metabolic legacy .....	145
5.1.3	Transcription .....	150
5.1.4	The EmbryoGENE platforms .....	151
5.2	Aims.....	153
5.3	Materials and methods.....	154
5.3.1	<i>In vitro</i> culture and metabolic profiling .....	154
5.3.2	Parallel extraction of total RNA and DNA .....	155
5.3.3	Quantification of RNA quantity and quality.....	156
5.3.4	T7 amplification of RNA .....	156
5.3.5	Transcriptomic microarray analysis .....	156
5.3.6	Hybridisation of labelled RNA samples to the microarray.....	157
5.3.7	Epigenetic microarray analysis.....	157
5.3.8	Analysis of microarray data.....	158
5.4	Results.....	159
5.4.1	Metabolic profiles .....	159
5.4.2	Summary of genetic changes .....	160
5.4.3	Transcriptomic microarray following L-carnitine treatment .....	162
5.4.4	Transcriptomic microarray following BMA treatment.....	167
5.4.5	Epigenetic microarray following L-carnitine treatment.....	176
5.4.6	Epigenetic microarray following BMA treatment .....	186
5.4.1	Overview of the L-carnitine treated blastocyst transcriptome and epigenome ....	194
5.4.1	Overview of the BMA-treated blastocyst transcriptome and epigenome .....	195
5.5	Discussion.....	196
5.5.1	Metabolic differences .....	196
5.5.2	Differential expression following promotion of $\beta$ -oxidation .....	197

5.5.3	Differential expression following inhibition of $\beta$ -oxidation .....	202
5.5.4	Differential methylation following promotion of $\beta$ -oxidation.....	206
5.5.5	Differential methylation following inhibition of $\beta$ -oxidation.....	210
5.5.6	Patterns in the transcriptome and epigenome.....	213
5.5.7	Strengths and limitations.....	214
5.5.8	General conclusions .....	215
5.6	Future studies .....	217
<b>6</b>	<b>General discussion .....</b>	<b>218</b>
6.1	Summary .....	220
6.1.1	Bioenergetic profiling of bovine embryos.....	220
6.1.2	$\beta$ -oxidation and metabolism .....	220
6.1.3	$\beta$ -oxidation and gene expression.....	221
6.2	Further work .....	223
6.3	Concluding remarks .....	225
<b>7</b>	<b>References .....</b>	<b>227</b>
<b>8</b>	<b>Appendix: suppliers and materials.....</b>	<b>273</b>
8.1	Suppliers.....	274
8.2	Materials .....	276

# List of tables

Table 1: Composition of stock solutions for holding medium. ....	35
Table 2: Composition of maturation additives for maturation media. ....	36
Table 3: Holding media and bovine maturation media recipes. Each type of media was prepared fresh before use. ....	37
Table 4: Preparation of Fert-TALP <i>in vitro</i> fertilisation medium and HEPES-TALP sperm washing medium.....	38
Table 5: Preparation of Percoll® Additives and SPTL solutions.. ....	40
Table 6: Preparation of 90% and 45% Percoll® .....	41
Table 7: Preparation of SOF BSA embryo culture medium and HEPES-SOF embryo handling and wash medium.....	42
Table 8: Preparation of 50x amino acid supplement stock.. ....	44
Table 9: Preparation of modified SOF analysis medium for glucose, lactate and pyruvate assays. ....	52
Table 10: Composition of the reaction mixture and standard solutions for the L-carnitine assay.....	57
Table 11: A summary of bovine blastocyst oxygen consumption from selected literature. ....	71
Table 12: Summary of the inhibitors used to measure aspects of bovine blastocyst oxygen consumption in this chapter .....	76
Table 13: Stoichiometry of ATP production from the oxidation of 1 mole palmitate.....	102
Table 14: Mean oocyte triglyceride content of mammalian species.....	103
Table 15: Example Nile Red staining image analysis.....	115
Table 16: Cleavage and blastocyst rates for control, BMA and L-carnitine treated embryos. Rates recorded over 7 independent experiments .....	130
Table 17: Composition of RNA hybridisation reaction mixture. ....	157

Table 18: Table highlighting the role and fold change of selected genes which were differentially expressed between L-carnitine treated and control blastocysts.....	163
Table 19: Table highlighting functional annotations of key genes which were differentially expressed following BMA treatment.. .....	171
Table 20: Differential methylation in CGIs between 5-50kbp of a promoter following promotion of $\beta$ -oxidation with L-carnitine. ....	180
Table 21: Intragenic CGI site differential methylation following promotion of $\beta$ -oxidation with L-carnitine. ....	184
Table 22: Table showing gene name and product function of the data shown above in Figure 56.....	188
Table 23: Table describing the gene name, product function, fold change and p value of the data shown above in Figure 57.....	191

# List of figures

Figure 1: Overview of the mammalian ovary and ovarian follicle.....	3
Figure 2: Overview of the bovine <b>oestrous cycle</b> .....	5
Figure 3: An overview of <i>in vitro</i> early bovine embryo development with approximate timings and stage information.....	11
Figure 4: The Tricarboxylic (TCA), Citric acid, or Krebs cycle.....	16
Figure 5: An overview of <i>in vitro</i> bovine preimplantation embryo metabolism at blastocyst stage.....	21
Figure 6: Diagram showing setup of <i>in vitro</i> maturation plate and BMM wash dish.....	37
Figure 7: Diagram showing fertilisation wash and 4-well plate for IVF.....	39
Figure 8: The layout of SOFaaBSA drops in a 40mm culture dish.....	43
Figure 9: An example standard curve for the pyruvate assay.....	54
Figure 10: An example standard curve for the glucose assay.....	55
Figure 11: An example standard curve for the lactate assay.....	56
Figure 12: Overview of oxidative phosphorylation.....	65
Figure 13: Diagram of the Q cycle.....	66
Figure 14: Overview of nano respirometry.....	72
Figure 15: Validation of the linearity of the BD OBS system.....	80
Figure 16: Analysis of OCR of different populations of bovine OCCs using the fluorescent BD OBS method.....	81
Figure 17: Comparison of OCR measured by nano respirometer and BD OBS methods.....	82
Figure 18: The effect of common solvents on blastocyst OCR.....	83
Figure 19: Blastocyst mitochondrial oxygen consumption.....	85
Figure 20: The coupled and uncoupled OCR of bovine blastocysts.....	86

Figure 21: Maximal respiratory rate and spare capacity of bovine blastocysts. . . . .	87
Figure 22: Complex I–dependent blastocyst OCR.....	88
Figure 23: Bioenergetic profile of bovine blastocyst oxygen consumption.. . . .	90
Figure 24: An overview of fatty acid transport and $\beta$ -oxidation in mammalian cells.. . . .	109
Figure 25: An example standard curve for the L-carnitine assay . . . . .	112
Figure 26: Example individual Nile Red images of early cleavage stage embryos. . . . .	114
Figure 27: Example analyses of embryo lipid droplet staining by Nile Red. 12 cross section images were taken for each embryo across the central 20 $\mu$ m.. . . .	114
Figure 28: An example image of a blastocyst stained with JC-1 and Hoescht 3342.....	116
Figure 29: The effect of inhibition of $\beta$ -oxidation with BMA on OCR during embryo development.. . . .	119
Figure 30: The effect of inhibition of $\beta$ -oxidation with BMA on blastocyst OCR with 0% and 5% FCS.. . . .	120
Figure 31: OCR of groups of 10 mixed blastocysts cultured with 0.1mM BMA, 5mM carnitine or control SOFaaBSA media.. . . .	121
Figure 32: Carbohydrate metabolism of embryos following manipulation of $\beta$ -oxidation with BMA, L-carnitine or Etomoxir.. . . .	123
Figure 33: L-carnitine concentration and consumption of L-carnitine during early cleavage stages.. . . .	124
Figure 34: The effect of increasing concentrations of FCS during culture on embryo lipid staining.....	125
Figure 35: The effect of increasing concentrations of FCS during culture on embryo mitochondrial polarisation ratio.. . . .	126
Figure 36: The effect of manipulating $\beta$ -oxidation during culture without FCS on embryo lipid staining.....	127
Figure 37: Mean polarisation ratio $\pm$ s.e.m of day 2-3 embryos of 2-8 cell stage chronically cultured with or without manipulators of $\beta$ -oxidation.....	128
Figure 38: The effect of manipulating $\beta$ -oxidation during culture +/- FCS on blastocyst lipid staining.....	129

Figure 39: Cell allocation of blastocysts following treatment with BMA, Etomoxir or L-carnitine..	130
Figure 40: Time of blastocoel expansion recorded using the Primovision system and Well-of-the-well culture of L-carnitine, BMA, Etomoxir treated or control embryos..	131
Figure 41: Summary of the effects of manipulation of endogenous fatty acid metabolism on embryo lipid content throughout <i>in vitro</i> development..	139
Figure 42: Metabolic profiling of blastocysts for microarray analysis..	159
Figure 43: Volcano plots indicating microarray results..	161
Figure 44: Volcano plot indicating the spread of transcriptomic probe binding between L-carnitine treated and control embryos.....	162
Figure 45: Differentially expressed genes of key interest in carnitine-treated blastocysts identified by microarray analysis..	164
Figure 46: Volcano plot indicating the spread of differentially expressed transcripts between BMA treated and control embryos.....	167
Figure 47: Differential expression of key genes by blastocysts following inhibition of $\beta$ -oxidation with $\beta$ -mercaptoacetate..	168
Figure 48: Epigenetic circular plot summarising all significantly different probe binding sites between control and L-carnitine treated blastocysts..	176
Figure 49: Volcano plot of all probes in methylation microarray between carnitine-treated and control embryos.....	177
Figure 50: Differential methylation at CGIs within 50kbp of promoter regions in blastocysts produced following culture with L-carnitine.....	178
Figure 51: Differential methylation of CpG islands within 1kbp of promoter regions in blastocysts following promotion of $\beta$ -oxidation with L-carnitine.....	179
Figure 52: Differential methylation at CGIs within 50kbp of a promoter following L-carnitine treatment.....	181
Figure 53: Differential methylation in intragenic regions following promotion of $\beta$ -oxidation with L-carnitine. ....	185

Figure 55: Volcano plot indicating the spread of Differentially Methylated Regions between BMA treated and control embryos.....	186
Figure 56: Epigenetic circular plot summarising all significantly different probe binding sites between control and BMA treated blastocysts.....	187
Figure 57: Differential methylation of CpG islands related to promoter regions following BMA treatment of embryos in culture.....	188
Figure 58: Differential methylation of intragenic CpG island regions following BMA treatment to blastocyst stage.....	190
Figure 54: Combined circular plot showing transcriptomic and epigenetic changes following promotion of $\beta$ -oxidation with L-carnitine..	194
Figure 59: Combined circular plot showing transcriptomic and epigenetic changes following inhibition of $\beta$ -oxidation with BMA.....	195
Figure 60: Summary figure combining key data from chapters 3-5..	226

# List of abbreviations

A.R. Grade	Analytical Reagent Grade
ACC	Acetyl-Coenzyme A Carboxylase
ACoA	Acetyl-Coenzyme A
ADP	Adenosine Diphosphate
AMH	Anti-Müllerian Hormone
AMP	Adenosine Monophosphate
AMPK	Adenosine Monophosphate-activated Protein Kinase
ANOVA	Analysis Of Variance
aRNA	antisense RNA
ART	Assisted Reproduction Technology
ATP	Adenosine Triphosphate
BD OBS	Becton-Dickinson Oxygen Biosensor System
BMA	$\beta$ -Mercaptoacetate
BMI	Body Mass Index
BMM	Bovine Maturation Media
BSA	Bovine Serum Albumin
CACT	Carnitine-Acylcarnitine Translocase
cDNA	complementary DNA
CGI	CpG Island

CI	Respiratory Complex 1
CII	Respiratory Complex 2
CIII	Respiratory Complex 3
CIV	Respiratory Complex 4
CoA	Coenzyme A
CpG	Cytosine-phosphate-Guanine (adjacent bases on same DNA strand)
CPT	Carnitine-Palmitoyl Transferase
CytC	Cytochrome C
D	Diffusion coefficient
DABA	Diaminobutyric Acid
DAVID	Database for Annotation, Visualisation and Integrated Discovery
ddH <sub>2</sub> O	double-distilled Water
DHAP	Dihydroxyacetone Phosphate
DMR	Differentially Methylated Region
DMSO	Dimethyl Sulphoxide
DNA	Deoxyribonucleic Acid
DNMT	DNA Methyltransferase
DNP	2,4-Dinitrophenol
DR	Dynamic Range
EDTA	Ethylenediaminetetraacetic Acid
EGA	Embryonic Genome Activation
EGF	Epidermal Growth Factor

EI complex	Enzyme Inhibitor complex
EPPS	3-[4-(2-Hydroxyethyl)-1-piperazinyl] propanesulphonic acid
ET water	Embryo Tested Water
ETC	Electron Transport Chain
EtOH	Ethanol
EX	Etomoxir™
F-1,6-BP	Fructose-1,6-Bisphosphate
F-6P	Fructose-6 Phosphate
FAD	Flavin Adenine Dinucleotide (oxidised)
FADH <sub>2</sub>	Flavin Adenine Dinucleotide (reduced)
FAO	Fatty Acid $\beta$ -Oxidation
FCCP	Carbonyl cyanide-4-(trifluoromethoxy) phenylhydrazone
FCS	Foetal Calf Serum
FFA	Free Fatty Acids
FGF	Fibroblast Growth Factor
FSH	Follicle Stimulating Hormone
G-6P	Glucose-6 Phosphate
G6PD	Glucose-6 Phosphate Dehydrogenase
GAP	Glyceraldehyde-3 Phosphate
GC	Granulosa Cell
gDNA	genomic DNA
GDP	Guanosine Triphosphate

GLUT	Glucose Transporter
GTP	Guanosine Diphosphate
GV	Granular Vesicle
GVBD	Granular Vesicle Breakdown
H3K4	Histone 3 Lysine 4
HDAC	Histone Deacetylase
HEPES	4-(2-hydroxyethyl)-1-piperazineethanesulphonic acid
hESC	human Embryonic Stem Cell
HK	Hexokinase
HM	Holding Media
HPLC	High Pressure Liquid Chromatography
HSOF	Hepes-SOF
HTML	3-Hydroxy-6-N-trimethyllysine
ICM	Inner Cell Mass
ICSI	Intra-Cytoplasmic Sperm Injection
IFN- $\tau$	Interferon tau
IGF	Insulin-like Growth Factor
IGF2R	Insulin-like Growth Factor 2 Receptor
IVC	<i>In Vitro</i> Culture
IVF	<i>In Vitro</i> Fertilisation
IVM	<i>In Vitro</i> Maturation
IVP	<i>In Vitro</i> Production

J	Diffusion flux
JC-1	5,5',6,6'-Tetrachloro-1,1',3,3'-tetraethylbenzimidazolylcarbocyanine
KSV	Stern-Volmer constant
LDH	Lactate Dehydrogenase
LDL	Low-Density Lipoprotein
LH	Luteinising Hormone
LIMMA	Linear Models for Microarray data
lncRNA	long non-coding RNA
LSD1	Lysine-Specific Demethylase 1
M199	Medium 199
MA	Maturation Additives
MAPK	Mitogen-Activated Phosphorylase Kinase
MBS	Main Beam Splitter
MI	Metaphase I
MII	Metaphase II
MPF	Mitogen Promoting Factor
MS	Microsoft
mtDNA	mitochondrial DNA
MZT	Maternal-Zygote Transition
NAD <sup>+</sup>	Nicotinamide Adenine Dinucleotide (oxidised)
NADH	Nicotinamide Adenine Dinucleotide (reduced)
NADP <sup>+</sup>	Nicotinamide Adenine Dinucleotide Phosphate (oxidised)

NADPH	Nicotinamide Adenine Dinucleotide Phosphate (reduced)
ncRNA	non-coding RNA
NEB	Negative Energy Balance
NEFA	Non-Esterified Fatty Acids
NRF	Normalised Relative Fluorescence
OCC	Oocyte-Cumulus Complex
OCR	Oxygen Consumption Rate
OSC	Oogonial Stem Cell
OVOB	Overweight and Obese
oxLDL	oxidised Low-Density Lipoprotein
OXPHOS	Oxidative Phosphorylation
P/O <sub>max</sub>	maximal ATP Phosphorylation/Oxygen reduction ratio
PA	Percoll™ Additives
PBS	Phosphate Buffered Saline
PDH	Pyruvate Dehydrogenase
Pen/Strep	Penicillin/Streptomycin
PES	Polyethersulphone
PFK	Phosphofructokinase
Pi	inorganic Phosphate
PMF	Proton-Motive Force
PPAR	Peroxisome Proliferator-Activated Receptor
PS	Polystyrene

PVA	Poly (Vinyl) Alcohol
PVP	Poly (Vinylpyrrolidone)
Q	Quinone (oxidised)
QH <sub>2</sub>	Quinone (reduced)
reNRF	relative Normalised Relative Fluorescence
RIN	RNA Integrity Number
RNA	Ribonucleic Acid
ROS	Reactive Oxygen Species
s.d	standard deviation
s.e.m	standard error of the mean
SGLT	Sodium-Dependent Glucose Transporter
SOD	Superoxide Dismutase
SOF	Synthetic Oviduct Fluid
SPTL	Sperm Tyrode's Lactate
TALP	Tyrode's Albumin Lactate Phosphate
TBARS	Thiobarbituric Acid Reactive Substances
TCA cycle	Tricarboxylic Acid cycle
TE	Trophectoderm
TEM	Transmission Electron Microscopy
TG	Triglyceride
THF	Tetrahydrofolate
TML	Trimethyllysine

Tsix	antisense to X-Ist Specific Transcript
UCP	Uncoupling Protein
ULS	Universal Linkage System
WoW	Well-of-the-Well
XACT	X Active Specific Transcript
XIST	X-Ist Specific Transcript
ZP	Zona Pellucida
$\Delta P$	Proton Gradient
$\Delta\Psi_m$	change in mitochondrial membrane potential

# Acknowledgements

I would like to thank my supervisors, Dr Roger Sturmeay and Prof Henry Leese for giving me the opportunity to work with them on this project and supporting me with advice, ideas and patience throughout my PhD and beyond. The guidance of my TAP chair, Dr Anne-Marie Seymour was also invaluable and I am very grateful for her support.

I have been fortunate to work with colleagues who have provided inspiration, advice and advanced banter in equal measure. Many thanks to my labmates, particularly big sister Maryam, Fabrice, Kosta, Pooja (Lesley), Tom, Fraser, Huw and Andrew; and to the other members of the CCMR and the Department of Biology at Hull.

I have also been lucky enough to meet researchers from other institutions who have kindly provided advice and insight. This included working with Prof. Marc-Andre Sirard, Isabelle Dufort, Dominique Gagne, Eric Fournier and Julie Nieminen as part of the EmbryoGENE project, a collaboration which produced huge amounts of fascinating data, some of which is presented in Chapter 5. The microarray work was performed by Isabelle and Dominique, while the bioinformatic analysis was carried out by Eric. This work would not have been at all possible without their support and understanding following a rather painful delay at the start of the project!

This PhD would not have been possible without my studentship from the University of Hull, who also supported my travel to present at the 2013 IETS conference and granted me a 2 month extension to make up for time lost due to injury. Thank you for your support. Thanks also to the University of York for allowing me to continue to use my old email address for a full 8 years.

Heartfelt thanks to my friends and family, none of whom I have spent much time with while I have been writing this, but whose support I have always counted on and appreciated.

Finally, this book is dedicated to Kirsty Louise Escolme, as am I.

# Author's declaration

I confirm that this work is original and that if any passage(s) or diagram(s) have been copied from academic papers, books, the internet or any other sources these are clearly identified by the use of quotation marks and the reference(s) is fully cited. I certify that, other than where indicated, this is my own work and does not breach the regulations of HYMS, the University of Hull or the University of York regarding plagiarism or academic conduct in examinations. I have read the HYMS Code of Practice on Academic Misconduct, and state that this piece of work is my own and does not contain any unacknowledged work from any other sources.

Paul J McKeegan

January 2015

# 1 Introduction

# 1.1 Bovine oocyte and embryo development

## 1.1.1 *In vivo* oocyte development

The ovary is comprised of interstitial glands set in stroma tissue. This interstitial tissue surrounds the ovarian follicles, each containing a single primary oocyte. Before birth, the primary oocyte remains in the follicle and is surrounded by flattened mesenchymal cells, termed pre-granulosa cells. These are surrounded by 2 layers of thecal cells, the theca interna and theca externa (Figure 1). In many mammalian species, oogonial germ cells cease mitosis during foetal development, and enter meiosis. Meiosis halts at the diplotene stage, at which time homologous chromosomes have paired (Mandelbaum 2000; Johnson 2012). The oocytes may remain in developmental arrest for many years; up to 50 in women. The primary oocyte contains an enlarged, vesicular nucleus known as the Germinal Vesicle (GV).

It was traditionally believed that the number of oocytes present in the mammalian ovary is fixed at birth, or shortly after (Moor et al. 1990). In humans  $1-2 \times 10^6$  oocytes are present at birth (Lobo 2003). However, recent studies in mice claimed that some oogenesis continues in early post-natal development via Oogonial Stem Cells (OSC). OSCs express the germ cell specific RNA helicase Ddx4 before differentiation to oocytes (Johnson et al. 2004; White et al. 2012). The authors also reported that a greater number of oocytes were found than expected from the rate of ovarian follicle loss and, while current understanding suggests that the number of follicles is fixed, it is possible that this is regulated by new oocyte formation from OSCs. Analogous Ddx4<sup>+</sup> OSCs have been found in human ovarian tissue, so it is possible that oogenesis could continue later into life, or perhaps that OSCs could be stimulated to generate new oocytes as part of new fertility treatments (White et al. 2012).

At the onset of puberty, the reproductive cycle begins, prompting the ovaries to initiate their cyclical endocrine characteristics to support development of the primary oocyte and primordial follicle.

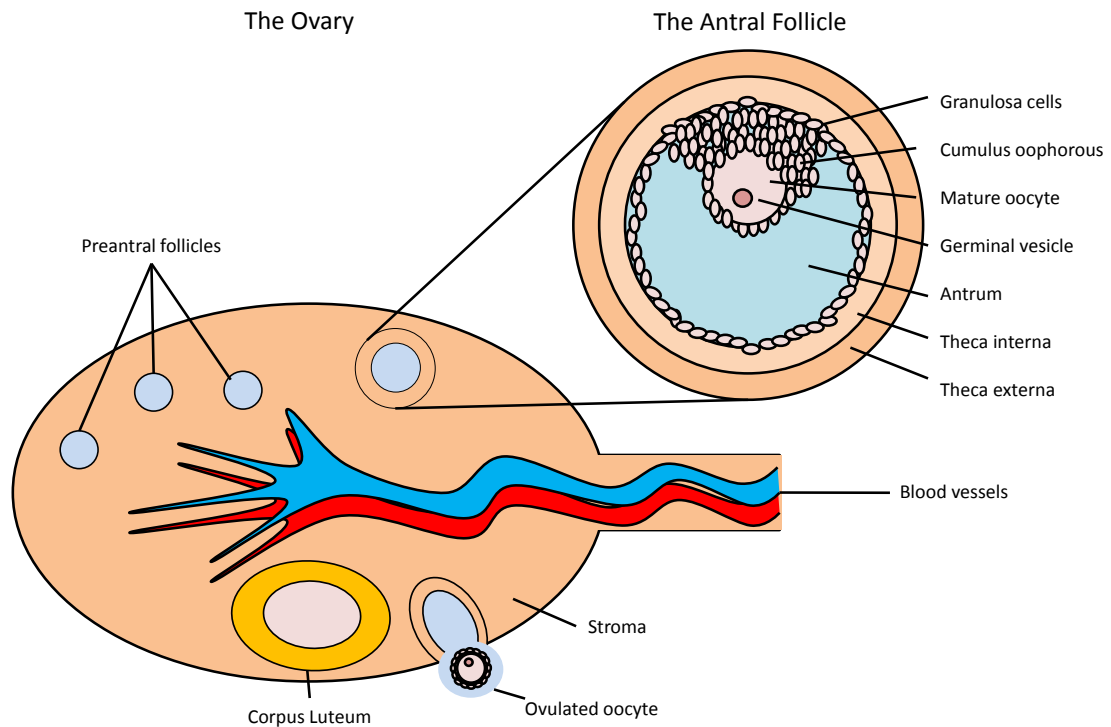


Figure 1: Overview of the mammalian ovary and ovarian follicle. In the developing **primary** or **preantral follicle**, the zona pellucida forms and oocyte genome is transcribed. The oocyte secretes signals stimulating further follicle development. Within the **secondary** or **antral follicle**, the **mature oocyte** has arrested at diplotene stage of meiosis and is surrounded by an expanding layer of **cumulus oophorus** cells. The follicle is lined with **granulosa cells** and contains a fluid-filled **antrum**, which continues to expand until the time of ovulation. The follicle is surrounded by the connective **theca interna** and vascular **theca externa**.

### 1.1.2 The ovarian cycle

The ovary undergoes the hormonally regulated ovarian cycle as part of the cyclical pattern of female episodic fertility. As the ovary cycles, several preantral follicles (7-11 in cattle and human) are recruited for growth to the preovulatory stage, in parallel to oocyte nuclear and cytoplasmic maturation (Zelevnik 2004). In the bovine, several waves of follicle recruitment, growth and regression precede growth and ovulation of the dominant follicle during the final wave (Fortune 1994). A single oocyte is ovulated and undergoes translocation to the site of fertilisation in the oviduct as well as preparing for the transition into a fertilised zygote. Each cycle, one oocyte is lost through ovulation; however, early stage oocytes are continually lost or reabsorbed through atresia; which may be defined as the loss of oocytes or follicles through any process other than ovulation. Follicle atresia is a hormonally regulated process controlled by apoptosis of

granulosa cells (Kaipia and Hsueh 1997). In parallel to the ovarian changes, the uterine lining is remodelled in preparation for a possible pregnancy.

The first 14 days following menstruation in the human and the first 2-3 days following oestrus in the cow (Austin 2001) constitute the follicular phase, in which levels of oestrogen, Follicle Stimulating Hormone (FSH) and Luteinising Hormone (LH) rise. This stimulates follicle growth and the phase ends with release of an oocyte through ovulation. The ruptured follicle folds in on itself, forming the corpus luteum in a process similar to wound healing (Smiths et al. 1994). The remaining 14 days in the woman and 18 days in the cow comprise the luteal phase, in which progesterone, derived from the corpus luteum, acts on the endometrium to allow implantation of a blastocyst and support early pregnancy.

The ovarian cycle affects the whole body and causes the sexually active and fertile period of oestrous, described as 'standing heat' in most mammals and giving rise to the term 'oestrous cycle'. If the ovulated oocyte is not fertilised, the endometrial lining of the uterus is reabsorbed during the luteal phase of the oestrous cycle. In higher primates, the ovarian cycle is instead termed the menstrual cycle due to the shedding of uterine endothelial tissue during the luteal phase of the cycle and the lack of physiological evidence of oestrous seen in other animals. The menstrual cycle is continuous and each cycle leads to the next. However, other mammals may have a limited number of cycles and fertile breeding seasons each year, such as monoestrous or dioestrous animals, with one or two oestrous cycles respectively. Polyestrous animals have many cycles per year, which can be seasonal, for example the ovine breeds during winter and the equine during summer. The bovine, however, is non-seasonal polyestrous, with many cycles per year, bearing more similarity to the human than other model species. However, cattle have a period of sexual inactivity, also termed dioestrous, between cycles.

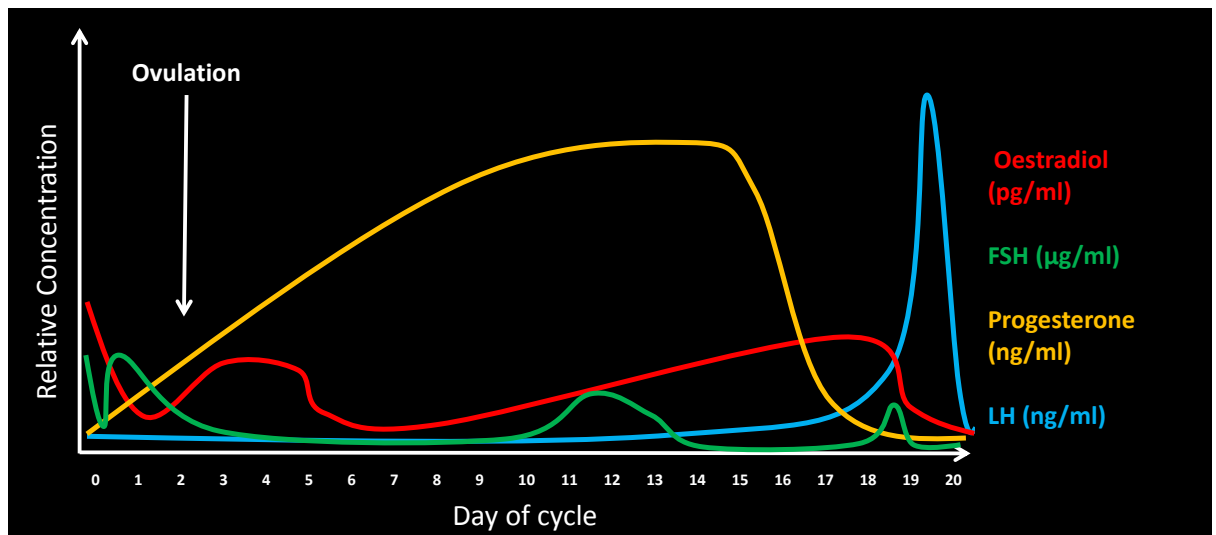


Figure 2: Overview of the bovine **oestrous cycle**. From the time of oestrous on day 0/20, **progesterone** is secreted by the corpus luteum and levels rise gradually until around day 15, then decrease rapidly. The dominant follicle secretes **oestradiol**, which inhibits **Follicle Stimulating Hormone (FSH)** secretion. When this follicle becomes non-functional, FSH secretion increases. FSH precedes recruitment of new follicles in 3 waves throughout the cycle. Levels of **Luteinising Hormone (LH)**, required for follicle growth, remain consistently low until the LH surge, which occurs in the absence of progesterone and stimulates ovulation. Data summarised from (**Wettemann et al. 1972; Austin 2001**).

### 1.1.3 Follicle development

Several follicles are thought to begin growth each day and must pass through the preantral, antral and preovulatory stages before a mature oocyte, with the potential to be fertilised, is released. Throughout the preantral and antral phases, granulosa cells express Follicle Stimulating Hormone (FSH) receptors and theca cells express Luteinising Hormone (LH) receptors. These gonadotrophins are secreted by the anterior pituitary gland and are required to stimulate follicle progression past the preantral stage (FSH) and the antral stage (LH) and to prevent the breakdown of the follicle by atresia. In FSH receptor knockout mice, follicular development is arrested at the preantral stage (Dierich et al. 1998; Kumar 2009), while LH receptor knockout mice arrest at the antral stage (Zhang et al. 2001). Theca cells of antral follicles secrete androgens, mainly testosterone, which stimulate granulosa cell proliferation. Theca cells secrete little oestrogen, but the androgens produced are converted to oestrogens by FSH-stimulated granulosa cells, such that these two cell types cooperate to maintain levels of oestrogen in the ovary and in the bloodstream. Low plasma levels of oestrogen inhibit secretion of FSH and LH from the pituitary gland, however the proliferation of granulosa cells and synthesis of oestrogen stimulated by the androgens creates a positive feedback system. Once the dominant follicle increases plasma oestrogen levels to the oestradiol threshold value, the pituitary

gland immediately secretes FSH and LH, leading to the LH surge in the late follicular stage (Figure 2). FSH and oestrogen stimulate granulosa cells to express LH receptors, which must also be present on the theca to respond to a brief LH surge and enter the preovulatory phase. The LH surge stimulates changes in follicle cells and the oocyte, triggering ovulation. LH also stimulates the shift from an autocrine follicle to a paracrine *corpus luteum*.

In the bovine adult, the majority of ovarian follicles are of primordial stage (Miyamura et al. 1996). During follicle growth, the pre-granulosa cells surrounding the oocyte proliferate and differentiate to form the cuboidal granulosa cells of the primary follicle (Fair, 2003). These cells continue to proliferate, forming at least two layers in the secondary follicle. At this stage, the theca cells differentiate to theca externa and theca interna layers. The granulosa cells secrete a fluid, which forms a number of small cavities that eventually merge to form the antrum (Eppig, 2001). This marks the preantral to antral transition. Those granulosa cells closest to the oocyte begin to form the cumulus oophorus, so called as it has the appearance of a 'little cloud', and push the oocyte into the newly formed antrum cavity. These cumulus cells will continue to support the oocyte through projections into the oolemma until it is fertilised or degraded.

Glucose transport is especially important as the oocyte has poor nutrient uptake mechanisms; instead pyruvate, which can be produced by cumulus cells, and endogenous triglyceride are the major substrates for ATP synthesis (Leese and Barton 1985; Sutton-McDowall et al. 2004; Harris et al. 2007). Glucose also fuels cumulus expansion, which involves mucification of proteoglycans and glycosaminoglycans, primarily the glycosaminoglycan hyaluronic acid (Nagyova 2012). This results in expansion of cumulus volume without significant proliferation. This occurs prior to breakdown of the germinal vesicle in rodents (Dekel 1979; Eppig 1980) but afterwards in pigs (Motlik et al. 1986). Cumulus expansion and hyaluronic acid synthesis is promoted by FSH and prostaglandin E2 (Eppig 1980; Lin et al. 1994).

#### 1.1.4 Oocyte maturation

Coinciding with these events, the oocyte increases protein synthesis and both cytoplasm and the germinal vesicle undergo significant remodelling. During follicle growth, the

bovine oocyte expands from 20µm to 130µm, while human oocytes expand to 120-160µm (Mandelbaum 2000). The surge in LH that precedes ovulation stimulates spindle formation in the oocyte and enables nuclear maturation (Kawamura et al. 2004). The activities of Maturation Promoting Factor (MPF) and Mitogen Activated Phosphorylase Kinase cause the chromatin in the germinal vesicle to breakdown (GVBD), which occurs within 8 hours of the LH surge in the bovine (Kruip et al., 1983). MPF is a heterodimeric protein complex comprised of Cyclin B and p34<sup>cdc2</sup> (Campbell et al. 1996). GVBD is inhibited by cyclic Adenosine Monophosphate (cAMP), which is produced from Adenosine Triphosphate (ATP) (Fan et al. 2002). This could allow ATP availability to regulate whether an oocyte undergoes GVBD or not. The nuclear envelope of the germinal vesicle also breaks down and the oocyte progresses to metaphase II of meiosis (Tripathi et al. 2010). Finally, before ovulation the oocyte must regain meiotic competence by resuming meiosis, completing MI, and then arresting at meiotic prophase I of MII (Eppig 2001).

The oocyte itself releases multiple signals to regulate primary follicle recruitment and development, including Insulin-Like Growth Factor (IGF), Epidermal Growth Factor (EGF) and Anti-Müllerian Hormone (AMH) (Fair, 2003), and may in turn be stimulated by Growth Differentiation Factor 9 (Eppig, 2001). During this time, the Zona Pellucida (ZP) is formed from sulphated glycoproteins secreted by the granulosa cells. The ZP is a proteinaceous matrix dividing the oocyte and pre-granulosa cells, which plays a vital role in fertilisation as well as protecting the embryo in the oviduct and uterus (Rankin and Dean, 2000). The granulosa cells establish projections through the ZP in order to transport substrates including glucose, nucleotides, amino acids and phospholipids to the oocyte (Moor et al. 1990).

The first meiotic division produces two diploid daughter cells with asymmetrical division of the cytoplasm. The larger of the two cells becomes the secondary oocyte, while the smaller, termed the first polar body, is extruded to the perivitelline space between the oocyte and ZP for degradation (Tripathi et al. 2010). This is necessary to enable the restoration of ploidy following meiosis. Crossing-over of homologous maternal and paternal chromosomes during meiotic prophase I allows exchange of sections of DNA producing unique chromosomes in each gamete. Additionally, independent assortment of these chromosomes during meiosis I randomly assigns maternal and paternal chromosomes to each daughter cell. The oocyte immediately enters a second meiotic

division and arrests at metaphase II. During oocyte development, ribosome count increases, mitochondria associate with the smooth endoplasmic reticulum and there is mass transcription and translation. This will cease and maternal mRNA and protein control metabolism and development until the embryonic genome is activated in early cleavage several days after fertilisation. At this stage, the presence of high MPF levels prevents further maturation (Campbell et al. 1996).

The granulosa cells express FSH receptors, which when activated stimulate the GC to secrete follicular fluid. After the LH surge, GCs also express LH receptors and convert androgens into progesterone, which is required for recognition of pregnancy. Proteolytic enzyme activity in the follicular fluid causes the follicle wall to thin as the follicle swells with fluid. At the point of ovulation the follicle ruptures, releasing the now mature oocyte into the oviduct and begins to form a corpus luteum (Rodgers and Irving-Rodgers 2010). Theca cells become small luteal cells while granulosa cells become large luteal cells. The Oocyte-Cumulus Complex (OCC) enters the peritoneal cavity between the ovary and oviduct and the oviductal fimbriae bind the cumulus cells to collect the OCC. It is then rapidly carried by cilia to the ampullary isthmic junction, which is the site of fertilisation. Meanwhile, the cells of the follicle reorganise to form the corpus luteum, coinciding with the luteal cells increasing oestrogen and progesterone secretion as described above.

### 1.1.5 Fertilisation

Tens to hundreds of spermatozoa are thought to reach the OCC and begin penetrating the cumulus oophorus, but only one spermatozoon must successfully fuse with the oocyte to initiate fertilisation. A capacitated spermatozoon must undergo the acrosome reaction to be capable of penetrating the zona pellucida. On contact with the zona pellucida, the cap-like acrosome over the spermatozoal head fuses with the oocyte plasma membrane, releasing enzymes and exposing cell surface antigens which are required for successful fertilisation. Sperm plasma membrane protein PH-20 has hyaluronidase activity and likely facilitates sperm movement through the hyaluronic acid-rich cumulus cells (Lin et al. 1994).

Traditional understanding is that only the sperm head penetrates the oocyte, however, evidence suggests that tail entry is sensitive to the presence of the microfilament inhibitor cytochalasin B and sperm tail filaments have been detected in mouse embryos

up to the morula stage (Simerly et al. 1993). Once the sperm enters the oocyte its mitochondria are degraded by ubiquitin-mediated autophagy in a process evolutionarily conserved from the nematode worm to the mouse, leaving only maternal mitochondria in the conceptus (Al Rawi et al. 2011). This process can fail in rare cases such that paternal mtDNA has been implicated in male infertility (May-Panloup et al. 2003). Sperm entry to the perivitelline space stimulates calcium oscillations originating from stores in the oocyte which promotes degradation of cyclin B1, one of the components of MPF. This deactivates MPF, which enables resumption and completion of meiosis II. A haploid set of chromosomes are again extruded to the perivitelline space forming a second polar body. The haploid maternal and paternal pronuclei align, establishing the unique embryonic genome and initiating the first embryonic cell cycle division.

### 1.1.6 Pre-implantation embryo development

The first embryonic cell cycle produces a nuclear diploid 2-cell embryo. Cell division in early embryonic development increases the number of cells without altering the size of the embryo, which is still enclosed within the zona pellucida.

The cells of the bovine embryo divide approximately every 24 hours from the point of fertilisation (Figure 3), although this is often asynchronous. This rate differs between species and is also affected by embryo sex and embryo quality. The supplies of mRNA and protein, inherited from the oocyte, regulate development during fertilisation and early cleavage stages. The embryonic genome is not transcribed immediately after fertilisation; instead, after a short period of transcription at the 2-4 cell stage in bovine *in vivo* derived embryos, major Embryonic Genome Activation (EGA) begins around the 8 cell stage in the bovine (Wrenzycki et al. 2004), 4-8 cell stage in the human (Braude et al. 1988; Telford et al. 1990) and 2 cell stage in the mouse (Niakan et al. 2012).

The developing embryo will compact to form a morula, defined morphologically as the point at which it is no longer possible to see the individual cells. The cells change shape and become wedge-like. This occurs on day 5 in the bovine (Holm et al. 2002). In parallel to cavitation, the cells of the morula begin to differentiate into two cell populations, the outermost cells become the trophectoderm (TE), and the inner cells form the inner cell mass (ICM). Following cavitation, the onset of differentiation and the subsequent formation of the fluid-filled blastocoel cavity, the embryo is referred to as the blastocyst.

Expansion of the blastocoel is driven primarily by the Sodium-Potassium-ATPase pump ( $\text{Na}^+$ ,  $\text{K}^+$ ATPase), a major consumer of ATP at this stage of blastocyst development. The  $\text{Na}^+$ ,  $\text{K}^+$  ATPase transports  $\text{Na}^+$  and  $\text{K}^+$  across the TE in opposing directions, increasing osmolarity within the cavity formed by morula compaction and increasing flux of water into this cavity, forming the blastocoel. Expansion continues for around 18 hours and is accompanied by thinning of the ZP. The bovine blastocyst begins to hatch from the ZP on day 7 (Figure 3). The ICM further differentiates to form epiblast and hypoblast, which subsequently form the three key embryonic lineages: ectoderm, mesoderm and endoderm. These stages are similar for all mammals, though timing and cell number differ (Telford et al. 1990). The embryo develops to about the morula stage within the lumen of the oviduct; however the next stage occurs in the uterus.

### 1.1.7 Predicting oocyte and embryo viability

Oocyte maturation, fertilisation and embryo development to the hatched blastocyst stage have been recapitulated *in vitro* in several model species including the bovine.

Morphology is widely used as a general marker for oocyte and embryo quality (Dokras et al. 1993; Gardner et al. 2004). There are, however differences between *in vivo* and *in vitro* embryo morphology and physiology, for example *in vivo* derived embryos tend to have a thicker zona pellucida, more obvious compaction and a higher inner cell number (Holm et al. 2002) as well as a wider perivitelline space between ooplasm and zona pellucida (Van Soom and de Kruif 1992). Several aspects of *in vitro* culture practices could cause these differences, in particular, an unphysiologically high oxygen tension (20% compared with ~5% *in vivo*) in some systems and the composition of culture media (Hawk and Wall 1994). However the subjective and relatively superficial nature of morphological assessment has led to substantial focus in developing non-invasive biochemical assays with the aim of producing a detailed metabolic profile of an embryo in terms of consumption of energy substrates including carbohydrates, amino acids and oxygen.

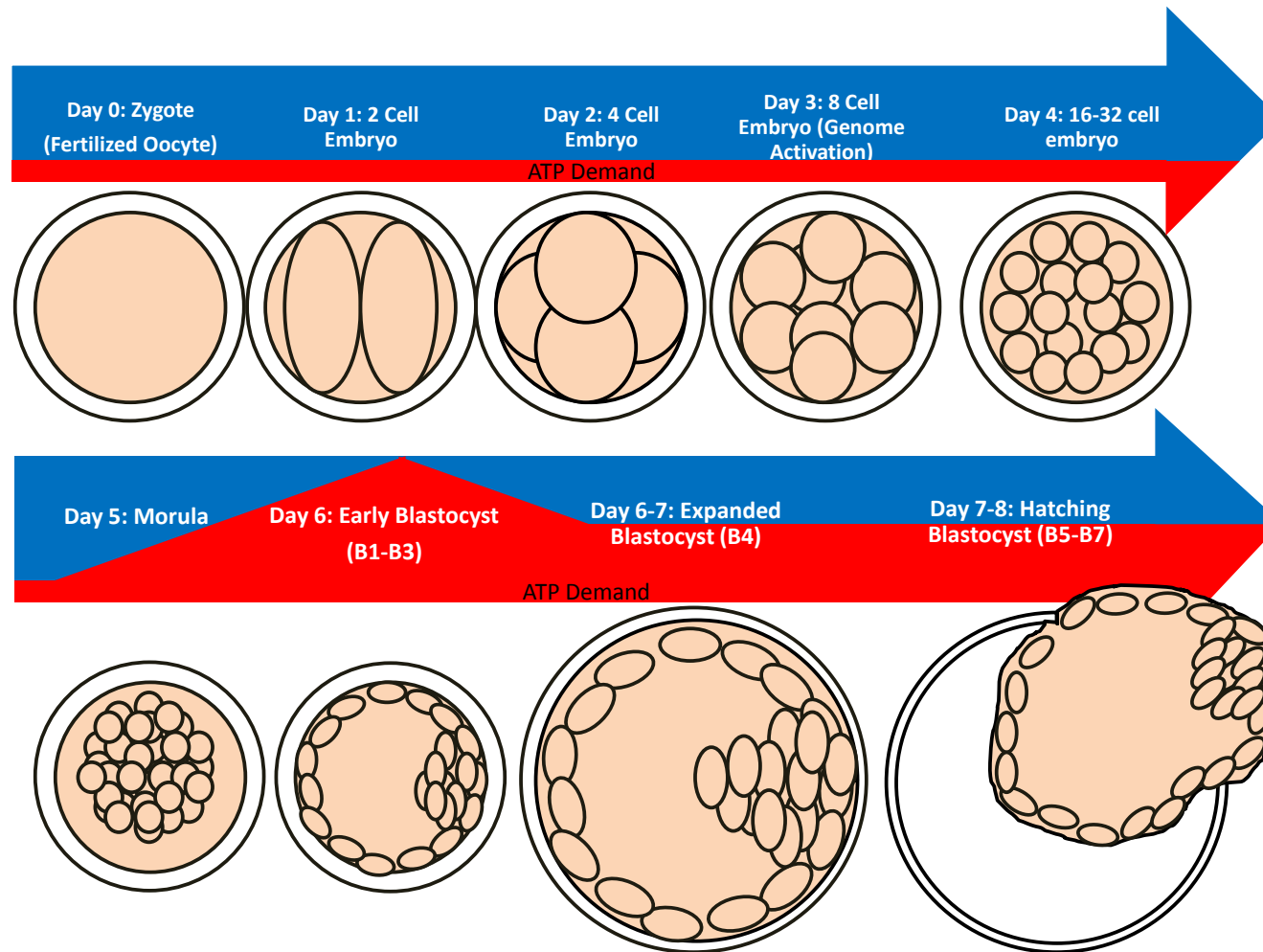


Figure 3: An overview of *in vitro* early bovine embryo development with approximate timings and stage information. Following fertilisation, the paternal and maternal genome combine and the zygote begins to divide approximately once every 24 hours. In the bovine and the human, the embryonic genome is activated on day 3 of development, between the 4-cell and 16-cell stages. During day 5, the cell mass compacts to form a morula. This is followed by the expansion of the fluid-filled blastocoel cavity, alongside differentiation of the Inner Cell Mass to one side of the expanding blastocyst and the single-cell layer of trophoctoderm cells. Blastocoel expansion continues, causing the blastocyst to expand in size as the zona pellucida thins. Finally, the blastocyst hatches from the zona. ATP demand remains relatively low and constant during the early cleavage stages (2-cell to morula) but increases during blastocoel expansion, finally reducing to an intermediate level once the blastocyst has fully expanded.

## 1.2 Eukaryotic energy metabolism

The oocyte, spermatozoon and embryo must complete a series of developmental events which require a constant but dynamic energy supply. Energy metabolism in all eukaryotic cells centres on the turnover of ATP, the primary chemical energy source in living cells. ATP is produced predominantly by aerobic respiration, but also through anaerobic glycolysis. In the early embryo there is little or no RNA or protein synthesis until the time of EGA and consequently DNA synthesis and mitosis are the major energy demands. Therefore ATP demand is relatively low throughout the first 3-4 days of development (Figure 3). A slight increase in energy demand has been reported following EGA, however the first major increase in energy demand occurs during morula compaction and blastocyst expansion, as ATP is required to fuel both the  $\text{Na}^+$ ,  $\text{K}^+$  ATPase and the dramatic rise in protein synthesis which coincides with the onset of growth (Leese et al. 2008). Once the blastocyst is established, ATP demand reduces to an intermediate level until implantation.

ATP is formed in the embryo through glycolysis and oxidative phosphorylation, processes shared by all eukaryotic cells. Energy substrates for oxidative phosphorylation include glucose, pyruvate, amino acids and free fatty acids. All of these can be broken down to form Acetyl Coenzyme A (ACoA), which enters the Tricarboxylic Acid (TCA), Citric acid, or Krebs cycle. The TCA cycle produces electron carriers for oxidative phosphorylation, providing ATP to meet the dynamic energy demands of the developing embryo.

### 1.2.1 Glycolysis

Glucose ( $\text{C}_6\text{H}_{12}\text{O}_6$ ) is a monosaccharide sugar and is a major energy substrate in many cell types. Most carbohydrates, such as starch, are broken down to glucose before ATP production is possible. Glucose is metabolised to pyruvate ( $\text{C}_3\text{H}_4\text{O}_3$ ) in the stoichiometric ratio 1:2 by a series of enzymatically-controlled reactions in the cytosolic process known as glycolysis. This produces 2 moles net ATP per mole of glucose, while a further 1 mole ATP can be generated by the entry of NADH to oxidative phosphorylation. Glucose must first be transported inside the cell by glucose transporter proteins such as the Facilitated Glucose Transporter (GLUT) or Sodium-Dependent Glucose Transporter (SGLT) families. In the

cytoplasm, hexokinase phosphorylates the 6-carbon of the glucose to glucose-6-phosphate (G-6P) by phosphoryl transfer from ATP. A divalent cation such as  $Mg^{2+}$  forms a complex with the ATP to enable this transfer. This first step of glycolysis ensures that the glucose molecule is retained in the cell, and is in common with the pentose phosphate pathway, which generates NADPH and pentose sugars. In glycolysis, the enzyme phosphoglucose isomerase catalyses the isomerisation of G-6P to its open-chain form, conversion of the aldehyde functional group to a ketone group (forming open-chain fructose-1,6-phosphate) and finally nucleophilic addition to form the five-member ring of fructose-6-phosphate (F-6P). F-6P is further phosphorylated by phosphofructokinase (PFK) to fructose 1,6-bisphosphate (F-1,6-BP). PFK is allosterically controlled by ATP, as high concentrations inhibit enzyme activity. This is the key regulatory step in glycolysis. F-1,6-BP is split into two 3-carbon molecules; dihydroxyacetone phosphate (DHAP) and glyceraldehyde 3-phosphate (GAP) by aldolase. Triose phosphate isomerase catalyses conversion of GAP to DHAP and vice versa. GAP is oxidised by glyceraldehyde 3-phosphate dehydrogenase to 1, 3-bisphoglycerate, producing NADH. 3-Phosphoglycerate kinase dephosphorylates 3-phosphoglycerate, producing net 1 mole of ATP. 3-Phosphoglycerate is finally converted to pyruvate via phosphoglyceromutase, enolase and pyruvate kinase, yielding a further mole of ATP per mole of substrate. Other monosaccharides including galactose are converted to glucose to undergo glycolysis, while fructose enters glycolysis after digestion to GAP by a separate mechanism.

Pyruvate has two principal fates in mammalian cells: conversion to lactate, yielding  $NAD^+$ , or decarboxylation to ACoA, which can enter the TCA cycle to produce ATP. While most pyruvate goes to ACoA, a balance must be maintained between pyruvate and lactate levels, as this directly controls the ratio between NADH and  $NAD^+$ , which must be maintained for glycolysis to proceed. Glycolysis is tightly controlled by several mechanisms, for example PFK catalyses an irreversible step and is a key control point. Competition between ATP and AMP for the active site of PFK enables allosteric control based on the ATP:AMP ratio; such that a relative decrease in ATP levels stimulates increased PFK activity. In addition, the  $NAD^+$ :NADH ratio is typically very high in the cell, favouring conversion of GAP to 1, 3-bisphosphoglycerate, which consumes  $NAD^+$ .

## 1.2.2 Fatty acid metabolism

Fatty acids are long chain hydrocarbons with a terminal carboxylate group which tend to exist in energy storage form as triacylglycerol (TG) or free fatty acids (FFAs) in cytoplasm. They are substrates for phospholipid production and are a key source of chemical energy. FFAs are linked to coenzyme A at the outer mitochondrial membrane, termed fatty acid activation, before being transported into the matrix by the L-carnitine shuttle. The fatty acyl-CoA then undergoes a series of reactions called  $\beta$ -oxidation to acyl-CoA and a 2-carbon shorter fatty acid, which also produces  $\text{FADH}_2$  and  $\text{NADH}$ .  $\beta$ -oxidation is described in detail in Chapter 4.  $\beta$ -oxidation of fatty acids produces more ATP per mole of substrate than glycolysis, as FFAs contain many more carbon-carbon covalent bonds than glucose. Additionally, lipid is anhydrous and highly reduced so more ATP can be produced per unit mass than for glucose.

## 1.2.3 Tricarboxylic acid cycle

The TCA cycle is a series of enzymatically controlled reactions regulating the stepwise oxidation of ACoA. Most substrates must be converted to ACoA to enter the TCA cycle, but glucogenic amino acids can also be degraded to provide intermediate substrates such as fumarate or oxaloacetate (Figure 4). This ACoA is used by citrate synthase to catalyse the carboxylation of oxaloacetate (4C) to citrate (6C). The enzymes of the TCA cycle then catalyse the reduction of citrate to oxaloacetate in several steps, producing the electron carriers  $\text{NADH}$  and  $\text{FADH}_2$ , as well as carbon dioxide,  $\text{GTP}$  and  $\text{H}^+$ . Components of the TCA cycle are also used as precursor substrates for biosynthesis.

Energy substrates, including carbohydrates, fatty acids and amino acids, are converted to Acetyl Coenzyme A (ACoA) by a variety of enzyme reactions. Glucose is converted to pyruvate in the cytosol by glycolysis, generating two moles of pyruvate, ATP,  $\text{NADH}$ ,  $\text{H}^+$  and  $\text{H}_2\text{O}$  per mole of glucose. Pyruvate can then be converted to ACoA, releasing  $\text{CO}_2$ , or converted to lactate, regenerating one mole of  $\text{NAD}^+$  per mole of pyruvate (Berg et al. 2002). Lactate production by anaerobic glycolysis in this way typically occurs in mammals when oxygen is limiting, however the regeneration of  $\text{NAD}^+$  is vital to maintaining redox balance and allowing further glycolysis to proceed. Redox state maintenance is vital to

controlling activity and stability of many proteins, transcription of certain genes, and may be involved in cell differentiation and patterning in some species (Coffman and Denegre 2007). ACoA then enters the TCA cycle by bonding its acetyl group to oxaloacetate to form citrate. 3 moles of NADH, 1 mole of FADH<sub>2</sub> and 1 mole of GTP are produced through coupled redox reactions as part of the cycle. The TCA cycle also produces succinate, which carries electrons to complex II, succinate dehydrogenase (CII), the only complex directly involved in the TCA cycle. NADH and FADH<sub>2</sub> act as electron carriers in the next step of aerobic respiration; oxidative phosphorylation.

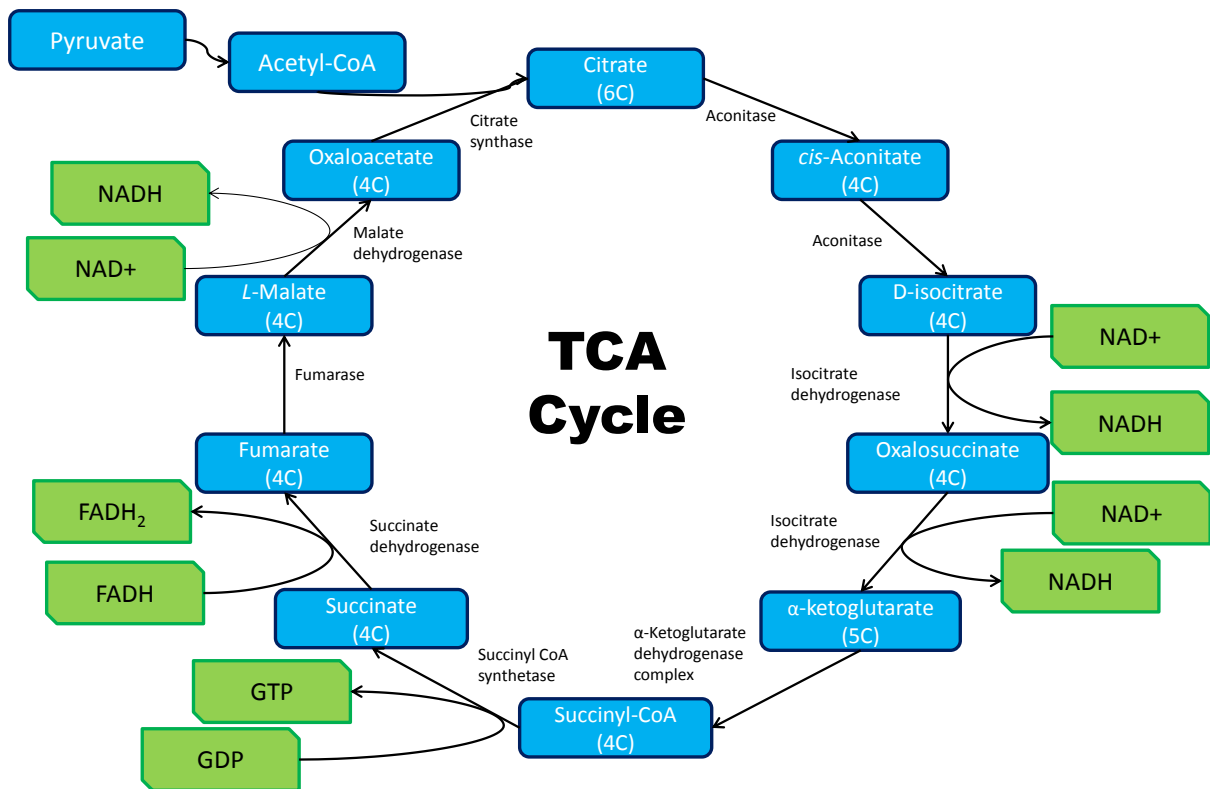
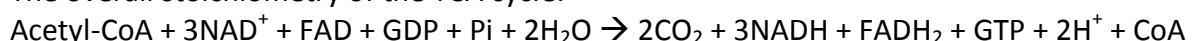


Figure 4: The Tricarboxylic (TCA), Citric acid, or Krebs cycle. Pyruvate is oxidised and conjugated to coenzyme A to form Acetyl-CoA. ACoA is also provided by fatty acid  $\beta$ -oxidation. Citrate synthase catalyses the condensation of Oxaloacetate with ACoA to form Citrate, releasing CoA to repeat this process. Citrate is isomerised to *D*-isocitrate via the unstable intermediate *cis*-Aconitase by the enzyme aconitase. Isocitrate is oxidised to oxalosuccinate, an unstable  $\beta$ -ketoacid, by isocitrate dehydrogenase. Isocitrate is spontaneously decarboxylated, releasing  $O_2$ . Both steps of this are coupled to reduction of  $NAD^+$ . The newly formed  $\alpha$ -ketoglutarate undergoes oxidative decarboxylation and is conjugated to CoA by the  $\alpha$ -ketoglutarate dehydrogenase complex to form succinyl-CoA. Cleavage of the energy-rich thioester succinyl-CoA by succinyl CoA synthetase is coupled to phosphorylation of a purine nucleotide diphosphate, here labelled as Guanosine Diphosphate (GDP). Succinate then undergoes several oxidation steps. First succinate dehydrogenase, complex II of the respirasome and the only complex to participate in the TCA cycle, oxidises succinate to fumarate. The energy released is insufficient to reduce NAD, so this reaction is coupled to the reduction of FAD and the only known cellular process producing  $FADH_2$ . Fumarate is then hydrolysed to malate by fumarase, followed finally by the oxidation of malate to oxaloacetate, catalysed by malate dehydrogenase. This reaction is again coupled to  $NAD^+$  reduction, for a total of 3 moles of NADH and 1 mole of  $FADH_2$  produced per complete cycle.

The overall stoichiometry of the TCA cycle:



## 1.2.4 Oxidative phosphorylation

The now universally accepted theory of oxidative phosphorylation was first published by Peter Mitchell (1965). Hitherto, the vast majority of researchers believed that high-energy chemical intermediates provided the energy for the production of ATP. However, Mitchell theorised that the energy came instead from a chemiosmotic gradient; an unorthodox idea at the time. However, evidence for the structure and mechanisms of the electron transport chain (ETC) complexes and ATP synthase supported the chemiosmotic theory (Boyer et al. 1973; Fry and Green 1980a; Fry and Green 1980b; Fry and Green 1981; Gresser et al. 1982). 4 protein complexes are bound to the inner mitochondrial membrane and form the mitochondrial ETC. NADH produced by the TCA cycle carries electrons to complex I (CI) of the ETC. FADH<sub>2</sub> generated by the TCA cycle carries electrons to CII.

Oxidative phosphorylation in eukaryotic cells involves the coupling of electron (e<sup>-</sup>) transfer (from substrate oxidation) to phosphorylation of Adenosine Diphosphate (ADP) to Adenosine Triphosphate by the creation of a proton (H<sup>+</sup>) gradient or proton-motive force (PMF) across the mitochondrial inner membrane. The protons flow down this proton gradient through ATP Synthase, and this drives ATP synthesis (Berg et al. 2001). However, there are many physiological factors which prevent this in reality. One consideration is proton leak, which is caused by uncoupling of the ETC from ATP Synthase. This is caused *in vivo* by the expression of Uncoupling Proteins (UCP). Uncoupled respiration releases heat energy, a process enhanced by UCP1 expression in tissues such as brown adipose tissue in mammals. This has a variety of roles, such as maintaining temperature in newborn, hibernating or cold-dwelling mammals, as well as a possible mechanism of body weight control (Harper et al. 2001; Divakaruni and Brand 2011). It is interesting to note, however, that oxidative phosphorylation using fatty acids provides 8-11% less ATP per mole of oxygen than carbohydrate oxidation (Hinkle et al. 1991), perhaps due to intrinsic uncoupling by fatty acid  $\beta$ -oxidation (Borst et al. 1962; Leverve et al. 1998).

Theoretically, 30-32 moles of ATP can be produced for every mole of glucose (Hinkle et al. 1991; Berg et al. 2002), while one mole of palmitic acid generates 109-129 moles of ATP (Darvey 2006). 87% of this ATP comes from oxidative phosphorylation, with the remainder coming partly from the TCA cycle and partly from glycolysis.

### 1.2.5 Productive and non-productive oxygen consumption

Oxygen acts as the final electron acceptor in the mitochondrial ETC. This is crucial to the mitochondrial conversion of ADP to ATP, the key endpoint of aerobic respiration. Therefore, consumption of oxygen can be considered to be representative of overall energy metabolism and the study of this energy transformation is part of bioenergetics. It is important to consider that some ATP can also be produced by non-oxidative sources such as non-aerobic glycolysis.

Factors affecting cellular oxygen consumption include:

- Cell metabolism and energy demand
- Cell cycle processes.
- Uncoupling of electron transport from ATP synthesis.
  - Caused by biological means e.g. Uncoupling protein activity
  - Caused by chemical means e.g. Uncoupler treatment
- Non-mitochondrial oxygen consumption as reactive oxygen species (ROS) or by oxygen-consuming enzymes, such as NADPH oxidase.

### 1.2.6 Mitochondrial function

The mitochondrion is the site of ATP production through oxidative phosphorylation in eukaryotic cells. Mitochondria are typically ellipsoid and 0.5-1 $\mu$ m in diameter. However they may change shape, fuse together and translocate by associating to microtubules, leading to many different morphologies. They consist of a specialised outer and inner membrane, giving rise to a narrow intermembrane space. The outer membrane contains porins which allow aqueous components of up to 5kDa in size into the intermembrane space. The inner membrane, however, is highly selective to energy substrates and enzyme co-factors and relatively impermeable to ions. This membrane is the site of oxidative phosphorylation and hosts the components of the ETC and ATP synthase. The central part bounded by the inner membrane is the matrix and contains enzymes involved in the TCA cycle and  $\beta$ -oxidation. The inner membrane forms projections into the matrix known as cristae, increasing surface area available for oxidative phosphorylation. The number of cristae varies to allow cells to adapt to energy demand, for example 3 times more cristae are present in cardiac muscle mitochondria than in hepatocytes. Mitochondrial energy transduction is plastic by necessity,

as the ATP demand depends directly on the energy requirements of the cell, which change throughout the cell cycle, growth and development. However, mitochondria may fail to perform these roles adequately leading to dysfunction. Mitochondrial dysfunction can be defined as any change to the ability of the mitochondria to produce sufficient ATP in response to the demands of the cell.

In addition to the primary function of ATP production, mitochondria also generate and detoxify Reactive Oxygen Species (ROS) as a toxic by-product of normal oxidative phosphorylation. ROS include superoxide ( $O_2^{\cdot-}$ ), hydroxide ( $\cdot OH$ ) and peroxide ( $H_2O_2$ ), all of which are highly reactive and can cause damage to organelles and macromolecules such as protein, lipid and DNA. This is termed oxidative damage or oxidative stress. ROS do have some productive cellular functions, including signalling pathways, apoptosis, calcium regulation, translocation of mitochondria and metabolism. A deficiency in any of these processes could also be described as a type of dysfunction (Brand 2011). An understanding of the number of moles of ATP produced by mitochondria is valued in terms of whole body health, as control of this biochemistry is essential for control of obesity. Proton leak or uncoupled oxygen consumption accounts for 20-40% total oxygen consumption (Buttgereit and Brand 1995). In the preimplantation embryo there is the additional factor of mitochondrial maturation, which may influence oxygen consumption and oxidative phosphorylation. During preimplantation development, mitochondria develop from a spherical condensed form to the classical elongated structure, which is discussed further in Chapter 3.

## 1.3 Bovine oocyte and embryo metabolism

Embryo metabolism is a source of great academic, clinical and commercial interest as the metabolic profile of an embryo may predict viability. Studies of embryo metabolism began by measuring turnover of radio-labelled substrate in-vitro. For example Wales and Brinster (1968) found that 2-8 cell mouse embryos consumed significantly more  $^{14}\text{C}$  glucose than oocytes or zygotes (Wales and Brinster 1968; Quinn and Wales 1973). The radiolabelling reduces developmental capacity, however, and is not suitable for routine screening before implantation.

Non-invasive fluorimetric methods were later developed (Leese and Barton 1984; Leese and Barton 1985) to measure glucose and pyruvate consumption and lactate depletion from the media (Gardner and Leese, 1986; Gardner and Leese, 1987; Hardy et al. 1989). This highly sensitive method measures the change in NAD or NADP fluorescence coupled to enzymatic breakdown of the measured substrate using a fluorescence microscope with photomultiplier tube. Since these procedures are time-consuming (Barnett and Bavister, 1996), a more high-throughput modification of this technique has been developed using a fluorimetric plate reader based on depletion or production of the substrate by individually cultured embryos over 24 hours and is described in detail in Chapter 2 (Guerif et al. 2013).

Many reports have proposed a link between metabolic activity and embryo viability, for example, those of Conaghan et al. (1993) for pyruvate, Houghton et al. (2006) for oxygen, Gardner and Leese (1987), Gardner et al. (2011) for glucose and Houghton et al. (2002), Brison et al (2004) for amino acids.

Measurement of various other factors secreted by embryos has also been carried out, including Human Chorionic Gonadotrophin (HCG) and Interferon-tau (IFN- $\tau$ ), but as yet the relationships between concentration of these factors and embryo viability has not been defined (Donnay et al. 2002).

# Bovine Embryo Metabolism

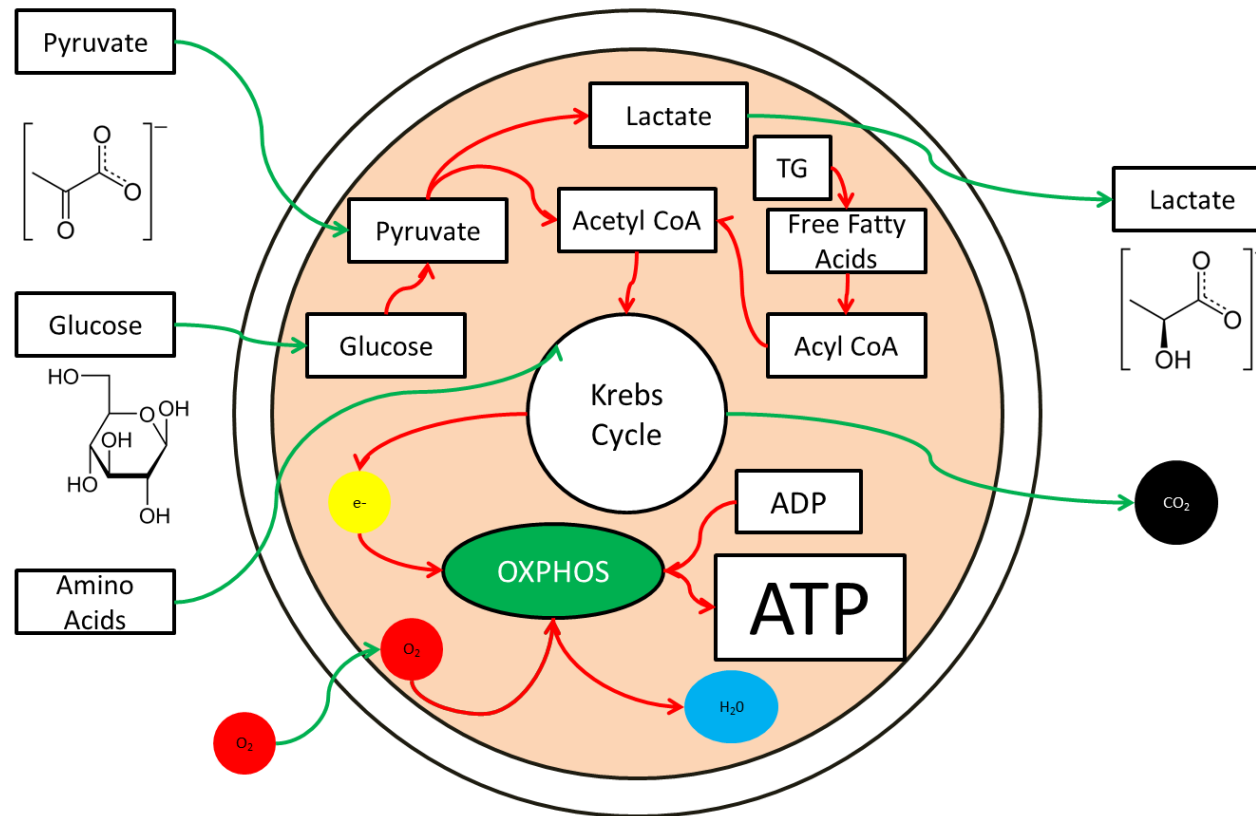


Figure 5: An overview of *in vitro* bovine preimplantation embryo metabolism at blastocyst stage. Green arrows indicate transport, red arrows indicate metabolic reactions. The bovine oocyte contains a large triglyceride (TG) store, used as an endogenous energy source during development. TG is hydrolysed to free fatty acids, which in turn are converted to Acyl-Coenzyme A by  $\beta$ -oxidation. Media is supplemented with glucose and pyruvate, which are consumed by anaerobic glycolysis, producing lactate, which is released, and oxidative phosphorylation (OXPHOS). Carbohydrates are digested to Acetyl-Coenzyme A (ACoA), which enters the Krebs or TCA cycle as described above. Amino acids are supplied in the media and can also be used as energy substrates, entering the Krebs cycle at various points. OXPHOS consumes diatomic oxygen (O<sub>2</sub>) and converts ADP to ATP, producing water.

### 1.3.1 Glucose, pyruvate and lactate

The preferred energy substrate of cleavage stage mammalian embryos is pyruvate as first demonstrated in the mouse (Leese and Barton 1984), and later shown in bovine embryos by Rieger and Guay (1988). Glucose uptake is limited due to low expression of the transport protein Glut1 (Pantaleon et al. 1997) and of low hexokinase activity (Hooper and Leese 1989; Martin et al. 1993; Martin and Leese 1999). Pyruvate is exchanged for lactate via a monocarboxylate carrier (Butcher et al. 1998). Pre-compaction embryos derive 85-90% of their ATP through oxidative phosphorylation (Thompson et al. 1996; Sturmey and Leese 2003). After compaction, ATP demand increases and this is accompanied by an increase in glycolysis (Thompson and Peterson 2000). As described above, the ratio of pyruvate to lactate is involved in regulation of redox equilibrium by maintaining the NADH:NAD ratio in the cytoplasm and an excess of pyruvate can impair development (Dumollard et al. 2007). Indeed, the majority of pyruvate uptake by early preimplantation human embryos is directed towards lactate production as a means of regulating intracellular pH (Butcher et al. 1998). However, the bovine embryo can develop, though in reduced numbers, to the morula stage using lactate as sole exogenous energy source (Takahashi and First 1992). Pyruvate uptake is maintained alongside increased glucose transport post-compaction in bovine embryos (Thompson et al. 1996). Guerif et al. (2013) reported a measureable 'optimum' range of pyruvate depletion by early cleavage stage bovine embryos which correlate with increased viability to the blastocyst stage.

Glucose is primarily used as an anabolic substrate, with up to 50% total glucose being used in the pentose phosphate pathway to build ATP, NAD, DNA and RNA at the 16 cell stage in the bovine (Javed and Wright 1991). At the blastocyst stage, glucose consumption greatly increases, and 50% is converted to lactate (Hardy et al. 1989; Conaghan et al. 1993; Sturmey and Leese 2003). However, as this process contributes only 2 moles ATP per mole glucose, compared to 32 moles through oxidative phosphorylation, the contribution of this to total ATP supply is relatively low. A greater increase in glycolysis is seen in response to stress in embryos and experiments conducted in sheep and mice suggest that embryos with higher rates of glucose metabolism are less viable (Leese et al. 1998; Leese 2002). High concentrations of glucose can, under some circumstances and depending on the species, have an inhibitory effect on embryonic

development and lead to reduced cell number and increased apoptosis (Jiménez et al. 2003). In hyperglycaemic conditions (10-30mM glucose), Glut1 expression and transcription are reduced and the result is essentially glucose starvation. It has also been reported that glucose is detrimental up to 120 hours after fertilisation, but beneficial after this point and increases blastocyst numbers (Kim et al. 1993).

In addition to the role of Glucose 6-Phosphate Dehydrogenase (G6PD) in the pentose phosphate pathway, it also metabolises and neutralises ROS (Lopes et al. 2007). Due to this detoxifying effect, G6PD has been described as cytoprotective against DNA damage and oxidative stress and it has been suggested that a deficiency in this enzyme in the embryo may reduce developmental capacity (Nicol et al. 2000). However, as moderate levels of ROS stimulate embryonic development (Rieger et al. 1992), this cytoprotective effect also delays female blastocyst development by controlling levels of ROS (Gutiérrez-Adán et al. 2001). G6PD is the only NADPH-producing enzyme to be activated during oxidative stress (Lopes et al. 2007). It has been suggested that the increased glucose metabolism during blastocyst expansion results in increased ROS production which stimulates greater expression of G6PD, rather than simply increased glucose consumption (Lopes et al. 2007). This is an intriguing idea, which suggests that greatly increased respiration in embryos is a product of ROS production and could indicate a more damaged embryo rather than a more viable one. More data on the non-oxidative phosphorylation component of oxygen consumption is required to support this theory.

Lactate production in the bovine accounts for 40% of glucose uptake on fertilisation, but increases at the blastocyst stage to 100% of glucose uptake (Thompson et al. 1996). Glucose is therefore directed to lactate production rather than entering the TCA cycle (Rieger et al. 1992). This does not appear to be related to oxygen availability, and instead may aid preparation of the embryo for the low-oxygen environment in the uterus (Fischer and Bavister 1993). Glycolysis provides both 2 moles net ATP per glucose and a range of intermediates for anabolic pathways, and along with high glutamine consumption, is common in rapidly dividing cell types (Newsholme et al. 1985) .

### 1.3.2 Fatty acids

Oocytes of many species contain a sizeable store of lipid as triglycerides (TG) and it seems likely that the fatty acid composition of this store is highly dependent on maternal diet (Leroy et al. 2011). Fatty acid metabolism is of particular interest in relation to human fertility in the case of overweight and obese (OVOB) females and in the declining fertility of the dairy cow (Diskin et al. 2006). However, research into the effects of specific fatty acids and more importantly, combined effects of fatty acids at different concentrations, has been largely ignored until very recently. This research was reviewed by McKeegan and Sturmey (2011) and is discussed in detail in Chapter 4.

A co-regulatory cycle between fatty acid and glucose, first proposed by Randle et al. (1963) exists in the whole body, as glucose and fatty acids compete for oxidation by tissues such as muscle and adipose. High insulin stimulates storage of lipids and carbohydrates, while high glucagon stimulates lipolysis in adipocytes and glucose production. However, a similar relationship at the cellular level has been proposed. Oxidation of one substrate inhibits production of the other. Briefly, production of Acetyl-CoA from  $\beta$ -oxidation inhibits conversion of pyruvate to ACoA by pyruvate dehydrogenase (PDH), while elevated cytosolic citrate inhibits glucose uptake and glucose-6-phosphate phosphorylation by Phosphofructokinase (PFK) (Cheema-Dhadli et al. 1976). ACoA normally regulates PDH activity by feedback inhibition to modulate glycolysis, but this mechanism enhances this effect, reducing PDH activity still further. Conversely, production of malonyl-CoA following glycolysis inhibits CPT1, reducing transport of NEFA into the mitochondria. Interestingly, the regulatory roles of a 'Randle-type' cycle are abrogated by a stress-related mechanism (Carling et al. 2003). A decrease in substrate supply or increase in energy demand increases the ratio of AMP:ATP, stimulating activity of AMP-activated protein kinase (AMPK). AMPK inhibits Acetyl-CoA Carboxylase (ACC), decreasing malonyl-CoA production and therefore malonyl-CoA inhibition of  $\beta$ -oxidation. In addition, AMPK stimulates glucose uptake and glycolysis. The net effect of this is the AMPK-dependent activation of ATP-generating processes and inhibition of ATP-consuming processes.

### 1.3.3 Amino acids

Non-invasive assays of bovine embryos have included amino acid profiling by High Performance Liquid Chromatography (HPLC), which makes it possible to predict viability based particularly on consumption and production of amino acids (Sturmey et al. 2009, 2010). As stated above, protein synthesis increases at the blastocyst stage and requires an increase in amino acid consumption (Partridge and Leese 1996). However, different amino acids are consumed at different rates, and amino acid profiling by reverse-phase HPLC has revealed signature profiles for different stages of embryo development in bovine (Thompson et al. 1996; Sturmey et al. 2010), porcine (Humpherson et al. 2005), mouse (Lamb and Leese 1994) and human embryos (Houghton et al. 2002). As with other markers of embryo viability, amino acid uptake and metabolism differs between *in vitro* and *in vivo* derived embryos (Partridge and Leese 1996) and is directly affected by the composition of the culture medium. For example, replacing Foetal Calf Serum (FCS) with Polyvinyl Alcohol reduced blastocyst rate and cell numbers, and led to quantitative and qualitative differences in amino acid turnover (Orsi and Leese 2004). Amino acid uptake is 30% lower in embryos cultured without FCS (Partridge and Leese 1996). FCS contributes a range of components to embryo culture medium, including protein, amino acids and fatty acids which may be of benefit to the embryo, but may also have some negative effects. FCS can also protect the *in vitro* embryos by buffering pH and chelating heavy metal ions. As well as direct uptake of amino acids, embryos endocytose FCS, BSA and other protein supplements from which they may derive amino acids.

Amino acids are also supplied as a supplement to the Synthetic Oviduct Fluid (SOF) medium used to culture bovine embryos. Often, essential and non-essential amino acids established by Eagle (1959) are added. It has been reported that provision of amino acids enhances the percentage of embryos progressing to blastocysts and increase cell number (Takahashi and First 1992). Aside from being utilised for protein synthesis, amino acids are also used as an energy source (Partridge and Leese 1996), a pH buffer (Baltz 1993; Baltz 2001) and may provide a defence against oxidative damage (Harding et al. 2003). Importantly, supplying amino acids to *in vitro* cultured embryos shifts gene expression towards a more *in vivo* profile, which is potentially beneficial when studying *in vitro* models of development (Ho et al. 1995).

A range of amino acids transporters have been discovered in embryos, some of which are specific to individual amino acids and others which transport specific groups such as branched amino acids or zwitterions (Whitewright and Leese 2008). Most of these are expressed from the blastocyst stage onward, though a few are expressed at early cleavage stages (Van Winkle 2001). It is assumed that maternally derived transporters are available until the embryonic genome is activated. Some patterns in transporter classes and the substrates carried are evident; for example all arginine transporters are sodium-dependent.

Glutamine metabolism is at its highest in two and four-cell bovine embryos, then decreases, in an inverse of the pattern of glucose metabolism (Rieger et al. 1992). This may be due to digestion of the maternal enzymes initially present in the embryo. However, the demand for glutamine increases during blastocyst expansion due to increased protein synthesis.

A by-product of amino acid metabolism is ammonia, some of which may also be produced by spontaneous breakdown of amino acids, especially glutamine (Gardner 1994). Ammonia is toxic and may cause morphological, structural and metabolic perturbations to the embryo (Gardner 1994; Walker et al. 1992).

As mentioned above, *in vitro* derived embryos exhibit significantly different amino acid profiles to *in vivo* derived embryos (Sturmeier et al. 2010) and it is likely that many other aspects of the metabolic profile will exhibit similar differences. Metabolic profiling also revealed sex-linked difference in amino acid depletion, particularly *in vitro* derived embryos. However, results from *in vitro* derived embryos are not directly comparable with those derived *in vivo*, but are useful in building an accurate model of embryo development in the physiological environment

### 1.3.4 Oxygen consumption

Consumption of oxygen has been investigated as an indicator for bovine embryo viability (Lopes et al., 2005). Oocyte Oxygen Consumption Rate (OCR) is a marker of quality for oocytes in humans (Tejera et al. 2011) and is affected by ovarian stimulation treatment, maternal age and FSH concentration (Scott et al. 2008).

A number of non-invasive techniques have aimed to measure oxygen consumption of embryos as sensitively as possible, starting with a 'Cartesian Diver' system (Fridhandler et al. 1956; Mills and Brinster 1967). This has since been succeeded by more sensitive methods such as the pyrene method used by the Leese group (Houghton et al. 1996; Sturmeay and Leese 2003). Currently, the most sensitive technique is nanorespirometry, which is used to assay single oocytes or embryos. It has been reported that nanorespirometry does not affect the viability of embryos, and hence could be an excellent candidate for accurate, non-invasive measurement on a clinical or commercial scale (Lopes et al. 2005). However, this technique does involve removing the embryo from its culture group, which may perturb metabolism in the embryos from certain species.

OCRs have been reported for both *in vivo* and *in vitro* derived preimplantation embryos. The techniques used have, in general, shown that mean OCR throughout the cleavage stages tends to be relatively consistent and low, in line with ATP demand, but increases from morula to blastocyst and from blastocyst to expanded blastocyst stages (Houghton et al. 1996; Overström 1996; Thompson et al. 1996; Donnay and Leese 1999; Lopes et al. 2005), reducing to an intermediate level once expansion is complete (Houghton et al. 1996; Thompson et al. 1996; Lopes et al. 2005). However there is often great variation between values for the same stage, for example the difference in blastocyst oxygen consumption between the reports of Overström (1.5 nl/h) and Thompson (0.7 nl/h). This is likely due to the different methods used to generate data. Indeed, large variation has been reported between embryos in the same experimental group at the blastocyst stage, which could be influenced by the degree of expansion when the measurements are made, especially as the onset of expansion involves a dramatic increase in protein content (Overström 1996; Shiku et al. 2001). A record of oxygen consumption of a blastocyst over time may be more revealing than a single time point. Differences between male and female blastocysts have also been reported (Agung et al. 2005).

Oxygen consumption by embryos can be affected by a variety of factors, including osmolarity and media composition. Observed differences between embryos derived *in vivo* and *in vitro* could be due to the change in conditions when removing embryos or oocytes from the *in vivo* to the *in vitro* situation. Glucose concentration in culture media has a particularly pronounced effect, as higher levels may result in reduced oxygen

consumption and increased lactate production through glycolysis (Donnay et al. 2002). This is similar to the 'Crabtree' effect in yeast (Seshagiri and Bavister 1991).

Linking the morphological grade of the embryo to oxygen consumption has met with some success, for example Shiku and colleagues (2001) found that *in vitro*-derived morulae graded as 'excellent' (even cell division, no fragmentation) tended to have higher rates of respiration and result in a greater number of expanded blastocysts. Agung et al. (2005) reported that oxygen consumption of embryos graded as 'excellent' had higher rates of oxygen consumption than those graded as 'good', although no significant difference was found between early and expanded blastocysts. However, other researchers have not reported such correlations (Overström 1996). The nanorespirometry method indicated that embryos of higher quality grades have moderate respiration rates (Lopes et al. 2005). Moreover, embryos with wider diameters at both day 3 and 7 have increased respiration. This is in agreement with earlier work which found that morulae with greater diameters had greater respiration rates (Shiku et al. 2001).

As indicated, ATP use is lowest in oocytes and cleavage stage embryos and the primary method for ATP production during these stages is oxidative phosphorylation (Leese et al. 2008). By the blastocyst stage, 85% of ATP is still produced by oxidative phosphorylation, but absolute rates are much higher, which may be attributed primarily to two factors involved in developing the blastocyst; increased protein synthesis, and increased activity of the  $\text{Na}^+, \text{K}^+$ ATPase, to which 30-40% ATP is directed (Leese et al. 2008). In the bovine blastocyst this enzyme is estimated to account for between 10.5 and 44% of oxygen consumption (Leese et al. 2001). It has been suggested that less viable embryos may be more permeable to sodium ions and have to devote more energy to sodium pumping to maintain intracellular osmolarity (Leese et al. 2007; Lopes et al. 2010).

A later study sought to use nanorespirometry to predict the development of early cleavage stage murine embryos to expanded blastocysts (Ottosen et al. 2007). The group found that there were significant increases in oxygen consumption moving from the 4 cell to 8 cell stage and again to the morula stage, followed by a doubling in rate at the expanded blastocyst stage. In general, embryos successfully reaching the expanded blastocyst stage tended to consume more oxygen than those which did not, though there was little difference between viable and poor 2 cell embryos. This oxygen consumption

data supports previous data in murine embryos (Houghton et al. 1996; Trimarchi et al. 2000).

### 1.3.5 Oxidative damage

As oxygen consumption increases with embryo development, so too does the production of Reactive Oxygen Species (ROS) (Lopes et al. 2010). However ROS production may be regulated independently of OCR (Barja 2007) and is perhaps more dependent on mitochondrial membrane polarisation and the degree of uncoupling. A cycle of proton pumping and proton loss by 'leaky' respiration account for a significant amount of overall metabolism in whole organisms, including up to 25% of metabolic rate in rats (Brand 2000). Although this proton cycle accounts for energy loss, it may be an evolutionarily conserved mechanism to reduce ROS production and oxidative damage (Brand 2000).

It has been suggested that ROS are more toxic *in vitro* than *in vivo* (Johnson and Nasr-Esfahani 1994) and this has led to the use of hypoxic incubators for *in vitro* embryo culture in order to improve blastocyst production. Indeed, *in vitro* matured oocytes exhibit upregulated expression of antioxidant enzymes compared to those matured *in vivo*, most likely in order to defend against the increased oxidative stress *in vitro* (Lonergan et al. 2003). An investigation into the effects of adding antioxidants to the culture medium revealed that ethylenediaminetetraacetic acid (EDTA) and culture at 5% oxygen gave the greatest increase in murine embryo development, while Superoxide Dismutase (SOD) and Catalase also had beneficial effects (Orsi and Leese 2001). These data agree with an earlier study of DNA damage to bovine embryos by ROS using a microgel electrophoresis technique (Takahashi et al. 2000). The authors observed a positive correlation with DNA damage when embryos were cultured in 20% O<sub>2</sub> compared to 5% O<sub>2</sub> – a finding confirmed for blastocysts by Sturmey et al. (2009). Many investigations have attempted to use an antioxidant to reduce ROS levels and hence improve embryo quality. In one study, embryos were treated with vitamins E and C alone and together, and it was observed that more embryos treated with vitamin E progressed to blastocyst stage (17%) compared to 11% in control media (Olson and Seidel 2000). In a separate experiment, *in vitro* produced bovine embryos transferred to recipients had a 63% higher surface area compared to controls when removed after 7 days. From these studies, it appears that ROS can have a deleterious effect on embryo development, and

efforts made to reduce ROS levels, such as incubating embryos in lower oxygen concentrations and treatment with antioxidants may be of benefit to the efficiency of embryo production.

Mammalian cells do, however, have an array of defences against ROS as well as sophisticated DNA repair mechanisms, and bovine embryos are no exception. In a recent study, 70% of the DNA repair genes investigated were expressed in human blastocysts (Jaroudi et al. 2009). These transcripts were detected at higher levels in oocytes, most likely due to the reliance of the oocyte and early embryo on maternal transcripts until embryonic genome activation. It also appears that female blastocysts may be more protected against ROS than male blastocysts as they have a higher antioxidative capacity and production of NADPH, both of which are due to increased pentose phosphate pathway activity; four times that of male blastocysts (Tiffin et al. 1991).

## 1.4 Aims

This literature review has revealed that rather little is known about the regulation of metabolism during preimplantation embryo development compared with the situation in somatic cells. In particular, there is a lack of information on the bioenergetic status of preimplantation embryos – particularly the components of oxygen consumption - a key consideration for tissues with dynamic changes in energy demand. Also, the role of lipid metabolism during the preimplantation phase has long been neglected – the focus having been on carbohydrate and amino acid metabolism. There is also a need to relate studies on metabolism to the outcome of embryo development, in phenotypic terms, i.e., the formation of a viable blastocyst and in terms of blastocyst gene expression and epigenetic modification.

The aim of this thesis was therefore to investigate the regulation of oxidative metabolism in individual mammalian embryos and the immediate and legacy effects of metabolic dysregulation. This involved the following objectives:

- Quantify the components of oxidative phosphorylation in the bovine embryo using oxygen consumption profiling techniques.
- Investigate the effects of dysregulated  $\beta$ -oxidation of fatty acids derived from endogenous triglyceride stores on energy metabolism during preimplantation embryo development.
- Examine the relationship between  $\beta$ -oxidation of endogenous fatty acids during *in vitro* embryo development and blastocyst gene expression.
- Investigate the epigenetic legacy of dysregulated  $\beta$ -oxidation during *in vitro* embryo development.

## 2 General materials and methods

## 2.1 Bovine embryo *In Vitro* Production (IVP)

### 2.1.1 Source of reagents

The reagents used in this research and their suppliers are listed in appendix I. Double distilled water (ddH<sub>2</sub>O) was taken from an ELGA water polisher.

### 2.1.2 Preparation of glassware and consumables for embryo culture

Glassware (volumetric flasks, funnels, beakers and Duran bottles) designated for the preparation of embryo culture media and stock solutions were washed and sterilised before use. Glassware was rinsed in ddH<sub>2</sub>O then submerged in an 8l bucket containing ddH<sub>2</sub>O + approximately 2% Decon 90™ for between 24hr – 2 weeks. Washed glassware was then removed from the Decon 90 solution, drained and rinsed three times by immersion in a rinsed 8l bucket containing ddH<sub>2</sub>O. Rinsed glassware was then drained and sealed with aluminium foil or appropriate lids, labelled with autoclave tape and sterilised in a Rodwell Ensign autoclave at 121°C for 2hr.

Non-sterile consumables including pipette tips, which were racked in appropriate boxes and eppendorf tubes, stored in glass jars or beakers, were sterilised in a Rodwell Ensign autoclave at 121°C for 2hr.

Autoclaved glassware and consumables were transferred to a drying oven at 80°C for at least 5h to evaporate all moisture before use.

Sterile plastic-ware including T25 and T75 culture flasks (Corning), tissue culture and petri dishes and universal tubes (Sarstedt) were tested for embryo culture before regular use.

### 2.1.3 Preparation of IVP media

The recipes used for media and solutions listed in this section are described below. All fertilisation and embryo culture media were made in large batches and stored as aliquots in sterile universal tubes (Sarstedt) at -20°C for 3 months. Stock solutions for holding media were kept at 4°C for the time indicated below.

Chemicals supplied as powder were weighed using a 4 decimal point (4 d.p) Sartorius or Ohaus balance. The balance was calibrated each day before use and cleaned after use with 70% Ethanol. Chemicals were weighed to siliconised weighing paper (Schleicher and Schuell) or a polystyrene weighing boat dependent on mass needed. Compounds were then transferred to a sterile volumetric flask through a sterile funnel and the appropriate volume of embryo tested (ET) water added (Fresenius Kabi). The flask was agitated by inversion or sonication or left at 4°C overnight until the chemicals were fully dissolved. Solutions were then sterilised using a 0.22µm PS Millipore syringe-top filter, discarding the first 6ml to be filtered as this carries embryotoxic compounds from the filter (Harrison et al. 1990). Sterile solutions were aliquotted to appropriate volumes using sterile T25 culture flasks, universal tubes or eppendorf tubes.

Media was tested for osmolarity in the appropriate range 280-290mOsm/kg using an Osmomat 030 osmometer (Gonotec GmbH, Berlin, Germany). Hepes-buffered and bicarbonate-buffered media to be used were within ±5mOsm/kg of each other to minimise osmotic shock to oocytes and embryos. If the osmolarity exceeded this range, the media was discarded and re-made. The osmometer was switched on 1 hour before use to allow cooling and calibrated to 0mOsm/kg using 100µl embryo tested water and to 300mOsm/kg H<sub>2</sub>O using 100µl commercial standard (Camlabs, Cambridge, UK). The probe was cleaned carefully with laboratory tissue between each measurement to prevent contamination and an empty 500µl micro tube attached to the probe when not in use.

## 2.1.4 Holding medium stocks

Stocks for preparation of HEPES-buffered Holding Media (HM) were prepared as described below. HEPES and HEPES Sodium Salt were stored in a sealed container at room temperature with desiccator crystals (Sigma-Aldrich, Dorset, UK).

Stock	Compounds	Mass	Relative molecular mass (Mr)	Final concentration	Final volume	Storage
Stock B	Sodium bicarbonate NaHCO <sub>3</sub>	0.42g	84.01	250mM	20ml	4°C for 2 weeks
Stock BSA	Bovine Serum Albumin Fraction V, Essentially Fatty Acid Free	2g		20% w/v	10ml	4°C for 6 weeks
Stock H	HEPES Free Acid	1.5g	238.3	126mM	50ml	4°C for 6 weeks
	HEPES Sodium Salt	1.625g	260.3	125mM		
Stock K	Kanamycin sulphate	0.5g	382.6	131mM	10ml	4°C for 6 weeks
Stock Heparin	Heparin (porcine)	0.2g		1% w/v	20ml	-20°C for 3 months

Table 1: Composition of stock solutions for holding medium.

## 2.1.5 FSH:LH stock

Lyophilised Menotrophin (Menopur) containing 75IU Luteinising Hormone (LH) and 75IU Follicle-Stimulating Hormone (FSH) was obtained from Ferring pharmaceuticals, West

Drayton, UK. The Menotrophin was reconstituted in 7.5ml of 1xM199 and mixed well before storing in 100µl aliquots at -20°C.

### 2.1.6 EGF:FGF stock

1mg Epidermal Growth Factor (EGF) from murine submaxillary gland was dissolved in 20ml BMM. 25µg Fibroblast Growth Factor (FGF) was dissolved in 1ml BMM. The EGF and FGF stocks were then combined in the ratio 4ml EGF to 185µl FGF, mixed well and stored in 200µl aliquots at 20°C.

### 2.1.7 Maturation additives

Maturation Additives were prepared as described below, sterile filtered and stored in 500µl aliquots at -20°C for 3 months. Gibco® Gultamax-II, containing a more stable dipeptide form of glutamine, L-alanyl-L-glutamine, was obtained from Life Technologies, Paisley, UK.

Compounds	Amount of chemical
Apo-transferrin	0.025g
Glutamax II	1ml
Pyruvate	0.11g
β-mercaptoethanol	7µl
Polyvinyl Alcohol (PVA)	0.025g
ET Water	24ml

Table 2: Composition of maturation additives for maturation media.

## 2.1.8 Preparation of holding and bovine maturation media

Holding medium (HM) and Bovine Maturation Medium (BMM) were prepared each day before use (Table 3). HM was pre-warmed to 39°C for 2 hours in a warming incubator, while maturation media drops were prepared as shown in Figure 6 and pre-equilibrated for 2 hours at 39°C and 5% CO<sub>2</sub> in air.

Holding Medium (HM)	
Solution	Volume
ET Water	80ml
10xM199	10ml
Stock B	2ml
Stock H	6ml
Stock K	100µl
Stock BSA	200µl
Final volume	98.3ml

Bovine Maturation Medium (BMM)	
Solution	Volume
1xM199	8ml
Stock B	1ml
Foetal Calf Serum (FCS)	1ml
Maturation Additives	222µl
Glutamax II	100µl
EGF:FGF	100µl
FSH:LH	200µl
Heparin	10µl
Final volume	10.522ml

Table 3: Holding media and bovine maturation media recipes. Each type of media was prepared fresh before use.

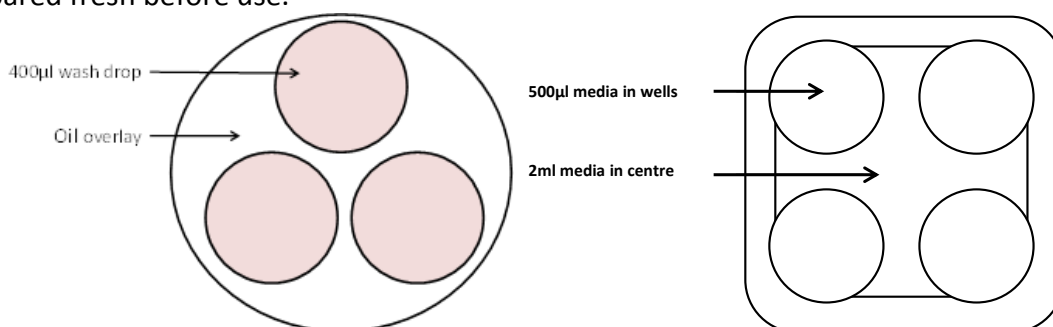


Figure 6: Diagram showing setup of *in vitro* maturation plate and BMM wash dish. 3x 400 µl drops of bovine maturation media (BMM) were placed in a 60mm petri dish and overlaid with oil. 500µl BMM was added to each well of a 4-well plate, with 1ml added to the centre to reduce evaporation.

## 2.1.9 Preparation of *in-vitro* fertilisation media

Fertilisation Tyrode's Albumin Lactate Pyruvate medium (Fert-TALP) and Hepes-TALP spermatozoa wash medium were prepared as shown below (Table 4) and frozen at -20°C for up to 3 months. Both media were defrosted on the day of use. Hepes-TALP was pre-warmed to 39°C for 2 hours in a warming incubator, while Fert-TALP drops were prepared as shown in Figure 7 and pre-equilibrated for 2 hours at 39°C and 5% CO<sub>2</sub> in air.

Hepes-TALP 250ml			Fert-TALP 202ml		
Component	Amount	Concentration	Component	Amount	Concentration
ET Water	248.393ml		ET Water	198.918ml	
NaCl	1.667g	114mM	NaCl	1.333g	114mM
KCl	0.06g	3.19mM	KCl	0.0476g	3.19mM
NaH <sub>2</sub> PO <sub>4</sub>	0.016g	0.45mM	NaH <sub>2</sub> PO <sub>4</sub>	0.0124g	0.45mM
Gentamycin	1.25ml	0.05mg/ml	Gentamycin	1ml	0.05mg/ml
NaHCO <sub>3</sub>	0.084	2mM	NaHCO <sub>3</sub>	0.42	2mM
Pyruvate	0.0144g	0.26mM	Heparin	0.002g	10µg/ml
Hepes free acid	0.45g	7.5mM	Pen-hyp stock	2ml	2µM/1µM
Hepes Na salt	0.488g	7.5mM	Pyruvate	0.0058g	0.26mM
CaCl <sub>2</sub> .2H <sub>2</sub> O	0.076g	2.06mM	CaCl <sub>2</sub> .2H <sub>2</sub> O	0.0605g	2.06mM
MgCl <sub>2</sub> .6H <sub>2</sub> O	0.025g	0.49mM	MgCl <sub>2</sub> .6H <sub>2</sub> O	0.02g	0.49mM
Na-Lactate	0.353ml	9.96mM	Na-Lactate	0.282ml	9.96mM
OSMOLARITY 280-290			OSMOLARITY 280-290		
BSA	1g	4mg/ml	BSA	0.8g	4mg/ml

Table 4: Preparation of Fert-TALP *in vitro* fertilisation medium and Hepes-TALP sperm washing medium. Medium was prepared in a sterile volumetric flask, sterile filtered and stored at -20°C for up to 3 months.

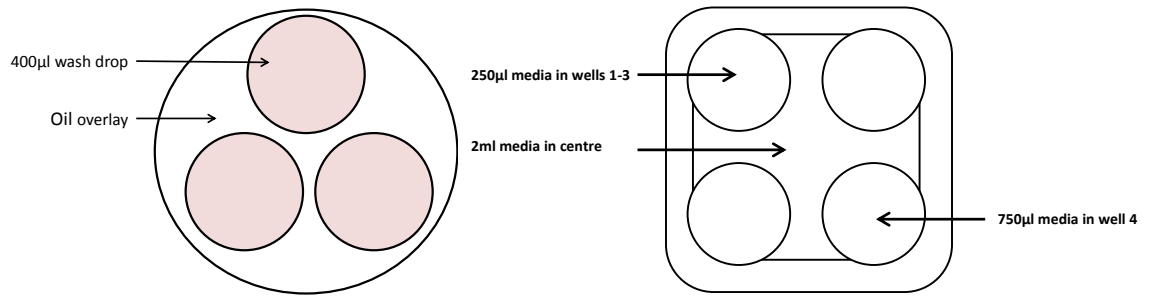


Figure 7: Diagram showing fertilisation wash and 4-well plate for IVF. 3x 400µl drops of Fertilisation media (Fert-TALP) were placed in a 60mm petri dish and overlaid with oil. 250µl Fert-TALP medium was added to wells 1-3, 750µl to the 4<sup>th</sup> well and 1ml Fert TALP to the central reservoir.

## 2.1.10 Preparation of Percoll® gradient

Motile spermatozoa were selected by centrifugation through a discontinuous Percoll® density gradient. Stocks of Percoll® Additives (PA) and Sperm Tyrode's Lactate (SPTL) were prepared as follows (Table 5). Both were sterile filtered and stored at -20°C. PA was aliquotted to 700µl and SPTL to 2ml. Percoll® was obtained from GE Healthcare, Uppsala, Sweden.

Percoll® Additives (PA)		Sperm Tyrode's Lactate (SPTL)	
Component	Amount	Component	Amount
ET Water	48.467ml	ET Water	50.15ml
NaCl	1.9479g	NaCl	0.292g
KCl	0.0958g	KCl	0.014g
NaH <sub>2</sub> PO <sub>4</sub> ·2H <sub>2</sub> O	0.0188g	NaH <sub>2</sub> PO <sub>4</sub> ·2H <sub>2</sub> O	0.003g
Hepes	0.4967g	Hepes	0.0754g
Hepes Sodium Salt	0.5425g	Hepes Sodium Salt	0.0814g
Sodium Lactate Syrup	1.533ml	Sodium Lactate Syrup	231 µL
NaHCO <sub>3</sub>	0.035g	CaCl <sub>2</sub> ·2H <sub>2</sub> O	0.0123g
CaCl <sub>2</sub> ·2H <sub>2</sub> O	0.0128g	MgCl <sub>2</sub> ·7H <sub>2</sub> O	0.0032g
MgCl <sub>2</sub> ·7H <sub>2</sub> O	0.0034g	Gentamycin	0.131ml
Gentamycin	2.083ml	Phenol Red	0.25ml
Phenol Red	4.17µl		
Final volume	50ml	Final volume	50.15ml

Table 5: Preparation of Percoll® Additives and SPTL solutions. Each was sterile filtered and stored at -20°C until required.

Percoll® was diluted to 90% using stock PA and 45% using stock SPTL as described below. The 4ml Percoll® gradient was then prepared by gently layering 2ml 45% Percoll® on top of 2ml 90% Percoll® as below and warmed to 39°C for at least 2 hours before use.

90% Percoll®	45% Percoll®
4.5ml Percoll®	2.0ml 90% Percoll®
600µl PA	2.0ml 1x SPTL

Table 6: Preparation of 90% and 45% Percoll®. Each was prepared fresh on the day of use.

### 2.1.11 Preparation of *in vitro* embryo culture media

Synthetic Oviduct Fluid embryo culture medium with BSA (SOF-BSA) and Hepes-SOF embryo wash medium were prepared as shown below (Figure 8) and frozen at -20°C for up to 3 months. Both media were defrosted on the day of use. Hepes-SOF was pre-warmed to 39°C for 2 hours in a warming incubator, while SOF-BSA drops were prepared as shown in Figure 8 and pre-equilibrated for 2 hours at 39°C and 5% CO<sub>2</sub> in air.

SOF-BSA 200ml			Hepes-SOF 250ml		
Component	Amount	Concentration (mM)	Component	Amount	Concentration (mM)
ET Water	To volume		ET Water	To volume	
NaCl	1.258g	108	NaCl	1.574g	108
KCl	0.106g	7.11	KCl	0.134g	7.2
KH <sub>2</sub> PO <sub>4</sub>	0.032g	1.18	KH <sub>2</sub> PO <sub>4</sub>	0.041g	1.2
NaHCO <sub>3</sub>	0.42g	25.00	NaHCO <sub>3</sub>	0.105	5.00
Glucose	0.054g	1.5	Glucose	0.06g	1.5
Pyruvate	0.007g	0.4	Pyruvate	0.009g	0.4
MgCl <sub>2</sub> .6H <sub>2</sub> O	0.020g	0.5	Hepes-free acid	0.6g	10
Glutamine	0.0058g	0.2	Hepes Na <sup>+</sup> salt	0.65g	10
Pen/Strep	1.199ml		CaCl <sub>2</sub> .2H <sub>2</sub> O	0.063g	1.7
CaCl <sub>2</sub> .2H <sub>2</sub> O	0.050g	1.7	MgCl <sub>2</sub> .6H <sub>2</sub> O	0.025g	0.5
			NEAA	2.5ml	
			EAA	5ml	
			Pen/Strep	1.5ml	
OSMOLARITY 280-290			OSMOLARITY 280-290		
BSA	1.598g	8% w/v	BSA	1g	4% w/v

Table 7: Preparation of SOF BSA embryo culture medium and Hepes-SOF embryo handling and wash medium. Medium was prepared in a sterile volumetric flask, sterile filtered and stored at -20°C for up to 3 months.

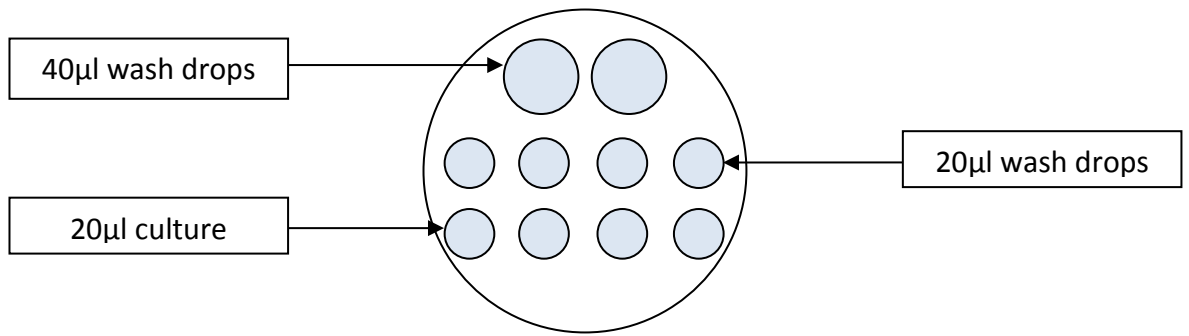


Figure 8: The layout of SOFaaBSA drops in a 40mm culture dish. These drops were covered with mineral oil to prevent evaporation and incubated under humidified 5% CO<sub>2</sub> in air at 39°C for 2 hours prior to addition of embryos for pre-equilibration.

## 2.1.12 Preparation of amino acid supplement

Amino acid stocks with defined concentrations were prepared as below (Table 8) and stored at  $-80^{\circ}\text{C}$  for up to 3 months. The stocks were diluted 50x in SOFaaBSA on the day of *in vitro* culture for final amino acid concentrations comparable to physiological levels (Tay et al. 1997).

50x concentrated amino acid supplement (200ml)			
Component	Amount (ml)	Final concentration (mM)	Final concentration in media ( $\mu\text{M}$ )
ET Water	200ml		
Arginine	0.4214	0.20	4.0
Cysteine	0.0315	0.02	0.4
Histidine	0.0838	0.04	0.8
Isoleucine	0.0262	0.02	0.4
Leucine	0.0787	0.06	1.2
Lysine	0.1096	0.06	1.2
Methionine	0.0298	0.02	0.4
Phenylalanine	0.033	0.02	0.4
Threonine	0.0596	0.05	1.0
Tryptophan	0.0408	0.02	0.4
Tyrosine	0.0725	0.04	0.8
Valine	0.0351	0.03	0.6
Alanine	0.098	0.11	2.2
Asparagine	0.0751	0.05	1.0
Aspartate	0.0399	0.03	0.6
Glutamate	0.1471	0.10	2.0
Glycine	0.03	0.04	0.8
Proline	0.023	0.02	0.4
Serine	0.042	0.04	0.8
Glutamine	0.2922	0.20	0.4
DABA	0.0516	0.05	1.0

Table 8: Preparation of 50x amino acid supplement stock. Solution was sterile filtered and aliquotted to 500 $\mu\text{l}$  microtubes and stored at  $-80^{\circ}\text{C}$  for up to 3 months.

### 2.1.13 Collection and *In Vitro Maturation* (IVM) of bovine oocytes.

Phosphate Buffered Saline (PBS) was prepared by adding 2x PBS tablets to 400ml ddH<sub>2</sub>O in 500ml Duran bottles and sterilised by autoclaving at 121°C for 2hr. Bovine ovaries were collected from a local abattoir (ABP Murton, York) and transported to the laboratory in an insulated canister with warm PBS. All further manipulations and culture of ovaries, oocytes, spermatozoa and embryos were performed at bovine physiological temperature of 39°C.

Upon arrival, ovaries were washed three times in fresh PBS at 39°C and stored in this solution on a heating plate. Follicular fluid containing oocytes was collected from antral follicles of <1cm diameter by aspiration with a pre-warmed 10 or 20ml syringe with 18 gauge needle containing a small amount of HEPES-buffered holding medium. Holding medium for OCC collection was supplemented with heparin to prevent agglutination of collected tissue. Once the fluid of approximately 10 ovaries was aspirated, the syringe was emptied to a 25ml universal tube and maintained upright at 39°C to allow the Oocyte-Cumulus Complexes (OCCs) to settle to the bottom.

The supernatant was removed using a sterile Pasteur pipette (Sarstedt) and the aspirate examined using an Olympus SZ11 stereomicroscope with Tokai Hit Thermo Plate heated stage (Olympus, Southend-on-Sea, UK) set to 39°C. Immature OCCs with a complete layer of cumulus cells were selected using a glass pipette in a 9cm petri dish with a marked grid. OCCs were washed twice in holding medium without heparin, then three times through 400µl pre-equilibrated BMM under mineral oil before transfer to 500µl BMM wells in groups of 50 in a 4-well plate (Nunc). OCCs were cultured for 24 hours at 39°C under 5% CO<sub>2</sub> in humidified air. BMM consisted of bicarbonate-buffered M-199 supplemented with 10% foetal bovine serum, 0.01IU FSH/LH (Ferring Pharmaceutical, Langley, UK), 0.40mg epidermal growth factor and 2.2ng fibroblast growth factor.

### 2.1.14 *In Vitro* Fertilisation (IVF)

Mature OCCs in BMM were collected in 40µl using a Gilson Pipetman and washed through three 400µl drops of pre-equilibrated Fert-TALP medium. This allows three 1 in 10 dilutions of the previous media for a total 1:1000 dilution, essentially removing the components of and waste products in the BMM. Cumulus expansion was used as a crude marker of OCC maturation and OCCs with poor cumulus expansion were not selected for IVF. OCCs were then transferred in groups of 50 to wells containing 250µl Fert TALP in a Nunc 4-well plate.

*In Vitro* Fertilisation (IVF) was carried out using frozen-thawed spermatozoa from a bull of proven fertility (Genus, Cheshire, UK). Cryopreserved spermatozoa were thawed for 10 seconds in a 50ml centrifuge tube (Sarstedt) containing tap water pre-heated to 40°C. The straw was dried and cut in sterile conditions before layering semen atop the 45% Percoll®. Sperm were centrifuged for 30 minutes at 760 x g in an accuSpin™ 400 centrifuge (Fisher Scientific, Loughborough, UK), the supernatant removed and the pellet resuspended in 4ml pre-warmed Hepes TALP. Percoll® is a viscous liquid through which only motile sperm can swim to form the pellet, while immotile sperm, sperm extender and protein debris from semen are removed in the supernatant. After centrifugation at 330 x g for a further 5 minutes, the supernatant was again removed and sperm resuspended in 200µl Fert-TALP. Sperm suspension was incubated at 39°C and 5% CO<sub>2</sub> in humidified air until required for fertilisation. Spermatozoa cell counts were performed using an Improved Neubauer Haemocytometer (Weber Scientific International, London, UK) and Leica LaborLux S microscope with 25x/0.5na objective, to calculate the correct volume of sperm suspension to co-incubate with mature OCCs at a concentration of 1x10<sup>6</sup>ml<sup>-1</sup>. Sperm and OCCs were co-incubated for 18-24hr at 39°C and 5% CO<sub>2</sub> in humidified air.

### 2.1.15 *In Vitro* Culture (IVC)

Embryo culture dishes were prepared using droplets of Synthetic Oviduct Fluid supplemented with 200µl 50x amino acids per 10ml (SOFaaBSA) under mineral oil as shown in Figure 8 and equilibrated at 39°C and 5% CO<sub>2</sub> in air for at least 2 hours. Hepes-buffered SOF was also warmed to 39°C for at least 2 hours before use. The putative zygotes were collected from IVF plates in a 2ml snap-cap centrifuge tube containing 500µl

of pre-warmed Hepes-SOF then denuded of remaining cumulus cells by vortexing for 2 minutes using a Vortex Genie 2 (Scientific Industries, New York, USA). The tube contents were poured into a 4cm culture dish and the tube washed twice with Hepes SOF. Putative zygotes were then selected in Hepes SOF using a stereomicroscope with heated stage and transferred to SOF culture medium in groups of 40 using a glass pipette. The zygotes were washed twice in SOFaaBSA before moving to 20 $\mu$ l culture drops in groups of 20. The culture dishes were then incubated in a Dry Seal desiccator containing approximately 150ml ddH<sub>2</sub>O with 150 $\mu$ l Antibiotic/Antimycotic (Ab/Am) solution. Air was purged from the desiccator and replaced with 5% CO<sub>2</sub>, 5% O<sub>2</sub>, 90% N<sub>2</sub> bubbled through a Dreschel bottle containing 100ml ddH<sub>2</sub>O + 100 $\mu$ l Ab/Am. Embryos were cultured for up to 8 days, with cleavage rate recorded on day 2 and blastocyst rate recorded on days 7 and 8.

## 2.2 Measurement of Oxygen Consumption Rate (OCR)

### 2.2.1 Measurement of OCR by the Becton-Dickinson Oxygen Biosensor System

#### 2.2.1.1 The Oxygen Biosensor System (OBS)

The Oxygen Biosensor System (OBS) is a 96-well plate with a proprietary fluorescent compound immobilised to the bottom of each well (BD Biosciences, Oxford, UK). The fluorophore is quenched in the presence of oxygen; therefore respiring cells reduce the dissolved oxygen concentration causing an increase in fluorescence intensity. An ambient oxygen blank (culture media without cells) and a 0% oxygen control (sodium dithionite) is used in each experiment. The fluorophore was excited at 485nm and read at 630nm in a Tecan Infinite (Tecan, Reading, UK) or BMG Labtech FLUOstar Omega fluorimetric plate reader with Atmospheric Control Unit (BMG Labtech, Buckinghamshire, UK). Fluorescence signal intensity can be converted to oxygen concentration in atm or  $\mu\text{mol/l}$  using the manufacturer guidance (Timmins and Haq 2006) and further converted to give Oxygen Consumption Rates (OCR) in  $\text{pmol/hr/embryo}$ .

100 $\mu\text{l}$  HEPES-buffered media was loaded to each well, with 2x media only wells adjacent to each well to be used as blank controls. 200 $\mu\text{l}$  sodium dithionite was loaded to a single well as a 0% oxygen control. The plate was sealed with HPLC film and incubated in the plate reader at 39°C for 1 hour. After this time, a single pre-blank reading was taken of each well with excitation at 485nm and emission at 630nm. The plate was then removed from the plate reader and transferred to a heated stage at 39°C for loading with samples. 10 $\mu\text{l}$  media was removed from each sample well and replaced with 10 $\mu\text{l}$  of HEPES media containing at least 10 embryos. 10 $\mu\text{l}$  of media in each blank well was also replaced with pre-warmed HEPES media. The plate was then re-sealed with HPLC film and incubated in the plate reader for 40 minutes with readings every 20 seconds to measure the change in oxygen over time.

#### 2.2.1.2 Analysis of data

Raw fluorescence data for each well at each time point was divided by the pre-blank value for the same well to calculate Normalised Relative Fluorescence (NRF). The NRF of

the sample wells was divided by the mean NRF of corresponding blank wells to calculate relative NRF (reNRF).

Dynamic Range (DR) was calculated by dividing the initial intensity of the sodium dithionite control by an average of the media well pre-blank. This value is expected to be around 6. DR is then used to calculate the Stern-Volmer constant ( $K_{SV}$ ), which is required to convert fluorescence data into oxygen concentrations. The ambient concentration of oxygen in media  $[O_2]_a$  was defined as  $209\mu\text{mol/l}$ .

$$K_{SV} = (DR - 1) / [O_2]_a$$

Finally,  $K_{SV}$  can be used to calculate the oxygen concentration ( $\mu\text{mol/l}$ ) at each time point for the sample wells:

$$[O_2] = (DR / \text{reNRF} - 1) / K_{SV}$$

$[O_2]$  was converted from  $\mu\text{mol/l}$  to  $\text{pmol/embryo}$  by multiplying by a factor of 100 and dividing by the number of embryos present. Oxygen concentration is then plotted against time. The gradient of this curve is the oxygen consumption rate (OCR) in  $\text{pmol/embryo/hr}$ .

This system was previously used to measure oxygen consumption by bovine oocytes, however this is the first time it has been employed to assess bovine blastocyst oxygen metabolism following inhibition of metabolic processes.

## 2.2.2 Measurement of OCR by nanorespirometry

### 2.2.2.1 The nanorespirometer

The method for nanorespirometry was adapted from Unisense (Unisense A/S, Aarhus, Denmark) guidance and the previous work of Ana Lopes (Lopes et al. 2005). The system uses a miniaturised electrode mounted on a motorised micromanipulator and connected to an oxygen sensor capable of  $0.1\mu\text{mol/l}$  resolution. The incubation beaker containing HEPES-buffered media is maintained at  $39^\circ\text{C}$  by a thermostatically controlled water bath and held in place by a standard laboratory clamp stand and boss. A two-point calibration was performed as follows. The 0%  $O_2$  control was set using 10ml of 100mM Sodium dithionite, generating a signal in the region of 0-2mV. The ambient control (21%  $O_2$ ) was

Hepes SOF (without BSA supplement in order to prevent foaming), which was maintained at 39°C and bubbled with air for 30 minutes to maximise dissolved oxygen.

#### 2.2.2.2 Loading and measurement of embryos

Embryos were loaded to a Drummond PCR micropipette (Alphalabs, Hampshire, UK) in 1µl of Hepes-buffered media and equilibrated for approximately 1hr in a 15ml falcon tube containing the same media. The embryo sinks to the bottom and consumes oxygen, building up a steady-state gradient of decreasing oxygen concentration with increasing depth. Tubes were sealed at the bottom with vacuum grease to prevent diffusion of oxygen from below the loaded embryo. For measurement, the micropipettes are mounted to a specifically designed rack in groups of four. This rack is held stably in an incubation beaker filled with Hepes-SOF to the level of the micropipette surface and maintained at 39°C with coiled tubing running from a Grant water bath. Alignment of the probe tip with the centre of each micropipette opening was performed using a horizontal dissecting microscope. Control of the oxygen sensor probe by the motorised micromanipulator during measurement was carried out using the SensorTrace Pro program (Unisense).

Readings were taken at 200µm intervals from -200µm to 4000µm, where 0µm is defined as the surface of the micropipette tube. The oxygen profile was visualised in real-time for an instant overview of the oxygen consumption by the embryo. However, the OCR gradient was calculated from the 3000 to 4000µm section of the profile to ensure comparability between more and less active embryos and avoid the loss of data due to evaporation at the top of the tube.

The probe is sensitive to temperature fluctuation (2-3% change in signal per 1°C) and so the temperature of the incubation beaker was monitored at all times using a thermometer (Lopes et al. 2005). However, evaporation of water at the surface of the media was unavoidable and may cause a slight decrease in temperature. Media volume was maintained by adding embryo tested water pre-heated to 39°C when required.

#### 2.2.2.3 Inhibitor treatment

To assess the contribution of different components of oxidative phosphorylation to the overall embryonic Oxygen Consumption Rate (OCR), embryos were loaded to

micropipettes as described above, except embryos were initially loaded in Hepes SOF + solvent control. This reduces potential deleterious effects of prolonged experiments and multiple manipulations with the same embryo and is acceptable as the basal OCR in Hepes SOF has been established in other experiments (0, 4.4.1) and the inhibitor effects must be calculated in reference to the solvent control OCR rather than basal OCR. In addition, the solvent control did not have a significant effect on OCR in other experiments (section 3.4.4-3.4.8). Following basal OCR measurement the embryo was removed from the micropipette to a pre-warmed solution of the inhibitor at the desired concentration in Hepes SOF using a stereomicroscope with heated stage. The embryo was then moved to a second pre-warmed dish containing the same inhibitor solution and loaded to a micropipette once more. Pre-equilibration and oxygen profiling were then carried out as before (section 2.2.2.2).

#### 2.2.2.4 Calculation of Oxygen Consumption Rate (OCR)

The oxygen consumption rate is essentially the slope of the steady-state gradient recorded by the probe. This was calculated using an MS Excel program developed by Unisense which adapts Fick's First Law of Diffusion:

$$J = -D(dc/dx)$$

Where J= diffusion flux (amount of oxygen that will flow through a small area during a short time interval in mol/m<sup>2</sup>/s) The solubility of oxygen in the media is 200µmol/l and diffusion coefficient (D) at 38.5°C is 3.37x10<sup>-5</sup> cm<sup>2</sup> s<sup>-1</sup>: (Garcia and Gordon 1992). The slope of the gradient (change in concentration over time) is denoted by dc/dx.

## 2.3 Energy substrate assays

Lactate production, glucose and pyruvate consumption by individual pre-implantation bovine embryos of 2-cell to blastocyst stage were assayed by the rapid, non-invasive fluorimetric technique developed by Guerif et al. (2013). Briefly, embryos were selected for analysis at 2-4-cell and blastocyst stages (days 2, 5, 6 or 7 of culture, respectively). Selected embryos were washed in and moved to a modified SOFaaBSA "analysis" medium containing 0.5mM glucose and 0mM lactate. This media was prepared as described in Table 9. Embryos were incubated individually in 4µl droplets for 18-24hr under mineral oil

at 39°C in a humidified atmosphere of 5% CO<sub>2</sub>, 5% O<sub>2</sub>, and 90% N<sub>2</sub>. Identical control droplets were incubated adjacent to embryo-containing droplets to account for non-specific degradation/appearance of compounds of interest.

SOF analysis (100ml)		
Component	Amount	Concentration (mM)
ET Water	To volume	
NaCl	0.629g	108
KCl	0.053g	7.11
KH <sub>2</sub> PO <sub>4</sub>	0.016	1.18
NaHCO <sub>3</sub>	0.21g	25.0
Glucose	0.009g	0.5
Pyruvate	0.0035g	0.4
CaCl <sub>2</sub> .2H <sub>2</sub> O	0.025g	1.7
MgCl <sub>2</sub> .6H <sub>2</sub> O	0.010g	0.5
Glutamine GLN	0.0029g	0.2
Pen/Strep	0.5995ml	1000 IU/ml
Amino acids 50x	2ml	1x
<b>OSMOLARITY</b>	<b>280-290</b>	
BSA	0.799g	8% w/v

Table 9: Preparation of modified SOF analysis medium for glucose, lactate and pyruvate assays. Medium was prepared in a sterile volumetric flask, sterile filtered and stored at -20°C for up to 3 months.

Following 24hr individual culture, the morphological status of each embryo was recorded and compared to the stage recorded prior to individual culture. Development was defined as early cleavage stage embryos increasing in cell count or morula and blastocyst progression to a higher stage. Dead or arrested embryos were excluded from further analysis. Embryos were removed and spent media samples were frozen under oil at -80°C until analysis.

Assay mixture was first loaded to each well of interest in a 96-well V-bottomed plate. Background fluorescence due to NAD<sup>+</sup> or NADP was measured using a BMG FLUOstar

plate reader with excitation/emission of 340/460nm. Sample medium was added to the assay mixture in the ratio 1:10 and incubated in the dark at 37°C for a period of time specific to the substrate of interest. Fluorescence intensity was measured once more and corrected for the background values. Intensity values for each sample were calibrated against a six-point standard curve to calculate concentration of substrate and change in concentration of substrate was calculated by comparison to control drops of medium. Consumption or production of substrate was expressed in pmol/embryo/hr  $\pm$  s.e.m.

### 2.3.1 Pyruvate

Pyruvate reaction cocktail containing 0.1mM NADH and 40IU/ml lactate dehydrogenase in 4.6mM EPPS buffer, pH 8.0 and supplemented with 50µg/ml Penicillin and 50µg/ml Streptomycin was prepared prior to use and stored at -20°C for 3 months. 10 µl of assay mixture was added per well using positive displacement and fluorescence measured to yield a pre-blank background measurement. Sample medium, control medium or standard solution (1µl) was added to each well and incubated at 37°C for 3 minutes before endpoint readings. A reduction in fluorescence due to NADH oxidation was monitored. Final concentrations in each spent culture droplet were determined against a six point standard curve from 0-0.45mM pyruvate and consumption was calculated relative to the mean pyruvate concentration of the control drops. Pyruvate standard 0.45mM obtained from Analox, London, UK. Standard curves with  $R^2 < 0.99$  were rejected.

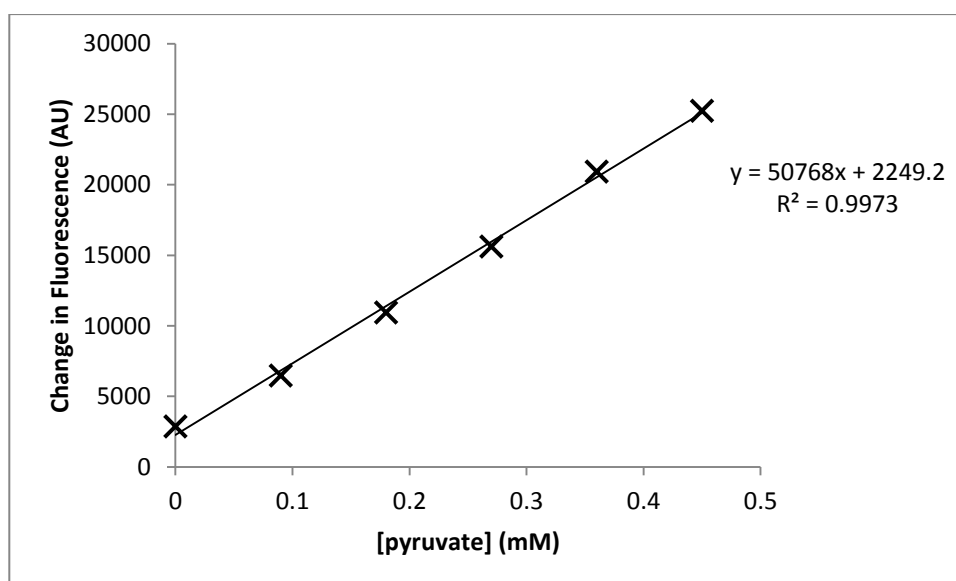
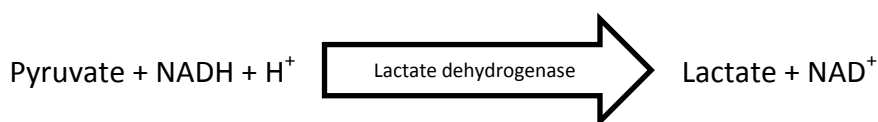


Figure 9: An example standard curve for the pyruvate assay.

### 2.3.2 Glucose

Glucose reaction cocktail containing 0.4mM dithiothreitol, 3.07mM MgSO<sub>4</sub>, 0.42mM ATP, and 1.25mM NADP<sup>+</sup>, 20 IU/ml hexokinase/glucose-6-phosphate dehydrogenase (HK/G6PD) in EPPS buffer at pH 8.0 was made prior to use and stored at -20°C for 3 months. 10 µl of assay mixture was added per well using positive displacement and fluorescence measured to yield a pre-blank background measurement. Sample medium (1µl) was added and incubated at 25°C for 10 minutes. Changes in fluorescence due to NADP<sup>+</sup> reduction were monitored. Final concentrations in each spent culture droplet were determined against a six point standard curve from 0-0.5 mM glucose. Standard curves with R<sup>2</sup> <0.99 were rejected.

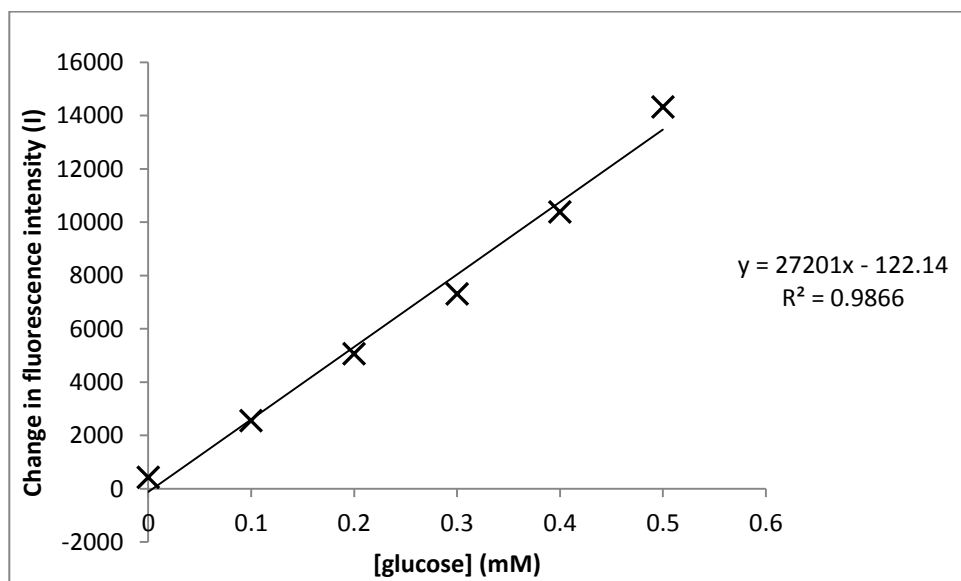
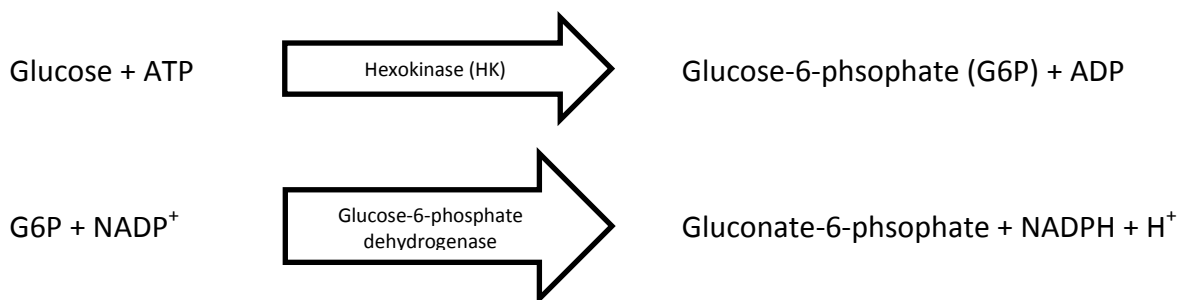


Figure 10: An example standard curve for the glucose assay.

### 2.3.3 Lactate

Assay mixture containing 40IU/ml lactate dehydrogenase (LDH) in a glycine-hydrazine buffer, pH 9.4 was prepared prior to use and stored at  $-20^{\circ}\text{C}$  for up to 3 months.  $10\mu\text{l}$  of assay mixture was added per well using positive displacement and fluorescence measured to yield a pre-blank background measurement. Sample medium ( $1\mu\text{l}$ ) was added to  $10\mu\text{l}$  of assay mixture and incubated at  $25^{\circ}\text{C}$  for 30 minutes. Changes in fluorescence due to  $\text{NAD}^{+}$  reduction were monitored. Final concentrations in each spent culture droplet were determined against a six point standard curve from 0-1.0mM lactate. Standard curves with  $R^2 < 0.99$  were rejected.

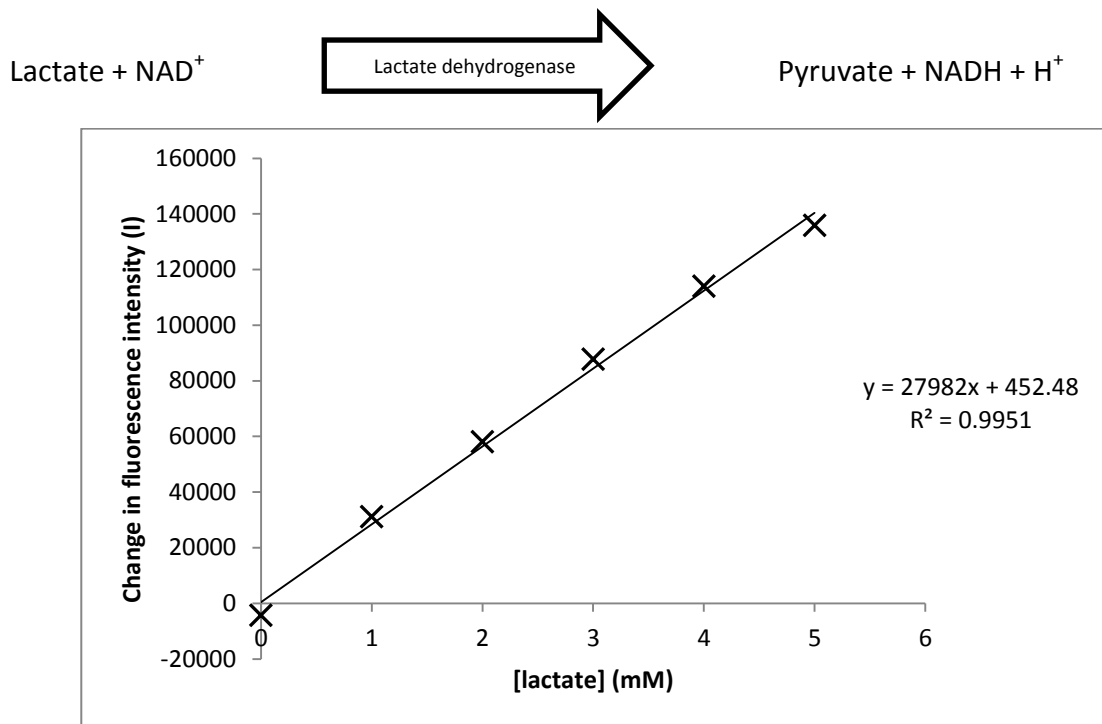


Figure 11: An example standard curve for the lactate assay.

## 2.4 L-carnitine assay

This assay was performed according to manufacturer instructions (Abcam, Cambridge). Briefly, the supplied 100mM standard was diluted to 1mM with ddH<sub>2</sub>O. A standard curve and reaction mixture were prepared as follows:

Standard	[L-carnitine] (mol/ $\mu$ l)	Reaction mix component	Volume per well ( $\mu$ l)
0	0	Assay buffer	4
1	0.04	Carnitine converting enzyme	0.2
2	0.08	Carnitine development mix	0.2
3	0.12	Substrate mix	0.4
4	0.16	Carnitine probe	0.2
5	0.2		

Table 10: Composition of the reaction mixture and standard solutions for the L-carnitine assay.

5 $\mu$ l reaction mix was loaded to each well and a blank reading taken at 535/587nm. A positive control well containing standard 5 and reaction mix was used to set the gain to its optimal level. 5 $\mu$ l standard or sample was added to each well and the plate incubated at room temperature inside the plate reader. The end point reading was measured at 535/587nm and a standard curve plotted.

## 2.5 Time-lapse imaging of embryo development using the Primo Vision system

Real-time monitoring of embryo development throughout the culture period was performed using the Primo Vision system (Vitrolife, Goteborg, Sweden) and 9-well dishes (Cryo Management Ltd, Hungary). Each individual well of the 9-well dish was filled with SOFaaBSA using a pulled glass pipette and then the main well filled with 40µl of the same media. This was overlaid with oil and incubated at 39°C in 5% CO<sub>2</sub>/5% O<sub>2</sub> for 2hr prior to loading embryos. 2-cell embryos were selected on day 1 of culture for transfer to the 9-well dish. Images were recorded every 10 minutes for 7 days of culture. Data was analysed using the Primo Vision analyser software.

## 2.6 Cell allocation ratios

Blastocyst cell counts and allocation ratio were taken using the method of Thouas et al. (2001). Blastocysts were incubated in Hepes SOF with 1% Triton X-100 (Sigma-Aldrich, Dorset, UK) and 100µg/ml propidium iodide (Sigma-Aldrich, Dorset, UK) for 30s. The Triton X-100 detergent permeabilises the zona pellucida, allowing propidium iodide to enter and stain trophoctoderm nuclei, but the blastocysts are moved before the dye reaches the inner cell mass. Blastocysts were moved to a fixative solution of 25µg/ml Hoescht 3342 in 100% ethanol overnight at 4°C. This dehydrates the blastocysts and allows the dye to stain all cells. Stained and fixed blastocysts were removed to a 1µl drop of glycerol on a sterile glass slide and fully flattened with a coverslip before labelling the embryo location. Images were taken on an Olympus IX51 inverted fluorescent microscope with 20x/0.5na UPlanF1 objective, ultraviolet lamp and excitation filters. Total cell number was recorded at 460nm and trophoctoderm only at 560nm. The TE:ICM ratio was then calculated for each blastocyst measured.

### 3 Bovine embryo bioenergetics

## 3.1 Introduction

### 3.1.1 Metabolic profiling of pre-implantation embryos

The topic of embryo metabolism is of great interest as it may yield biomarkers that can be used to select viable embryos for transfer in clinical and commercial Assisted Reproduction Technologies (ARTs). In addition is the importance of understanding the fundamental relationship between embryo metabolism and development. Ideally, studies on embryo metabolism should be non-invasive so that it is possible to relate metabolic activity to subsequent development. In addition, such assays should not perturb the embryo, affect its viability, or introduce any compounds, toxic or non-toxic, which may interfere with any aspect of development. Non-invasive methods should permit the assessment of an individual embryo and include the measurement of the consumption or production of various substrates in the culture medium, including glucose, pyruvate, lactate (Thompson et al. 1996; Sturmey and Leese 2003) and amino acids (Gopichandran and Leese 2003; Humpherson et al. 2005; Sturmey et al. 2010) whilst allowing assessment of ongoing development. As the embryonic genome activates at the 8-16 cell stage in the bovine (King et al. 1988; Telford et al. 1990; Wrenzycki and Niemann 2003), assessments of metabolism at earlier stages are assumed to relate more directly to oocyte quality and maternal legacy effects rather than the physiology of the developing embryo (Donnay et al. 2002); after this stage metabolism is increasingly thought of as a marker of embryo viability.

The general pattern of embryo energy metabolism throughout development based on our current level of knowledge is summarised in figures 1 and 2, in Chapter 1. Briefly, overall metabolic activity remains at a relatively low rate during the cleavage stages, from the zygote to morula, but increases sharply at the blastocyst stage largely to meet the increased demands for metabolic energy. During blastocyst formation, 30-40% of total Adenosine Triphosphate (ATP) is consumed by the enzyme  $\text{Na}^+/\text{K}^+$  ATPase, which is critical in forming the blastocoel cavity. This accounts for 10-44% of oxygen consumption (Leese et al. 2008).

### 3.1.2 Oxygen consumption

Consumption of oxygen has been proposed as an indicator for embryo viability (Houghton et al. 1996; Trimarchi et al. 2000b; Shiku et al. 2001; Lopes et al. 2005; Lopes et al. 2010). The major fate of consumed oxygen is as the final electron acceptor in the electron transport chain of respiration, releasing energy for ATP production by oxidative phosphorylation (Thompson et al. 1996). Mammalian mitochondria produce approximately 4.8 moles of ATP via oxidative phosphorylation for every mole of diatomic oxygen (O<sub>2</sub>) consumed. This equates to a maximal ADP phosphorylation to oxygen reduction ratio (P/O<sub>max</sub>) of 2.4 (Brand et al. 2005). Using this value, it is possible to estimate the total ATP produced by oxidative phosphorylation on the basis of OCR (Brand et al. 2005; Birket et al. 2011; Trimarchi et al. 2000).

Oxygen consumption by embryos can be affected by a variety of factors, including media composition, solute concentration and whether the embryo is produced *in vitro* or *in vivo* (Lopes et al. 2007). The concentration of glucose in culture media has a particularly pronounced effect. For example, Synthetic Oviduct Fluid (SOF), based on the biochemical composition of sheep oviduct fluid (Restall and Wales 1966), contains 1.5mM glucose (Tervit et al. 1972). Increasing the glucose concentration to 5.5mM reportedly leads to a reduction in OCR and increased lactate production from glycolysis (Donnay et al. 2002). High glucose also leads to chromatin degradation and apoptosis in murine embryos (Leunda-Casi et al. 2002). In addition the mechanism of fertilisation might alter embryo metabolic activity, For example, Tejera et al. (2012) reported that the OCR of human embryos decreases following ICSI, from 19.2pmol/embryo/hr at zygote stage to 16.52pmol/embryo/hr after 52 hours post-ICSI (approx. 8 cell stage). However, embryos of higher quality, which were transferred to prospective mothers, had higher OCR than poor quality embryos (19.15 compared to 18.1pmol/embryo/hr). In the same study, it was reported that the OCR of transferred embryos which successfully implanted continued to rise 52 hrs post-ICSI, while OCR of non-implanting embryos continued to fall (Tejera et al. 2012). These data suggest that OCR may relate to viability. As yet, however the metabolic legacy of ART is relatively unexplored and could involve subtle changes with relevance to health, disease and longevity.

### 3.1.3 Embryo mitochondria

The mitochondria of the mammalian oocyte and cleavage stage embryo have a distinctive morphology, appearing spherical with a diameter of less than 1 $\mu$ m, and fewer, shorter cristae than the classical elongated form seen in most differentiated cell types (Van Blerkom 2011). Despite this morphology, the mitochondria remain active and supply the oocyte and early embryo with ATP by oxidative phosphorylation. Maternal mitochondria increase in number from a tiny complement (<10) in the primordial oocyte until maturation is complete, at which point they may number in the hundreds of thousands (Van Blerkom 2004). All embryo mitochondria, including all their mtDNA, are maternally inherited; mitochondria from the spermatozoon are destroyed by ubiquitin-mediated proteolysis following fertilisation (Sutovsky et al. 1999; Cummins 2000). Interestingly, this process seems to have evolved autonomously many times, most likely to avoid inheritance of oxidative damage-prone spermatozoan DNA (Cummins 1998). In general, oxidative damage to mtDNA is particularly common as around 2% of electrons 'leak' from the electron transport chain to form reactive oxygen species (ROS) and defence or repair mechanisms do not exist in the mitochondria to prevent DNA damage (Cummins 2002). As the spermatozoa undergo significant shifts in oxygen concentration from low levels in the testis, to ambient levels in the vagina and again to low concentrations in the oviduct, spermatozoan mtDNA tends to accumulate mutations and a significant number of mtDNA deletions are found in the majority of normospermic men (Max 1992; Cummins 1998). In mammals, inheritance of paternal mtDNA is rare, linked to mitochondrial disease and seems to occur only in dysfunctional oocytes (St John et al. 2000).

Embryo mitochondria gradually elongate and develop more extensive cristae as cleavage progresses, beginning at around the 16-cell stage and finally attaining a more classical morphology during blastocyst formation and expansion in the cow (Plante and King 1994) and human (Sathananthan and Trounson 2000). This change in morphology coincides with the increased energy demand associated with blastocoel cavity formation (Figure 3). Occasionally, 'giant' mitochondria with a diameter up to 2 $\mu$ m or unusual 'dumbbell' shaped forms are seen in mature oocytes, but fusion and fission are rare (Sathananthan and Trounson 2000; Van Blerkom 2011). The total complement of mitochondria, therefore, appears fixed from the MII oocyte stage until components required for mitochondrial replication are expressed post-implantation (Larsson et al. 1998; Ekstrand

et al. 2004). Measurement of mitochondrial DNA (mtDNA) is often used as a proxy for mitochondrial number, however mtDNA is not limited to one copy per organelle; rather there seems to be little consistency in the number of copies of mtDNA per mitochondria (Van Blerkom 2011), although it is thought that the mitochondria of the mature human oocyte contain only one mtDNA genome copy (Cummins 2002). In addition, there is little correlation between mtDNA copy number and the number of mitochondria or mitochondrial function. For example, expression of human mitochondrial transcription factor A in mouse embryos significantly increases mtDNA copy number, but with no detectable effect on mitochondrial number, measured by mitochondrial mass or maximal respiratory capacity (Ekstrand et al. 2004). However, in the human, as well as the mouse, lower mtDNA copy number correlates with reduced viability, suggesting some benefit to increased copy number (Stojkovic et al. 2001; Santos et al. 2006; Ge et al. 2012).

### 3.1.4 Oxidative phosphorylation

Oxidative phosphorylation in eukaryotic cells involves the coupling of the transfer of electrons that arise from substrate oxidation to the phosphorylation of Adenosine Diphosphate (ADP) to ATP (Figure 12 and Figure 13). The major sources of electrons in the Electron Transport Chain (ETC) are the reducing equivalents NADH, FADH<sub>2</sub> and succinate, which are produced by the TCA cycle (Figure 4). Electrons from these reducing equivalents flow along four respiratory protein complexes – NADH dehydrogenase, succinate dehydrogenase, cytochrome bc<sub>1</sub> complex and cytochrome c oxidase, which are bound to the inner mitochondrial membrane and associate tightly, forming a superstructure termed the respirosome (Dudkina et al. 2010; Dudkina et al. 2011; Winge 2012). The flow of electrons across these proteins enables the establishment of a proton (H<sup>+</sup>) gradient that generates a proton-motive force (PMF) across the mitochondrial inner membrane. The protons flow down the proton gradient through ATP Synthase and the energy released enables ATP synthesis (Berg et al. 2002).

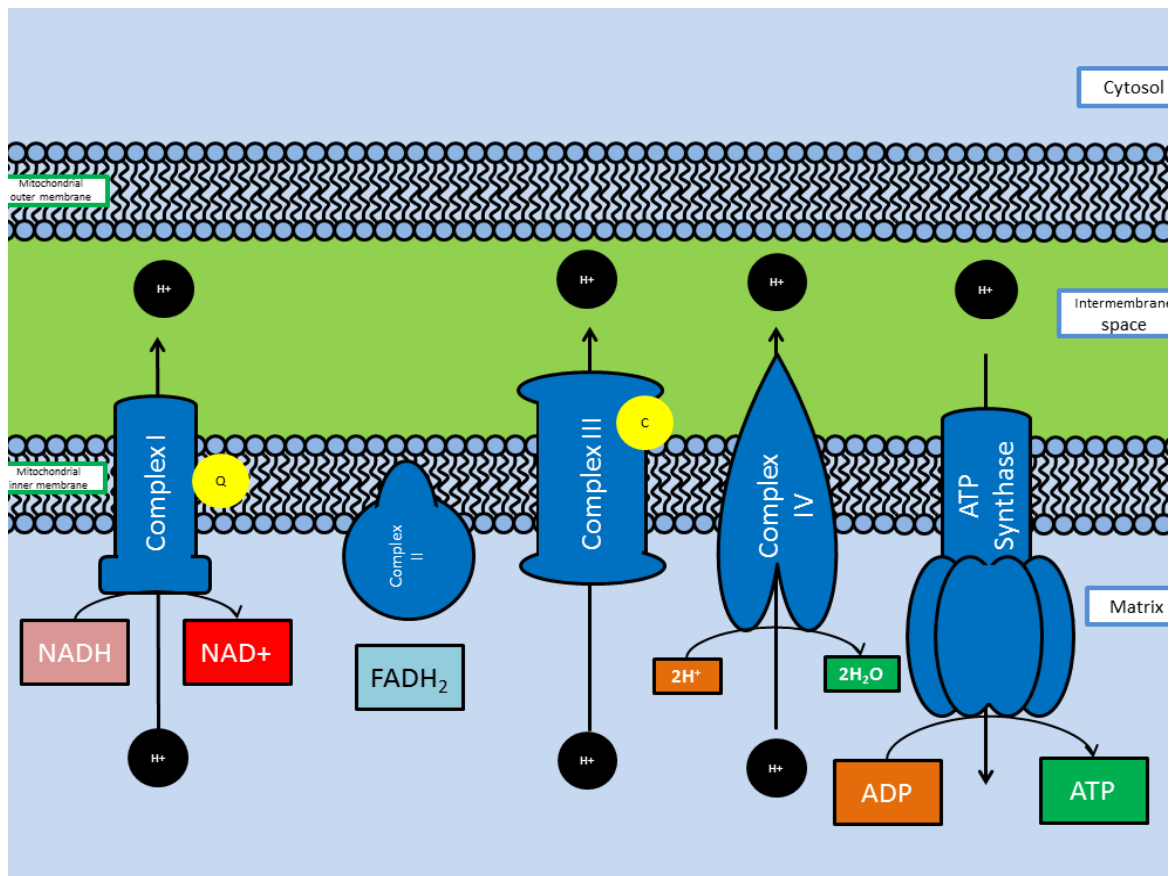


Figure 12: Overview of oxidative phosphorylation. The electron transport chain, or respirasome, consists of ATP synthase and 4 enzyme complexes; Complex I: NADH-Q Oxidoreductase, Complex II: Succinate-Q Reductase, Complex III: Q-Cytochrome c Oxidoreductase, Complex IV: Cytochrome c Oxidase. Electrons are carried to the respirasome by NADH and  $\text{FADH}_2$  generated by the TCA cycle. NADH binds to Complex I, which transfers electrons to Coenzyme Q (ubiquinone) for transport to Complex III. At Complex II, Coenzyme Q also accepts electrons from  $\text{FADH}_2$ . Reduced Coenzyme Q transfers electrons to complex III, which uses donated electrons to reduce a second co-factor, Cytochrome c. Cytochrome c translocates to Complex IV, where the final electron acceptor, oxygen, is reduced. Electron transfer at Complex I, III and IV is coupled to active transport of protons across the inner mitochondrial membrane, maintaining a proton gradient or proton-motive force from within the intermembrane space to the matrix. Protons flow spontaneously through the proton channel of ATP synthase, providing the energy required for the formation of ATP from ADP and  $\text{P}_i$  and subsequent release of ATP.

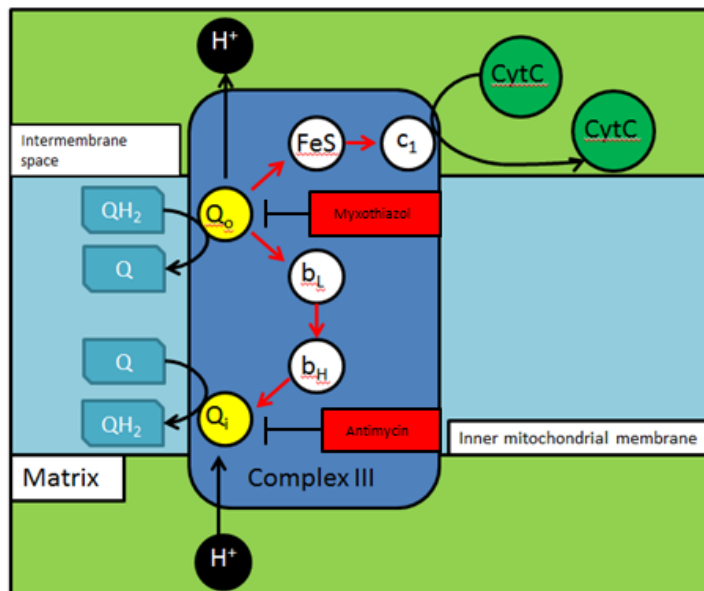


Figure 13: Diagram of the Q cycle. Ubiquinol ( $\text{QH}_2$ ) binds at the ubiquinol oxidation site ( $\text{Q}_o$ ) to transfer one electron to a bound Rieske iron-sulphur protein (FeS), which then reduces cytochrome c (CytC). The two protons of  $\text{QH}_2$  are released to the intermembrane space.  $\text{QH}_2$  also transfers a second electron to a series of haem groups; cytochromes  $\text{b}_L$  and  $\text{b}_H$ . A second quinone (Q) binds at the ubiquinone reduction site ( $\text{Q}_i$ ) and is reduced, removing 2 protons from the matrix and contributing to the maintenance of the proton gradient. Myxothiazol competitively binds the  $\text{Q}_o$  site, blocking electron transfer to cytochrome c and hence any further electron transport. Antimycin binds at the  $\text{Q}_i$  site, inhibiting electron transfer and hence proton flow.

### 3.1.5 Classification of respiration

While the majority of oxygen consumption in most cell types is driven by mitochondrial oxidative phosphorylation, other cellular processes also consume oxygen. These include oxygen-consuming enzymes, as well as the production of reactive oxygen species (ROS) either as a spontaneous by-product of normal metabolism or in some cases as signalling molecules. Oxygen-consuming enzymes include xanthine oxidase, NADPH oxidase and squalene monooxygenase, which may be inhibited specifically to deduce their individual contribution to overall OCR. Total non-mitochondrial oxygen consumption can be assessed by treating cells with an inhibitor of respiratory complex III (or cytochrome bc1 complex), since all electrons flowing through the electron transport chain must pass through complex III, transfer to cytochrome c via the Q cycle and transport to complex IV.

Myxothiazol is a competitive inhibitor of ubiquinol, binding at the ubiquinone reduction site ( $Q_o$ ) of the complex and prevents electron transfer from quinol to the Rieske iron-sulphur protein (Figure 13). A further inhibitor is antimycin A, which binds the  $Q_i$  site, preventing transfer of electrons from the haem group to oxidised quinone (Figure 13).

Oxygen consumed by each of the respiratory components can be quantified by using inhibitors specific to each process. Theoretically, approximately 30 moles of ATP can be produced for every mole of glucose (Berg et al. 2001). The majority (87%) of this total ATP comes from oxidative phosphorylation, with the remainder coming from substrate-level phosphorylation in the TCA cycle and glycolysis. Other pathways, including creatine dephosphorylation by creatine kinase in the mouse embryo (Forsey et al. 2013), do generate ATP, but their overall contribution is small. However, there are many physiological factors which reduce the yield of ATP per unit glucose. For example, the proportion of oxygen consumption which is ATP-producing; i.e. coupled to ATP synthesis by ATP Synthase - is typically 60-80% (Birket et al. 2011); the remaining 20-40% is lost from potential ATP Synthase and is described as uncoupled from ATP synthesis. One cause of uncoupling is the passive leak of protons across the inner mitochondrial membrane without flow through the proton channel of ATP Synthase, leading to partial uncoupling of electron transport from ATP Synthase. To investigate this *in vitro*, a range of respiratory inhibitors can be used. Oligomycin binds to the proton channel, effectively abolishing aerobic respiration, although some oxygen may still be consumed by non-ATP-productive processes. This is uncoupled oxygen consumption, as it is independent of ATP Synthase activity. The difference between measured basal OCR and the OCR following oligomycin treatment is considered to be the coupled OCR (Brand and Nicholls 2011):

$$\text{Total Basal OCR} - \text{Oligomycin-sensitive OCR} = \text{Coupled OCR}$$

Coupled OCR rates in somatic cells range from 60-80%, although some carcinoma cell lines are only 30% (Affourtit and Brand 2009; Birket et al. 2011; Divakaruni and Brand 2011).

### 3.1.6 Uncoupled respiration

The majority of uncoupled OCR is considered to be proton leak, although it does have at least one defined purpose, in whole body homeostasis and roles specific to some cell

types. Thus, in adipocytes uncoupled respiration is used to generate heat (Rousset et al. 2004) and regulate non-ATP dependent carbon flux between anaerobic glycolysis and oxidative phosphorylation (Si et al. 2009), while uncoupling protein expression by pancreatic  $\beta$ -cells modulates their insulin secretion and (Chan et al. 2001). Uncoupling even has a role in photosynthesis; UCP1 expression is required to maintain mitochondrial redox state in *Arabidopsis*, while knockout of UCP1 reduces the overall rate of photosynthesis (Sweetlove et al. 2006). Furthermore, the 'uncoupling to survive' hypothesis of Martin Brand suggests that uncoupling regulates the proton gradient ( $\Delta P$ ), limiting mitochondrial superoxide production to prevent extensive oxidative damage and resulting conditions (Brand 2000). The majority of cellular reactive oxygen species (ROS) are generated by mitochondria (Boveris and Chance 1973). However, in isolated mitochondria, increasing respiration rate with ADP or an uncoupler such as DNP decreases the amount of ROS produced (Boveris and Chance 1973; Boveris et al. 1976). Uncoupling electron transport from ATP synthesis reduces the protonmotive force, which has been proposed to alter the redox state of the mitochondrial ubiquinone (Q) pool, reducing the concentration of QH $\cdot$  (Brand 2000). The net effect of this is to reduce formation of ROS. However, a similar observation has not been reported in whole cell experiments and the physiological relevance of isolated mitochondria manipulations under artificial conditions is doubtful. Further evidence of this idea comes from a finding that polymorphisms in uncoupling protein genes are associated with human longevity (Rose et al. 2011). It therefore appears that while uncoupling of respiration may reduce ATP production, it also has a beneficial regulatory role.

### 3.1.7 Oxygen profiling methods in oocytes and embryos

The analysis of oxygen consumption in rabbit oocytes and mouse embryos was first reported by Fridhandler et al. (1956; 1957). The authors used a Cartesian diver technique and noted that oxygen consumption by rabbit oocytes increased during development and subsequent embryo development to the blastocyst stage, but did not vary in response to serum. In addition, supplementation of the culture medium with pyruvate, glucose or TCA cycle substrates fumarate or malonate did not cause a detectable change in OCR. However, embryos were sensitive to cyanide treatment, reducing OCR of early cleavage stage embryos by 95%, and that of blastocysts to an undetectable level (Fridhandler et al. 1957). The technique was further refined by Mills and Brinster (1967) to validate the non-

invasive measure of oxygen consumption in the mouse, as 8-cell embryos continued to develop on return to culture. This was a complex and labour-intensive method, requiring large groups of embryos or oocytes to detect changes in oxygen concentration.

Spectrophotometric methods were used in mouse blastocysts (Nilsson et al. 1982) and single human oocytes and blastocysts (Magnusson et al. 1986). This technique was based on the amount of oxyhaemoglobin converted to haemoglobin due to oxygen consumption and as such was indirect and lacked sensitivity.

Methods to improve sensitivity were developed; the first method to measure oxygen consumption of single embryos with oxygen electrodes was developed by Overstrom et al. (1992). This method found that respiration rates of individual embryos correlated with survival following embryo transfer. However, the method was time-intensive and lacked sensitivity, so was not widely used.

Oxygen consumption by small groups of murine, bovine and porcine embryos was measured using pyrene as a fluorescent marker of oxygen depletion, described by (Houghton et al. 1996; Thompson et al. 1996; Sturmey and Leese 2003). Pyrene is a non-toxic, hydrophobic compound whose fluorescence is quenched in the presence of oxygen. The change in fluorescence is proportional to the change in oxygen concentration and can be measured using a quantitative fluorescence microscope. This method is non-invasive and embryos can be returned to culture and grown to the blastocyst stage. However, embryos must be assayed in groups and the technique is very time-demanding, requiring manual measurements every 15 minutes for up to 6 hours. Using this technique, murine embryo OCR was relatively constant at 6.7pmol/embryo/hr throughout cleavage stages, significantly increasing to 18.3pmol/embryo/hr at the blastocyst stage (Houghton et al. 1996). A similar pattern was seen in the bovine, increasing from 10.7-12.1pmol/embryo/hr during cleavage stages, to 17.4pmol/embryo/hr during morula compaction and to 40.2pmol/embryo/hr in the expanded blastocyst (Thompson et al. 1996). In the porcine, a significant increase in oxygen consumption again occurred at the blastocyst stage, from around 20pmol/embryo/hr to 50pmol/embryo/hr with considerable biological variation for each stage measured throughout *in vitro* development of oocytes and embryos (Sturmey and Leese 2003). The pyrene technique

uses a closed system and so precludes dynamic experiments where compounds that might modulate OCR can be added.

A self-referencing electrode technique was used to measure the OCR of mouse embryos (Trimarchi et al. 2000). The technique required the zona pellucida to be removed; an invasive process. Trimarchi and colleagues reported that the proportion of oxygen consumed by oxidative phosphorylation altered dramatically during early embryonic development, from 30% at early cleavage stages to 60-70% at the blastocyst stage, however the non-mitochondrial oxygen consumption stayed constant throughout development. Therefore, the cleavage stage embryo generates the majority of its ATP through glycolysis, whereas the blastocyst relies on oxidative phosphorylation. 50-70% of oxygen consumed was not used to produce ATP during the early cleavage stages.

A scanning electrochemical microscopy technique was developed by Shiku et al. (2001). Bovine morulae with greater diameters had higher respiration rates than those with smaller diameters when measured by scanning electrochemical microscopy, suggesting a link between metabolic activity and total embryo volume. This pattern was later corroborated by Lopes and colleagues who, using an electrochemical method (discussed in detail in the following section) found that day 3 and day 7 bovine embryos with above average diameters had increased respiration (Lopes et al. 2005). Furthermore, Abe (2007) found that respiration rates of individual embryos correlated with morphological quality; higher ranked morulae tended to have greater OCR. A summary of reported OCR for bovine blastocysts is given below in Table 11.

### 3.1.8 Nanorespirometry

Lopes and colleagues validated a technique called 'nanorespirometry' to measure the OCR of bovine single oocytes or embryos (Lopes et al. 2005). The system uses a miniaturised Clark electrode mounted on a motorised micromanipulator and connected to an oxygen sensor capable of 0.1µmol/l resolution. Embryos are maintained at 39°C in HEPES-buffered media for the duration of equilibration and oxygen profile measurement. Pre-equilibration allows the build-up of a steady state of oxygen consumption, where the concentration is lowest in close proximity to the embryo and highest at the media surface. This gradient in oxygen concentration is measured directly by the oxygen sensor and is converted to oxygen consumption in nl/hr. Nanorespirometry does not affect the viability of embryos, and hence could be a candidate for accurate, non-invasive measurement on a clinical or commercial scale (Lopes et al. 2005). However, this technique does involve removing the embryo from its culture group. Moreover, working with the embryos under atmospheric gas conditions in HEPES-buffered medium, may perturb metabolism.

OCR (pmol/embryo/hr)	OCR (nl/embryo/hr)	Reference	Method
58	1.3nl/hr	Lopes 2005	Nanorespirometer
67	1.5nl/hr	Overström 1996	Self-Referencing Electrode
31	0.7 nl/hr	Thompson 1995	Pyrene

Table 11: A summary of bovine blastocyst oxygen consumption from selected literature.

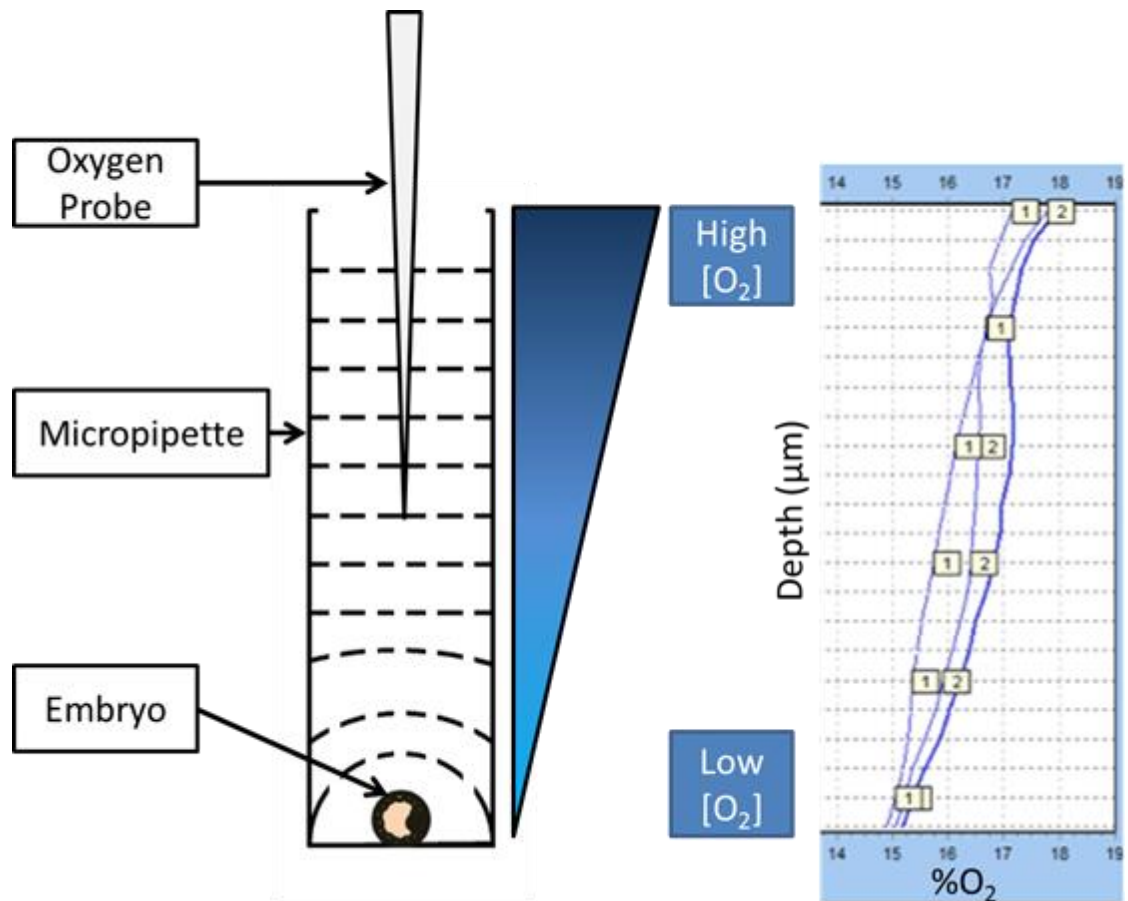


Figure 14: Overview of nanorespirometry. An embryo is aspirated to a 5 $\mu$ l micropipet and incubated at 39 $^{\circ}$ C under Hepes SOF for 1hr. During this time the embryo settles to the bottom of the tube and establishes a steady state gradient of oxygen consumption. The oxygen concentration is measured in 200 $\mu$ m intervals, moving towards the embryo. This generates an oxygen profile, shown here as % oxygen saturation vs depth in  $\mu$ m. Example data collected using Unisense A/S $\text{\textcircled{C}}$  SensorTrace Pro 3.0 and the nanorespirometer system.

Using nanorespirometry, Lopes et al. reported that the OCR increased during development, from 0.38nl/hr for day 3 embryos to 1.3nl/hr for day 7 embryos. In the same study, it was claimed that blastocysts with a higher morphological quality tended to have a higher OCR, with a mean of 1.72nl/hr. By contrast, blastocysts of lower morphological quality had a significantly lower OCR (Lopes et al. 2005). These data suggest that, in terms of OCR, the embryos with elevated metabolism tend to be the most viable. However this was based on subjective morphological analysis of blastocyst quality/viability.

The nanorespirometer method has revealed additional data which suggests that embryos with higher quality grades have average respiration rates, with rogue high and low values indicative of reduced viability in the bovine (Lopes et al. 2005).

In a later study, Ottosen and colleagues used nanorespirometry to predict the capacity of early cleavage stage murine embryos to develop to expanded blastocysts (Ottosen et al. 2007). There were significant increases in oxygen consumption between the 4 cell to 8 cell stage and again to the morula stage, followed by a doubling in rate at the expanded blastocyst stage. In general, embryos that successfully reached the expanded blastocyst stage consumed more oxygen than those that did not, though there was little difference between viable and poor morphological quality 2 cell embryos. This supported previous data collected in murine embryos (Houghton et al. 1996).

### 3.1.9 Fluorometric techniques

While other fluorescence methods have been discussed above, so far the BD Oxygen Biosensor System (BD OBS), employing a proprietary fluorophore quenched by oxygen, has yet to be applied to oocytes or embryos. It has been used to assay oxygen consumption of somatic cells (Fraker et al. 2006) and spermatozoa from different bulls, identifying differences in respiration which correlated with the non-return rate, representing relative fertility (Garrett et al. 2008). However the present research is the first time the method has been applied to bovine oocytes and blastocysts.

## 3.2 Aims

As described above, several studies have assayed oxygen consumption by oocytes and embryos, using a variety of methods, but a thorough assessment of the components of oxygen consumption has hitherto yet to be performed, limiting our understanding of the degree and possible effects of uncoupling and the capacity of embryos to adapt to metabolic challenges. The aim of this chapter is to quantify the ATP-producing oxygen consumption of bovine oocytes and embryos. This involved the following objectives:

- Evaluate two different methods of measuring oocyte and early embryo oxygen consumption.
- Measure the non-mitochondrial oxygen consumption of bovine embryos by acute inhibition of mitochondrial OCR with myxothiazol
- Quantify the ATP-producing rate of oxygen consumption in bovine oocytes and embryos using acute inhibition of ATP synthase with oligomycin.
- Determine the 'spare' respiratory capacity of bovine embryos using acute treatment with the uncoupling agent 2, 4-Dinitrophenol.
- Identify the contributions of the Tricarboxylic Acid Cycle to bovine embryo OCR using rotenone, an inhibitor of complex I.

## 3.3 Materials and methods

Unless otherwise described, *in vitro* maturation and fertilisation of oocytes, *in vitro* culture and grading of embryos and measurement of oxygen consumption by nanorespirometry were performed as described in Chapter 2.

### 3.3.1 Linearity of the BD Oxygen Biosensor System

Experiments using the BD OBS system were performed at either atmospheric oxygen (21%) or 5% oxygen using the gas control module. Mean fluorescence intensity of 0% sodium dithionite controls was plotted alongside blank Hepes-buffered media 5% and 21% using data from 5 separate experiments to form a 3-point standard curve to check for linearity (Figure 15).

### 3.3.2 Validation of the BD Oxygen Biosensor System

Prior to performing experiments using embryos, the BD oxygen biosensor system was tested with 4 randomly assigned groups (30, 50, 60 and 80) of mature oocyte-cumulus complexes (OCCs) following IVM. The change in absolute oxygen (pmol) was calculated from fluorescence intensity according to the manufacturer's guidance (as described in Chapter 2.2.2.4) and the change in concentration normalised to individual OCC relative to time as plotted below (Figure 16). The gradient of this curve is the oxygen consumption rate in pmol/embryo/hr.

### 3.3.3 Comparison of the BD Oxygen Biosensor System and Nanorespirometer oxygen profiling methods

To validate whether the BD OBS method was accurate, and reproducible, multiple oxygen consumption measurements of groups of in-vitro produced blastocysts at a range of stages of expansion were performed for comparison with mean OCR data collected by nanorespirometry, which has previously been validated with bovine embryos (Lopes, 2005). For analysis by BD Oxygen Biosensor System (BD OBS), blastocysts were assigned randomly into groups of approximately 10. For analysis by nanorespirometry, blastocysts were loaded individually into PCR micropipets. Nanorespirometer oxygen profiles were

analysed using a manufacturer designed MS Excel program. BD OBS data was analysed according to manufacturer guidance using MS Excel.

### 3.3.4 Optimisation of solvent

Analytical Reagent (A.R.) Grade Absolute Ethanol was diluted in Hepes SOF to achieve stock concentrations of: 0.01%, 0.1%, 1%, and 10% (v/v). Embryos were cultured to the blastocyst stage as described in chapter 2 and assigned into groups of approximately 10 mixed stage blastocysts for analysis by BD OBS in 50µl HSOF, as described above. Basal OCR of blastocysts was measured for 30 minutes by the BD OBS method, before injecting increasing concentrations of ethanol in 5µl volumes to reach approximate final concentrations of 0.001%, 0.01%, 0.1%, and 1% (v/v), again measuring for 30 minutes for each treatment.

### 3.3.5 Inhibitor preparation.

A range of inhibitors were used to assess the components of oxygen consumption. Details are given below in Table 12.

Inhibitor name	Solvent	Concentration used	Site affected	Value ascertained
Oligomycin	DMSO/Ethanol	0.05µg/ml	ATP Synthase	Uncoupled OCR
Myxothiazol	Ethanol	1.6nM	Complex III	Non-mitochondrial OCR
Antimycin A	Ethanol	0.2µM	Complex III	Non-mitochondrial OCR
2,4-dinitrophenol (DNP)	Ethanol	10µM	Proton Gradient	Maximal OCR
Rotenone	Ethanol	0.01µM	Complex I	Complex I-independent OCR

Table 12: Summary of the inhibitors used to measure aspects of bovine blastocyst oxygen consumption in this chapter

### 3.3.6 Coupled oxygen consumption

In order to establish the optimum concentration of oligomycin to be used, the OCR of a group of 10 blastocysts was recorded prior to and after addition of increasing concentrations of the ATP synthase inhibitor oligomycin (Table 12). Groups of 10 blastocysts were loaded into the BD OBS plate and OCR was measured every 20s for one hour at 485/600nm without mixing. After one hour, a vehicle control solution of DMSO was injected into the sample wells and OCR read for another hour. The injector was manually washed to remove the DMSO solution and primed with 0.05µg/ml oligomycin in HM. This procedure was timed for exactly 5 minutes to maintain an identical interval between measurements. Measurements were taken for a further 20 minutes before injecting 0.005µg/ml of the oligomycin and OCR measured for 30 min. This step was repeated for 0.05µg/ml and 0.5µg/ml oligomycin.

These experiments were repeated with oligomycin solubilised in 100% Ethanol, n=40 across 4 independent experiments.

### 3.3.7 Non-mitochondrial oxygen consumption

Non mitochondrial OCR was determined by addition of myxothiazol or antimycin, both inhibitors of complex III (Table 12). Following basal OCR measurement by BD OBS, 0.001% ethanol (vehicle control) was added to the well containing groups of embryos and basal OCR measured for 20min. After this, increasing concentrations of myxothiazol in HEPES SOF in the range 0.16-16nM (Garrett et al. 2008) were injected and OCR measured for 20min in the same way. Mitochondrial OCR was calculated by subtracting myxothiazol-treated OCR from basal OCR.

For antimycin treatment, blastocysts were profiled using nanorespirometry (n=20) across 4 independent experiments. Following measurement of basal OCR in the presence of 0.001% ethanol, measurement of the same embryos was repeated following treatment with increasing concentrations of antimycin in HEPES SOF in the range 0.02-2µM, in line with concentrations used in embryonic stem cells as described by (Birket et al. 2011). The OCR of 20 individual blastocysts was measured before and after treatment with 0.2µM antimycin A across 4 independent experiments from 3 independent IVP cohorts. Mitochondrial OCR was calculated by subtracting antimycin-treated OCR from basal OCR.

### 3.3.8 Maximal rate and spare respiratory capacity

Maximal OCR was determined using DNP, an ionophore that abolishes the proton gradient, removing all regulation of mitochondrial OCR and forcing mitochondria to consume the maximum volume of oxygen. Embryos were first titrated with increasing concentrations of DNP in Hepes SOF in the range 10-1000 $\mu$ M (Macháty et al. 2001) to determine the optimal concentration.

Maximal OCR was determined using nanorespirometry (n=14) across 3 independent experiments. Following basal measurement, blastocysts were treated with 10 $\mu$ M DNP, increasing OCR. Spare respiratory capacity was calculated by subtracting the basal OCR from maximal OCR for each blastocyst.

### 3.3.9 NADH and FADH<sub>2</sub>-dependent OCR

NADH-dependent OCR was determined by addition of rotenone, an inhibitor of complex I, which receives electrons from NADH only (Table 12). To determine the optimal concentration of rotenone, a group of 30 blastocysts were first profiled by BD OBS. Following basal OCR measurement, 0.001% ethanol (vehicle control) was added to the well containing groups of embryos and basal OCR measured for 20min. After this, increasing concentrations of rotenone in Hepes SOF in the range 0.001-1 $\mu$ M, in line with concentrations used in embryonic stem cells as described by (Birket et al. 2011).were injected and OCR measured for 20min in the same way.

Next, individual embryos were profiled using nanorespirometry. Following measurement of basal OCR in the presence of 0.001% ethanol, measurement of the same embryos was repeated following treatment with 0.01 $\mu$ M rotenone in Hepes SOF. Complex I or NADH-dependent OCR was calculated by subtracting the remaining OCR from basal. Complex II or FADH<sub>2</sub>-dependent OCR was calculated by subtracting the complex I dependent value from estimated coupled OCR based on Figure 20; 66% of basal OCR.

$$\text{Basal OCR} - \text{Rotenone-insensitive OCR} = \text{Complex I-dependent OCR}$$

$$\text{Basal OCR} \times 0.66 = \text{Estimated coupled OCR}$$

$$\text{Estimated coupled OCR} - \text{Complex I-dependent OCR} = \text{Complex II-dependent OCR}$$

### 3.3.10 Statistical analyses

Data were compared between groups by ANOVA with post-hoc Bonferroni test, or Dunn's test in the case of unequal groups. Significance threshold was  $p < 0.05$ . Specific details of numbers of observations and replicates are given in appropriate figure legends.

## 3.4 Results

### 3.4.1 Linearity of the BD Oxygen Biosensor System

Mean fluorescence intensity of the sodium dithionite control at 0% oxygen was  $215209 \pm 1806$ , while blank media at 5% oxygen was  $203425 \pm 1146$ , decreasing to  $47287 \pm 1825$  in blank media at 21% oxygen. Plotting this data as a standard curve produces a trend line with  $r^2=0.97$  (Figure 15). Plotting this data as a standard curve suggests that the change in fluorescence of the BD OBS in response to changing oxygen concentration is linear (Figure 15).

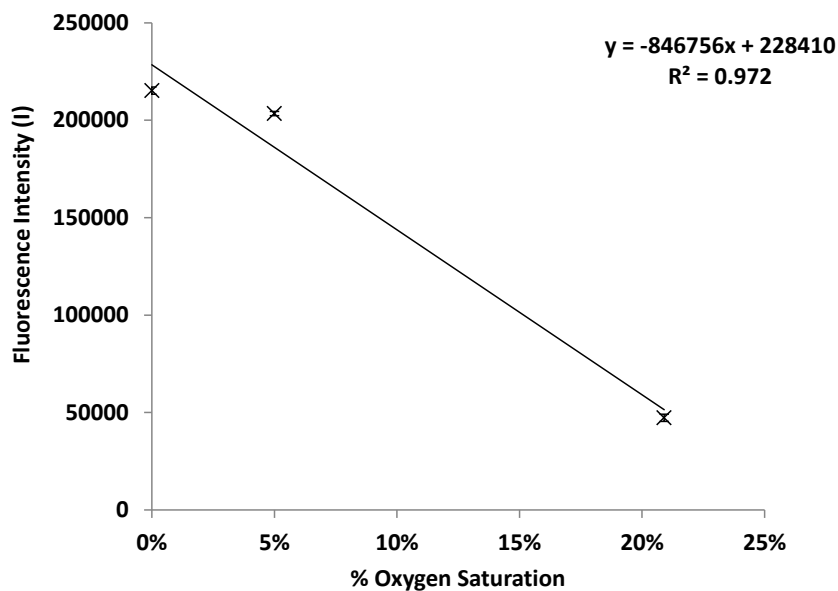


Figure 15: Validation of the linearity of the BD OBS system. Data from 5 separate experiments conducted at 5% or 21% oxygen with corresponding 0% oxygen controls. data shown as mean intensity  $\pm$ s.e.m. 0% O<sub>2</sub>:  $215209 \pm 1806$ , 5% O<sub>2</sub>:  $203425 \pm 1146$ , 21% O<sub>2</sub>:  $47287 \pm 1825$ .

### 3.4.2 Validation of the BD OBS system with OCCs

Figure 16A shows that fluorescent signal increased over time, in response to depletion of oxygen (Figure 16B) and was able to detect the oxygen consumption of as few as 30 OCCs (Figure 16C). Change in fluorescence over time correlates with the number of OCCs per well. Figure 5C also shows that when OCR per oocyte is largely equivalent regardless of group size.

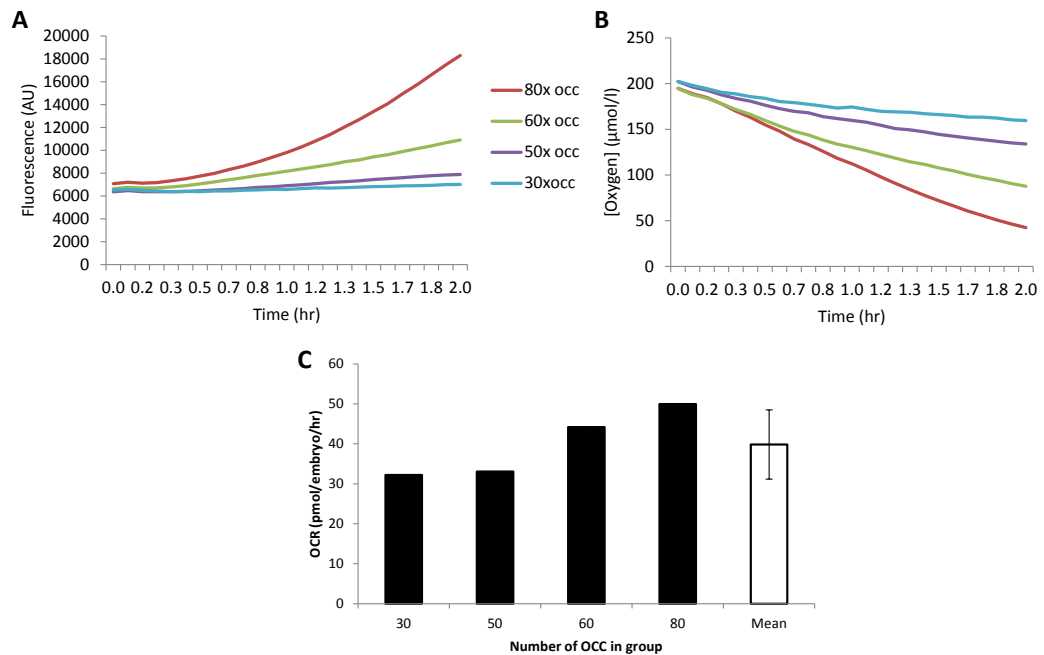


Figure 16: Analysis of OCR of different populations of bovine OCCs using the fluorescent BD OBS method. A) Change in fluorescence over time B) Change in oxygen concentration over time C) Individual OCR of OCCs measured in different population sizes from 30-80 OCCs per group. Mean value =  $39.8 \pm 8.6$ . Measured individual OCR was not different dependent on population size  $p=0.9$ .

### 3.4.3 Comparison of blastocyst OCR profiles by nanorespirometry and BD OBS

The mean OCR value for groups of mixed stage blastocysts measured by BD OBS was  $27.2 \pm 2.9$  pmol/embryo/hr, while the mean OCR of single blastocysts of mixed stages measured by nanorespirometry was  $21.7 \pm 1.3$  pmol/embryo/hr (Figure 17), with no significant difference between the two measurement types ( $p=0.9$ ). These values are comparable to published data (Lopes et al. 2005).

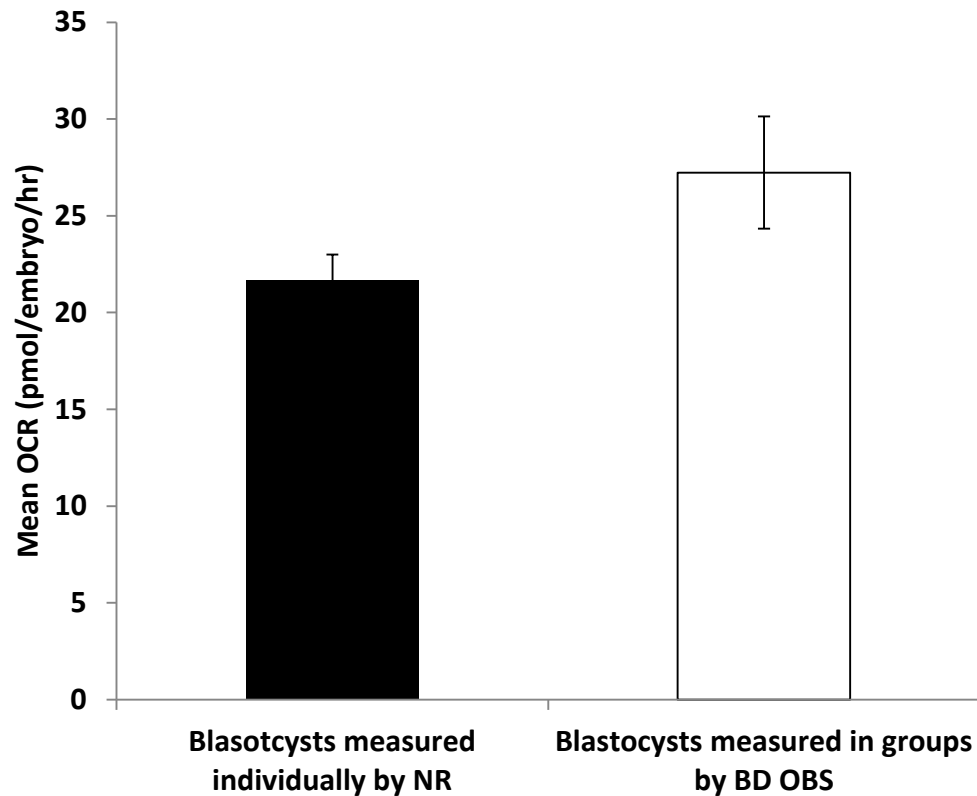


Figure 17: Comparison of OCR measured by nanorespirometer and BD OBS methods. Nanorespirometry:  $n=97$  individual blastocysts measured across 10 independent experiments, BD OBS  $n= 40$  blastocysts in groups of 10 across 4 independent experiments. Presented as mean OCR (pmol/embryo/hr) $\pm$ s.e.m: NR:  $21.7.6 \pm 1.3$ ; BD OBS:  $27.2 \pm 2.9$ .

### 3.4.4 Optimisation of solvent for respiratory inhibitor experiments

Figure 18A shows that 0.005% (v/v) dimethyl sulphoxide (DMSO) had no significant effect on blastocyst oxygen consumption rate as measured by BD OBS ( $p=0.6$ ). Figure 18B shows that injection of 0.001% analytical reagent (A.R) grade ethanol in Hepes SOF significantly reduced OCR from a basal level of 26.7 to 9.6 pmol/embryo/hr ( $p=0.001$ ). Injection of higher concentrations of ethanol abolished OCR entirely (Figure 18B). However, oxygen consumption of bovine blastocysts in the presence of molecular biology (M.B.) grade absolute ethanol in Hepes SOF (>99.5%) was 19.7 pmol/embryo/hr, which did not differ significantly from basal OCR measurement (28.2 pmol/embryo/hr;  $p=0.3$ ).

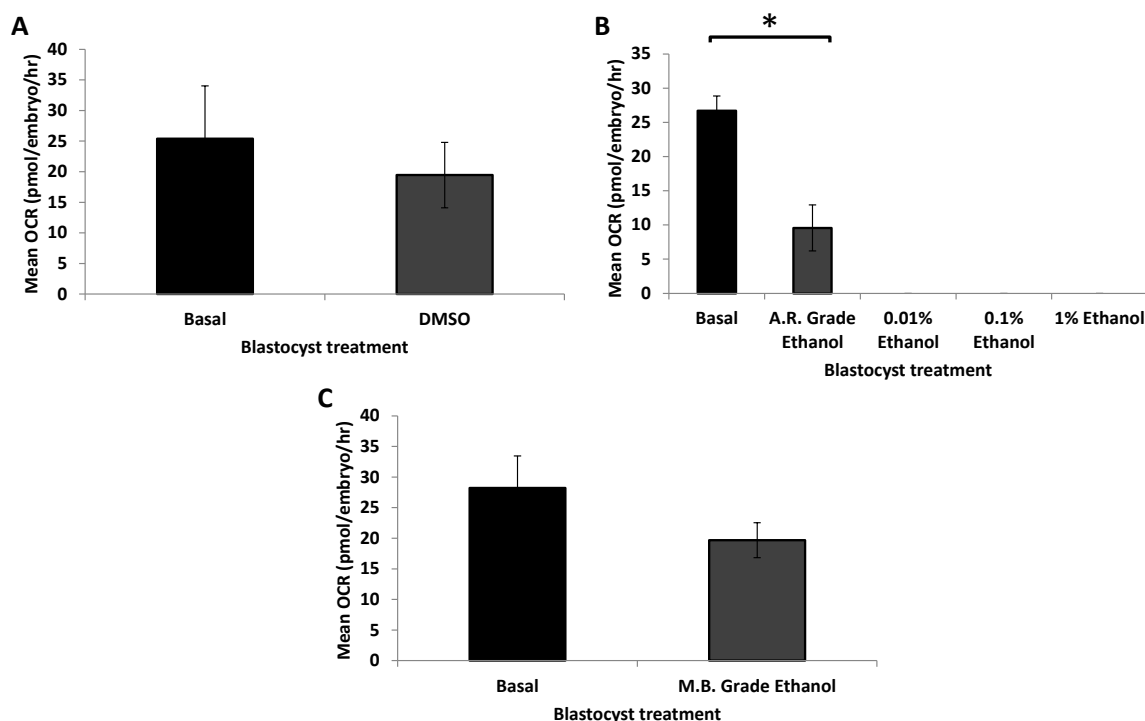


Figure 18: The effect of common solvents on blastocyst OCR. Data presented as OCR (pmol/embryo/hr) ± s.e.m. A) The effect of DMSO on grouped blastocyst OCR measured over 3 independent experiments ( $n=30$ ). B) The effect of A.R grade ethanol on blastocyst OCR measured over seven independent experiments ( $n=70$ ). Mean OCR decreased from  $26.7 \pm 2.2$  to  $9.6 \pm 3.4$  on addition of 0.001% ethanol. Injection of higher concentrations of solvent ablated OCR. C) The effect of 0.001% M.B grade ethanol on blastocyst OCR measured over 3 independent experiments ( $n=30$ ). Mean OCR decreased from  $28.2 \pm 5$  to  $19.7 \pm 3$ .

### 3.4.5 Non-mitochondrial oxygen consumption rate

Addition of 1.6nM myxothiazol reduced OCR from 29.64pmol/embryo/hr to 1.5pmol/embryo/hr, abolishing 95% of OCR compared to the solvent control (Figure 19A-B). Injecting higher concentrations of myxothiazol ablated embryonic oxygen consumption entirely, suggesting toxicity above 1.6nM.

As described in section 3.3.6, titrating antimycin concentration from 0.02μM, 0.2μM and 2μM dramatically altered OCR. At the lowest concentration, 0.02μM, OCR was reduced by 60% from 28.9±5.9 to 11.3±3.3 pmol/embryo/hr. By comparison, 0.2μM antimycin consistently reduced OCR by 88% to 3.6±2.1pmol/embryo/hr ( $p=0.006$ ), while 2μM consistently reduced blastocyst OCR to zero and was likely toxic (Figure 19C). Therefore, 0.2μM was used in subsequent experiments.

Figure 18D shows that the mean OCR in the presence of vehicle control was 26±3.6 pmol/embryo/hr, which fell to 2.3±1. pmol/embryo/hr after addition of 0.2μM antimycin A ( $p<0.001$ ). This suggests that 12.8% of basal OCR was non-mitochondrial (Figure 18E). It should be noted that on a few occasions, antimycin treatment reduced OCR to zero. These embryos were not included in the calculation of non-mitochondrial OCR as it is likely that they died during the assay, thus this was not true OCR.

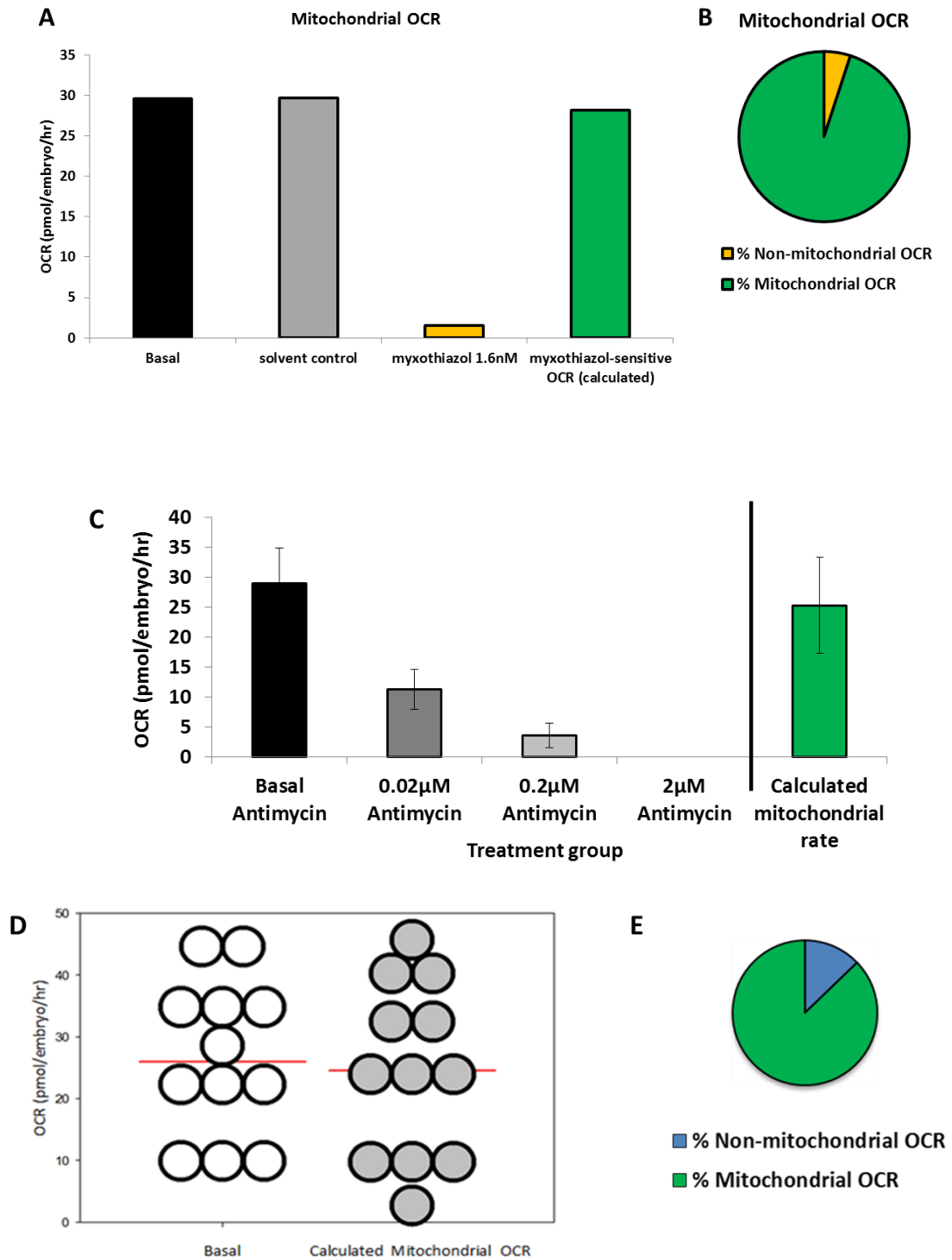


Figure 19: Blastocyst mitochondrial oxygen consumption. A) Blastocyst OCR measured by BD OBS (n=14) (B) Overall mitochondrial and non-mitochondrial OCR using myxothiazol (%; n=14). C) The effect of increasing concentrations of antimycin on OCR (n=20; 4 replicates) D) Basal and mitochondrial OCR of single blastocysts (n=12; 3 replicates) E) Overall mitochondrial and non-mitochondrial OCR using antimycin.

### 3.4.6 Coupled oxygen consumption

As shown in Figure 20, addition of 0.05 $\mu$ g/ml oligomycin had no effect on overall OCR, while concentrations above 0.5 $\mu$ g/ml abolished oxygen consumption entirely, suggesting toxicity. Therefore, 0.05 $\mu$ g/ml was selected as the appropriate concentration. When this was added to groups of 10 blastocysts, OCR was reduced from 19.7 $\pm$ 2.8pmol/embryo/hr to 6.4 $\pm$ 2.3pmol/embryo/hr (Figure 20B). The coupled rate of oxygen consumption was determined to be 13.3 $\pm$ 0.7pmol/embryo/hr (Figure 20B), suggesting that 66% of *in vitro* produced bovine embryo oxygen consumption is coupled to ATP production, while 33% is uncoupled (Figure 20C).

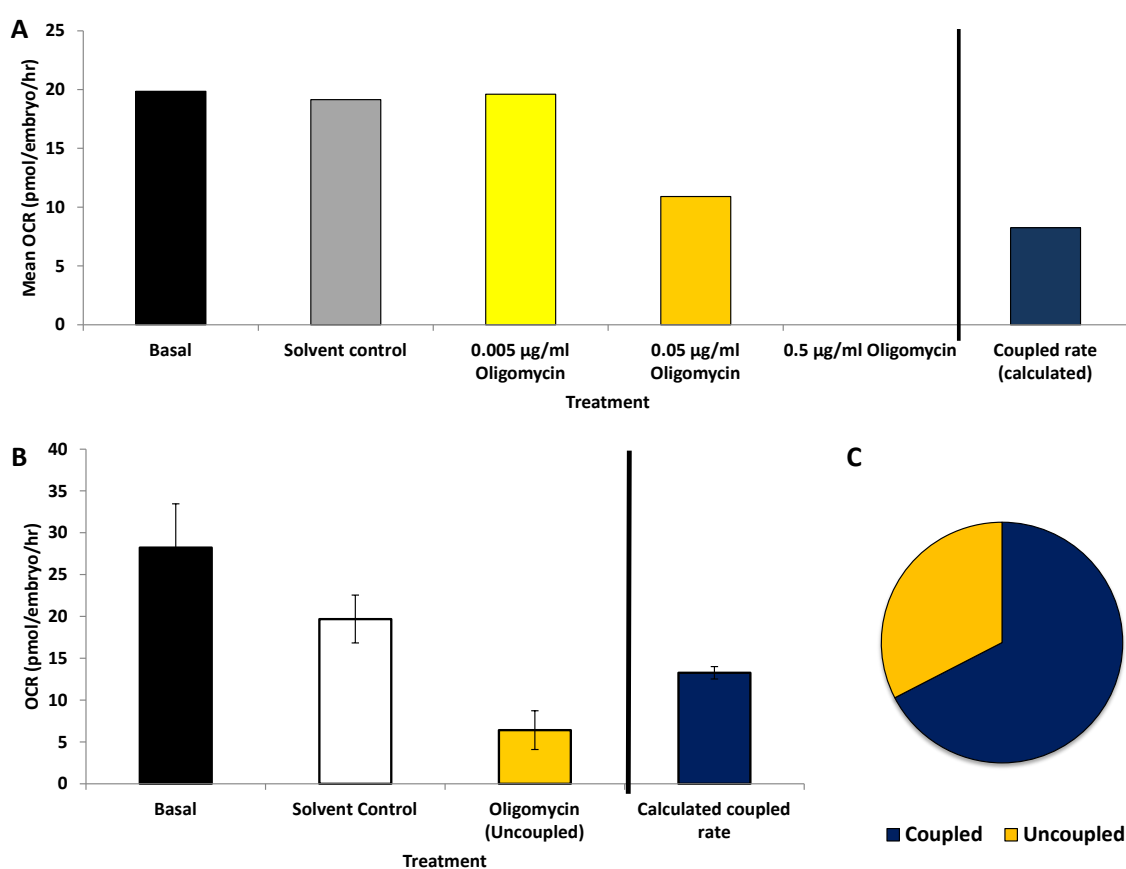


Figure 20: The coupled and uncoupled OCR of bovine blastocysts. A) Oligomycin titration using a group of 10 blastocysts. B) Oligomycin sensitive proportion of OCR (n=40, 4 independent replicates). Coupled rate calculated as basal OCR – oligomycin-treated OCR. Data presented as mean OCR $\pm$ s.e.m C) Coupled (32.6%) and uncoupled rate (67.4%) as a percentage of basal OCR.

### 3.4.7 Maximal rate and spare respiratory capacity

Individual embryos had varied basal OCR between 4.5 and 38pmol/embryo/hr, however OCR consistently and significantly rose after addition of DNP (14 - 49pmol/embryo/hr),  $p < 0.001$  (Figure 21). Mean OCR increased from  $17.1 \pm 2.5$  pmol/embryo/hr to  $32.3 \pm 2.7$  pmol/embryo/hr following addition of DNP (Figure 21A). The difference between the basal and maximal values, known as the spare respiratory capacity, was 15.2pmol/embryo/hr. This suggests that basal OCR accounts for 53% of maximal OCR, with a 47% spare respiratory capacity (Figure 21B).

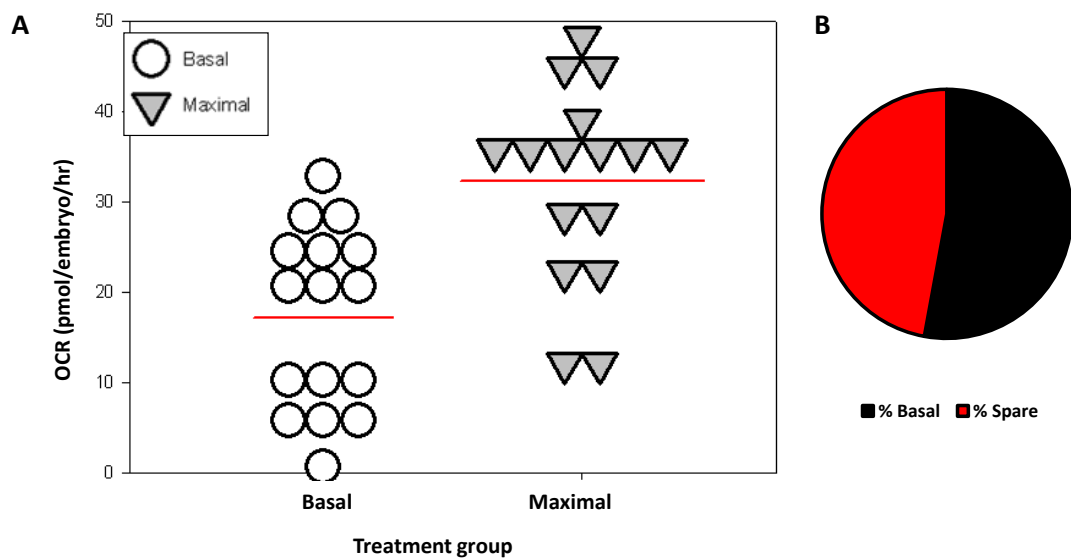


Figure 21: Maximal respiratory rate and spare capacity of bovine blastocysts. A) OCR increases to maximal following DNP treatment ( $p < 0.001$ ,  $n = 14$ ; 3 independent replicates) B) Spare respiratory capacity, as calculated by subtracting basal from maximal OCR. Data presented as individual OCR (A) and % maximal OCR (B).

### 3.4.8 NADH-dependent OCR

Addition of 0.01 $\mu$ M rotenone reduced the mean OCR from 16.5pmol/embryo/hr to 7.1pmol/embryo/hr, a reduction of 57% (Figure 22). This analysis was subsequently repeated using nano respirometry on individual blastocysts. Mean basal OCR fell from 27.7 $\pm$ 1.6pmol/embryo/hr, to 11.6 $\pm$ 0.9pmol/embryo/hr following treatment with 0.01 $\mu$ M rotenone (Figure 22). This suggests a mean complex-I or NADH-dependent OCR of 16.1 $\pm$ 1.1pmol/embryo/hr, or 58% of basal OCR.

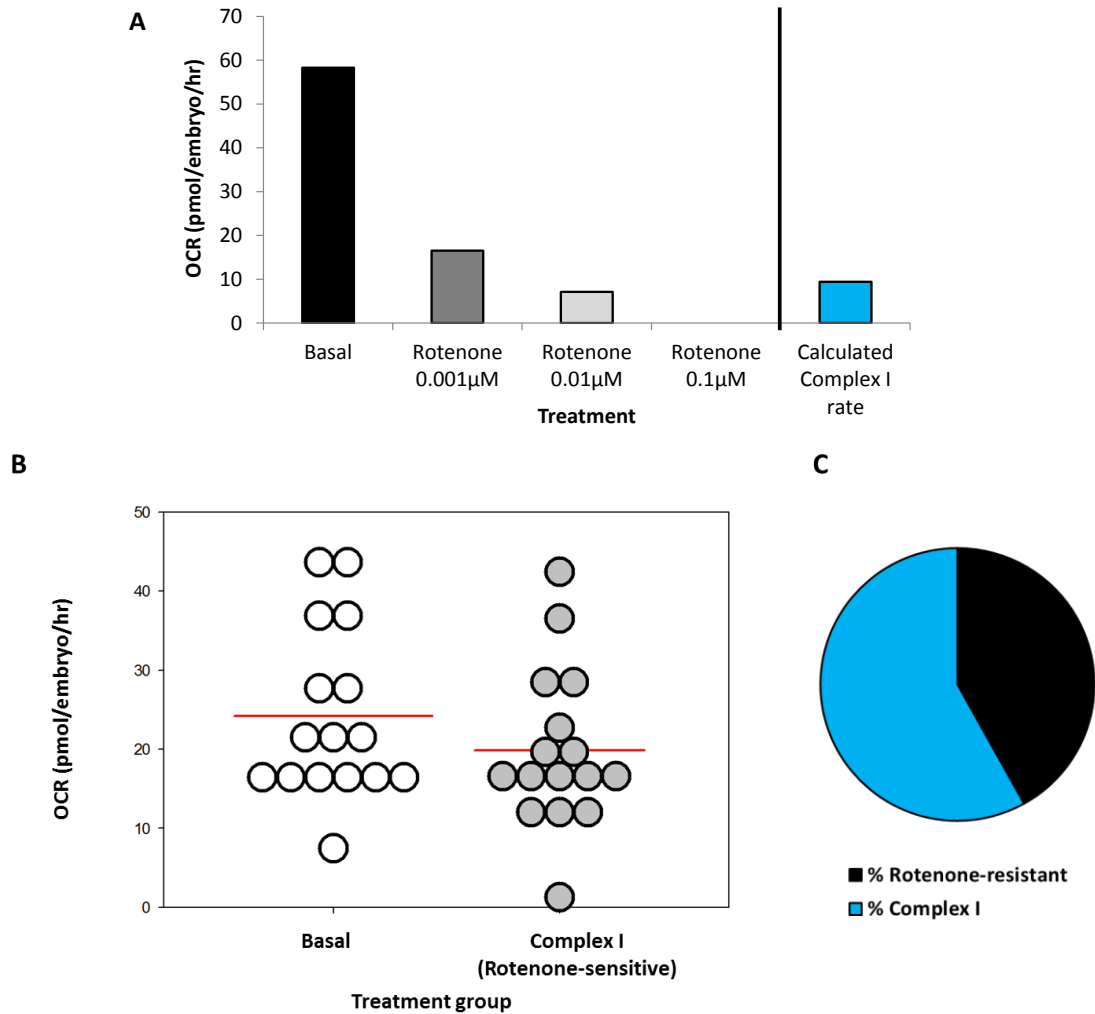


Figure 22: Complex I-dependent blastocyst OCR. A) The effect of increasing concentrations of rotenone on grouped blastocyst OCR (n=30) B) Basal and rotenone-sensitive or complex I-dependent OCR of single blastocysts C) Overall complex I-dependent and independent OCR (%).

## 3.5 Discussion

### 3.5.1 Overview

The aim of this research was to quantify the components of oxygen consumption rate (OCR) in individual bovine blastocysts. In order to do this, the following experimental sequence was completed:

- Validated the use of the BD Oxygen Biosensor System to measure OCR of groups of embryos against nanorespirometry
- Optimised the use of solvents for respiratory inhibitor experiments
- Measured non-mitochondrial OCR of bovine blastocysts using myxothiazol and antimycin A.
- Calculated the amount of OCR coupled to ATP synthesis in bovine blastocysts using the ATP synthase inhibitor oligomycin.
- Determined the maximal rate and spare respiratory capacity of bovine embryos using the uncoupler protonophore 2,4-Dinitrophenol.
- Identified the contributions of tricarboxylic acid cycle products NADH and FADH<sub>2</sub> to OCR using the complex I inhibitor rotenone.

### 3.5.2 Bioenergetic profile of bovine blastocysts.

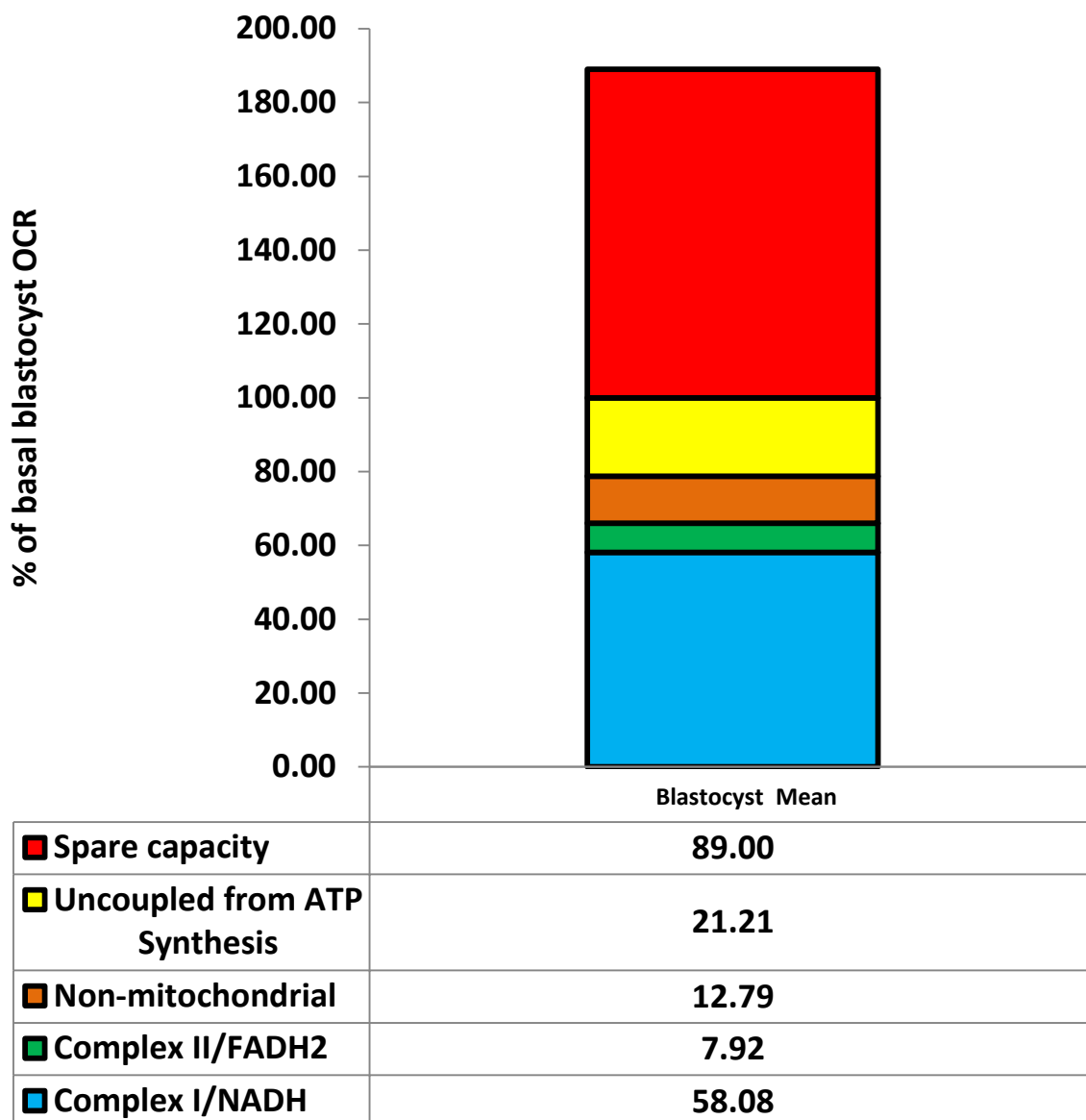


Figure 23: Bioenergetic profile of bovine blastocyst oxygen consumption. Percentage contribution of each component was calculated using all of the preceding data.

Analysis of oxygen consumption using a range of inhibitors has revealed for the first time a comprehensive and detailed breakdown of the fate of consumed oxygen by the bovine blastocyst, which is summarised in Figure 23. Spare respiratory capacity allows a potential 89% increase in OCR. This might be of importance during high energy demand processes such as blastocoel expansion, acting as a 'buffer' to enable ATP synthesis by mitochondrial oxidative phosphorylation to increase on demand. Around 21% of basal OCR is uncoupled from ATP synthesis but not used by non-mitochondrial processes and may contribute to ROS generation, or have an alternative role such as activity of oxygen-consuming enzymes such as membrane-bound NADPH oxidase (Manes and Lai 1995) or

peroxisomal enzyme activity. Finally, 66% of basal OCR is coupled to ATP production, with the majority, 58% of basal, coming from electron flow from NADH to complex I and the remaining 8% of basal from electron flow from FADH<sub>2</sub> to complex II.

### 3.5.3 Linearity of the BD Oxygen Biosensor System

Data recorded using the BD Bioscience oxygen biosensor system (BD OBS) at 0%, 5% and 21% oxygen across 5 different experiments were plotted to form a 3-point standard curve with  $r^2=0.972$  (Figure 15). This suggests that the change in fluorescence of the BD OBS in response to changing oxygen concentration was linear.

### 3.5.4 Validation of the BD Oxygen Biosensor System

The BD Bioscience oxygen biosensor system (BD OBS) has previously been applied to a wide range of somatic cell types (Wodnicka 2000; Stitt et al. 2002; Guarino et al. 2004; Fraker et al. 2006), however this is the first time the system has been used with mammalian embryos. Initially, the system was tested with 4 groups of mature OCCs, ranging from 30–80 OCCs per well to establish sensitivity, potential toxicity and reproducibility. The system was sufficiently sensitive to detect the OCR of 30 bovine OCCs, though increasing the number reduced an observed fluctuation in the fluorescent signal, suggesting that having more biological replicates reduces heterogeneity; alternatively the lower limit of sensitivity may have been reached. The system also gave a similar value for OCR per OCC regardless of the number (mean 55pmol/embryo/hr), suggesting sufficient reproducibility to compare different groups of OCCs or embryos where appropriate.

On the basis of signal variability (Figure 16B) it was decided that 50 OCCs per group was the optimum group size for further experiments. In addition, all assayed OCCs were returned to culture after assay and fertilised as normal, resulting in similar blastocyst rates to control cognate OCCs not used in the experiment. The, BD OBS is therefore a sensitive, robust, non-toxic method for measuring OCC oxygen consumption and could be used to measure embryo OCR.

### 3.5.5 Comparison of techniques

In addition to the BD OBS system, it was possible to use a nano respirometer (Lopes et al. 2005) to measure OCR. This method is technically challenging, but allowed the OCR to be measured on individual embryos. It was necessary to confirm that mean OCR values for individual blastocysts did not differ according to the method of assay. As shown in Figure 17, there were no significant difference between the two measurement types ( $p=0.9$ ).

These data are broadly comparable to published findings. For example, when expressed as nl/embryo/hr, mean OCR as measured by nano respirometry was 0.96nl/embryo/hr, compared to the 0.7nl/embryo/hr reported by Thompson et al. (1996) using the pyrene method and slightly lower than the value of 1.3 nl/embryo/hr published by Lopes et al. (2005) or 1.8nl/embryo/hr published by (Van Hoeck et al. 2011), both using nano respirometry. These modest differences in OCR between published reports could be due to differences in culture technique, which have been well-described as having an impact on embryo metabolism (Takahashi and First 1992; Gardner and Sakkas 1993; Leese 1995; Gandhi et al. 2001).

### 3.5.6 Optimisation of solvent for respiratory inhibitor experiments

The majority of publications using water immiscible respiratory chain inhibitors such as oligomycin and DNP report using DMSO as the vehicle, without significant negative effects on somatic cell, stem cell or embryo physiology (Harvey et al. 2004; Birket et al. 2011). In initial experiments, treating embryos with DMSO using the plate reader injector system had no significant effect on embryo OCR, hence DMSO was chosen for respiratory inhibitor experiments. However, addition of DMSO to the nano respirometer lead to irreparable damage to the probe. Furthermore, DMSO has been reported in a variety of systems to interfere with gene expression (David et al. 2012) and increase oxidative damage by converting hydroxyl radicals to methyl radicals, which can react with  $O_2$  to form more reactive secondary radicals (Burkitt and Mason 1991); factors which could interfere with physiological measurement of oxygen consumption. Consequently, DMSO was excluded from further experiments and ethanol was tested as an alternative (Trimarchi et al. 2000).

A titration experiment was therefore carried out in which increasing concentrations of analytical reagent (A.R) grade ethanol, ranging from 0.0001% to 1%, were tested for their effect on bovine blastocyst oxygen consumption rate. When this was done OCR was greatly reduced at all concentrations including the lowest, in which the mean basal OCR of 20 blastocysts reduced by 60% on addition of 0.001% ethanol in Hepes SOF (170 $\mu$ M). Injection of higher concentrations of ethanol abolished oxygen consumption completely and was likely toxic to the blastocysts. However, when repeated with molecular biology grade ethanol, no detrimental effect was observed. This observation was confirmed in subsequent experiments where Molecular Biology (M.B.) grade ethanol was used as a vehicle and shown not to affect ongoing embryo development. It is possible that the analytical reagent grade ethanol contained impurities such as methanol which interfered with embryo metabolism (Andrews et al. 1993; Abbott et al. 1995). M.B. grade ethanol was therefore chosen as an appropriate solvent for solubilisation of water immiscible chemicals used in the determination of oxygen consumption.

### 3.5.7 The non-mitochondrial OCR of bovine blastocysts

The majority of total oxygen consumption in the bovine blastocyst is due to mitochondrial oxidative phosphorylation, however a significant portion has been reported to be consumed by non-mitochondrial processes, such as oxygen-consuming cyclooxygenase or NADPH dehydrogenases (Trimarchi et al. 2000; Manes and Lai 1995). Addition of 1.6nM myxothiazol reduced mean OCR of 20 blastocysts from 29.55 to 1.5pmol/embryo/hr, abolishing 95% of OCR compared to the solvent control. This suggests that the remaining 5% of blastocyst OCR is used in non-mitochondrial processes. Treatment with higher concentrations of the inhibitor caused a decrease in fluorescent signal, reflecting an increase in oxygen concentration (Guarino et al. 2004). This suggests that at higher concentrations the inhibitor is toxic and the resulting loss of respiring embryos removes the site of oxygen consumption. As the BD OBS is an open system, this change allows oxygen to diffuse into the well down the concentration gradient, returning it eventually to ambient concentration.

In order to confirm the data for non-mitochondrial oxygen consumption obtained from blastocysts cultured in groups, individual embryo respiratory measures were performed. A second inhibitor of complex III, antimycin, was used in order to compare the effects of

inhibiting mitochondrial respiration at a different stage of the Q cycle (Figure 13). Furthermore, this was an opportunity to compare published data of mitochondrial OCR in mammalian embryos using the same inhibitor (Trimarchi et al. 2000). Addition of 0.2 $\mu$ M antimycin in HEPES SOF caused the mean blastocyst OCR to fall from 26 $\pm$ 4.7 pmol/embryo/hr to 2.3 $\pm$ 1.3 pmol/embryo/hr, suggesting that the true mean mitochondrial OCR was 24.5 $\pm$ 4.1 pmol/embryo/hr. From these data, it may be concluded that 12.8% of blastocyst OCR was used for non-mitochondrial purposes. This is higher than was observed using myxothiazol. However, individual blastocyst data collected using nanorespirometry is likely to be more reliable than data for groups using fluorescence as the nanorespirometer is a more sensitive system and blastocysts in group analysis which may be more sensitive to toxic effects of the inhibitor cannot be detected and removed from the BD OBS analysis.

The proportion of non-mitochondrial OCR was similar to that in many somatic cell types at around 10% (Porter and Brand 1995; Wu et al. 2007; Affourtit and Brand 2008; Amo et al. 2008; Kenney et al. 2014) and significantly lower than the 23.2% reported for embryonic stem cells (Birket et al. 2011). The non-mitochondrial component of oxygen consumption observed here was lower than that reported previously in murine blastocysts (Trimarchi et al. 2000); in that study, 30% of blastocyst OCR was insensitive to cyanide or 1mM antimycin A treatment, inhibiting complexes IV and III respectively. The proportion of non-mitochondrial oxygen consumption reported by Trimarchi et al. (2000) is in agreement with the work of Manes and Lai (1995), who determined that 30% of rabbit blastocyst OCR was caused by H<sub>2</sub>O<sub>2</sub>-producing oxygenase enzymes, reporting activity of an unidentified NADPH oxidase and identified superoxide and peroxide radicals present on the blastocyst surface (Manes and Lai 1995). These processes might include enzymatic activity, such as NADPH dehydrogenase, cyclooxygenases and xanthine oxidase. The differences between the present data and that reported by Manes and Lai may arise from species differences. Other metabolic pathways also differ between species, for example murine embryos consume significantly less glucose and pyruvate than bovine (Leese and Barton 1984; Leese et al. 1986). Further investigation comparing mitochondrial OCR between different mammalian species such as human, sheep and pig is clearly required.

### 3.5.8 Coupled OCR of bovine blastocysts

The mean basal OCR of groups of 10 bovine embryos with multiple degrees of blastocyst expansion was  $19.7 \pm 2.8$  pmol/embryo/hr or 0.44 nl/embryo/hr, a value comparable to the data of Lopes et al. (2005). Treatment with 0.05  $\mu$ g/ml oligomycin reduced the OCR to  $6.4 \pm 2.3$  pmol/embryo/hr; approximately 33% of total. While this figure is in agreement with studies in somatic cells (Brand and Nicholls 2011), it remains surprising to find that only 66% of OCR in *in vitro* produced bovine blastocysts is coupled to ATP synthesis since it is often assumed that more viable embryos tend to have lower overall metabolism (Leese 2002) and an embryo with high uncoupled OCR must increase its overall OCR to maintain sufficient ATP production. It is tempting to speculate that the ratio of coupled to uncoupled oxygen consumption in individual blastocysts will have a role in embryo viability. For example, an embryo with a greater than average proportion of coupled OCR could be expected to produce enough ATP for basal metabolism and development while consuming less exogenous and endogenous substrate and producing less ROS by leaky respiration. In contrast, an embryo with a greater than average proportion of uncoupled OCR could be expected to produce greater levels of ROS, increasing lipid peroxidation, DNA damage and the amount of ATP required for repair of this damage.

The present data (Figure 20B) also enable re-interpretation of previously published data. For example, we can consider the widely accepted data of Thompson et al. (1996), who reported total blastocyst OCR of 0.9 nl/embryo/hr (40.2 pmol/embryo/hr). If coupled OCR is 66% of total, coupled OCR was 26.5 pmol/embryo/hr. The quantification of the coupled proportion of oxygen consumption suggests that ATP production is lower than previously thought, for example Thompson et al. (1996) reported 221 pmol/embryo/hr ATP, a value calculated from total OCR. However, using the coupled OCR of 26.5 pmol/embryo/hr and the  $P/O_{max} = 2.4$  (per single oxygen), total ATP production by OXPHOS is  $26.5 \times 4.8 = 127.3$  pmol/embryo/hr ATP. Furthermore, we can estimate ATP production from aerobic glycolysis, since 1 mole of lactate equates to 1 mole of ATP. Thus, if individual bovine blastocyst lactate production was 31.9 pmol/embryo/hr, again as determined by Thompson et al. (1996), ATP produced from glycolysis is 31.9 pmol/embryo/hr, giving a total production of  $127.3 + 31.9 = 159.2$  pmol/embryo/hr ATP. This value is significantly below the value reported by Thompson and colleagues (1996) in the absence of information relating to coupled OCR. However, using the newly calculated figures,

approximately 20% of ATP is produced by glycolysis, while 80% ATP is produced by coupled OXPHOS. This is broadly in agreement with Sturme and Leese (2003), who reported that the overwhelming majority of ATP in the porcine blastocyst came from oxidative processes, despite not having access to data on the ratio of coupled: non-coupled OCR.

It should be noted that since oligomycin treatment slightly increases proton leak by inhibiting phosphorylation of ATP, the calculated coupled rate may be artificially lower than the true value; an unavoidable effect of the experimental intervention (Affourtit and Brand 2009; Divakaruni and Brand 2011).

### 3.5.9 Maximal rate and spare respiratory capacity

Spare respiratory capacity, which may be described as providing the ability of oxidative metabolism to adapt to changing ATP demand (Brand and Nicholls 2011), was determined by measuring OCR in the presence of DNP. Basal OCR was  $17.1 \pm 2.5$  pmol/embryo/hr, while maximal OCR following DNP treatment was  $32.3 \pm 2.7$  pmol/embryo/hr. The spare respiratory capacity of bovine blastocysts was therefore  $32.3 - 17.1 = 15.2$  pmol/embryo/hr, or 47% of maximal OCR (Figure 21). In other words, under control conditions, the bovine blastocyst used only 53% of its possible maximal oxygen consumption. While there was high individual variation between embryos, it is interesting to note that the mean percentage change was similar for that established using the BD OBS method above

As 33% of basal OCR is uncoupled from ATP synthesis (Figure 20), this implies that the bovine blastocyst uses only 35% of its potential maximal oxygen consumption for energy metabolism. Individual embryos had wide ranging basal OCR between 4.5 and 38 pmol/embryo/hr; however all exhibited a dramatic increase in OCR on DNP treatment, which rose to between 14 and 49 pmol/embryo/hr. Individual variation in sensitivity to the uncoupler FCCP by murine embryos has previously been reported by Trimarchi et al. (2000), so it is possible that the precise concentration of DNP was not ideal in all cases. However, in the interest of controlling the independent variable, the concentration of DNP was titrated using a group of 20 blastocysts to find the most appropriate concentration for the majority.

A large spare respiratory capacity is common in cell types which require variable ATP demand, including neurons, muscle cells (Yadava and Nicholls 2007; Choi et al. 2009; Flynn et al. 2011) and most likely, embryos. Spare respiratory capacity in bovine blastocysts was measured as 89% over basal, much lower than somatic cells with dynamic ATP demand, such as rat neurones, with a spare respiratory capacity of 217% over basal (Brand and Nicholls 2011). However this still represents a relatively large buffer for energy demand processes in the embryo. Additionally, the maximal OCR is theoretically dependent, to some extent, on the number of mitochondria and thus may be fixed during embryo development (Van Blerkom 2011). Conversely a small spare capacity suggests mitochondrial dysfunction. Indeed, maximal OCR is also fixed throughout the early cleavage stages (Trimarchi et al. 2000). While basal OCR differs between species, similar fluctuations in OCR throughout pre-implantation development have been reported in mouse (Houghton et al. 1996), porcine (Sturmey and Leese 2003) and bovine embryos (Lopes et al. 2005).

This spare respiratory capacity may be vital to support the changing energy demands of the developing pre-implantation embryo and throughout the cell cycles of individual blastomeres. As the number of mitochondria is fixed during this period of development, the maximal respiratory capacity may also remain fixed. This large potential reserve may therefore be necessary for the sudden and dramatic increase in energy demand on blastocoel expansion, caused by increasing protein synthesis, differentiation, growth and activity of the  $\text{Na}^+/\text{K}^+$  ATPase (Donnay and Leese 1999). Membrane potential differs between mitochondria in the inner cell mass and trophectoderm cells; the trophectoderm, which will contribute to the placenta, consumes significantly more oxygen, contains ~80% of the total embryonic ATP and significantly more mitochondria, which tend to be more polarised than the comparatively quiescent ICM, from which the foetus will develop (Houghton et al. 1996; Houghton 2006). This distribution may help restrict ROS production in the ICM and developing postimplantation embryo until ATP demand increases, while the TE and resulting placenta are much more metabolically active.

### 3.5.10 NADH and FADH<sub>2</sub>-dependent OCR

Having established the coupled rate of oxygen consumption in individual embryos (76%), it was decided to quantify the relative contributions of respiratory complexes I and II to the coupled rate. As complex I accepts electrons from NADH only and complex II from FADH<sub>2</sub> only, this provides an insight into the activity of the TCA cycle in the bovine blastocyst. Addition of 0.01 $\mu$ M Rotenone, an inhibitor of complex I, caused individual blastocyst OCR to fall from 27.7 $\pm$ 1.6pmol/embryo/hr, to 11.6 $\pm$ 0.9pmol/embryo/hr; a reduction of 58% (Figure 22). This suggests that 16.1pmol/embryo/hr or 58% of total OCR is generated by complex I activity, which requires electron transfer from NADH. If 66% OCR is coupled, the difference between the two, that is 66%-58%=8% or 2.2pmol/embryo/hr of embryo OCR due to complex II, which requires electron transfer from FADH<sub>2</sub>. The ratio of OCR due to complex I compared to II is 58/8=7.25. This is unsurprising as NADH is more abundant in the mammalian cell than FADH<sub>2</sub>, the Krebs cycle theoretically producing four times as much NADH as FADH<sub>2</sub> and moreover, electron transfer from FADH<sub>2</sub> releases less energy than that from NADH (Berg et al. 2002). It is possible that experimental analysis of this relationship using malate would result in a different FADH<sub>2</sub>-dependent rate due to the deleterious effects of experimental manipulations and the technical difficulties of performing both analyses on the same embryo; it is likely that the ratio is specific to each embryo.

### 3.5.11 Linking components of oxygen consumption to ATP supply

From the relative proportions of oxygen consumption reported above, it is possible to recalculate components of ATP supply assuming that 1) the ADP phosphorylation/oxygen reduction ratio P/O<sub>max</sub>=2.4 (Brand et al. 2005); 2) the average bovine blastocyst has an OCR of 27.23 $\pm$ 2.9pmol/embryo/hr (Figure 17); 3) that 32pmol/embryo/hr ATP is produced by glycolysis (Thompson et al. 1996) and 4) 66% of total OCR is coupled to ATP synthesis as reported above (Figure 20). Thus, the coupled OCR was 18pmol/embryo/hr, which can, theoretically support the generation of approximately 86pmol/embryo/hr ATP. The NADH-dependent Complex I, contributing 58% of the total oxygen consumption, accounts for approximately 16pmol/embryo/hr of oxygen consumption and 76.8pmol/embryo/hr ATP production. This suggests that FADH<sub>2</sub>-dependent complex II

accounts for 2pmol/embryo/hr O<sub>2</sub> and 4.8pmol/embryo/hr ATP produced. Total ATP production per blastocyst including glycolysis was 118pmol/embryo/hr, such that oxidative phosphorylation accounts for approximately 72% of bovine blastocyst ATP production.

### 3.5.12 Evaluation of methodology

In many somatic cell types, it is possible to treat cells sequentially with a range of inhibitors over a short period of time to calculate several components of oxygen consumption (Brand and Nicholls 2011). By contrast, individual embryos were less robust in withstanding manipulation of mitochondrial function without death or complete dysregulation of energy metabolism. Early experiments attempting a similar approach by nanorespirometry failed as individual embryos must be pre-equilibrated, with inhibitor for an hour before measurement can be made. Attempting a second profile with a new inhibitor gave varied responses between embryos, but most often the embryos became unstable or ceased respiring altogether. In both experimental methods, it appeared that treatment of embryos with two inhibitors in series result in toxic effects. Separate experiments were therefore used to improve accuracy.

### 3.5.13 Strengths and limitations

Chapter 3 describes a detailed breakdown of the fate of consumed oxygen in the bovine blastocyst. Embryos responded consistently to the individual inhibitors in the experiments detailed above. However, embryos tended to be sensitive to the toxic effects of multiple inhibitors in series, preventing analysis of multiple components, such as uncoupled and non-mitochondrial OCR, in the same embryos. This approach is possible with somatic cells (Birket et al. 2011) but embryos may be more sensitive to metabolic poisons, or toxicity may be exacerbated by the 1hr equilibration time between nanorespirometer profiles. The BD OBS method may be more appropriate for a multiple inhibitor approach, but inhibiting oxidative phosphorylation tends to reduce the OCR below the lower limit of sensitivity using the number of blastocysts tested to date. Furthermore, repeating each bioenergetic profiling experiment with different preimplantation stages, such as zygote, pre-EGA cleavage stages or morulae, could illustrate dynamic changes in energy demand and OCR during preimplantation development.

### 3.5.14 Conclusion

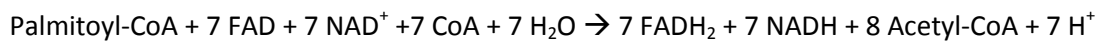
This chapter reports a detailed breakdown of bovine blastocyst oxygen consumption, which reflects the dynamic nature of mammalian embryo energy metabolism. Most oxygen is consumed in response to the activity of the NADH-dependent complex I, with a smaller proportion by FADH<sub>2</sub>-dependent complex II. The activity of these complexes is coupled to ATP synthase activity, producing sufficient ATP to meet the energy demands of the blastocyst, including protein and DNA synthesis, cell division and structural changes. However, a sizeable proportion of oxygen consumed, which varied between individual embryos, is uncoupled from ATP synthesis. A small proportion of this is due to non-mitochondrial oxygen consuming processes, such as cyclooxygenases, but the remainder is apparently due to proton 'leak' and potentially causes oxidative damage to DNA, protein and lipid throughout the embryo. Finally, the blastocyst maintains a significant spare respiratory capacity, allowing an increase in coupled rate, perhaps in order to accelerate ATP production during energy-demanding processes such as blastocoel expansion.

## 4 The effects of manipulating bovine embryo lipid metabolism

## 4.1 Introduction

### 4.1.1 Fatty acid metabolism

Cellular fatty acids are stored in uncharged lipid droplets composed of triacylglycerol esters (TGs). In adult mammals, most TG is stored in the adipocyte; a specialised cell composed almost entirely of a single large lipid droplet. However, mammalian oocytes from many species contain comparatively high quantities of lipid stored as droplets in the ooplasm (Kruip et al. 1983; Cran 1985; Abe et al. 2002; Leroy et al. 2005; Sturmey et al. 2006; Aardema et al. 2011), with considerable inter species variation (Table 14). It has been suggested that, on the basis of oxygen consumption, there is sufficient lipid to support the metabolic requirements of oocyte maturation as a sole energy source (Sturmey et al. 2009b). For example, oxidation of each mole of palmitate ( $C_{16}H_{32}O_2$ ) produces net 106 moles ATP. The stoichiometry of the complete oxidation of palmitate is as follows:



Producing the following proportions of ATP:

Product/Process	No. produced per mole palmitate	Moles ATP produced per oxidation	Net ATP produced
Acetyl-CoA	8	10	80
NADH	7	2.5	17.5
FADH <sub>2</sub>	7	1.5	10.5
Total ATP produced			108
Initial activation			-2
Total Net ATP produced			106

Table 13: Stoichiometry of ATP production from the oxidation of 1 mole palmitate. Palmitate activation to palmitoyl-CoA requires 2 moles ATP. Data reproduced from (Brand 1994; Meisenberg and Simmons 2011).

Until relatively recently, the importance of the endogenous lipid store in oocytes has been largely overlooked, however a growing body of research has highlighted the vital

role of fatty acid metabolism in embryo development (Sturmeay and Leese 2003; Sturmeay et al. 2009).

Species	Triglyceride content (ng/nl volume of oocyte)
Pig	37.3
Sheep	21.2
Cow	15
Mouse	6.25

Table 14: Mean oocyte triglyceride content of mammalian species. Data reproduced with kind permission from H. Leese (2012).

Oocyte development from the primordial to a pre-ovulatory follicle housing an oocyte in metaphase II involves periods of growth, nuclear maturation and cytoplasmic development, however the precise period when the oocyte accumulates endogenous lipids is largely unknown. *In vitro*, the final stages of oocyte maturation are the most susceptible to modification of cytoplasmic lipid content. Ferguson and Leese reported that triglyceride content of bovine oocytes decreased from  $59 \pm 1.37$  ng to  $46 \pm 0.85$  ng during *in vitro* maturation (Ferguson and Leese 1999). In traditional cell or embryo culture, the major source of fatty acids in the medium is foetal calf serum (FCS) or bovine serum albumin (BSA), which also has bound lipids – and is obligatory whereas serum is less so, which influences the morphology and composition of the bovine oocyte and embryo (Sata et al. 1999). During bovine embryo development without serum, triglyceride content is relatively constant from 2 cell to hatched blastocyst stage at around  $34 \pm 0.76$  ng, but addition of 10% serum led to an increase in triglyceride content from  $33 \pm 0.65$  ng at the 5-6 cell stage to  $62 \pm 1.14$  ng in the hatched blastocyst (Ferguson and Leese 1999). Non-esterified fatty acids (NEFA) are retained by bovine oocytes before and during meiotic maturation (Aardema et al. 2011) and modification of the fatty acid content of *in vitro* maturation (IVM) media alters tolerance of the resulting embryos to cryopreservation (Shehab-El-Deen et al. 2009); an indicator of lipid content and composition (Nagashima et al. 1994). These studies indicate that the lipid profile of the *in vitro* matured oocyte is dynamic and dependent on the culture environment. On this

basis, it is widely thought that the lipid profile of the oocyte *in vivo* reflects the fatty acid composition of the follicular fluid.

#### 4.1.2 Diet and fatty acid composition

The composition of fatty acids contained in the blood plasma is influenced by maternal diet and can have very significant effects on oocyte and embryo development, reviewed by McKeegan and Sturmeay (2011). For example, oocytes of canids and felids contain a rich store of lipid (Guraya 1965) and it has been proposed that a carnivorous diet leads to increased oocyte fatty acid (Spindler et al. 2000).

Maternal metabolic stress is reported to have major effects on the fatty acid composition of blood and follicular fluid. A particularly well-studied model is the high yielding commercial dairy cow (Leroy et al. 2008a; Leroy et al. 2008b). Sustained high-volume milk production leaves the high yielding dairy cow in a state of permanent Negative Energy Balance (NEB), which is associated with reduced fertility and altered follicular fatty acid composition (Leroy et al. 2005b, 2010; Vanholder et al. 2005). Feeding the dairy cow a specialised diet including increased saturated and polyunsaturated lipid, known as ‘fat feeding’, can alleviate some of the negative effects of NEB by providing a rich energy source and reducing fatty acid content in milk (Leroy et al. 2013). NEB can be modelled *in vitro* by supplementing oocyte and embryo culture media with Non-Esterified Fatty Acids (NEFA), leading to altered oocyte and embryo fatty acid content, metabolism and gene expression (Van Hoeck et al. 2011). The embryos arising from NEFA-treated oocytes tend to have increased apoptosis and fewer total cells at blastocyst stage. Treatment with a mixture of NEFA including stearate, palmitate and oleate, the most abundant in the follicle, resulted in more dramatic perturbations to the embryo than stearate alone, including more greatly reduced blastocyst development rate, along with altered differential gene expression, amino acid and carbohydrate metabolism. This reinforces the need for more investigations incorporating a range of treatments at physiological concentrations and ratios, rather than isolated fatty acids in excess.

In the human, maternal overweight and obesity (OVOB) is associated with subfertility (Dunning et al. 2010; Jungheim et al. 2011). Several studies have focused on the composition of the follicular fluid in OVOB women, since this is the environment in which

the oocyte matures prior to ovulation and is the first key stage in establishing the embryo's metabolic and genetic phenotype during the periconceptual period in mammals (Steegers-Theunissen et al. 2013). A recent study by Valckx and colleagues (2012) reported that in OVOB women (BMI 25+), the increased serum content of C-Reactive Protein (CRP), triglycerides and insulin was reflected in the follicular fluid. This corroborated the earlier data of Robker et al (2009), who reported that obesity was associated with elevated follicular triglyceride and CRP levels, as well as lactate and androgen concentrations. Bausenwein et al. (2010) reported that oxidised Low-Density Lipoproteins (oxLDL) levels are significantly higher in the serum and follicular fluid of obese women and that the activities of catalase, glutathione oxidase and glutathione reductase were also increased (Bausenwein et al. 2010). In the whole body, oxLDL cause cardiovascular conditions such as atherosclerosis and coronary heart disease (Toshima et al. 2000), upregulate cellular ROS generation and Hypoxia-Inducible Factor 1 $\alpha$  expression (Guarino et al. 2004).

In the bovine, oocytes can mature and embryos can progress through multiple cleavage stages without exogenous substrates, relying only on endogenous TG stores (Ferguson and Leese 2006; Sturmey et al. 2009). Oocytes matured in this way were successfully fertilised and developed to blastocyst stage in normal media (Ferguson and Leese 1999; Sturmey et al. 2009). Mouse oocytes have a much smaller TG store and arrest within 15hrs of culture without exogenous substrates (Downs and Hudson 2000). Similarly, when bovine oocytes were cultured without exogenous substrate and with an inhibitor of  $\beta$ -oxidation, they arrest (Ferguson and Leese 2006). Furthermore, culture of bovine zygotes from zygote stage without exogenous substrates but supplemented with 5mM L-carnitine increased the number of morulae compared to media without L-carnitine or exogenous carbohydrate, although only 32% of these morulae developed into blastocysts (Sutton-McDowall et al. 2012). These data suggest that  $\beta$ -oxidation of endogenous TG stores is vital to oocyte maturation and resulting embryo development.

#### 4.1.3 Lipids in the oviduct and uterus.

Compared to our knowledge of the ovarian follicle, little is known about the lipid profile of oviduct and uterine fluid which support early embryo development. This gap in our understanding is presumably due to the technical challenges associated with the

collection of fresh samples from the oviduct and uterine lumen (Iritani et al. 1969, 1971, 1974; Khandoker et al. 1997, 1998; Coyne et al. 2008; Hugentobler et al. 2008; Leese et al. 2008). As a consequence, relatively little is known about lipid metabolism by preimplantation embryos *in vivo*. It was suggested that NEFA in the rabbit oviduct lumen may provide an energy substrate for early embryo development, since these oocytes can be cultured *in vitro* in simple salt-based medium supplemented with a sole NEFA such as palmitate, oleate or stearate together with BSA (Kane 1979). However, lipids have roles in addition to the provision of an oxidisable substrate for ATP synthesis, an illustration of which is given by Menezo et al. (1982) who reported that total fatty acid content of the bovine embryo increased between day 11 and 13 of development, with a specific increase in arachidonic acid; the precursor for prostaglandins, at Day 14. This could indicate the start of prostaglandin synthesis, vital to recognition of pregnancy, and suggests a more complex regulatory role for NEFA.

For an overview of the pathways discussed below, see Figure 24.

#### 4.1.4 Lipid metabolism and mitochondria

In mice, a high fat diet is associated with a deleterious mitochondrial phenotype in the oocyte (Grindler and Moley 2013). These mitochondria tend to have fewer cristae, reduced matrix electron density and an increased number of mitochondrial vacuoles (Luzzo et al. 2012). Mitochondria tend to cluster (Igosheva et al. 2010) and have reduced membrane polarisation (Wu et al. 2010), which is consistent with other tissues wherein an increase in FAO versus carbohydrate oxidation tends to decrease membrane potential (Rigoulet et al. 1998). In addition, the high fat diet oocyte tends to have fragmented spindles and clustered chromosomes (Luzzo et al. 2012).

#### 4.1.5 The role of L-carnitine in fatty acid metabolism

Metabolism of endogenous long-chain fatty acids occurs in the matrix of the mitochondria. The transport of fatty acid moieties into the mitochondrial matrix requires L-carnitine, an essential co-factor (Vaz and Wanders 2002). The transport of fatty acids into the mitochondrial matrix is a two-step process: cytosolic fatty acids in the form of fatty acyl-CoA are transesterified to L-carnitine by the enzyme Carnitine Palmitoyl Transferase 1 (CPT1B). The fatty acyl-carnitine passes through the outer mitochondrial

membrane and is transported to the matrix by carnitine-acylcarnitine translocase (CACT). CPTII transesterifies the fatty acids to mitochondrial CoA, releasing the L-carnitine to be transported by CACT back across the mitochondrial membranes. These reactions maintain fatty acid transport to the mitochondrion for  $\beta$ -oxidation and control the intracellular balance between free CoA and acyl-CoA (Vaz and Wanders 2002). Free carnitine is taken in through the diet, but can also be synthesised from lysine and methionine in mammals and other animals (Vaz and Wanders 2002). Synthesis takes place in the liver and involves the enzymes TML dioxygenase, HTML aldolase, TAMABA dehydrogenase and butyrobetainedioxygenase (BBD). Conversion of butyrobetaine to carnitine has been reported in many mammalian tissues, including the rat testis (Tanphaichitr and Broquist 1974; Vaz and Wanders 2002), although activity of these enzymes has not been reported. L-carnitine synthesis has yet to be confirmed in the early embryo, although it is possible, especially when the embryo is viewed as a discrete organism with the potential to express every gene and carry out every biological process possible in the eventual organism.

CPT1B expression has been confirmed in mouse blastocysts, though not in the zygote, 2-cell or 8-cell stages (Dunning et al. 2010). However, inhibition of CPT1B with Etomoxir significantly reduced blastocyst rates, whereas supplementing medium with L-carnitine to facilitate increase  $\beta$ -oxidation caused an increase in blastocyst rate (Dunning et al. 2010). The importance of fatty acid  $\beta$ -oxidation (FAO) is especially interesting in this case considering that the endogenous store of triglyceride in the mouse oocyte (6.25ng/nl) is significantly smaller than other organisms studied. Furthermore, again in the mouse, inhibition of CPT1B with Etomoxir or malonyl CoA arrests oocyte maturation by a mechanism that may be rescued by supplying L-carnitine or palmitic acid in the medium (Downs et al. 2009).

In addition to these effects *in vitro*, oral administration of L-carnitine to superovulated mice protects oocytes against oxidative stress (Miyamoto et al. 2010). The mechanism by which this occurs might be linked to the observation that L-carnitine supplementation causes an increase in  $\beta$ -oxidation and hence reduces the endogenous lipid stores available for lipid peroxidation (Dunning et al. 2010). However, anti-oxidant roles for L-carnitine have been well documented. For example, Wu et al. (2011) found that addition of L-carnitine to the immature porcine oocyte improved maturation and reduced ROS levels, most likely by upregulating the production of the biological antioxidant

glutathione. It is clear that L-carnitine plays an important role in early embryo development. Theoretically, addition of L-carnitine facilitates increased fatty acid  $\beta$ -oxidation, but the relationship between L-carnitine treatment and carbohydrate, amino acid and oxygen metabolism remains unknown.

#### 4.1.6 Inhibition of fatty acid $\beta$ -oxidation

An alternative approach to investigate the role of endogenous lipid stores in the early embryo is to inhibit, rather than increase  $\beta$ -oxidation.  $\beta$ -Mercaptoacetate (BMA) is a competitive inhibitor of palmitoyl-CoA dehydrogenase (long-chain 3-hydroxyacyl-coenzyme A dehydrogenase), preventing complete  $\beta$ -oxidation of fatty acids to fatty acyl-CoA and acetyl-CoA (Bauche et al. 1981). This inhibitor acts downstream of L-carnitine transport by CPT1B and can be used to investigate the mechanism proposed by Downs et al. (2009), who reported that inhibition of  $\beta$ -oxidation with Etomoxir or Malonyl-CoA decreased oocyte maturation, but that this effect was rescued by addition of L-carnitine. The authors suggested an AMPK-dependent mechanism, inhibiting malonyl-CoA formation to relieve the inhibition of  $\beta$ -oxidation. The effect of BMA on early porcine embryo development has previously been investigated (Sturmey et al. 2003). However, the effects of inhibiting endogenous  $\beta$ -oxidation during preimplantation bovine embryo development on oxidative metabolism have yet to be studied.

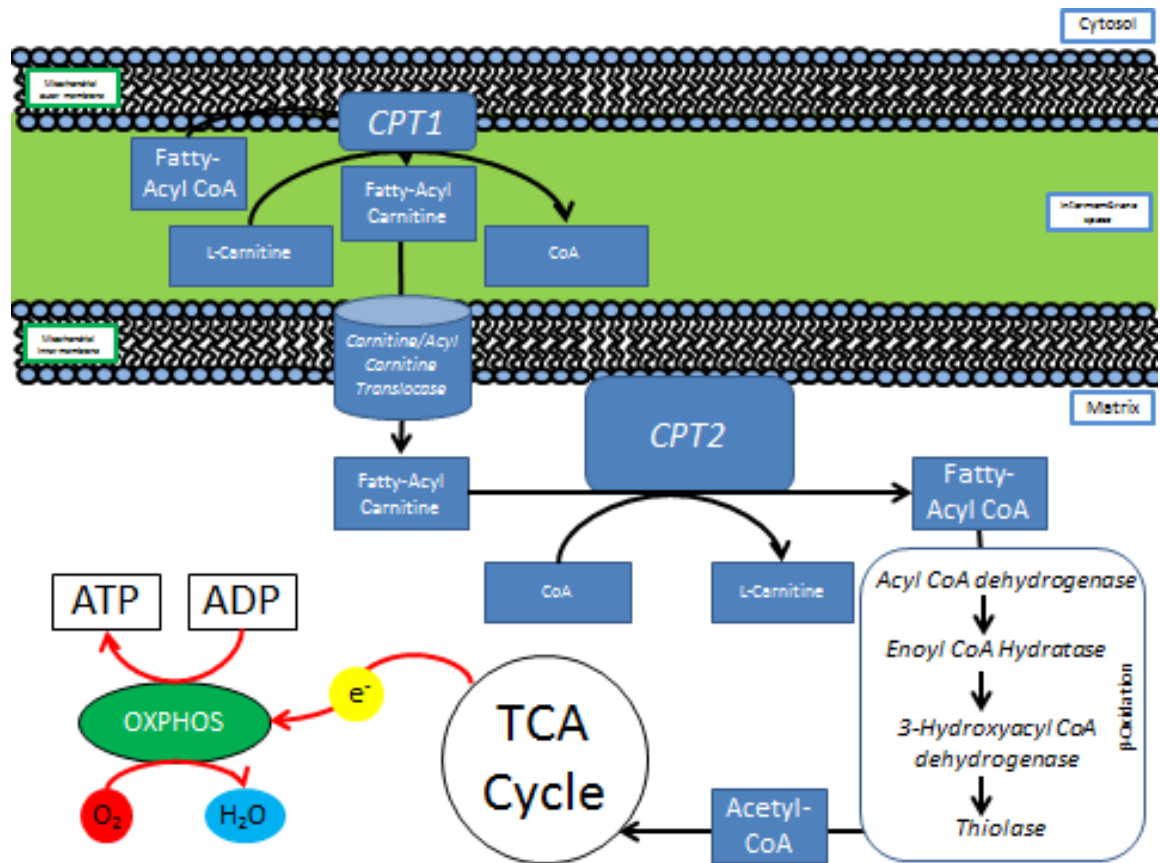


Figure 24: An overview of fatty acid transport and  $\beta$ -oxidation in mammalian cells. Fatty acids must be transported across the mitochondria; inner membrane for entry to the  $\beta$ -oxidation pathway. Fatty acyl groups conjugated to Coenzyme A (Fatty Acyl-CoA) are conjugated to L-carnitine by the mitochondrial outer membrane-bound enzyme Carnitine Palmitoyl Transferase I, releasing CoA. The fatty acyl-carnitine is transported across the mitochondrial inner membrane by the transport channel carnitine/acyl carnitine translocase, after which the L-carnitine moiety is exchanged for another CoA by carnitine palmitoyl transferase II, bound to the mitochondrial inner membrane on the matrix side. The L-carnitine is transported back into the intermembrane space by carnitine/acylcarnitine translocase. Remaining bound to CoA, the fatty acyl group undergoes  $\beta$ -oxidation, regulated by a series of 4 enzymes; Acyl-CoA dehydrogenase, Enoyl CoA hydratase, 3-Hydroxyacyl-CoA dehydrogenase (also known as long-chain fatty acyl dehydrogenase); and Thiolase. This sequence releases a fatty acid chain which is reduced in length by 2 carbons, which can undergo further  $\beta$ -oxidation, along with an Acetyl-CoA, which enters the tricarboxylic acid (TCA) cycle, providing electrons to drive ATP synthesis through oxidative phosphorylation. Figure adapted from **(Berg et al. 2002)**.

## 4.2 Aims

The aim of this chapter is to assess the effects of manipulating fatty acid metabolism on oxidative metabolism in bovine embryos. Specific objectives are to:

- Investigate the effect of manipulating  $\beta$ -oxidation of endogenous fatty acid on oxygen consumption rate and mitochondrial polarisation.
- Measure the effects of modifying endogenous stores by supplementing the culture medium with foetal calf serum and measuring embryonic lipid content, mitochondrial polarity and response to manipulation of  $\beta$ -oxidation.
- Determine the metabolic impact of supplementing the culture medium with L-carnitine.

## 4.3 Methods

Embryos were produced as described in Chapter 2. Measurement of oxygen consumption and carbohydrate turnover were carried out as described in sections 2.2 and 2.3.

### 4.3.1 The effect of acute BMA treatment on bovine blastocyst oxygen consumption measured by nanorespirometry

It was first necessary to assess the effect of inhibiting fatty acid  $\beta$ -oxidation on bovine blastocyst oxygen consumption over a short period of time. This was done by nanorespirometry. After recording the basal oxygen profile in 1 $\mu$ l Hepes SOF, 1 $\mu$ l of 0.1mM BMA in Hepes SOF was injected to each of the micropipettes carrying the blastocysts (n=3) making a final volume of 2 $\mu$ l and left to re-equilibrate for 30 minutes. Oxygen profiles were taken again for each blastocyst and data analysed using a manufacturer-designed MS Excel program.

### 4.3.2 Measurement of the effect of chronic BMA treatment on bovine blastocyst oxygen consumption by nanorespirometry

Embryos (n=110) were randomly grouped and cultured in standard SOFaaBSA or SOFaaBSA supplemented with 0.1mM BMA; a concentration that has been shown not to reduce oocyte maturation or blastocyst rate in the pig (Sturmeay and Leese 2003). Blastocysts were staged according to the Gardner protocol (Trounson and Gardner 2000) and transferred to individual culture, in single 4 $\mu$ l droplets of SOFaaBSA + 0.1mM BMA. After 24 hours, blastocysts were staged and those which had developed to the required stage were loaded into micropipettes for oxygen profiling as described in Chapter 2. At the conclusion of the assay, embryos were returned to a fresh droplet of culture medium in group conditions and allowed to develop further. This procedure was repeated to collect oxygen profiles for 4 cell, 8 cell, morula and blastocyst stage embryos. At each stage of development, data were collected for an equivalent number of control embryos cultured in SOFaaBSA.

### 4.3.3 The effect of enhanced $\beta$ -oxidation on OCR

Putative zygotes (n=120) were randomly assigned to groups and cultured in SOFaaBSA + 5mM L-carnitine, SOFaaBSA + 0.1mM BMA or standard SOFaaBSA. Embryos were cultured to the blastocyst stage on Day 8 before selection of 10 blastocysts to be profiled in the control and treatment group by BD OBS. The OBS method was performed as described previously.

### 4.3.4 Determination of follicle L-carnitine

Follicular fluid was aspirated from mature follicles (n=21), centrifuged to remove debris and stored at  $-20^{\circ}\text{C}$ . The L-carnitine fluorimetric assay kit (Abcam) was used according to the manufacturer's instructions to assay the concentration of L-carnitine in *in vivo* derived follicular fluid, FCS for cell culture (Sigma-Aldrich, Dorset, UK) and SOFaaBSA media. In this assay, an acetyl group is transferred from Acetyl-CoA to L-carnitine, followed by the oxidation of the proprietary probe with fluorescence change measured at 535/587nm. L-carnitine concentrations are calculated by calibration to a 6-point standard curve in the range 0-10mM.

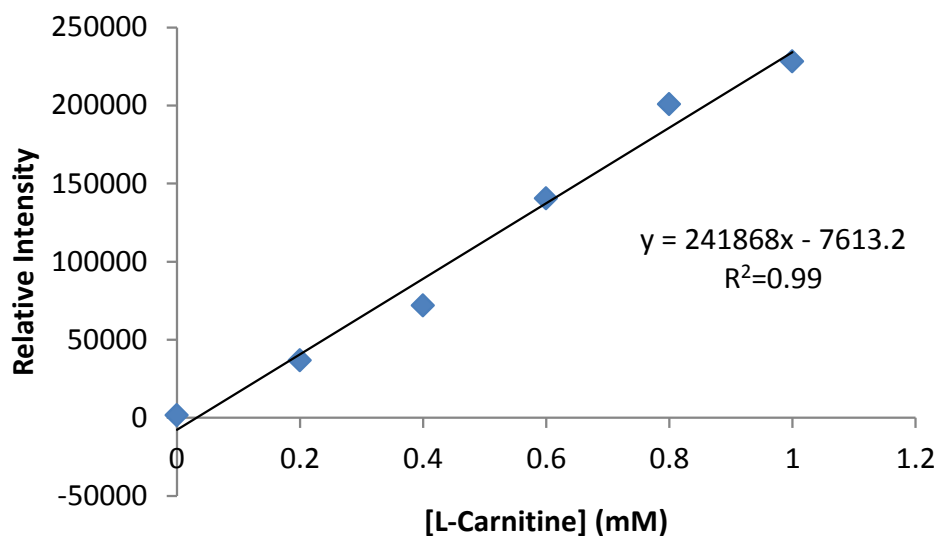


Figure 25: An example standard curve for the L-carnitine assay

### 4.3.5 Assessment of embryonic lipid content by confocal microscopy

Lipid droplets were stained with Nile Red according to the method described by Leroy et al. (2005), with the following adaptations: Embryos were selected at the relevant developmental stage and morphological quality and fixed overnight in 500 $\mu$ l 0.9% PBS with 1mg/ml Polyvinylpyrrolidone (PVP), 2% formaldehyde and 2% glutaraldehyde in groups. Fixed embryos were transferred to staining solution (250 $\mu$ l 0.9% PBS with 1mg/ml PVP (PBS/PVP) and 100nM Nile Red stain) for 2hr. Embryos were then mounted in custom-made chambers containing 50 $\mu$ l PBS/PVP for imaging.

Images were obtained on a Zeiss LSM 710 Confocal Microscope with Plan-Apochromat 40x air-based objective. Fluorophores were excited at 458nm and emission data collected at 571-741nm using a MBS 458/561 dichromatic beam splitter. Data were collected in a Z-stack of the mid 20 $\mu$ m above and below the embryo equatorial across 12 individual images (Figure 27A). This allowed representative data to be collected from each cell of early cleavage stage embryos to be assessed.

Images were analysed post-collection using Image J (NIH, <http://rsbweb.nih.gov/ij/>). Each of the 12 individual images per embryo was thresholded before specifically measuring the signal intensity.

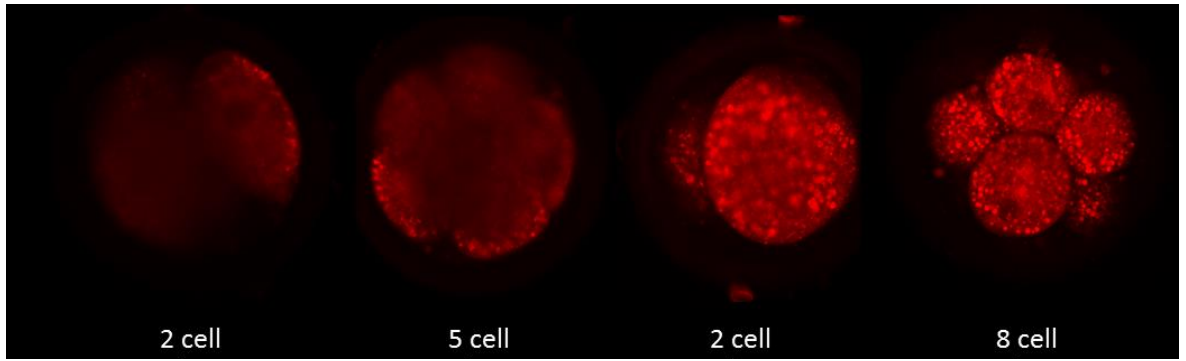


Figure 26: Example individual Nile Red images of a range of early cleavage stage embryos.

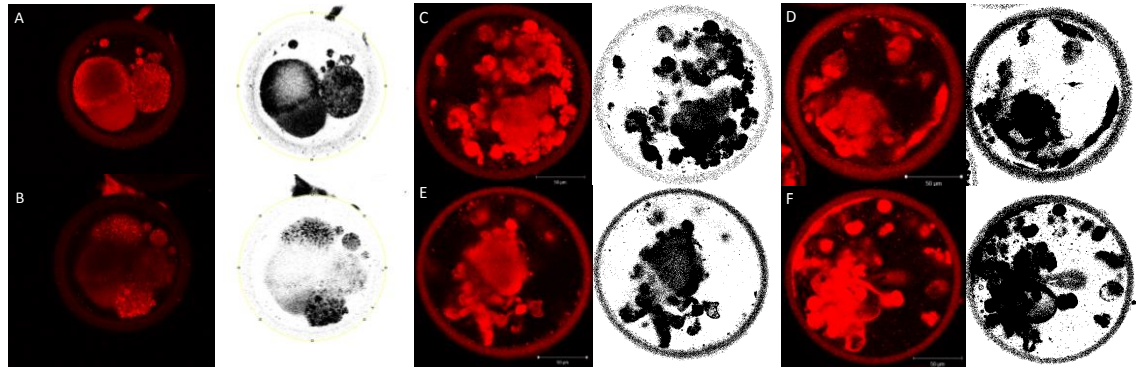


Figure 27: Example analyses of embryo lipid droplet staining by Nile Red. 12 cross section images were taken for each embryo across the central 20 $\mu$ m. Images were thresholded using ImageJ to convert the raw grayscale image to a binary image. A and B) Example images 1 and 12 from the same 5-cell embryo are shown in raw and binary form. Mean intensity was measured in a defined area for each embryo as shown in the binary images above. C-F) Raw and binary blastocyst cross-section images incorporating ICM.

Image no.	Mean intensity (raw)	Relative signal value (post-threshold)
1	1183.33	79.78
2	1131.68	74.70
3	1075.92	68.29
4	1021.84	61.48
5	978.12	55.78
6	950.07	51.61
7	928.91	48.31
8	912.77	46.01
9	895.23	43.44
10	877.81	41.37
11	857.39	38.98
12	833.07	36.59
<b>Mean</b>	<b>970.51</b>	<b>53.86</b>
<b>s.d.</b>	<b>111.4</b>	<b>14.33</b>

Blastocyst	Relative signal value (post-threshold)
A	100.69
B	109.59
C	86.54
D	112.07
<b>Mean</b>	<b>102.22</b>
<b>s.d.</b>	<b>11.54</b>

Table 15: Example Nile Red staining image analysis. Table A shows the differences in raw and binary intensity for all 12 images taken of the embryo shown in Figure 26 images 1 and 12. Only the post-threshold intensity was used for image analysis. Table B shows relative signal value of the binary blastocyst images shown in Figure 26C-F.

#### 4.3.6 Assessment of mitochondrial polarity by confocal microscopy

Blastocysts were incubated with 0.2mg/ml JC-1 and 0.05µg/ml Hoescht 3342 in pre-warmed HSOF at 39°C for 30 minutes before mounting in custom-made chambers containing 50µl HSOF at 39°C. Images were obtained on a Zeiss LSM 710 Confocal Microscope with Plan-Apochromat 40x air-based objective, with numerical aperture 0.6-1.3. JC-1 was excited at 488nm using an MBS-488 dichromatic beam splitter and emission data was collected at 511-549nm (Red) and 578-625nm (Green). Hoescht 3342 was excited at 405 using an MBS-405 dichromatic beam splitter and emission data collected at 414-501nm. Each image was analysed in ImageJ, auto-thresholded, and the area showing the embryo selected and pixel intensity measured for each channel (Figure 28). Polarisation ratios are calculated by dividing red/total (green + red) intensity. A higher ratio suggests polarisation, whereas a lower value suggests depolarisation. Mean

polarisation ratio was calculated for each experimental group and data from independent experiments combined for statistical analysis by ANOVA with post-hoc Bonferroni test, or Dunn's test if groups were unequal.

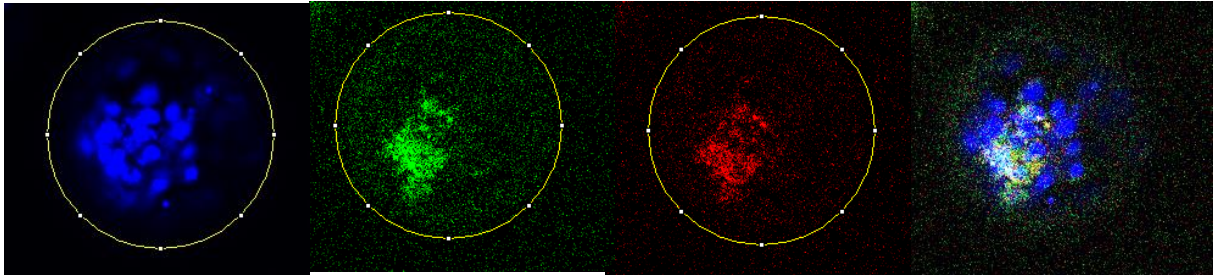


Figure 28: An example image of a blastocyst stained with JC-1 and Hoescht 3342. From left to right: (blue) the nuclear stain Hoescht 3342 (green) and (red) the ratiometric dye JC-1 which tends to form monomers with green fluorescence in depolarised mitochondria and J-aggregates with red fluorescence in more polarised mitochondria. The final image combines all 3 colours. The area highlighted in yellow in each image was analysed for fluorescence intensity with these values used to generate the depolarisation ratios for each blastocyst.

### 4.3.7 Statistical analyses

All data presented in this chapter were analysed using SigmaPlot. Data was first tested for normality using the Shapiro-Wilke test, followed by analysis of variance (ANOVA) with post-hoc Bonferroni test for equal groups or Dunn's test for unequal groups. The significance threshold was  $p < 0.05$ .

## 4.4 Results

### 4.4.1 Inhibiting FAO during embryo development increases OCR

Figure 29A shows that inhibition of  $\beta$ -oxidation with 0.1mM BMA throughout embryo culture led to significant increases in OCR at the morula ( $p=0.010$ ) and at all blastocyst stages, including B1-B7 ( $p=0.050$ ). At each stage, several embryos had very low OCR however, overall OCR increases with stage, as does the range of OCR.

Oxygen consumption of bovine blastocysts increased with blastocyst development (Figure 29B). In general, mean OCR of blastocysts treated with BMA was greater than that of the control at the equivalent stage. This was a significant difference at the fully hatched blastocyst stage, B7 ( $p=0.036$ ).

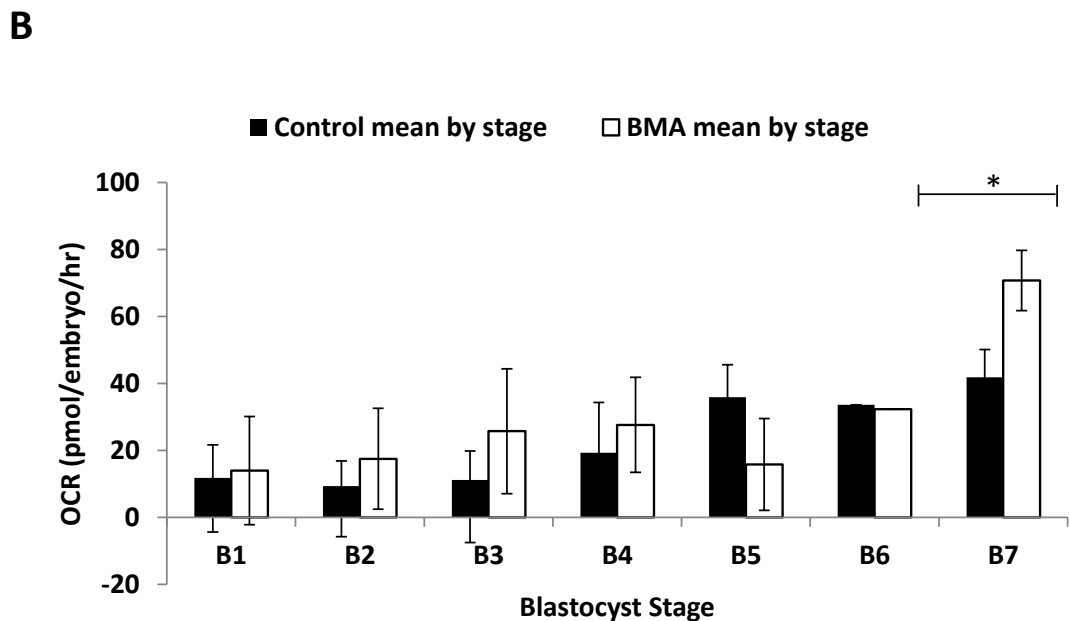
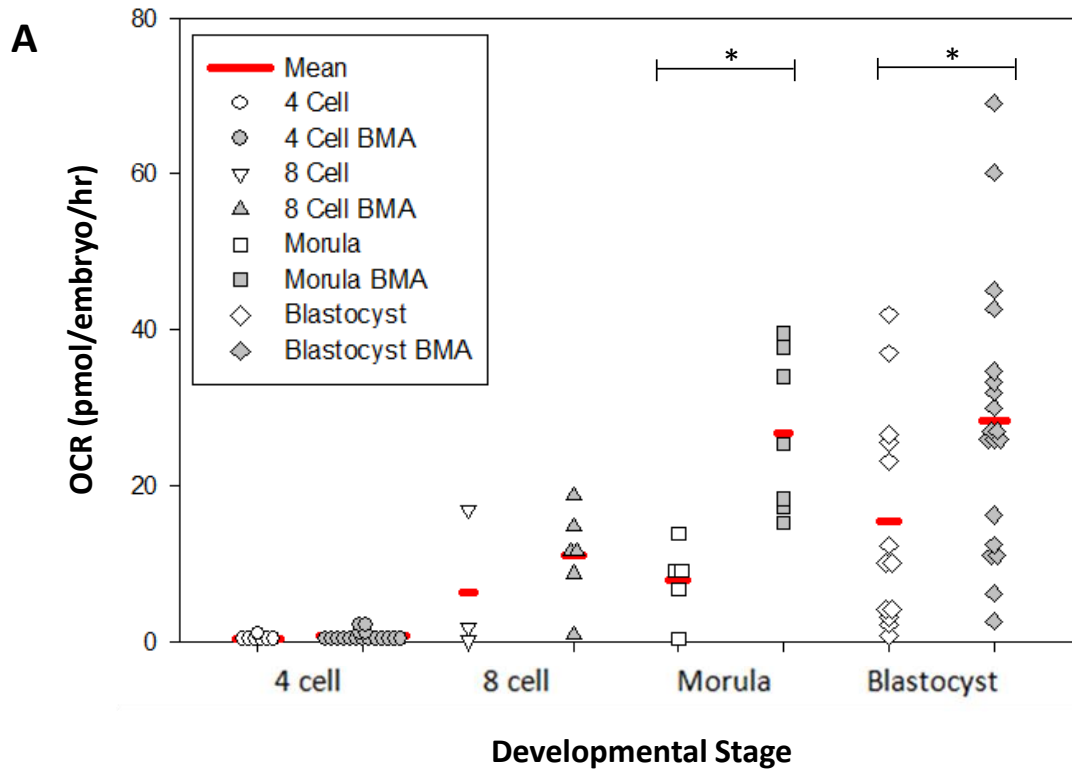


Figure 29: The effect of inhibition of  $\beta$ -oxidation with BMA on OCR during embryo development. A) The basal OCR of embryos at each stage of early development following chronic culture with 0.1mM BMA versus control embryos cultured without supplement. OCR values in pmol/embryo/hr $\pm$ 1 s.d. 4 cell: control OCR 24.4 $\pm$ 27.77 (n=7) BMA OCR=83.49 $\pm$ 47.67, n=17. 8 cell: control OCR=12.51 $\pm$ 14.9, n=12 BMA OCR=21.99 $\pm$ 25.84 n=14. Morula control OCR=2.18 $\pm$ 1.86 n=3 BMA OCR=74.71 $\pm$ 36.06, n=7. Blastocyst control OCR=30.85 $\pm$ 27.73, n=21 BMA OCR=56.49 $\pm$ 34.54, n=27. Total n=106 over 12 independent experiments. B) Mean OCR $\pm$ 1 s.d. of individual blastocysts cultured in SOFaaBSA control or SOFaaBSA + 0.1mM BMA from the zygote stage and measured on day 6, 7 or 8. Blastocysts were staged according to the Gardner Scale as described in Chapter 2.

#### 4.4.2 Acute BMA treatment increases OCR of blastocysts dependent on FCS supplementation

Following basal OCR measurement, 0.1mM BMA in HSOF was injected directly into the tube containing the respiring embryo. Acute treatment of bovine blastocysts with BMA tended to cause an immediate and dramatic increase in measured OCR, which varied between blastocysts (Figure 30B).

By contrast, individual blastocysts cultured without FCS had variable responses to acute BMA treatment, with no significant difference overall (Figure 30A).

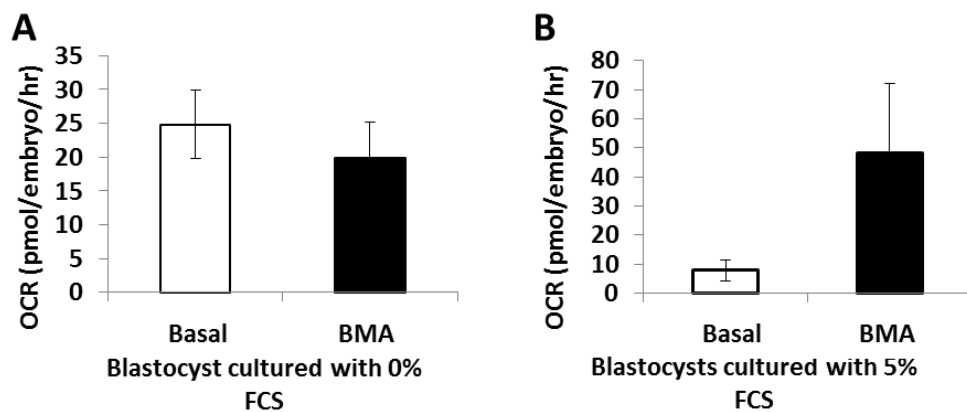


Figure 30: The effect of inhibition of  $\beta$ -oxidation with BMA on blastocyst OCR with 0% and 5% FCS. A) Blastocysts cultured with 0% FCS did not exhibit altered OCR following acute BMA treatment n=7. B) Blastocysts cultured with 5% FCS increase OCR following acute BMA treatment n=3.

#### 4.4.3 Manipulating fatty acid $\beta$ -oxidation significantly alters OCR.

Measurement of bovine blastocysts by the OBS method (Figure 31) correlated well with the nanorespirometry data shown in Figure 29. The control blastocyst OCR was  $25 \pm 5$  pmol/embryo/hr, while the BMA-treated blastocyst OCR was  $48 \pm 9$  pmol/embryo/hr (Figure 31) compared to  $56.5$  pmol/embryo/hr by nanorespirometry (Figure 31). Furthermore, treatment with L-carnitine throughout of culture decreased OCR to  $16 \pm 4$  pmol/embryo/hr.

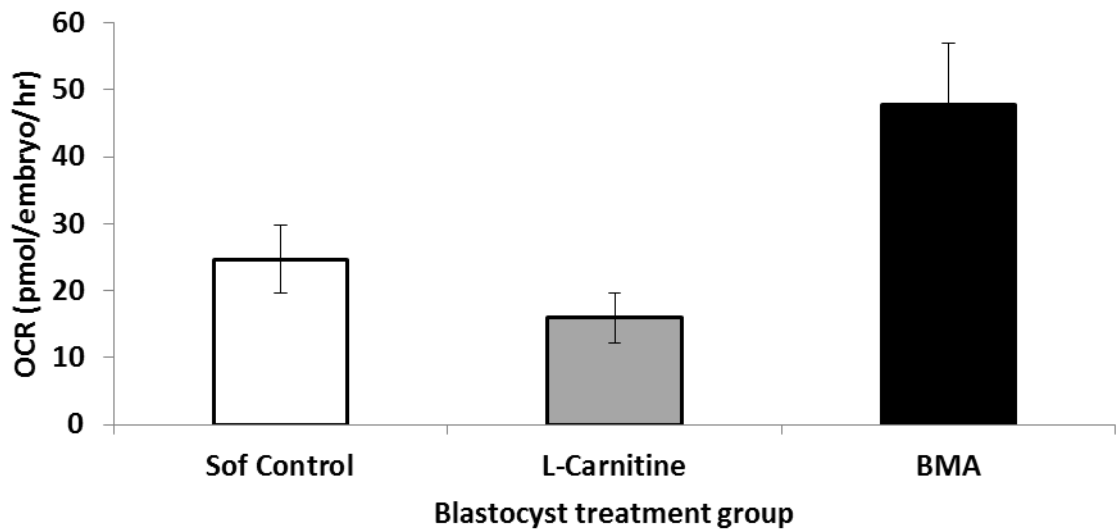


Figure 31: OCR of groups of 10 mixed blastocysts cultured with 0.1mM BMA, 5mM carnitine or control SOFaaBSA media. Measurement by BD OBS assay across 4 independent experiments. Presented as mean OCR  $\pm$  s.e.m. Control:  $24.7 \pm 5.1$ , L-Carnitine:  $15.9 \pm 3.7$ , BMA:  $47.7 \pm 9.2$ .

#### 4.4.4 Manipulating fatty acid $\beta$ -oxidation alters carbohydrate metabolism.

Treatment with L-carnitine had little effect on glucose consumption (Figure 32A,  $p=0.46$ ) but decreased pyruvate uptake at the early cleavage stages (Figure 32D,  $p<0.001$ ) and increased lactate production at blastocyst stages (Figure 32C,  $p=0.004$ ). Blastocysts treated with Etomoxir (EX) to inhibit FAO consumed significantly more glucose than equivalent blastocysts cultured with L-carnitine (Figure 32A,  $p=0.009$ ), BMA (Figure 32A,  $p=0.025$ ) and control blastocysts (Figure 32A,  $p=0.005$ ). BMA and EX treated embryos both had increased pyruvate consumption versus controls ( $p=0.018$  and  $p=0.006$  respectively) and L-carnitine treated embryos (Figure 32E,  $p=0.018$  and  $p=0.006$  respectively) (Figure 32D and E).

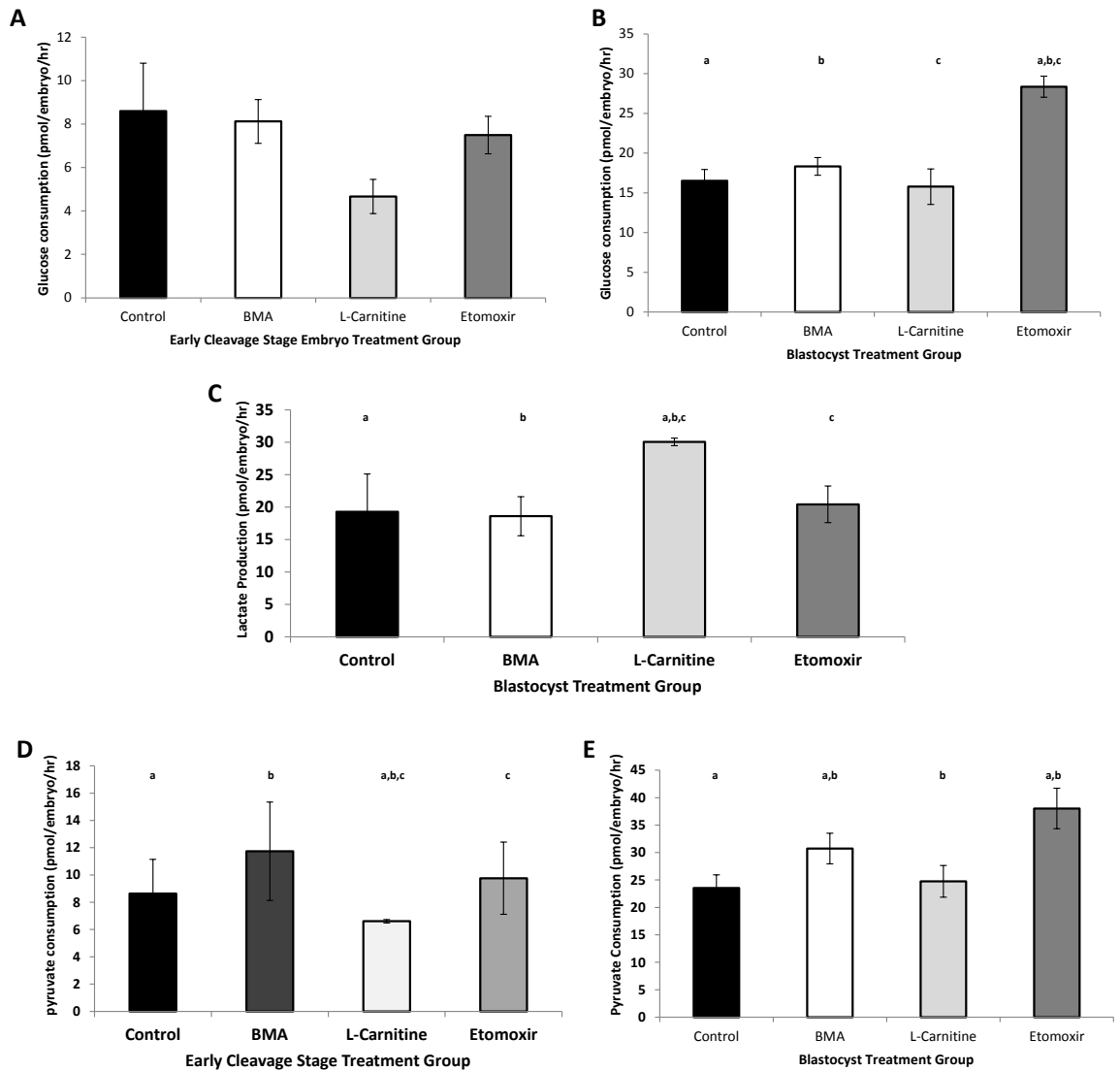


Figure 32: Carbohydrate metabolism of embryos following manipulation of  $\beta$ -oxidation with BMA, L-carnitine or Etomoxir. A) Cleavage stage glucose consumption in mean pmol/embryo/hr  $\pm$  s.e.m, n=30. Control:  $8.6 \pm 2.2$ , BMA:  $8.1 \pm 1.1$ , L-carnitine:  $4.6 \pm 0.8$ , Etomoxir:  $7.5 \pm 0.9$ . B) Blastocyst glucose consumption in mean pmol/embryo/hr  $\pm$  s.e.m, n=35. Control:  $16.5 \pm 1.4$ , BMA:  $18.3 \pm 2.2$ , L-carnitine:  $15.8 \pm 1.3$ , Etomoxir:  $28.4 \pm 1.1$ . C) Blastocyst lactate production in mean pmol/embryo/hr  $\pm$  s.e.m, n= 30. Control  $19.3 \pm 5.8$  pmol/embryo/hr, BMA  $18.6 \pm 3.0$  pmol/embryo/hr, L-carnitine  $30.0 \pm 0.6$  pmol/embryo/hr, Etomoxir  $20.4 \pm 2.8$  pmol/embryo/hr. D) Cleavage stage pyruvate consumption in mean pmol/embryo/hr  $\pm$  s.e.m, n=30. Control:  $8.6 \pm 2.5$ , BMA:  $11.7 \pm 3.6$ , L-carnitine:  $6.6 \pm 0.1$ , Etomoxir:  $9.8 \pm 2.6$ . E) Blastocyst pyruvate consumption in mean pmol/embryo/hr  $\pm$  s.e.m, n=35. Control:  $23.5 \pm 2.4$ , BMA:  $30.7 \pm 2.8$ , L-carnitine:  $24.8 \pm 2.9$ , Etomoxir:  $38.0 \pm 3.7$ . Data bars with the same letter are significantly different from each other.

#### 4.4.5 L-carnitine is present in follicular fluid and FCS

The concentration of L-carnitine in FCS was 0.1mM (Figure 33), while the concentration of L-carnitine in preovulatory follicles with a diameter greater than 1cm was 0.22mM and varied little between follicles from different bovine ovaries (n=21). Consumption of L-carnitine from the SOFaaBSA culture medium supplemented with 0.5mM L-carnitine was  $0.84\pm 0.04$ pmol/embryo/hr in day 1 embryos, increasing to  $1.66\pm 0.32$ pmol/embryo/hr in day 2 embryos.

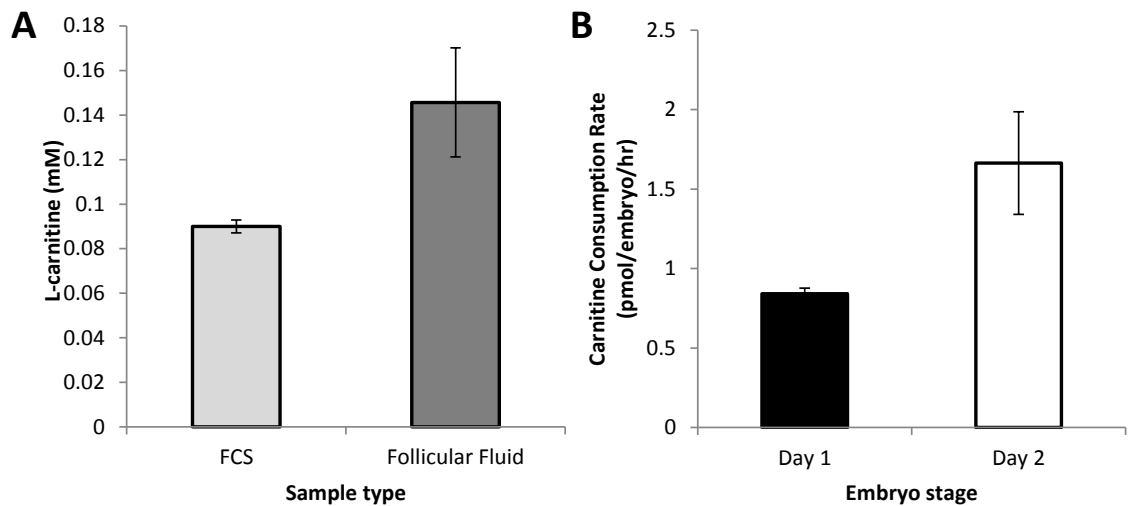


Figure 33: L-carnitine concentration and consumption of L-carnitine during early cleavage stages. A) Mean L-carnitine concentration of FCS ( $0.09\pm 0.003$ ) and follicular fluid ( $0.15\pm 0.02$ ) in  $\text{mM}\pm\text{s.e.m.}$  Data collected from 5 separate collections over three independent experiments. B) Consumption of L-carnitine of Day 1 n=5 and Day 2 n=10 embryos measured in groups of 5 over 24hr presented as  $\text{mean}\pm\text{s.e.m.}$

#### 4.4.6 FCS supplementation increases lipid content in day 2-3 embryos

Embryos were cultured for 8 days in the presence of FCS at a range of concentrations (0-10%). Embryos supplemented with FCS had significantly increased lipid staining intensity than controls, suggesting higher lipid content (Figure 34A). However, there was no linear correlation between lipid droplet content and FCS concentration (Figure 34C). At the blastocyst stage, there were no significant differences in lipid content regardless of FCS concentration used (Figure 34B and D).

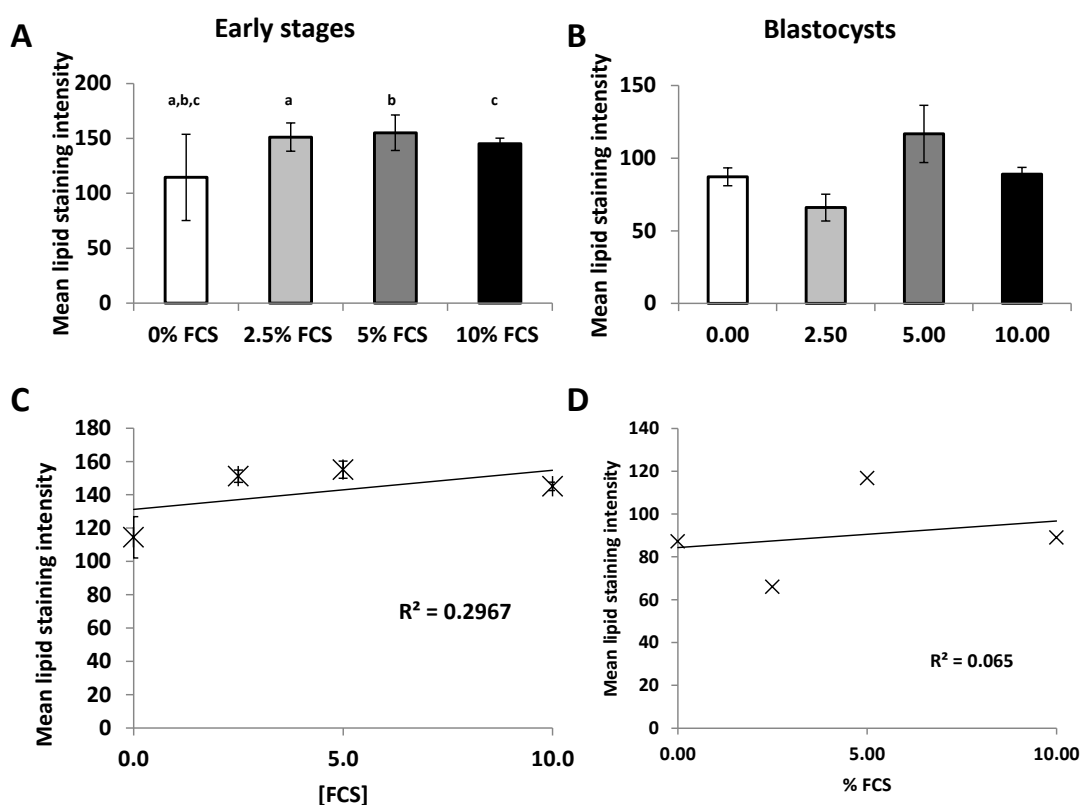


Figure 34: The effect of increasing concentrations of FCS during culture on embryo lipid staining. A) Mean lipid staining intensity (arbitrary units)±s.e.m. of day 2-3 embryos of stages 2-8 cell produced with 0% (n=21), 2.5% (n=22), 5% (n=21) or 10% (n=9) FCS. There is not a linear relationship between % FCS and lipid staining intensity. B) Mean lipid staining intensity (arbitrary units)±s.e.m. of day 2-3 embryos of stages 2-8 cell produced with 0% (n=16), 2.5% (n=5), 5% (n=12) or 10% (n=4) FCS. Data points with the same letter are significantly different from each other.

#### 4.4.7 Increasing FCS concentration correlates with decreased mitochondrial polarisation of day 2-3 embryos

Embryos cultured in SOFaaBSA supplemented with 5% and 10% (v/v) FCS had significantly more depolarised mitochondria in comparison to control embryos cultured without FCS (Figure 35A). There was a negative correlation between FCS concentration (0-10%) and mean polarisation ratio (Figure 35B,  $p=0.018$ ).

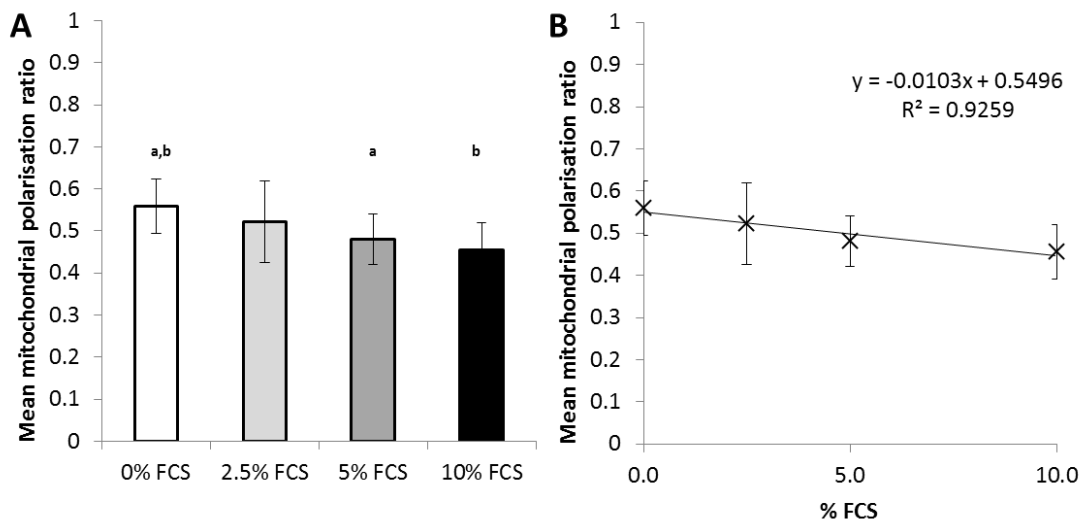


Figure 35: The effect of increasing concentrations of FCS during culture on embryo mitochondrial polarisation ratio. A) Mean polarisation ratio  $\pm$  s.e.m of day 2-3 embryos of 1-8 cell stages across 5 independent experiments. 0% FCS  $n=17$ , 2.5% FCS  $n=18$ , 5% FCS  $n=17$ , 10% FCS  $n=7$ . Data points with the same letter are significantly different from each other. B) Linear correlation of data presented in a),  $p=0.018$ .

#### 4.4.8 Manipulating $\beta$ -oxidation of endogenous stores significantly alters lipid droplet staining

Figure 36A shows that cleavage stage embryos exposed to L-carnitine throughout development ('chronic exposure') had significantly decreased lipid staining intensity compared to control embryos ( $p=0.009$ ) and BMA-treated embryos (Figure 36A,  $p<0.001$ ). Day 7 Blastocysts treated with 0.1mM BMA had significantly higher intensity than controls or L-carnitine treated blastocysts (Figure 36B,  $p=0.022$ ).

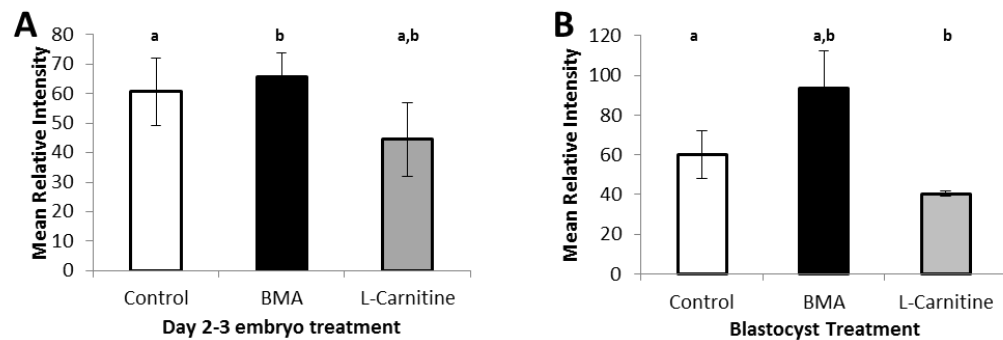


Figure 36: The effect of manipulating  $\beta$ -oxidation during culture without FCS on embryo lipid staining. A) Mean lipid staining intensity (arbitrary units) $\pm$ s.e.m. of day 2-3 embryos of stages 2-8 cell produced with 0% FCS. Control ( $n=8$ ), 0.1mM BMA ( $n=13$ ), L-carnitine ( $n=10$ ) across 2 independent experiments. B) Mean lipid staining intensity (arbitrary units) $\pm$ s.e.m. of Day 7 blastocysts produced with 0% FCS. Control ( $n=6$ ), 0.1mM BMA ( $n=7$ ), L-carnitine ( $n=5$ ) across 2 independent experiments. Data points with the same letter are significantly different from each other.

#### 4.4.9 Manipulating FAO without FCS significantly decreases mitochondrial polarisation ratio during early cleavage

The mitochondrial polarisation ratio was significantly reduced in BMA-treated and L-carnitine treated embryos compared to controls (Figure 37,  $p=0.002$ ). However, there were no significant differences in blastocyst mitochondrial polarisation.

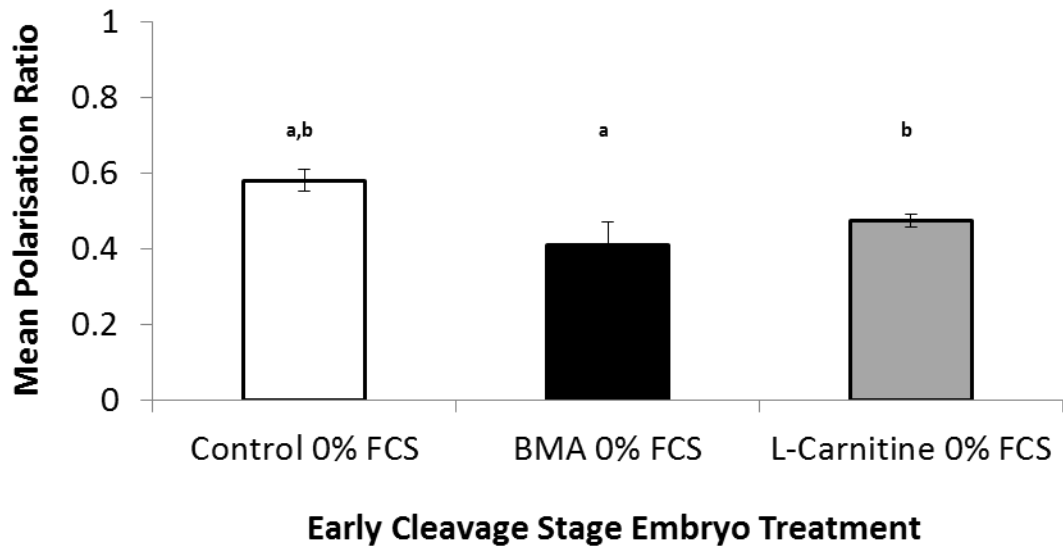


Figure 37: Mean polarisation ratio  $\pm$  s.e.m of day 2-3 embryos of 2-8 cell stage chronically cultured with or without manipulators of  $\beta$ -oxidation. Control  $n=9$ , BMA  $n=10$ , L-carnitine  $n=13$  across 2 independent experiments. Data points with the same letter are significantly different from each other.

#### 4.4.10 Manipulating FAO does not affect blastocyst polarisation ratio with or without FCS

Figure 38 shows that there was no change in mitochondrial polarisation rate in blastocysts following culture with 0% (A) or 5% (B) FCS.

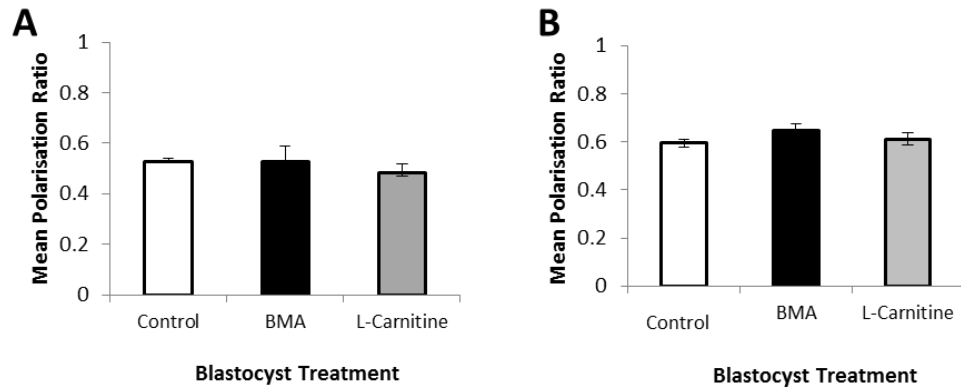


Figure 38: The effect of manipulating  $\beta$ -oxidation during culture +/- FCS on blastocyst lipid staining. A) Mean polarisation ratio  $\pm$  s.e.m of day 7 blastocysts cultured with or without chronic manipulators of  $\beta$ -oxidation and 0% FCS. Control n=8, BMA n=5, L-carnitine n=5 across 2 independent experiments. No significant differences between treatments were apparent. B) Mean polarisation ratio  $\pm$  s.e.m of day 7 blastocysts cultured with or without chronic manipulators of  $\beta$ -oxidation and 5% FCS. Control n=6, BMA n=8, L-carnitine n=7, L-carnitine + BMA n=5 across 3 independent experiments. No significant differences between treatments were apparent.

#### 4.4.11 Treatment with BMA, Etomoxir or L-carnitine does not alter development rate or blastocyst cell allocation.

Cleavage and blastocyst development rates were recorded over 7 independent experiments and did not differ between control embryos and embryos treated with BMA or L-carnitine (Table 16). Embryos were cultured to blastocyst stage in the presence of BMA, Etomoxir or L-carnitine and stained for differential cell counting as described above (Section 2.6). Blastocysts of different treatment groups had similar mean cell counts (Figure 36A) and trophoctoderm to inner cell mass ratios (Figure 39B). Additionally, inclusion of 5% FCS in culture medium had no effect on cell count or TE:ICM ratio ( $p=0.83$ ).

	Control	BMA	L-carnitine
Cleavage rate	73%	81%	72%
Number cleaved/total	218/298	114/140	152/211
Blastocyst rate	25%	24%	24%
Number of blastocysts/total	58/235	50/208	24/99

Table 16: Cleavage and blastocyst rates for control, BMA and L-carnitine treated embryos. Rates recorded over 7 independent experiments.

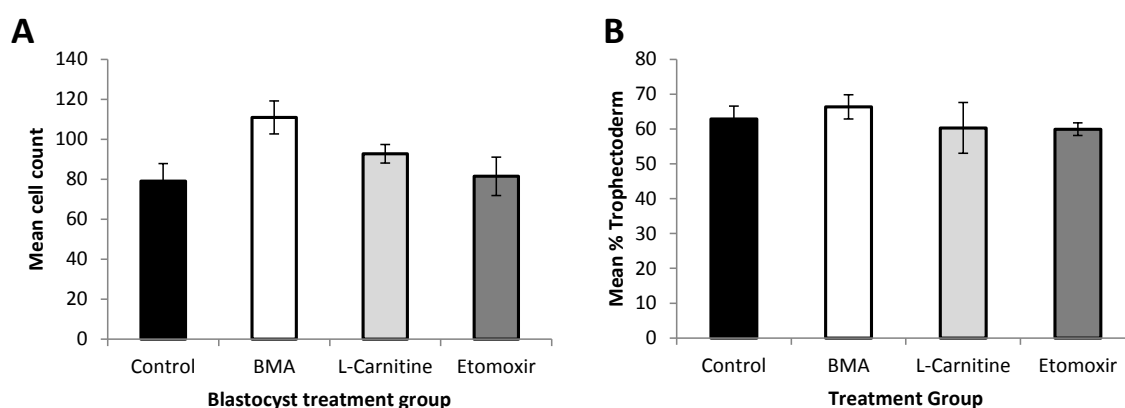


Figure 39: Cell allocation of blastocysts following treatment with BMA, Etomoxir or L-carnitine. A) Mean total cell count did not differ between control, BMA, L-carnitine and Etomoxir treated blastocysts displayed as mean s.e.m. Control:  $79 \pm 8.74$ , BMA:  $111 \pm 8.21$ , L-carnitine:  $93 \pm 4.59$ , Etomoxir:  $81 \pm 9.55$ . B) Differential counts of blastocysts cultured with BMA, L-carnitine or Etomoxir versus controls presented as % Trophectoderm. Control  $63.1 \pm 3.7$  %,  $n=8$ ; BMA  $66.3 \pm 3.5$ ,  $n=6$ ; L-carnitine  $60.3 \pm 9.4$ ,  $n=3$ ; Etomoxir  $59.9 \pm 1.8$ ,  $n=3$ . Data collected over 3 independent collections and experiments.

#### 4.4.12 Treatment with L-carnitine may accelerate blastocyst development

In order to assess differences in embryo development rate following manipulation of  $\beta$ -oxidation, the Primo Vision embryo tracking system was used. One cohort of 9 2-cell embryos from a specific treatment group (BMA, L-carnitine, Etomoxir or controls) were allocated to a well-of-the-well (WoW) culture dish to track development over 8 days of development.

Times of morula formation, blastocoel expansion and cell death were recorded. Data collected using the Primo Vision system (Figure 40) suggest that embryos treated with L-carnitine may begin blastocoel expansion sooner than controls (5.08 days compared to 6.75,  $p=0.017$ ) or Etomoxir-treated embryos (7.2 days,  $p=0.003$ ).

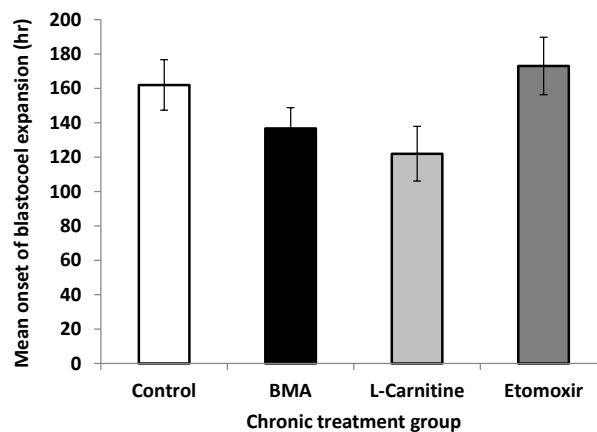


Figure 40: Time of blastocoel expansion recorded using the Primovision system and Well-of-the-well culture of L-carnitine, BMA, Etomoxir treated or control embryos. Treatment groups measured independently over a series of 12 independent collections and experiments. Data recorded as mean number of hours post-fertilisation  $\pm$  s.d. Control  $162 \pm 15.9$  hr,  $n=6$ ; BMA  $136.7 \pm 5.7$  hr,  $n=3$ , L-carnitine  $122 \pm 5.1$  hr,  $n=3$ ; Etomoxir  $173 \pm 7.2$  hr,  $n=3$ .

## 4.5 Discussion

The bovine embryo has a large endogenous store of triglyceride, which is affected by maternal diet *in vivo* (Leroy et al. 2011; Leroy et al. 2013) and culture media composition *in vitro* (Ferguson and Leese 1999; Van Hoeck et al. 2011). Manipulation of oocyte fatty acid metabolism by inhibiting  $\beta$ -oxidation with BMA, Etomoxir or other inhibitors or promoting  $\beta$ -oxidation with L-carnitine affects oocyte maturation and subsequent embryo developmental competence (Downs et al. 2009; Dunning et al. 2010; Sutton-McDowall et al. 2012). In this chapter, the effects of manipulating the metabolism of endogenous stores during embryo development were investigated. The aim was to highlight the importance of fatty acid  $\beta$ -oxidation (FAO) on embryo development, oxidative metabolism and mitochondrial function.

### 4.5.1 Inhibiting $\beta$ -oxidation during embryo development increases OCR

Individual bovine embryo OCR increased with stage of development (Figure 29A), corroborating data collected by other methods (Thompson et al. 1996; Trimarchi et al. 2000a; Lopes et al. 2005).

Reducing FAO in embryos with 0.1mM BMA throughout culture led to a significant rise in oxygen consumption at the morula and blastocyst stages. The increased OCR may be more pronounced at the later stages due to increased metabolic activity associated with blastocoel expansion. Furthermore, inhibition of  $\beta$ -oxidation in the cleavage stage embryo could lead to legacy effects on metabolism at the blastocyst stage, alongside the switch from generating ATP from glycolysis at the cleavage stages to OXPHOS at the later stages (Trimarchi et al. 2000b).

This increase in OCR was surprising, since the inhibition of fatty acid oxidation might be expected to limit access to a major endogenous energy source. Thus one might predict that inhibition of FAO would result in reduced metabolism and OCR. The increased OCR observed (Figure 29) may have arisen from an intrinsic uncoupling effect of fatty acids due to UCP activation (Rousset et al. 2004; Fedorenko et al. 2012) or accumulation of NEFA in the mitochondrial inner membrane, since oxidation to remove the fatty acids was

inhibited. An increase in OCR due to NEFA analogous to the effects of uncouplers such as FCCP or DNP has been reported in a variety of cell types (Rottenberg and Hashimoto 1986; Luvisetto et al. 1990; Nobes et al. 1990). This would reduce the coupling of electron transport to oxidative phosphorylation, leading to inefficiency, where a greater consumption of oxygen would be required to produce a sufficient level of ATP. To investigate this possibility in the future, the coupled OCR of BMA-treated blastocysts could be measured alongside control blastocysts. A second possibility is that the additional oxygen consumption was non-mitochondrial in origin. This could be investigated by treating BMA-treated blastocysts with myxothiazol, which inhibits electron transfer by complex III, abolishing all mitochondrial oxygen consumption.

#### 4.5.2 Manipulating fatty acid $\beta$ -oxidation significantly alters OCR

L-carnitine is an essential co-factor for the transport of fatty acyl-CoA into mitochondria and plays a pivotal role in fatty acid oxidation (Bremer 1983). Supplementing embryo culture media with L-carnitine resulted in a 33% decrease in OCR. This was somewhat surprising as L-carnitine has been reported to stimulate fatty acid oxidation in oocytes and embryos (Dunning et al. 2010; Valsangkar and Downs 2013). Consequently one might have expected OCR to increase to reflect an increase in  $\beta$ -oxidation of fatty acids.

One explanation for this apparent discrepancy might be a change in the strategy by which ATP is synthesised. The total energy demands of the developing embryo are not likely to be changed in the L-carnitine treated group, however, by promoting FAO, a higher proportion of ATP may be supplied at the expense of other pathways. Since FAO is the most efficient way of generating ATP it is possible that a partitioning towards FAO and concomitant fall in activity in other pathways was seen as an overall fall in OCR.

#### 4.5.3 Manipulating fatty acid $\beta$ -oxidation alters carbohydrate metabolism.

L-carnitine treatment of bovine embryos led to a rise in lactate production and fall in pyruvate consumption, suggesting that more glucose and pyruvate were converted to lactate by glycolysis rather than entered the Krebs cycle for complete oxidation. This suggested a switch from carbohydrate to fatty acid oxidation and a reduction in OCR used

for carbohydrate metabolism. The idea that increased FAO leads to a fall in glucose metabolism was proposed by Randle and colleagues (Randle et al. 1963; Randle 1998). This finding is analogous to the recent study by Van Hoeck and colleagues, who reported that supplementation of bovine embryo cultures with a mixture of fatty acids caused a reduction in glucose uptake, lending more support to the idea that increased FAO in embryos inhibits carbohydrate metabolism (Van Hoeck et al; 2011).

A number of reports have used Etomoxir, which irreversibly inhibits CPT1 activity and hence FAO during oocyte maturation and embryo development (Downs et al. 2009; Dunning et al. 2010; Paczkowski et al. 2013). This inhibition is upstream of BMA, so comparison of embryos treated with both inhibitors could determine whether the mechanism involved in increasing OCR is due specifically to inhibition of fatty acid transport and  $\beta$ -oxidation, as well as highlight any difference in metabolism dependent on the site of inhibition. Etomoxir inhibition of mouse OCCs *in vitro* prevented subsequent embryo maturation to the blastocyst stage (Dunning et al. 2010). However, treatment with methyl palmoxirate, another inhibitor of CPT1, from the 2 cell stage reduced but did not abolish mouse blastocyst production (Hewitson et al. 1996). This suggests that FAO plays a vital role on mouse oocyte maturation. However, in this study bovine blastocyst rates were unaffected in embryos cultured with BMA or Etomoxir from the zygote stage (Table 16). Potentially, treatment with BMA or Etomoxir allows  $\beta$ -oxidation of short and medium-chain fatty acids to continue.

Blastocysts treated with Etomoxir to inhibit FAO consumed more pyruvate than L-carnitine treated embryos and took up more glucose than equivalent blastocysts in all other treatment groups, suggesting a more extreme phenotype than with BMA. This was perhaps due to the difference in site of action, as Etomoxir acts upstream of BMA. In addition, Etomoxir is irreversible while BMA is a competitive inhibitor, so it is possible that Etomoxir inhibited FAO more effectively. In a recent study by Valsangkar and Downs (2013), L-carnitine stimulated meiotic resumption in mouse oocytes, while BMA and Etomoxir each inhibited meiotic resumption. Furthermore, Dunning et al. (2010) reported that Etomoxir treatment during oocyte development or zygote cleavage reduced rates of blastocyst formation, while L-carnitine treatment during oocyte maturation increased  $\beta$ -oxidation 2-fold as well as improving subsequent blastocyst rate. While it appears that manipulation of FAO during oocyte maturation rather than during early cleavage has

more dramatic effects on subsequent embryo development, the present data show that inhibiting or promoting FAO modification during embryo development affects other aspects of oxidative metabolism.

#### 4.5.4 L-carnitine is present in the follicular environment and consumed by early cleavage stage embryos

L-carnitine is present at a concentration of  $24 \pm 5.5 \mu\text{mol/l}$  in serum and  $29 \pm 6.6 \mu\text{mol/l}$  in follicular fluid in the human (Leroy et al. 2011; Valckx et al. 2012). In the present study, the *in vivo* concentration of L-carnitine in bovine antral follicles was more than double that of FCS (0.09mM) at 2mM. This value is also much higher than that reported for bovine plasma; 270-700 $\mu\text{M}$  (Carlson et al. 2007) and suggests that L-carnitine accumulates in the ovarian follicle. The presence of L-carnitine in the follicular environment is particularly interesting in light of the triglyceride stores present in the bovine oocyte and the consumption of triglyceride during *in vitro* maturation (Ferguson and Leese 1999; Sturmey and Leese 2003; Ferguson and Leese 2006). It would be interesting to measure the concentration of L-carnitine in follicular fluid at different stages of follicle development and discover if the concentration changes, perhaps to support *in vivo* oocyte maturation.

The presence of L-carnitine in follicular fluid; the natural environment, presents a strong physiological argument for the inclusion of L-carnitine in oocyte maturation systems. The presence of L-carnitine in *in vitro* maturation media has previously been shown to boost maturation and subsequent embryo development (Dunning et al. 2010; Sutton-McDowall et al. 2012; Valsangkar and Downs 2013). However, the concentrations used greatly exceeded those found in the follicle. Taken together, these findings suggest that L-carnitine may have an important role in oocyte maturation *in vivo* and might improve the physiological relevance of the bovine model. Serum, which includes L-carnitine, is often a constituent of *in vitro* maturation systems and could account for one of the benefits of serum addition. Foetal Calf Serum is also widely used in cell culture practices generally and the addition of L-carnitine should be considered as having physiological relevance.

In the FAO manipulation experiments (results sections 4.4.3, 4.4.4, 4.4.9-0), SOF medium was supplemented with 5mM L-carnitine, a concentration reported to improve the proportion of bovine zygotes which develop to blastocysts (Sutton-McDowall et al. 2012).

To the best of my knowledge, the concentration of L-carnitine in reproductive tract fluids, such as uterine and oviduct fluids, has not been measured, however the concentration of L-carnitine found in follicular fluid ( $0.15\pm 0.02\text{mM}$ ) was much lower than in the culture medium (5mM, Figure 33). This highlights the discrepancy between physiological levels of compounds and the concentrations used in laboratory studies and the relevance of data collected in supra-physiological conditions.

The data in Figure 33C shows that bovine embryos depleted carnitine from the *in vitro* culture environment. Consumption of L-carnitine by bovine embryos increased from Day 1 to Day 2.

#### 4.5.5 FCS supplementation increases lipid content in day 2-3 embryos

Foetal Calf Serum has long been added to embryo culture medium where it improves success rates by providing a range of metabolic substrates, including fatty acids, and growth factors, although it has been reported to lower mitochondrial number and efficiency (Crosier 2001). Lipid content was increased in early cleavage stage embryos cultured with FCS (Figure 34), in agreement with the findings of Ferguson and Leese (1999). However accumulation of lipid was not dependent on the concentration of FCS (2.5%-10%) in the medium. This suggests that embryos can replenish or maintain their TG reserves from the FCS, maintaining endogenous TG to a relatively constant level regardless of FCS concentration. It is possible that the absence of FCS or another source of NEFA in *in vitro* culture media leads to a fall in  $\beta$ -oxidation, although *in vivo* derived blastocysts have similar TG content to those produced *in vitro* without serum (Ferguson and Leese 1999). This is in agreement with the data of Leroy et al. (2005), who reported that bovine embryos cultured in the presence of 5% FCS had significantly more TG by the morula stage, and that of Aardema et al. (2011), who reported that supplementation of *in vitro* oocyte maturation media with oleic acid increased TG content. As in its natural environment, the embryo is exposed to a source of NEFA, culture with FCS, or at least a source of exogenous lipid, may be a more physiologically relevant culture technique.

#### 4.5.6 Increasing FCS concentration correlates with decreased mitochondrial polarisation of day 2-3 embryos

A reduction of mitochondrial transmembrane potential ( $\Delta\Psi_m$ ) is a direct marker of mitochondrial function and can be caused by apoptosis and/or impaired mitochondrial regulation. To assess transmembrane potential in preimplantation embryos, the ratiometric dye JC-1 was used. Mitochondrial polarisation ratios were calculated by dividing red/total intensity (green + red). A higher ratio suggests polarisation, whereas a lower value suggests depolarisation. This method of quantification obviates artefacts commonly detected in the use of the marker JC-1 (Brand and Nicholls 2011) since non-specific staining similar to green and red channels is cancelled out.

A linear correlation was found between increasing FCS concentration and decreasing polarisation ratio in early cleavage stage embryos. This is in agreement with the data of Wu et al. (2010), who reported a decrease in mitochondrial membrane polarisation oocytes from mice fed a high fat diet. When considered with the lipid-staining data (Figure 34), this suggests that increased embryonic lipid content is related to mitochondrial phenotype. Even mildly hyperlipidaemic conditions could compromise embryonic mitochondrial polarity.

No significant correlation was found between polarisation ratios and lipid staining intensity, since lipid uptake appeared to increase very dramatically on addition of the lowest concentration of FCS and reach a threshold. A positive correlation was found between FCS concentration and lipid stain intensity. Treatment with FCS also reduced the variation in lipid content between embryos.

#### 4.5.7 Manipulating $\beta$ -oxidation of endogenous stores significantly alters lipid droplet staining

While it seems likely that mammalian embryos utilise TG as an energy source during development, a decrease in lipid content between the oocyte and blastocyst stages has not been observed (Sturmey et al. 2009a; McKeegan and Sturmey 2011). Several studies have reported that bovine embryos take up lipid from the culture media, perhaps suggesting that it serves to replenish endogenous stores (Ferguson and Leese 1999; Aardema et al. 2011).

In the present study, addition of L-carnitine to promote  $\beta$ -oxidation throughout the embryo culture period led to significantly reduced lipid content at the early cleavage stages (Figure 36), implying that these embryos consumed TG more rapidly than control or BMA-treated embryos. Treatment with BMA to inhibit  $\beta$ -oxidation led to significantly increased lipid content at blastocyst stage ( $p=0.022$ ), suggesting these embryos had consumed less TG than control or L-carnitine-treated embryos. Taken together, these data strongly suggest that L-carnitine promotes fatty acid  $\beta$ -oxidation and accelerates the metabolism of lipid at early pre-implantation stages, while BMA inhibits  $\beta$ -oxidation so that most lipid remains, even at the blastocyst stage. This supports the hypothesis that bovine embryos can develop to the blastocyst stage even though lipid metabolism is inhibited.

Treatment with L-carnitine also reduced variation in lipid staining, suggesting that supplementation had overcome individual variation in the concentration of L-carnitine present in the oocyte, or perhaps levels of synthesis in the embryo, forcing embryos to consume most of their lipid store. There was no significant difference between L-carnitine treatment and controls at the blastocyst stage, supporting the hypothesis that additional L-carnitine has no beneficial effect on bovine embryos cultured without serum. The variation in the BMA-treated group could be due to variation in oocyte TG content, based on maternal age, diet or variation in metabolism of medium and short-chain fatty acids.

When bovine embryos were supplemented with L-carnitine or BMA in the presence of 5% FCS during embryo culture, no differences were observed in lipid droplet staining during early cleavage or blastocyst stages. Taken with the above data, this strongly suggests that bovine embryos consume endogenous TG during normal *in vitro* development, replenishing endogenous stores when an exogenous supply of lipid, such as NEFA found in FCS, is available. These findings are summarised below in Figure 41.

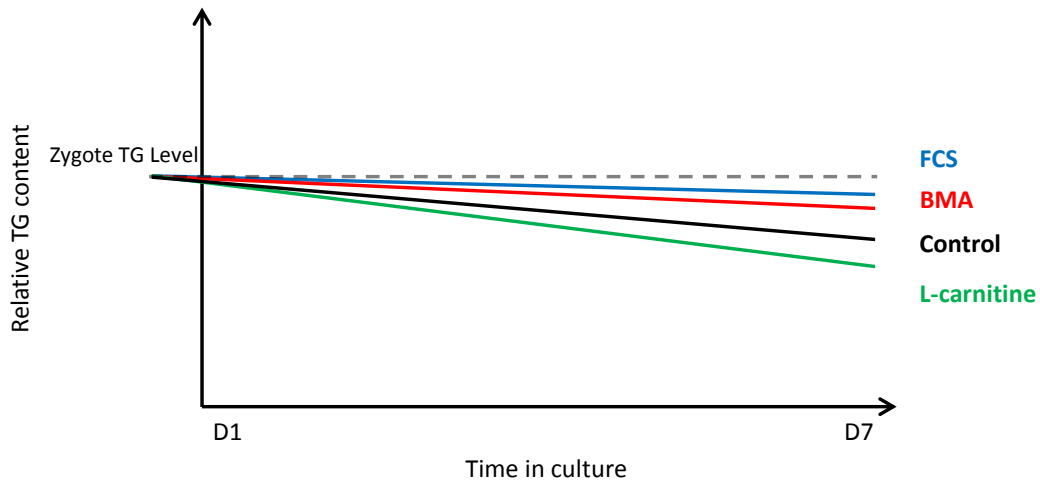


Figure 41: Summary of the effects of manipulation of endogenous fatty acid metabolism on embryo lipid content throughout *in vitro* development. Dotted line represents zygotic TG level. Supplementation with FCS (2.5-10%) allows the embryo to maintain high TG content to the blastocyst stage on D7 (Blue). BMA (Red) inhibits long chain fatty acid  $\beta$ -oxidation so BMA-treated embryos have relatively higher TG than control embryos (Black). L-carnitine (Green) promotes  $\beta$ -oxidation, accelerating TG consumption but reaching a level similar to control embryos at the blastocyst stage.

#### 4.5.8 Manipulating FAO without FCS significantly decreases mitochondrial polarisation ratio in day 2-3 embryos

In early cleavage stage embryos, cultured in the absence of FCS, inhibition or promotion of  $\beta$ -oxidation throughout the culture period led to a fall in mitochondrial polarisation ratio compared to controls (Figure 37). It has been reported that an increase in cellular fatty acid provision leads to decreased oocyte mitochondrial polarity in mouse oocytes (Wu et al. 2010) and other tissues (Borst et al. 1962; Rigoulet et al. 1998; Hue and Taegtmeyer 2009). However, others have reported that provision of fatty acids increases membrane potential in the bovine oocyte (Van Hoeck et al. 2013) and other tissues (Nobes et al. 1990). BMA inhibits  $\beta$ -oxidation beyond fatty acyl-CoA transport across the mitochondrial inner membrane. It is possible, therefore, that fatty acyl residues accumulate and could interfere directly with the mitochondrial membrane, reducing the voltage gradient. Similarly, supplementation with excess L-carnitine may result in increased transport of fatty acids into the intermembrane space, resulting in an accumulation of fatty acids and allowing for a similar interaction with the phospholipid membrane. Both of these scenarios could result in an uncoupling effect, reducing membrane polarisation (Luvisetto et al. 1987; Pietrobon et al. 1987). In addition, as fatty

acids are required for the activation of uncoupling proteins, the depolarisation could also be caused by increased UCP activity (Rousset et al. 2004; Fedorenko et al. 2012).

The potential uncoupling caused by fatty acid accumulation in the mitochondrial inner membrane discussed above may be decreased in L-carnitine treated embryos, since the metabolism of these fatty acids is increased and hence their tendency to accumulate over time in the mitochondrial matrix could be expected to decrease. In addition, L-carnitine has been shown to increase production of glutathione and thereby reduce ROS levels. This would correlate with higher coupled respiration in L-carnitine treated embryos, such that the same ATP generation is achieved while the demand for substrates, including oxygen, is decreased. To investigate this, the coupled OCR of L-carnitine treated blastocysts was investigated.

#### **4.5.9 Manipulating FAO does not significantly affect blastocyst polarisation ratio with or without FCS**

There were no significant differences in polarisation ratio between blastocysts treated with inhibition or promotion of  $\beta$ -oxidation, regardless of whether FCS was present. This is surprising, given the significant changes in oxygen consumption induced by these treatments in FCS-treated blastocysts. It is therefore possible that embryos can overcome mitochondrial depolarisation during early cleavage by a regulatory mechanism and that altered OCR is a legacy of this effect. This could result in a change in cell number at the blastocyst stage or a change in mitochondrial copy number following the activation of the embryonic genome at the 8-16 cell stage. Alternatively it could simply reflect the shift in metabolic strategy from the use of lipid at early cleavage stages, which usually depletes lipid stores by the blastocyst stage, to minimal lipid metabolism in the blastocyst, thus alleviating the detrimental effects of dysregulated lipid metabolism.

#### **4.5.10 Treatment with BMA, Etomoxir or L-carnitine does not alter cell allocation ratio**

TE cells contain the majority of mitochondria in the blastocyst and are more metabolically active as they have to carry out the ion pumping required to maintain the blastocoel cavity (Barnett et al. 1996; Van Blerkom 2008). ICM cells have lower ATP demand and so have fewer and less active mitochondria (Hewitson and Leese 1993; Houghton 2006). The

TE therefore has a higher OCR than the relatively quiescent ICM and an increase in TE:ICM ratio would explain a higher overall OCR.

Embryos cultured to the blastocyst stage following stimulation of  $\beta$ -oxidation with L-carnitine or inhibition of  $\beta$ -oxidation with BMA or Etomoxir each had similar mean cell counts and trophectoderm:inner cell mass ratios, regardless of the presence or absence of FCS ( $p=0.83$ ). These findings indicate that manipulation of  $\beta$ -oxidation of endogenous stores has no effect on blastocyst cell count or the allocation to TE or ICM lineages. Furthermore, the differences in metabolism are not due to a difference in TE:ICM ratio or of total cell number.

#### 4.5.11 Treatment with L-carnitine may accelerate blastocyst development

Timing of embryo cleavage, particularly the initial zygotic cleavage from one to two cells, has been proposed as a non-invasive marker of developmental capacity (Kirkegaard et al. 2012; Cetinkaya et al. 2014). In humans, early cleavage is associated with increased pregnancy rates and reduced rate of abortion (Van Montfoort et al. 2004). Similarly, the time of zygotic cleavage is linked to increased developmental competence in the bovine embryo (Yadav et al. 1993; Lonergan et al. 1999; Lonergan et al. 2000; Lee et al. 2012).

Data collected using the Primovision™ system (Figure 40) suggested that embryos treated with L-carnitine may begin blastocoel expansion earlier than controls ( $p=0.017$ ) or Etomoxir-treated embryos ( $p=0.003$ ). Instead, it may be that the addition of L-carnitine better supports development of bovine embryos in individual culture. Faster development may be linked to chromosomal aberration (Magli et al. 2014), fragmentation (Alikani 2000), loss of genomic imprinting and altered gene expression (Market Velker et al. 2012). However, since development rates were poor when using the 9-well culture dishes and only one treatment group could be cultured per week, few biological replicates were possible. While the system is excellent when using human embryos which develop well when incubated individually, bovine embryos which normally develop best in groups of around 20 (Gopichandran and Leese 2006) may be too isolated for autocrine or paracrine communication to provide support for embryos in a 9-well culture dish.

#### 4.5.12 Strengths and limitations

Chapter 4 describes the differences in metabolism of embryos cultured with promotion of  $\beta$ -oxidation or inhibition of  $\beta$ -oxidation from the zygote to blastocyst stage. Analysis of relative lipid content by confocal microscopy was successful, but further study with a quantitative method of sufficient sensitivity could be a powerful addition to this study. Analysis of mitochondrial polarisation was also successful, but analysis of mitochondrial localisation and physiology using Transmission Electron Microscopy (TEM) would add further detail to the mitochondrial phenotype of embryos with dysregulated  $\beta$ -oxidation. Investigation of development rates and time of blastulation following manipulation of  $\beta$ -oxidation with the Primo Vision system was limited by the relatively poor development of bovine embryos in the well-of-the-well dishes, presumably due to the increased distance between embryos, reducing paracrine signalling (Stokes et al. 2005; Gopichandran and Leese 2006). Additionally, only one treatment group could be analysed per development cycle, reducing the total number of replicates.

#### 4.5.13 Conclusions

The role of fatty acid metabolism in mammalian reproduction has long been neglected but is an important area of investigation, especially in humans, since an increase in fat content of the oocyte and embryo, as in maternal obesity, is linked to infertility (Leary et al. 2014). It is also important in the dairy industry, where the dairy cow has reduced fertility due to negative energy balance (Leroy et al. 2005). An understanding of the underlying mechanisms affecting oocyte and early embryo development is therefore vital to improving assistive reproductive technologies (ARTs) in domestic animals and man.

Fatty acid metabolism is undoubtedly a critical component of early embryo development (Sturmey et al. 2009b). Recent studies investigating the role of  $\beta$ -oxidation have suggested that successful FAO is vital for oocyte maturation (Sturmey and Leese 2003; Dunning et al. 2011) and the fatty acid composition of bovine reproductive fluids *in vivo* (Leroy et al. 2012) and during *in vitro* culture (Leroy et al. 2009) affects the outcome of early development. The present study provides evidence that modification of endogenous fatty acid  $\beta$ -oxidation in bovine embryos impacts on overall energy metabolism, including basal oxygen consumption rate, carbohydrate turnover, lipid metabolism, mitochondrial polarisation and possibly the coupling of electron transport and oxidative

phosphorylation. In addition, supplementation of culture media with FCS increased embryo lipid content, while decreasing mitochondrial polarity, providing further evidence for a link between lipid content and mitochondrial phenotype.

In the present study, L-carnitine was shown to be present in the ovarian follicular environment, providing a justification for supplementing the culture medium for *in vitro* maturation with this component.

5 The effects of manipulating bovine embryo lipid metabolism on gene expression and methylation

# Introduction

## 5.1.1 Gene expression in mammalian embryos

Mammalian preimplantation embryos are made up of relatively few cells; from one in the fertilised egg to around 200 in the bovine blastocyst and rely on maternal protein and mRNA transcripts during the early cleavage stages since the embryonic genome is not transcribed immediately following fertilisation. Embryonic Genome Activation (EGA) begins around the 8 cell stage in the bovine, 4-8 cell stage in the human and the late 1 cell stage in the mouse (Niakan et al. 2012). Thus, there is relatively little RNA present in the preimplantation embryo. These factors produce a range of challenges for studying gene expression in early embryos. Several reports have focused on specific gene expression in single blastomeres using qPCR, or alternatively, take a whole-genome approach using microarray technology and small groups of embryos. In this study, groups of ten blastocysts with matched pyruvate and oxygen consumption rates were collected (within  $\text{mean} \pm 2\text{s.d}$ ) to obtain a representative sample of genetic changes with minimal variation. This enabled analysis of how gene expression differed in relation to metabolic changes following promotion of  $\beta$ -oxidation with L-carnitine and inhibition of  $\beta$ -oxidation with BMA.

## 5.1.2 Epigenetics and metabolic legacy

As proposed by Barker (1986), changes during early development can predispose the developing organism to disease. From the first report of a link between infant birth weight and adult coronary heart disease, to recent studies investigating the relationship between ART and adult health, it is increasingly well understood that early development is crucial to the health of the adult. The embryo is entirely dependent on the maternal environment and a harmful, but sublethal, environment, potentially produced by maternal diet and lifestyle, can have permanent implications for the organism's health and development, the embryo giving rise eventually to all cell types, including the placenta and other extraembryonic tissues (Sinclair et al. 2007; Sinclair and Singh 2007; Fleming et al. 2011; Lucas 2013; Steegers-Theunissen et al. 2013).

One mechanism connecting the preimplantation environment to development, metabolism and gene expression is epigenetics (Lucas 2013). Meaning 'above genetics',

epigenetics is the study of heritable changes in gene expression through means other than DNA modification. Examples of such modifications include DNA methylation, histone modification and RNA methylation, which enable cells to express a subset of the genome, allowing the tissue-specific gene expression associated with differentiated cells. DNA methylation is the most stable and heritable type of epigenetic modification, as well as the best understood since it is less complex than histone modification (Jones 2012). Certain areas of the mammalian genome are GC-rich and termed CpG islands (CGIs), defined as comprising at least 55% CpG dinucleotides and an observed to expected ratio of CpG of  $>0.6$  (Takai and Jones 2002). Cytosine residues can be methylated to 5-methylcytosine to control gene expression. Some 80-90% of human CpG sites are methylated, and 60-80% of CGIs occur around transcription promoter sites (Davuluri et al. 2001; Takai and Jones 2002). Traditionally, methylation of DNA was perceived to repress gene expression (Phillips 2008), however a more complex picture is now emerging. Promoter methylation tends to repress gene expression, while intragenic methylation has gene-specific effects. Intergenic methylation has few well described effects and is much less common (Guo et al. 2014), highlighting the specific regulatory role of methylation.

The methylation of CpG islands is largely regulated by a class of enzymes termed DNA Methyltransferases (DNMT). DNMT1 is responsible for 'maintenance methylation', required for cell differentiation and proliferation. DNMT2 methylates transfer RNA, allowing epigenetic control at an additional level of transcription. DNMT3a and DNMT3b, assisted by the non-catalytic DNMT3L, perform *de novo* methylation in the early embryo (Gowher et al. 2005). DNA methylation may work in tandem with histone modification to silence gene expression (Fuks 2005), however as histone modifications are reversible, it is debated whether they are a true epigenetic mechanism. DNA methylation is essential to cell differentiation and proliferation, with somatic cells retaining methylation patterns throughout their lifespan. Aberrant DNA methylation is implicated in many diseases, including developmental conditions and metabolic syndrome (Barres and Zierath 2011; Milagro et al. 2012; Carless et al. 2013).

Epigenetic alterations are heritable, as changes to DNA persist in daughter cells following cell division. However, these alterations must be removed in order to allow the new organism's epigenetic modifications to be applied. Germ cells undergo reprogramming to remove the vast majority of epigenetic modifications, though reports state that the

spermatozoon and oocyte have different levels and regions of methylation in mouse (Kobayashi et al. 2012) or relatively similar levels in humans (Guo et al. 2014). Furthermore, following oocyte fertilisation, the paternal genome is immediately demethylated (Yoshizawa et al. 2010; Ma et al. 2012; Smith et al. 2012), with maternal demethylation continuing until the blastocyst stage. In the mouse, demethylation starts in the zygote stage and most is completed by the end of the 2 cell stage (Guo et al. 2014). Paternal demethylation is reduced in IVF or ICSI-produced zygotes compared to *in vivo*-derived zygotes (Ma et al. 2012). During postimplantation development up to gastrulation, selective *de novo* methylation establishes the organism's unique methylation pattern as the ICM further differentiates (Smith et al. 2012; Hackett and Surani 2013). Again, there are some similarities in remethylation patterns in humans and animal models (Fulka et al. 2004), as well as some variation (Beaujean et al. 2004). DNMT activity has been detected in pregastrulation embryos and embryonic stem cells, but not in differentiated ESCs or somatic cells such as fibroblasts (Jaenisch 1997). Furthermore, DNMT knockout mouse embryos do not develop beyond gastrulation, while DNMT knockout ESCs do not survive differentiation (Li et al. 1992; Lei et al. 1996).

Some genes are "imprinted" meaning that selective methylation is used to ensure only one parental allele of certain genes is expressed. These genes may be protected from remodelling during postimplantation development to an extent (Li et al. 1993; Smallwood et al. 2011; Hackett and Surani 2013) although several reports suggest that imprinted genes are prone to remodelling (Radford et al. 2012; Huntriss et al. 2013) and respond to the maternal environment (Puumala et al. 2012). Imprinted genes are often involved with growth and development (Lucas 2013), though some have argued that they are more important to somatic cell function than early development (Jaenisch 1997). Imprinting is vital in X-inactivation in mammalian females, preventing over expression of genes absent from the male Y chromosome, but mutations affecting imprinting are implicated in a variety of diseases. The active X chromosome tends to be hypermethylated within gene sequences and hypomethylated at promoter regions, with double the allele-specific methylation of the inactive X chromosome (Hellman and Chess 2007), leading to enhanced activity (Ball et al. 2009; Aran et al. 2011). The XIST gene (X inactive specific transcript) encodes a lncRNA component of the X-chromosome inactivation centre (Sado and Sakaguchi 2013) and is demethylated during gamete development but remethylated post-implantation (Norris et al. 1994; Beard et al. 1995). The XIST gene is expressed only

on the inactive X chromosome, which is always paternal in the placenta (Takagi and Sasaki 1975), but randomised in the actual embryo. An antisense transcript known as Tsix is encoded at the Xist locus and inhibits Xist transcription on the same chromosome (Lee et al. 1999; Migeon et al. 2001). Another X-linked lncRNA, XACT, was recently discovered (Vallot et al. 2013). The extraembryonic tissues tend to be more demethylated than the embryo (Sado et al. 2000). In the mouse, Xist RNA tends to accumulate on the paternal X chromosome during the 4-8 cell stage. Xist remains on the TE and portion of the ICM destined to form endoderm, but disappears from the rest of the ICM complement (Mak et al. 2004; Okamoto et al. 2004). Another example is the intronic methylation of maternal IGF2R during oogenesis (Stöger et al. 1993) alongside the paternal-specific methylation upstream of the H19 promoter region during spermatogenesis (Tremblay et al. 1995). These modifications work in synergy; paternal H19 expression is suppressed, while maternal IGF2R is enhanced. These specific modifications are unaffected through demethylation in the zygote and *de novo* methylation in the postimplantation embryo (Jaenisch 1997), maintaining optimal expression of these genes throughout early development.

Not all regulatory CGIs are found in promoter regions; CGIs several kbp away from a promoter can affect its transcription (Deaton and Bird 2011; Wittkopp and Kalay 2012). Regions known as 'alternative promoters' within genes can suppress or enhance transcription (Maunakea et al. 2010) and have phenotypic manifestations. Differential methylation of CGIs adjacent to splice sites can affect the efficiency of splicing, leading to expression of one splice variant of a protein over another (Edwards et al. 2010; Shukla et al. 2011). In general, around half of all genomic CGIs are known as 'orphan' CGIs and often show evidence of initiating transcription or dynamic expression. The orphan CGIs are primarily methylated during embryo development, as opposed to promoter CGIs (Illingworth et al. 2010). In addition, 42-60% of orphan CGIs had promoter activity in the human (Illingworth et al. 2010). The authors found that hypomethylated orphan CGIs were associated with expression of certain genes, while hypermethylation was associated with transcriptional repression (Illingworth et al. 2010). It seems possible that orphan CGI products are non-coding RNAs with regulatory roles and methylation of these sites could regulate tissue-specific gene expression (Illingworth et al. 2010). Increased intragenic methylation correlates with increased transcription in some cases (Deaton and Bird 2011), however in other reports intragenic methylation decreased expression by

promoting a closed chromatin structure to prevent RNA Polymerase II binding (Lorincz et al. 2004). Thus, intragenic and intergenic methylation regulates gene expression, but the enhancing or suppressing effect of each modification is specific to each gene and cannot be easily predicted.

While the total population of humans born through ART is increasing and the earliest ART children are entering adulthood, the majority of research linking ART, preimplantation conditions and epigenetic modifications is performed in animal models, primarily mouse, but also sheep, rat, rabbit and cow (Lucas 2013). Broadly speaking, animal models and the human have exhibited similar relationships between maternal diet and cardiovascular change, behaviour, bone development and the immune response in the progeny (Fleming et al. 2011). For example, a maternal diet deficient in methyl donors, such as tetrahydrofolate (THF), causes altered methylation status in the liver of foetal sheep (Sinclair et al. 2007). Similar effects were maintained in the rat until adolescence, but were rescued by dietary supplementation with folate (Lillycrop et al. 2005; Burdge et al. 2009). Cooper et al. (2012) recently reported that supplementation of human maternal diet with folate, zinc, and vitamins A, B, C, and D altered DNA methylation status of offspring in a gender-specific manner, with hypomethylation of IGF2R in females and GTL2-2 in males. These changes were detected in cord blood, although not replicated at 9 months in venous blood (Cooper et al. 2012). Such studies suggest that methylation status is affected by maternal diet, but remains dynamic to an extent throughout an organism's life.

Epigenetic modification is intricately linked to metabolism through a number of mechanisms. Acetyl-CoA, supplied by the TCA cycle, is the substrate for histone acetyltransferase enzymes, which perform histone modifications (Lee and Workman 2007; Shahbazian and Grunstein 2007). The primary methyl group donor for DNA and RNA methylation is S-adenosylmethionine (SAM), which is produced during the conversion of methionine to succinyl CoA for entry to the TCA cycle (Figure 4, Chapter 1). A further link to the TCA cycle is the FAD-dependent enzyme LSD1, which demethylates H3K4, a common histone modification site which increases transcription when trimethylated (H3K4me3) (Shi et al. 2004). LSD1 also influences DNA metabolism, perhaps through this histone modification (Lan et al. 2008; Ciccone et al. 2009; Wang et al. 2009). Another methyl donor is tetrahydrofolate, which is converted to N<sup>5</sup>N<sup>16</sup>-methylenetetrahydrofolate

by the glycine cleavage system (Kaelin and McKnight 2013). In humans, genes with the H3K4me3 promoter modification tend to remain hypomethylated throughout gamete maturation and preimplantation development (Guo et al. 2014). During postimplantation development, and in hESCs, such genes tend to be highly methylated and actively expressed (Guo et al. 2014). Evolutionarily younger DNA elements tend to resist demethylation to a greater degree than 'older' elements.

### 5.1.3 Transcription

Transcriptomics is the study of the complete set of genes expressed by a cell type, and includes expression of messenger RNA (mRNA) and non-coding RNA (ncRNA). The majority of mRNAs may be similar between tissue types, but abundantly expressed mRNAs are often specific to a tissue. In general, around 10% of expressed genes are specific to a differentiated cell type, while many genes are constitutively expressed in all cell types (Lewin 2004). Microarray chip analysis allows an overview of expression of the entire genome to be recorded simultaneously, revealing genes that are differentially expressed between tissue types or treatments. Such comparisons may be made in experimental settings to examine the effect of an intervention or in clinical settings to compare the impact of a disease state. In studies in early development, microarray analysis opens the possibility to identify differences in gene expression pattern as a function of developmental stage and in response to manipulations and interventions.

Recent studies using large-scale expression analysis have revealed a new cohort of candidate genes involved in aspects of embryo metabolism, development and successful pregnancy. For example, El-Sayed et al. (2006) established links between bovine embryo gene expression and developmental competence by analysing biopsies of day 7 blastocysts which were later transferred to surrogate recipients. The authors found that blastocysts resulting in successful pregnancies, as measured on day 25, tended to express greater levels of genes including thioredoxin and cyclooxygenase 2, which are involved in prostaglandin synthesis, CDX2, a trophoblast-specific transcription factor, PLAU, a plasminogen activator, ALOX15, required for carbohydrate metabolism, BMP15, a growth factor, and PLAC8, a placental gene specific to invasion. However, embryos that had been reabsorbed by day 25 had increased expression levels of KRT8, a protein phosphorylase, PGK1 and AKR1B1, both involved in glucose metabolism; embryos resulting in no pregnancy had increased TNF cytokine, CD9, an inhibitor of implantation and EEF1A1,

involved in amino acid binding. These data indicate that there are differences in gene expression at the blastocyst stage in cattle that reflect developmental competence.

#### 5.1.4 The EmbryoGENE platforms

The EmbryoGENE transcriptomic and methylomic microarray platform was first developed and validated by Robert et al. (2011). The transcriptomic EmbryoGENE bovine microarray comprises 42,242 probes in total, of which 21,139 are known reference genes; 9,322 are novel transcribed regions (NTRs); 3,677 are alternatively spliced exons; 3,353 are 3'-tiling probes; and 3,723 are controls.

The transcriptomic microarray platform has since been used in numerous studies. Gad et al. (2012) found transcriptomic changes between embryos moved between *in vitro* and *in vivo* culture conditions before and after EGA, at the 4 or 16 cell stages. Embryos cultured *in vitro* until the 4 cell, 16 cell stages or blastocyst stage had significantly down-regulated gene products related to lipid metabolism, while 68 transcripts including development and proliferation-related genes were differentially expressed between embryos cultured *in vitro* at the time of genome activation and those cultured *in vivo* during embryonic genome activation. Another recent study found that embryos cultured under *in vitro* conditions, including embryo co-culture with buffalo rat liver cells, had significantly upregulated genes involved in cell death, and oxidative stress, as well as altered expression of lipid metabolism pathways than *in vivo* derived oocytes (Plourde et al. 2012). These data suggest that transcription in the embryo is dynamically linked to embryo production method and culture conditions.

A recent study by Cagnone and Sirard (2014) reported that culture of bovine embryos with serum lipid induced an altered transcriptomic phenotype at the blastocyst stage. Genes connected with oxidative stress and inflammation were upregulated, while pluripotency genes were downregulated. Another study reported that culturing bovine OCCs with L-carnitine boosted blastocyst rate, total cell count and a possible increase in mitochondrial content, along with decreased expression of fatty acid transporters SLC27A1 and SLC22A5 and increased expression of FAO enzymes CPT1B and CPT2 (Ghanem et al. 2014).

The EmbryoGENE bovine methylomic microarray platform was first developed and validated by Saadi et al. (2014). The authors found that bovine sperm DNA tended to be

more methylated than blastocyst DNA and validated this by selecting 7 DMRs for analysis by bisulphite pyrosequencing, which showed a similar pattern. However, the present study is the first use of this method in conjunction with parallel transcriptome analysis.

## 5.2 Aims

The aim of this chapter is to quantify the effects of manipulating preimplantation embryo  $\beta$ -oxidation on gene expression and DNA methylation status. This aim will be addressed by carrying out the following series of experiments:

- Metabolic profiling of bovine blastocysts produced following promotion of  $\beta$ -oxidation with L-carnitine or inhibition of  $\beta$ -oxidation with  $\beta$ -mercaptoacetate.
- Microarray analysis of transcriptional differences.
- Microarray analysis of DNA methylation status.

## 5.3 Materials and methods

The techniques described below in sections 5.3.1 and 5.3.2 were carried out in-house. RNA quantification (5.3.3) of the initial group of 12 samples was carried out at Université Laval by the author with the guidance of Isabelle Dufort. As several of these samples had degraded in transit, another group of samples were prepared on return to the UK. Quantification of these RNA samples was carried out by Sally James of the University of York. Once the final group of 12 samples were received at Université Laval, the techniques described in sections 5.3.4, 5.3.5, 5.3.6 and 5.3.7 were carried out by Isabelle Dufort and Dominique Gagne of Université Laval. Bioinformatic analysis (section 5.3.8) was carried out by Eric Fournier of Université Laval. Subsequent gene ontology analysis was carried out in-house by the author (section 5.3.8). All data shown below, including the metabolic profiles shown in section 5.4.1, relates only to the final group of 12 samples.

### 5.3.1 *In vitro* culture and metabolic profiling

Embryos were produced using the *in-vitro* production protocol as described in Chapter 2. However, immediately after fertilisation, at the *in vitro* culture stage, zygotes were randomly assigned to SOFaaBSA culture media supplemented with 0.1mM  $\beta$ -mercaptoacetate (BMA, a competitive inhibitor of long-chain acyl-CoA dehydrogenase), 5mM L-carnitine (a co-factor required for transport of Fatty Acyl-CoA across the inner mitochondrial membrane) or unaltered SOFaaBSA. Culture media was SOFaaBSA + 5% FCS. As previously reported (Section 4.5, Figure 39), there was no difference in cleavage or blastocyst development rates between treatments. Embryos were cultured without interference to the blastocyst stage (Day 7), at which point blastocysts were removed for individual metabolic profiling of oxygen consumption rate by nanorespirometry and pyruvate consumption rate by fluorimetric assay as described in sections 2.2.2 and 2.3.1. Four samples were prepared for each group; BMA, L-Carnitine and Control, for a total of 12 samples. Each sample contained a group of 10 blastocysts with pyruvate and oxygen consumption rates within mean $\pm$ 2.s.d. Samples were immediately frozen in 5 $\mu$ l PBS on dry ice and stored at -80°C prior to RNA and DNA extraction using the AllPrep DNA/RNA micro kit (Qiagen).

### 5.3.2 Parallel extraction of total RNA and DNA

RNA and DNA were extracted from frozen blastocysts using the QIAshredder kit and AllPrep DNA/RNA micro kit (Qiagen) following manufacturer's guidance with the following modifications. Frozen blastocyst samples were transported to the preparation hood on dry ice and suspended in 75µl buffer RLT plus. The suspension was moved to a QIAshredder column and the original tube rinsed with a further 275µl RLT plus to ensure all blastocyst material was removed. The QIAshredder column was centrifuged at 10,000 x g for 2min to lyse blastocysts and liberate all DNA and RNA. The homogenised lysate was then transferred to an AllPrep DNA spin column and centrifuged at 10,000 x g for 30s to separate DNA and RNA. DNA was bound to the spin column membrane and stored in a collection tube at room temperature until RNA extraction was completed.

RNA purification as carried out as described by the manufacturer. Briefly, the lysate containing RNA was mixed with an equal volume of 70% ethanol, transferred to an RNeasy spin column and centrifuged at 10,000 x g for 15s, binding RNA to the column membrane. Bound RNA was then washed with a series of buffers and centrifuged at 10,000 x g; 700µl RW1 for 15s, 500µl RPE for 15s and 500µl 80% ethanol for 2min. The 80% ethanol wash removes any components which can interfere with downstream RNA labelling (described below). Carryover from previous washes was minimised by transferring the spin column to a fresh collection tube and spinning for a further 1min. Finally, RNA was eluted to a fresh collection tube in 12.5µl RNasefree water. RNA samples were transported on dry ice and stored at -80°C until required.

DNA samples, still bound to the AllPrep DNA spin column, were washed with 500µl buffer AW1 and centrifuged at 10,000 x g for 15s to wash the membrane. The flow-through was discarded and the spin column membrane washed with 500µl buffer AW2 at 10,000 x g for 2min. DNA was extracted in 37µl buffer EB in a fresh collection tube AllPrep DNA/RNA micro kit. RNA and DNA samples were stored at -80°C before shipment to Université Laval on dry ice for transcriptomic and epigenetic analysis. DNA samples were stored at -20°C until required.

### 5.3.3 Quantification of RNA quantity and quality

RNA quality was analysed using the Agilent Bioanalyser 2100 system (Agilent Technologies Inc., Santa Clara, CA). RNA samples with an RNA Integrity Number (RIN) of 7.5 or greater, along with their DNA counterparts, were included in microarray analyses.

### 5.3.4 T7 amplification of RNA

RNA samples of >2ng with RIN >7.5 were amplified using the RiboAmp<sup>®</sup> HS<sup>Plus</sup> RNA Amplification Kit (Applied Biosystems) as described by Robert et al. (2011). Briefly, 1<sup>st</sup> strand cDNA was synthesised using 1<sup>st</sup> Strand Synthesis components and Superscript<sup>™</sup> II Enzyme (Invitrogen). Following this, 2<sup>nd</sup> Strand DNA synthesis was performed and DNA was purified again using kit components. *In vitro* transcription was performed and the resulting anti-sense RNA (aRNA) purified. The resulting aRNA was then processed through another round of cDNA synthesis, cDNA purification, aRNA transcription and aRNA purification. The final aRNA was quantified using a NanoDrop system (Thermo Fisher Scientific, Wilmington, USA) and was around 50µg per sample.

### 5.3.5 Transcriptomic microarray analysis

RNA samples were first labelled in a dye-swap design with the Universal Linkage System (ULS) (Kreatech/Leica Biosystems, Ontario). Briefly, 2µl of CY3-ULS or CY5-ULS were added to 2µg RNA and 2µl Labelling Solution and the mixture was incubated at 85°C for 15 minutes to allow the proprietary ULS moieties to bind to the N7 position of guanine on RNA molecules. Labelled RNA was separated from non-reacted ULS-label using the PicoPure<sup>™</sup> RNA isolation Kit (Qiagen). Briefly, the RNA spin column was preconditioned using 250ml conditioning buffer and centrifuged at 16,000 x g. The labelled RNA sample was mixed with 100µl Extraction Buffer and 120µl 70% Ethanol, and then added to the preconditioned RNA column. Labelled RNA was bound to the column by centrifugation at 100 x g for 2min, then flow-through was removed by further centrifugation at 16,000 x g. Bound RNA was then washed with Wash Buffer 1 and washed twice with Wash Buffer 2 with centrifugation at 8000 x g and 16,000 x g. Bound RNA was eluted to a fresh collection tube by incubating with 11µl elution buffer and centrifugation at 16,000 x g.

### 5.3.6 Hybridisation of labelled RNA samples to the microarray

Next, ULS-labelled RNA samples were conjugated to the microarray. Briefly, lyophilised 10X blocking agent was reconstituted in 500µl nuclease free water, 2ml 10% Triton X-102 was added to wash buffer and 0.005% Triton X-102 to gene expression buffers 1 and 2. Next, each of the following reagents (Table 17) were added to a 500µl microtube and mixed gently.

Substance	Amount
Cyanine 3-labeled RNA	825ng
Cyanine 5-labeled RNA	825ng
Agilent spike, 0.01X	2.75µl
Nuclease-free water	to volume
10X Blocking Agent	11µl
25X Fragmentation Buffer	2.2µl
<b>Total Volume</b>	<b>55µl</b>

Table 17: Composition of RNA hybridisation reaction mixture.

The mixture was incubated at 60°C for exactly 15min to fragment the RNA, then immediately cooled on ice for 1min before adding 55µl hybridisation buffer Hi-RPM to halt fragmentation. 100µl sample was then immediately loaded to the gasket slide within the chamber base, distributing evenly across the slide surface. An Agilent microarray slide was then gently lowered on top of the gasket slide and the chamber cover firmly attached to the base. The chamber was held vertically to check for a single large bubble and then loaded to a rotating rack within the pre-warmed hybridisation oven at 65°C. The microarrays were rotated at 10rpm and 65°C for 17hr.

Microarray chambers slides were then gently removed from the oven and array-gasket slides removed from the chambers. Each array-gasket slide was submerged in Gene Expression Buffer (GEB) 1 and separated. The array slide was then transferred to the staining dish containing pre-warmed GEB 1 for 3 min, then transferred to another slide staining dish containing GEB 2 for 3min. Slides were scanned immediately.

### 5.3.7 Epigenetic microarray analysis

Analysis of blastocyst DNA methylation status was performed using the EmbryoGENE platform as described below (de Montera et al. 2013). Briefly, blastocyst gDNA samples

were fragmented with the non-methylation dependent restriction enzyme MseI. Linker primers MseLig21 and MseLig12 were added by incubation with T4 DNA ligase for 20min. Following this, DNA samples were treated with the methyl-sensitive restriction enzymes HpaII, AclI and HinfI, which specifically digest non-methylated DNA fragments. Real-time qPCR was performed to verify digestion success and if insufficient digestion was observed (defined as a difference of <5 copies between digested and non-digested DNA), digestion was repeated. Methylated fragments were then amplified exponentially by PCR. Following this, non-methylated fragments were digested using MseI to remove linkers and then linearly amplified by PCR. This method leads to selective enrichment of methylated fragments, allowing differences in methylation between DNA samples to be detected.

The amplified DNA samples were labeled with Cy3 and Cy5 dyes using the ULS Fluorescent Labelling Kit as described above (Kreatech, Ontario). Labelled DNA samples were hybridized to the Agilent-manufactured EmbryoGENE slides as described above for RNA samples, with the following modifications: Hybridisation was at 65°C for 40hr, after which microarray slides were washed in Oligo aCGH Wash Buffer 1 for 5min at room temperature, in Oligo aCGH Wash Buffer 2 for 1min at 37°C, in 100% acetonitrile for 10s at room temperature and finally in Stabilization and Drying Solution (Agilent, Diegem, Belgium) at room temperature for 30s. Slides were scanned immediately with PowerScanner (Tecan, Männedorf, Switzerland), followed by features extraction with ArrayPro 6.4 (MediaCybernetics, Bethesda, MD).

### 5.3.8 Analysis of microarray data

Microarray data analysis was performed by Eric Fournier using Flex array version 1.6 ([genomequebec.mcgill.ca/FlexArray](http://genomequebec.mcgill.ca/FlexArray)) and the Linear Models for Microarray data (LIMMA) R package. Differentially expressed or differentially methylated genes identified by LIMMA analysis (exceeding fold change 0.5 and p value of 0.05) were analysed in-house using DAVID online functional annotation software (<http://david.abcc.ncifcrf.gov/>).

## 5.4 Results

### 5.4.1 Metabolic profiles

Blastocysts produced following chronic BMA treatment, chronic L-carnitine treatment, or control conditions, were metabolically profiled for oxygen and pyruvate consumption immediately prior to cryopreservation for microarray analyses as described above (Section 5.2). BMA-treated blastocysts ( $40.4 \pm 7.1$  pmol/embryo/hr) had a significantly higher mean oxygen consumption rate (OCR) than L-carnitine-treated blastocysts ( $23.2 \pm 2.7$  pmol/embryo/hr,  $p=0.034$ , Figure 42). Control blastocysts had an intermediate OCR ( $29.3 \pm 6.5$  pmol/embryo/hr). BMA-treated blastocysts also had significantly higher pyruvate consumption ( $23.6 \pm 7.1$  pmol/embryo/hr) than L-carnitine treated blastocysts ( $13.8 \pm 0.8$  pmol/embryo/hr,  $p=0.018$ , Figure 42). Control blastocysts had similar pyruvate consumption ( $13.1 \pm 3.3$  pmol/embryo/hr) to L-carnitine treated blastocysts, albeit with greater variation.

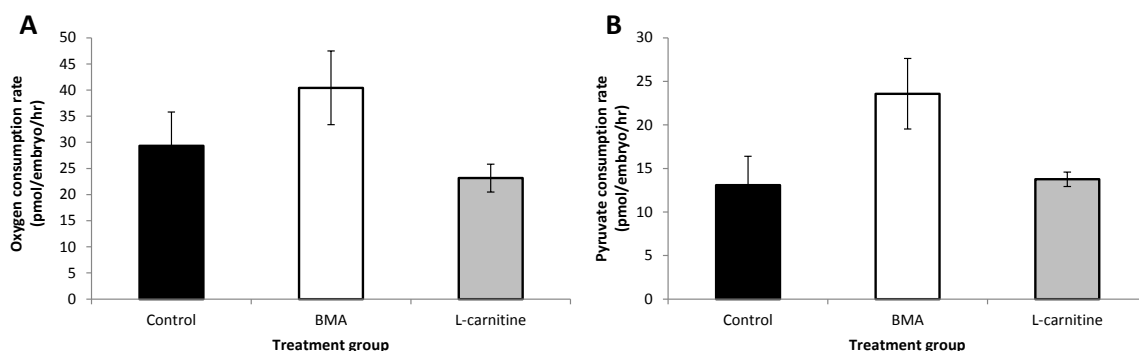


Figure 42: Metabolic profiling of blastocysts for microarray analysis. A: Mean oxygen consumption rate of Control, BMA and L-carnitine treated embryos used in the following microarray experiments. BMA-treated OCR was significantly higher than L-carnitine-treated OCR ( $p=0.034$ ). B: Pyruvate consumption assays of the same embryos. Control:  $13.1 \pm 3.3$ ; BMA:  $23.6 \pm 7.1$ ; L-carnitine:  $13.8 \pm 0.8$ . BMA pyruvate consumption was significantly higher than L-carnitine ( $p=0.018$ ). Data in both cases shown as mean  $\pm$  s.e.m.

## 5.4.2 Summary of genetic changes

DNA and RNA were extracted from groups of 10 blastocysts in each treatment group for microarray analysis. BMA and L-carnitine treated blastocysts were compared to control embryos to generate a dataset of differentially expressed genes and differentially methylated regions (DMRs). Transcriptomic analyses revealed that 152 genes were differentially expressed in L-carnitine treated blastocysts (Figure 43A), while 582 genes were differentially expressed following BMA treatment (Figure 43B) ( $p < 0.05$ , fold change  $> \log_2(0.5)$ ). Epigenomic comparison revealed 1414 DMRs between L-carnitine treated and control blastocysts (Figure 43C) and 2494 DMRs between BMA-treated and control blastocysts (Figure 43D) ( $p < 0.05$ , fold change  $> \log_2(0.5)$ ).

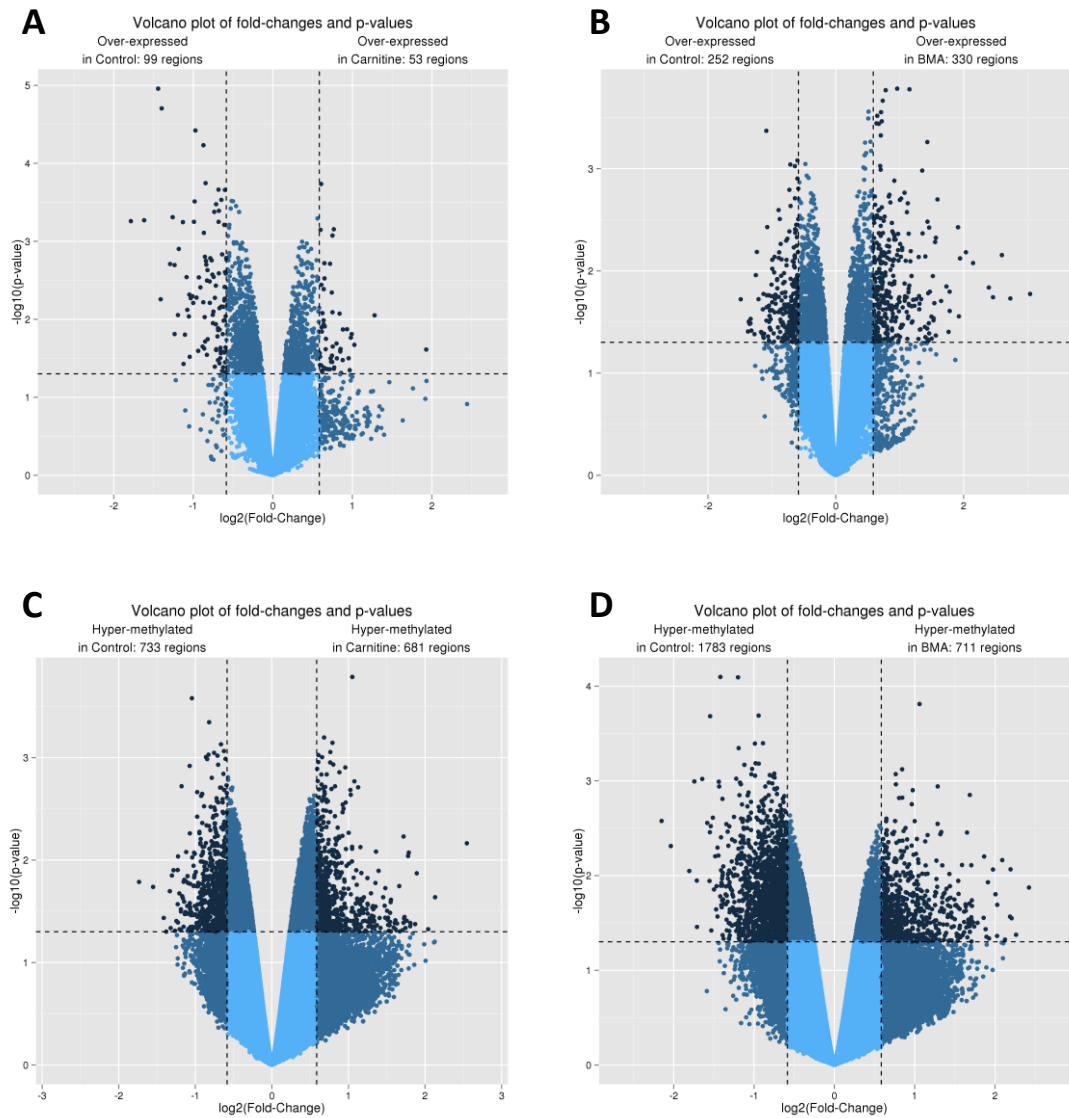


Figure 43: Volcano plots indicating microarray results. A) Differential gene expression between L-carnitine treated and control blastocysts. B) Differential gene expression between BMA treated and control blastocysts. Data points located on the upper left side of the plot are significantly downregulated genes following treatment, whereas the points located on the upper right side of the plot are those which are significantly upregulated. C) Differential methylation between L-carnitine treated and control embryos. D) Differential methylation between BMA treated and control embryos. Data points located on the upper left side of the plot are significantly hypomethylated genes following treatment, whereas the points located on the upper right side of the plot are those which are significantly hypermethylated. Dashed lines indicate significance thresholds of  $p < 0.05$  and fold change  $> \log_2(0.5)$ .

### 5.4.3 Transcriptomic microarray following L-carnitine treatment

L-carnitine-treated blastocysts analysed using the EmbryoGENE transcriptomic microarray platform had 152 differentially expressed transcripts compared to control blastocysts (Figure 44), including 102 genes, 40 novel products and 1 pseudogene. These genes had a variety of functions, and a full list of annotations were found using online DAVID analysis software (Huang et al. 2009). However we will initially focus on genes involved in embryo metabolism and development, including oxidative damage and resistance, DNA and protein turnover, apoptosis and proliferation (Table 18 and Figure 45).

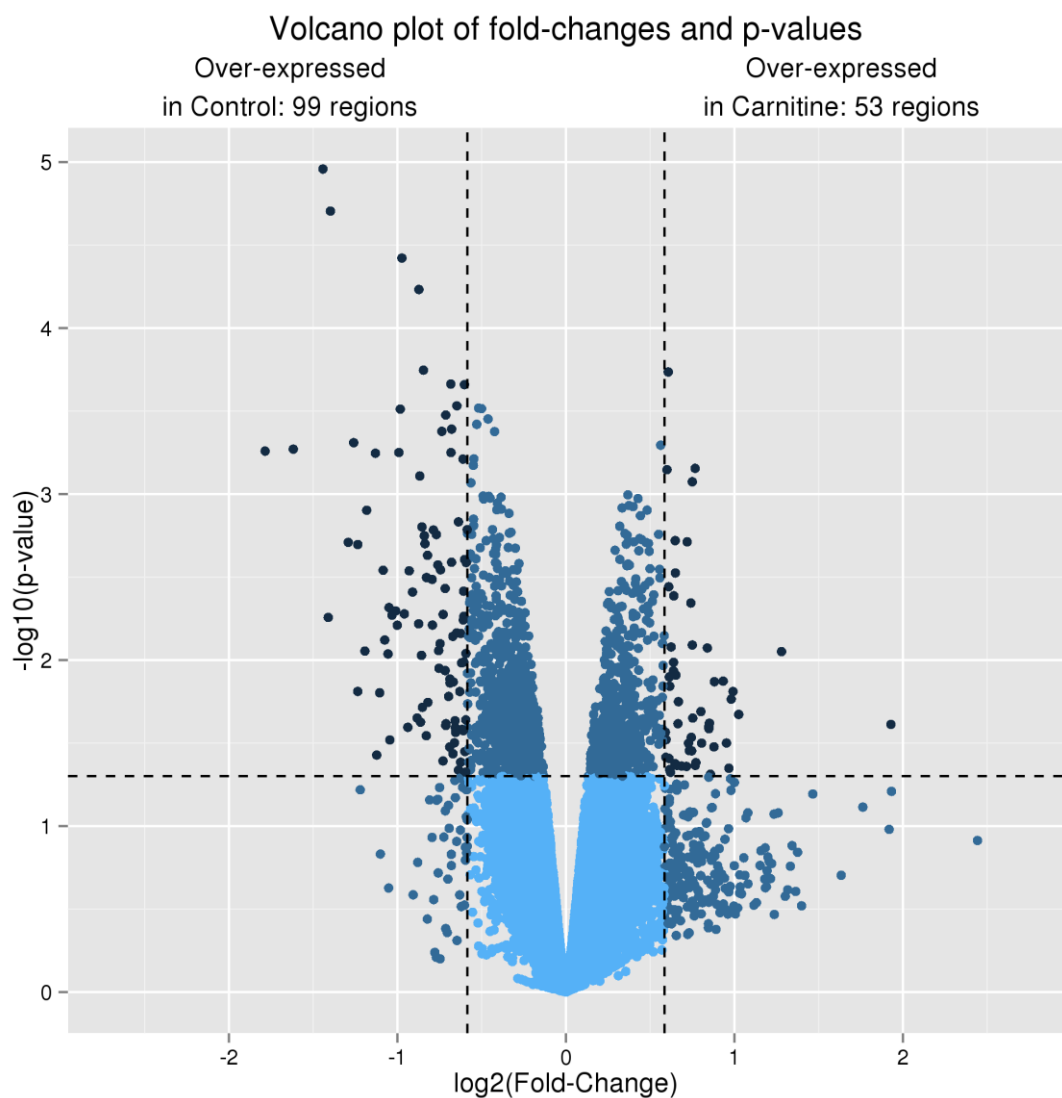


Figure 44: Volcano plot indicating the spread of transcriptomic probe binding between L-carnitine treated and control embryos. The dark points indicate probes which exceed the significance thresholds of  $p < 0.05$  and fold change  $> \log_2(0.5)$ . A total of 152 regions were differentially expressed between control and L-carnitine treated embryos.

Annotation Group	Gene ID	Product name	Role	Fold change
Mitochondria	ALAS2	Delta-aminolevulinatase synthase 2	Catalyses first step of haem biosynthesis	+0.60
	RAB32	Ras-related protein 32	Mitochondrial fission	+0.75
	HEBP2	heme binding protein 2	Oxidative-stress induced apoptosis , mitochondrial membrane permeability	-0.97
Metabolism	STBD1	Starch binding domain 1	May have the capability to bind to carbohydrates, involved in glycogen metabolism	+0.84
	ELOVL1	Elongation of very long chain fatty acids 1	Elongation of very long chain fatty acids	-0.68
	ACOT4	Acyl-CoA thioesterase 4	Degradation/synthesis of fatty acids. Hydrolyses succinyl-CoA	-0.86
	ACSL6	Acyl-CoA synthetase long-chain 6	Long-chain FA synthetase	-0.66
	THEM4	Thioesterase superfamily member 4	Has acyl-CoA thioesterase activity towards medium and long-chain (C14 to C18) fatty acyl-CoA substrates	-0.60
	TPI1	Triosephosphate isomerase 1	Converts Glyceraldehyde-3-phosphate (GAP) <-> Dihydroxyacetone-phosphate (DHA) for TG synthesis	-0.85
	CYP4A22	Cytochrome P450	Catalyses the omega- and (omega-1)-hydroxylation of various fatty acids such as laurate and palmitate, no activity towards arachidonic acid and prostaglandin A1	+0.98
Obesity	MTMR9	Myotubularin related protein 9	Control of cell proliferation Relevance to obesity and diabetes.	-0.61
	CLDN23	Claudin 23	Possible link to childhood obesity	-1.44
Pregnancy	IFNT	Interferon- $\tau$	Primary signal for maternal recognition of pregnancy	-1.41
	PAG2	Pregnancy-associated glycoprotein 2	Low expression related to abortion.	-1.24
	PAG12	Pregnancy-associated glycoprotein 12	Involved in implantation and placentogenesis	-0.94
	PTGS2	Prostaglandin-endoperoxide synthase 2 or cyclooxygenase 2	Key enzyme in prostaglandin synthesis	-0.84
	TIA1	T-Cell-Restricted Intracellular Antigen-1	Silences COX-2 expression	-0.76
ROS	GSTO1	Glutathione S-transferase omega-1	Glutathione-ascorbate cycle antioxidant metabolism	-0.61
Gap junctions	GJB4	Component of gap junctions.	Calcium Regulation in the Cardiac Cell. Membrane Trafficking	-0.59
Oxygen-consuming	SQLE	Or squalene monooxygenase.	1st oxidation in cholesterol synthesis, likely rate-limiting. Oxygen consuming.	-0.65
Protein turnover	QSOX1	Sulfhydryl oxidase 1	Catalyses oxidation of thiol groups to sulphides	-0.73
	CHST10	Carbohydrate sulphotransferase 10	Transfers sulphate to the of terminal glucuronic acid of protein-and lipid-linked oligosaccharides.	+0.65
	TGM2	Transglutaminase 2	Catalyze the crosslinking of proteins	+0.93
Transcription	NUPR1	Nuclear protein, transcriptional regulator 1	Inhibits MSL1 activity on Histone H4'Lys-16' acetylation	-0.60
	TFAP2A	Transcription factor AP-2 alpha	KO represses placental gene expression in trophoblasts. Related to apoptosis, caspase and wnt.	-1.01
	ZNF187	Zinc finger and SCAN domain containing 26	Zinc Finger And SCAN Domain Containing 26. transcriptional regulation	+0.62
	TAF7	TATA Box Binding Protein (TBP)-Associated Factor, RNA Polymerase II	Component of the DNA-binding general transcription factor complex TFIID, mediating promoter responses to various activators and repressors	+0.65
	FOXP1	Forkhead box protein G1	Transcription repression factor which plays an important role in the establishment of the regional subdivision of the developing brain	+0.69
	ZNF354A	Zinc finger protein 354A	Promotion of cardiogenesis in vertebrates and MAPK signalling	+0.73
	NR3C2	Nuclear receptor 3 C2 or mineralocorticoid receptor	Ligand-dependent transcription factor	+0.77
	TBX18	T-box 18	Embryonic development transcriptional repressor	+0.85

Table 18: Table highlighting the role and fold change of selected genes which were differentially expressed between L-carnitine treated and control blastocysts.

### Differentially expressed genes following promotion of $\beta$ -oxidation with L-carnitine

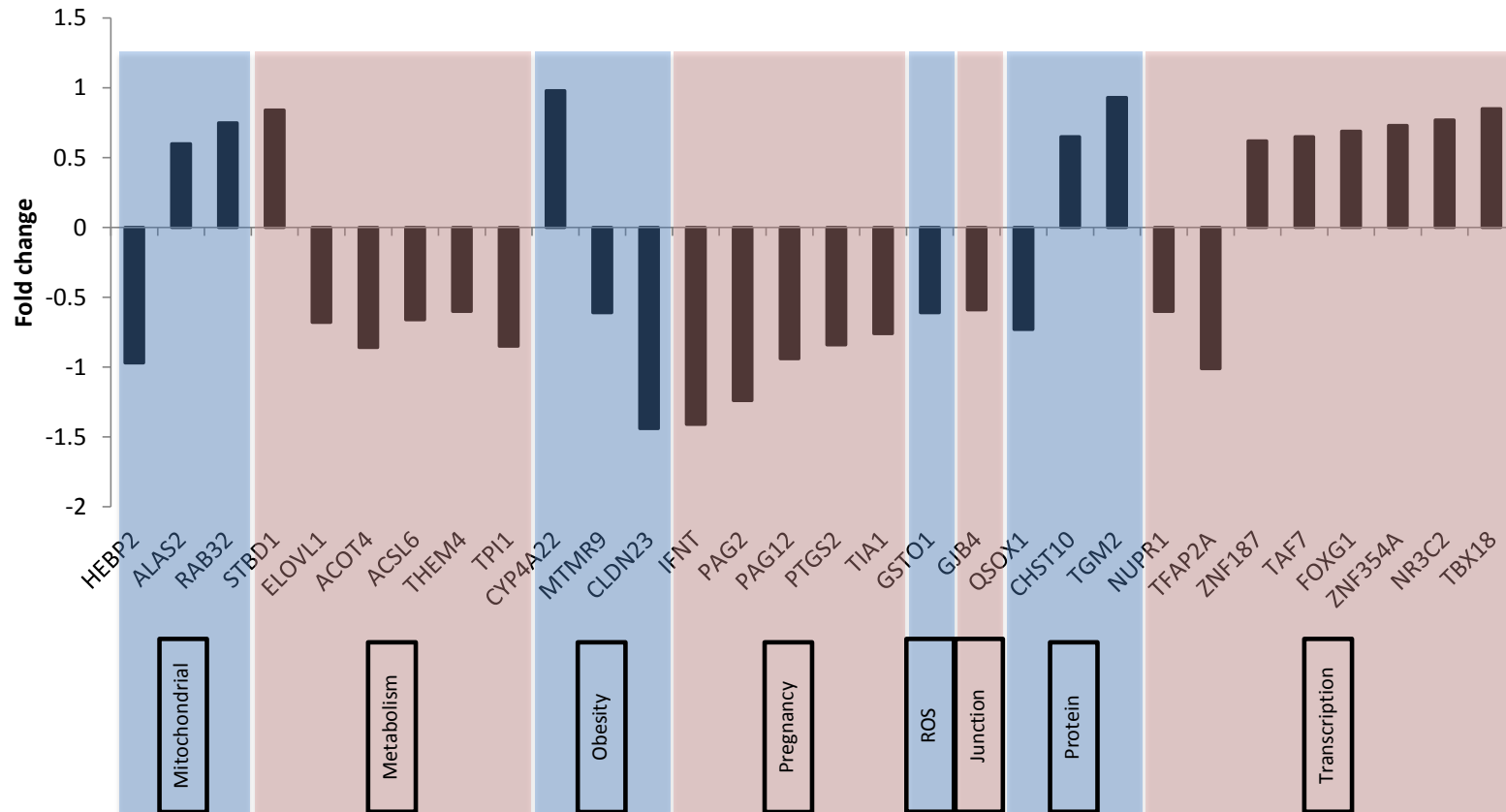


Figure 45: Differentially expressed genes of key interest in carnitine-treated blastocysts identified by microarray analysis. These genes are involved in embryo metabolism and development, including oxidative damage and resistance, recognition of pregnancy, DNA and protein turnover, apoptosis and proliferation. Genes presented exceed significance thresholds of  $p < 0.05$  and fold change  $> \log_2(0.5)$ .

#### 5.4.3.1 Genes involved in mitochondrial permeability and morphology

Culturing embryos in the presence of L-carnitine led to a change in transcription of a number of genes involved in mitochondrial behaviour. HEBP2, involved in apoptosis and mitochondrial membrane permeability, was downregulated at transcript level (-0.97 fold change). ALAS2, which catalyses the first step of heme biosynthesis, along with RAB32, a protein required for mitochondrial fission, were upregulated compared to controls (+0.6 and +0.75 fold increase respectively).

#### 5.4.3.2 Genes involved in metabolism

A number of genes related to fatty acid  $\beta$ -oxidation were modulated at transcript level following promotion of  $\beta$ -oxidation with L-carnitine. In contrast, only one gene directly related to carbohydrate metabolism was altered. Five genes involved in fatty acid elongation and synthesis of triglyceride were downregulated following carnitine exposure; ELOVL1 (-0.68 fold change), ACOT4 (-0.80 fold change), ACSL6 (-0.66 fold change), THEM4 (-0.6 fold change), TPI1 (-0.85 fold change), while one transcript required for  $\beta$ -oxidation, CYP422A, was upregulated (+0.98 fold change). STBD1, starch binding domain 1, involved in carbohydrate metabolism, was upregulated in carnitine-treated blastocysts (+0.84 fold change).

#### 5.4.3.3 Genes involved in successful pregnancy

Three transcripts related to successful pregnancy were down-regulated in carnitine-treated blastocysts compared to controls; IFNT (Interferon- $\tau$ ), the primary signal for maternal recognition (-1.41 fold change), as well as pregnancy-associated glycoproteins PAG2 (-1.24 fold change) and PAG12 (-0.94 fold change).

#### 5.4.3.4 Genes involved in glutathione metabolism

The gene GSTO1, encoding the cytoplasmic enzyme Glutathione S-transferase omega-1, was downregulated in L-carnitine-treated embryos (-0.61 fold change).

#### 5.4.3.5 Intracellular junctions

GJB4, encoding a component of gap junctions with roles including calcium regulation and membrane trafficking, had reduced expression following L-carnitine treatment (-0.59 fold change).

#### 5.4.3.6 Oxygen-consuming enzymes

SQLE, encoding squalene monooxygenase, had reduced expression compared to control blastocysts following L-carnitine treatment (-0.65 fold change).

#### 5.4.3.7 Protein turnover and post-translational modification

L-carnitine treatment led to altered expression of a number of genes involved in protein turnover. QSOX1, catalysing oxidation of thiol groups to sulphides, was downregulated (-0.73 fold change), while CHST10, which transfers sulphate groups to glycoproteins and glycolipids, along with TGM2, involved in protein crosslinking were upregulated (+0.65 and +0.93 fold change respectively).

#### 5.4.3.8 Transcription factors and transcription suppressors

A number of genes encoding transcription factor or suppressor products were altered following promotion of  $\beta$ -oxidation with L-carnitine. Two transcription repressors were upregulated; TBX18, which represses genes involved in embryo development (+0.85 fold change); and FOXG1, which represses genes involved in brain development (+0.69 fold change). These changes might inhibit development of a viable embryo. Interestingly, TFAP2A (transcription factor AP-2 alpha) was downregulated (-1.10 fold change), an effect reported to repress placental gene expression in trophoblast. Additionally, NUPR1, encoding an inhibitor of histone acetylation was downregulated (-0.6 fold change).

#### 5.4.4 Transcriptomic microarray following BMA treatment

In blastocysts treated with BMA, a total of 582 sites were differentially expressed, with 330 upregulated and 252 downregulated versus controls (Figure 46). Of these, 440 were differentially expressed genes, 62 were novel products and 14 were pseudogenes. The remaining 66 were internal 'degenerate' controls based on genes included in the microarray but with a number of mismatches. These were differentially expressed as their corresponding genes were differentially expressed and are included in the total of 440.

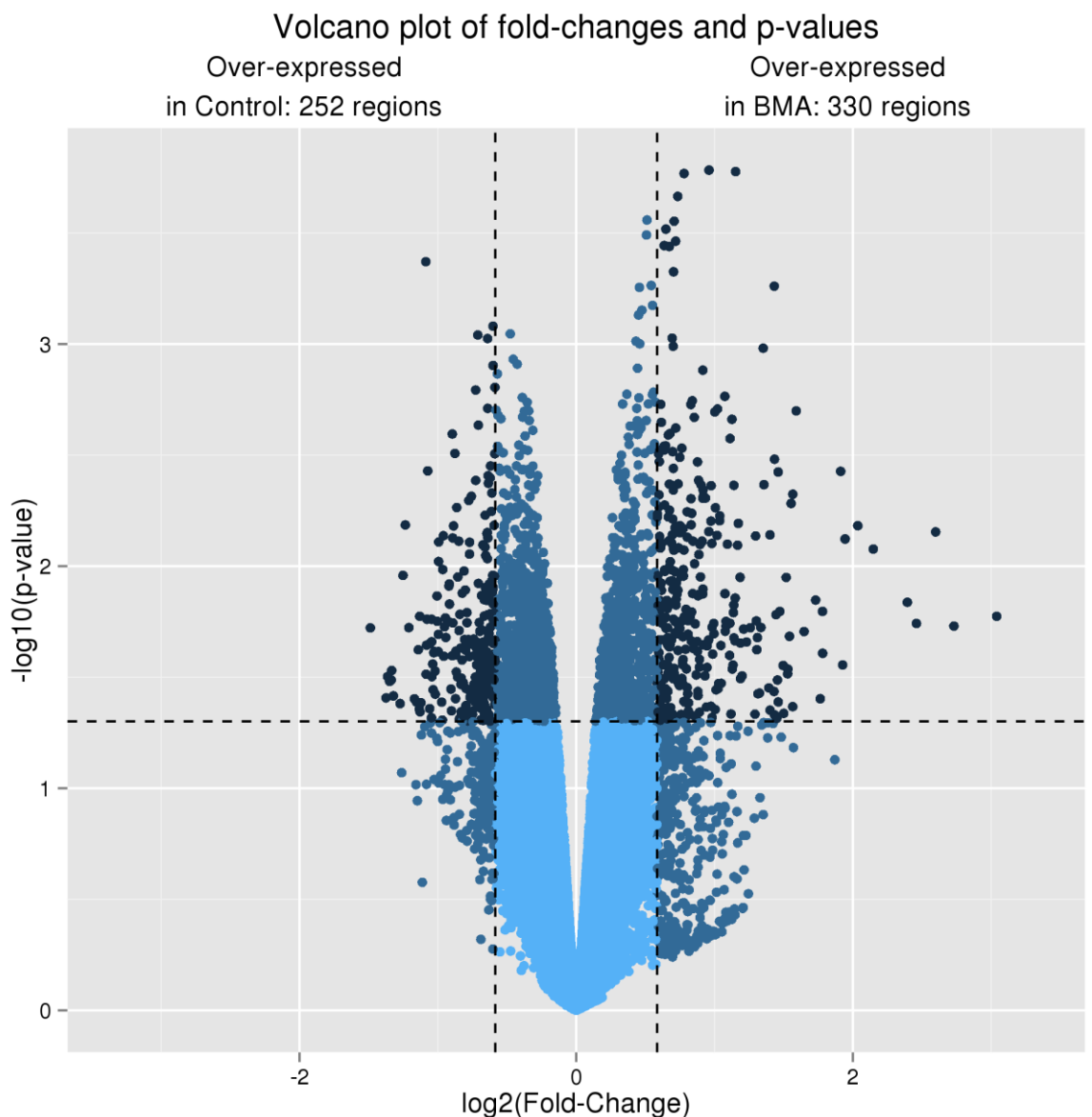


Figure 46: Volcano plot indicating the spread of differentially expressed transcripts between BMA treated and control embryos. The dark points indicate probes which exceed the thresholds of  $p < 0.05$  and  $\text{fold change} > \log_2(0.5)$ . A total of 582 transcripts were differentially expressed.

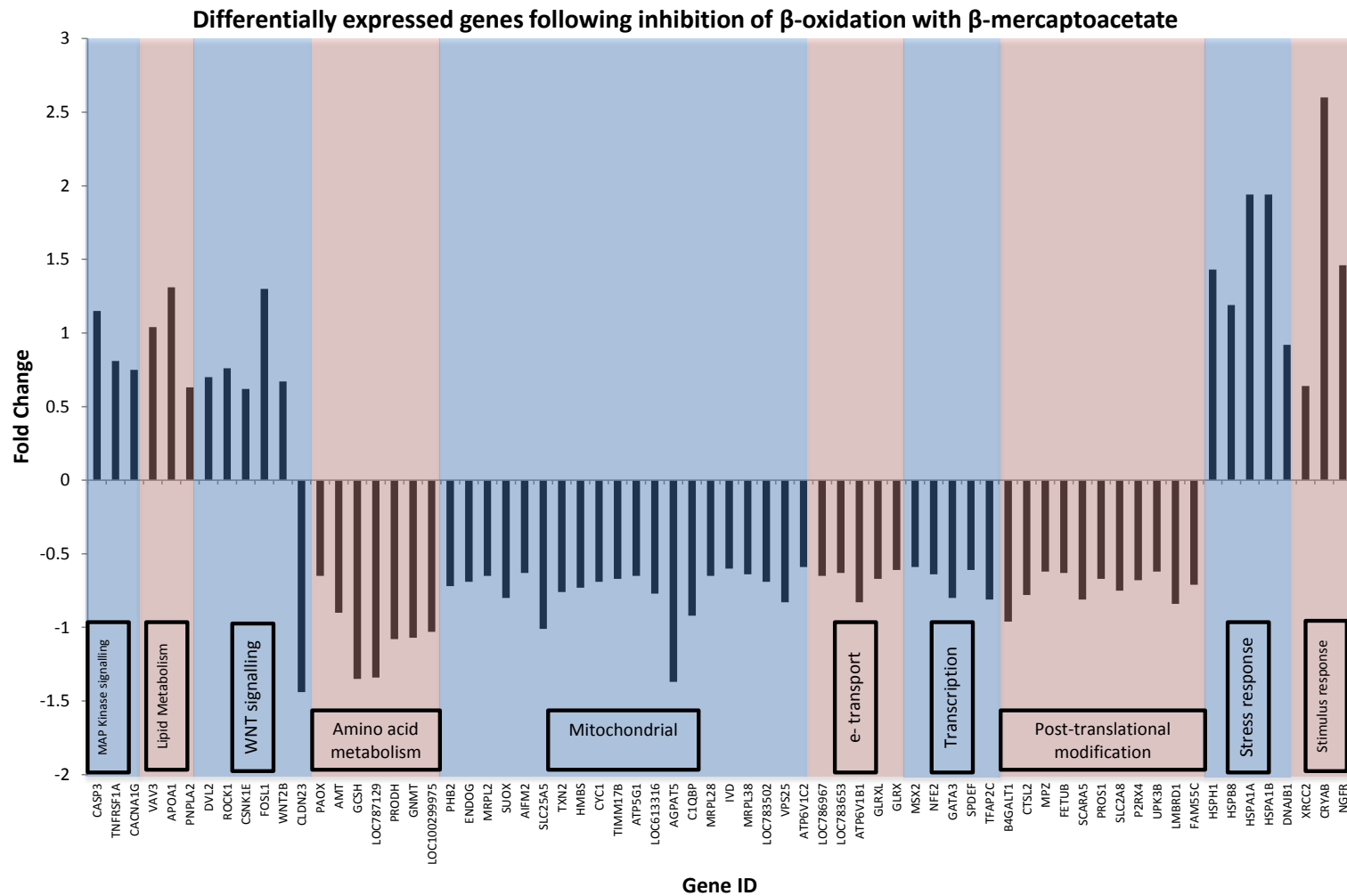


Figure 47: Differential expression of key genes by blastocysts following inhibition of  $\beta$ -oxidation with  $\beta$ -mercaptoacetate. Genes grouped by functional classification. Genes displayed exceed significance thresholds of  $p < 0.05$  and fold change  $> \log_2(0.5)$ .

Annotation Group	Gene ID	Product name	Role	Fold change
MAP Kinase signalling	CASP3	Caspase 3	Apoptosis-Related Cysteine Peptidase	1.15
	TNFRSF1A	Tumour necrosis factor receptor 1A	Activates NF-kB, regulates apoptosis via caspase 8 and inflammation	0.81
	CACNA1G	Voltage-dependent calcium channel, T A1g	Low voltage activated calcium channel involved in pacemaker activity and	0.75
lipid metabolism	VAV3	Vav 3 guanine nucleotide exchange factor	Acts with Rho GTPases to stimulate cytoskeletal rearrangements, regulates lipid processes	1.04
	APOA1	Apolipoprotein A-I	Major component of high density lipoprotein	1.31
	PNPLA2	Patatin-like phospholipase containing 2	Catalyses the first step of lipolysis in lipid droplets.	0.63
WNT signalling	DVL2	Dishevelled Segment Polarity Protein 2	Promotes internalisation of frizzled receptors following wnt signalling.	0.70
	ROCK1	Rho-Associated, Coiled-Coil Protein Kinase 1	Rho kinase, regulates cytoskeleton and cell polarity	0.76
	CSNK1E	Casein Kinase 1, Epsilon	Negative regulator of circadian rhythmicity	0.62
	FOSL1	FOS-Like Antigen 1	Dimerises with JUN proteins to form transcription factor complex AP-1, regulates proliferation and differentiation.	1.30
	WNT2B	Wingless-Type MMTV Integration Site 2B	Ligand for frizzled receptor, developmental signalling	0.67
	CLDN23	Claudin 23	Possible link to childhood obesity	-1.44
Amino acid metabolism	PAOX	Polyamine oxidase (exo-N4-amino)	Flavoenzyme oxidising N(1)acetyl spermidine to spermidine or putrescine.	-0.65
	AMT	Glycine cleavage system T	Aminomethyltransferase	-0.90
	GCSH	Glycine cleavage system H	One of four glycine components of glycine cleavage system	-1.35
	LOC787129	Similar to GCSH		-1.34
	PRODH	Proline dehydrogenase (oxidase) 1	Mitochondrial FAD binding catalysing first step in proline degradation.	-1.08
	GNMT	Glycine N-methyltransferase	Methionine metabolism	-1.07
	LOC100299975	Similar to GCSH		-1.03
Mitochondrial structure and function	PHB2	Prohibitin 2	Oestrogen receptor-selective coregulator with antiestrogens.	-0.72
	ENDOG	Endonuclease G	Mitochondrial endonuclease, cleaves DNA at GC tracts	-0.69
	MRPL2	Mitochondrial ribosomal protein L28	39S subunit of mitoribosome	-0.65
	SUOX	Sulphite oxidase	Intermembrane matrix protein oxidising sulphite to sulphate	-0.80
	AIFM2	Apoptosis-inducing factor, mitochondrion-associated, 2	Oxidoreductase mediating p53-dependent apoptosis.	-0.63
	SLC25A5	Solute carrier family 25, member 5	Translocates ADP from cytoplasm to mitochondrial matrix and ATP from matrix to cytoplasm.	-1.01
	TXN2	Thioredoxin 2	Mitochondrial thioredoxin.	-0.76
	HMBS	Hydroxymethylbilane synthase	Third enzyme of heme biosynthetic pathway	-0.73
	AMT	Glycine cleavage system T	Aminomethyltransferase	-0.90
	CYC1	Cytochrome C-1	Heme-containing Cytochrome b-c1 components	-0.69
	TIMM17B	Translocase of inner mitochondrial membrane 17 homolog B (yeast)	Integral component of mitochondrial TIM23 complex.	-0.67
	ATP5G1	ATP synthase, H+ transporting, F0, C1 (9)	Subunit of ATP synthase.	-0.65
	LOC787129	Similar to Glycine cleavage system H protein		-1.34
	LOC613316	Similar to ubiquinol-cytochrome c reductase		-0.77
	AGPAT5	1-acylglycerol-3-phosphate O-acyltransferase 5	Integral mitochondrial membrane protein catalysing 2 <sup>nd</sup> step in de novo phospholipid synthesis.	-1.37
	C1QBP	Complement component 1, q binding protein	Complement subcomponent inhibiting C1 activation.	-0.92
	MRPL28	Mitochondrial ribosomal protein L28	39S component of mitoribosome	-0.65
	IVD	Isovaleryl Coenzyme A dehydrogenase	Mitochondrial matrix enzyme catalysing leucine metabolism.	-0.60
	MRPL38	Mitochondrial ribosomal protein L38	39S component of mitoribosome	-0.64
	LOC783502	Similar to ubiquinol-cytochrome c reductase		-0.69
	VPS25	Vacuolar protein sorting 25 homolog	(S. cerevisiae) homolog. Endosomal sorting complex component	-0.83
	ATP6V1C2	ATPase, H+ transporting, lysosomal 42kDa, V1 C2	Subunit of vacuolar ATPase	-0.59

Annotation Group	Gene ID	Product name	Role	Fold change
Electron transport chain	ATP6V1C2	ATPase, H+ transporting, lysosomal 42kDa, V1 subunit C2	Subunit of vacuolar ATPase	-0.59
	LOC786967	Similar to Glutaredoxin-1	Similar to (Thioltransferase-1) (TTase-1)	-0.65
	TXN2	Thioredoxin 2	Mitochondrial thioredoxin.	-0.76
	CYC1	Cytochrome C-1	Heme-containing Cytochrome b-c1 components	-0.69
	LOC783653	Similar to Glutaredoxin-1	Similar to (Thioltransferase-1) (TTase-1)	-0.63
	ATP5G1	ATP synthase, H+ transporting, mitochondrial F0 complex, C1 subunit 9	Subunit of ATP synthase.	-0.65
	ATP6V1B1	ATPase, H+ transporting, lysosomal 56/58kDa, V1 subunit B1	Subunit of vacuolar ATPase	-0.83
	LOC783502	Similar to ubiquinol--cytochrome c reductase		-0.69
	GLRXL	Glutaredoxin (thioltransferase)-like		-0.67
	GLRX	Glutaredoxin (thioltransferase)	Redox enzyme involved in antioxidant defence, uses glutathione as cofactor.	-0.61
	LOC613316	Similar to ubiquinol--cytochrome c reductase		-0.77
Transcription	NFE2	Nuclear factor (erythroid-derived 2), 45kDa	NF-E2 complex essential for regulating erythroid and megakaryocytic maturation and development	-0.64
	MRPL28	Mitochondrial ribosomal protein L28	39S subunit of mitochondrial ribosome, role in protein synthesis within mitochondria	-0.65
	GATA3	GATA binding protein 3	Tissue specific roles: regulate T cell development and mammary epithelial cell differentiation	-0.80
	PHB2	Prohibitin 2	Oestrogen receptor selective coregulator. Essential for mitochondrial activation, loss leads to diabetes	-0.72
	SPDEF	SAM pointed domain containing ets1 transcription factor	Androgen-independent activator of prostate specific antigen promoter.	-0.61
	TFAP2C	Transcription factor AP-2 gamma (activating enhancer binding protein 2 gamma)	Involved in mammary development and hormone responsive breast cancer	-0.81
	VPS25	Vacuolar protein sorting 25 homolog ( <i>S. cerevisiae</i> )	Component of endosomal sorting complex, role in sorting ubiquitinated proteins. Regulates transcription via ELL (elongation factor RNA polymerase II)	-0.83
Post-translational modification	B4GALT1	UDP-Gal:betaGlcNAc beta 1,4- galactosyltransferase, polypeptide 1	Golgi form involved in lactose production, N-linked oligosaccharides and carbohydrate moieties of glycolipids. Cell surface form involved in cell-cell recognition in events including fertilisation.	-0.96
	CTSL2	Cathepsin L2	Lysosomal cysteine peptidase, role in corneal physiology and certain cancers.	-0.78
	MPZ	Myelin protein zero	Vital structural component of myelin sheath. Deficiency implicated in heritable neurological diseases.	-0.62
	LOC786967	Similar to Glutaredoxin-1 (Thioltransferase-1) (TTase-1)		-0.65
	TXN2	Thioredoxin 2	Regulation of mitochondrial membrane potential and protection against ROS-induced apoptosis	-0.76
	FETUB	Fetuin B	Protease inhibitor required for oocyte fertilisation	-0.63
	LOC783653	Similar to Glutaredoxin-1 (Thioltransferase-1) (TTase-1)		-0.63
	SCARA5	Scavenger receptor class A, member 5 (putative)	Ferritin receptor, mediates non-transferrin-dependent delivery of iron	-0.81
	PROS1	Protein S (alpha)	Vitamin K-dependent glycoprotein. Binds complement component C. Role in blood clotting.	-0.67
	GLRXL	Glutaredoxin (thioltransferase)-like		-0.67
	GLRX	Glutaredoxin (thioltransferase)	Redox enzyme involved in antioxidant defence, uses glutathione as cofactor.	-0.61
	SLC2A8	Solute carrier family 2 (facilitated glucose transporter), member 8	GLUT8. Insulin-regulated glucose transporter. Binds cytochalasin B and inhibited by fructose.	-0.75
	P2RX4	Purinergic receptor P2X, ligand-gated ion channel, 4	ATP-activated ligand binding ion channel. Forms homomeric or heteromeric trimmers.	-0.68
	UPK3B	Uroplakin 3B	Component of urothelial asymmetric unit membrane	-0.62
	LMBRD1	LMBR1 domain containing 1	Lysosomal protein involved in export of cobalamin for its conversion to cofactors.	-0.84
FAM55C	Family with sequence similarity 55, member C	Also known as Neurexophilin And PC-Esterase Domain 3.	-0.71	

Annotation Group	Gene ID	Product name	Role	Fold change
Stress response	HSPH1	Heat Shock 105kDa/110kDa Protein 1	Prevents aggregation of denatured protein following cell stress	1.43
	HSPB8	Heat Shock 22kDa Protein 8	Temperature-sensitive chaperone protein, oestrogen sensitive.	1.19
	HSPA1A	Heat Shock 70kDa Protein 1A	Stabilises protein against aggregation.	1.94
	HSPA1B	Heat Shock 70kDa Protein 1B	Stabilises protein against aggregation.	1.94
	DNAJB1	DnaJ (Hsp40) Homolog B1	Interacts with and stimulates ATPase activity of Hsp70s	0.92
Stimulus response	CASP3	Caspase 3,	Apoptosis-Related Cysteine Peptidase	1.15
	XRCC2	X-Ray Repair Complementing	(Defective Repair In Chinese Hamster Cells) DNA repair	0.64
	CRYAB	Crystallin, Alpha B	Stabilises proteins against aggregation.	2.60
	HSPB8	Heat Shock 22kDa Protein 8	Temperature-sensitive chaperone protein, oestrogen sensitive.	1.19
	NGFR	Nerve Growth Factor Receptor	Regulates translocation of GLUT4 to the cell surface	1.46
	HSPA1B	Heat Shock 70kDa Protein 1B	Stabilises proteins against aggregation.	1.94
Cellular remodelling	STMN2	Stathmin 2	Regulates microtubule stability, activated by MAP8	0.77
	KLC1	Kinesin Light chain 1	Component of Kinesin. Transports intracellular cargo towards the + terminus of microtubules	0.59
	SWAP70	Switch-associated protein 70	PI3P-dependent guanine exchange factor (GEF). Regulates membrane ruffling, actin cytoskeleton via RAC	0.98
	UCHL1	Ubiquitin carboxyl-terminal esterase L1	Thiol protease involved in ubiquitin precursor processing. Protects monoubiquitin from degradation.	1.11
	S100A11	S100 calcium binding protein A11	Regulation of cell cycle progression and differentiation	1.78
	TUBB6	Tubulin $\beta$ 6	Major constituent of microtubules, interacts with Kinesin (+ end) and Dynein (- end)	0.85
	CDH2	Cadherin 2	Calcium dependent cell-cell adhesion glycoprotein. Role in left-right asymmetry in gastrulation.	1.08
	KLC2	Kinesin light chain 2	Component of Kinesin. ATP-dependent transport of organelles and vesicles.	0.62
	ACTG2	Actin $\gamma$ 2	Cell motility and maintenance of cytoskeleton	0.65
	CASP3	Caspase 3	Apoptosis-Related Cysteine Peptidase	1.15
	PNPLA2	Patatin-like phospholipase containing 2	Catalyses the first step of lipolysis in lipid droplets.	0.63
	CAMK2N2	Calmodulin-dependent protein kinase II	Negative regulator of Ca <sup>2+</sup> /calmodulin kinase II, regulates cell growth	0.63
	GCH1	GTP cyclohydrolase 1	Positive regulation of nitric oxide synthesis, dopamine synthesis. Role in pain sensitivity and persistence.	0.78
	AP1S2	Apoptosis-related protein complex 1 $\sigma$ 2	Subunit of clathrin-associated adaptor protein complex I, protein sorting in late golgi/endosome	0.86
	SPTBN1	Spectrin beta chain	Actin crosslink or scaffold protein linking cytoskeleton to membrane. Role in Ca <sup>2+</sup> -dependent movement	0.96
	SEC24D	SEC 24 family D	Component of COPII coat, role in transport of ER-derived vesicles to the golgi.	1.07

Table 19: Table highlighting functional annotations of key genes which were differentially expressed following BMA treatment. Genes displayed exceeded the significance thresholds of  $p < 0.05$  and  $\text{fold change} > \log_2(0.5)$ .

#### 5.4.4.1 Genes involved in MAP kinase signalling

3 Genes involved in MAP kinase signalling were upregulated following BMA treatment, including CASP3, a caspase involved in apoptosis (-+1.15 fold change) and TNFRSF1A, which activates NF- $\kappa$ B and regulates apoptosis via caspase 8 (+0.81 fold increase). CACNA1G, a voltage-dependent calcium channel, was also upregulated (+0.75 fold increase). The MAP kinase pathway typically responds to stimuli including mitogens but also osmotic or heat stress, and regulates proliferation, mitosis, apoptosis and gene expression. An increase in expression of MAP kinase components suggests that the BMA-treated embryo is under stress and may have altered cell division and apoptosis rates.

#### 5.4.4.2 Genes involved in lipid metabolism

Two genes with a role in lipid metabolism were differentially expressed following BMA treatment; APOA1, the main protein component of high density lipoproteins (1.31 fold increase,  $p=0.04$ ) and PNPLA2 a target of PPAR $\gamma$  with downstream roles in lipid metabolism (+0.63 fold change,  $p=0.03$ ).

#### 5.4.4.3 Genes involved in WNT signalling

5 genes involved in the wnt signalling cascade, a vital pathway to embryonic development, were upregulated in response to BMA treatment. These include DVL2, involved in frizzled receptor internalisation (0.7 fold increase,  $p=0.01$ ), ROCK1, a vital Rho kinase (0.76 fold increase,  $p=0.03$ ), CSNK1E, a casein kinase (0.62 fold increase,  $p=0.05$ ), FOSL1, a transcription factor complex (1.3 fold increase,  $p=0.02$ ) and WNT2B, a ligand for frizzled receptors. This suggests an overall increase in wnt activity.

#### 5.4.4.4 Genes involved in amino acid metabolism

A total of 5 genes involved in amino acid degradation were downregulated following BMA treatment, including 2 subunits of the glycine cleavage system, AMT (0.9 fold decrease,  $p=0.0$ ) and GCSH (1.35 fold decrease,  $p=0.03$ ). Additionally, polyamine oxidase (PAOX, 0.65 fold decrease,  $p=0.04$ ), glycine methyltransferase (1.07 fold decrease,  $p=0.004$ ), and proline dehydrogenase (PRODH, 0.9 fold decrease,  $p=0.02$ ).

#### 5.4.4.5 Genes involved in mitochondrial structure and function

A total of 24 genes involved in mitochondrial structure and function were downregulated following BMA treatment. These include ADP/ATP carrier SLC25A5 (-1.01 fold change,  $p=0.01$ ), prohibitin PHB2 (-0.72 fold change,  $p=0.04$ ), Endonuclease ENDOG (0.69 fold change,  $p=0.03$ ), Mitochondrial ribosome subunits MRPL2 (-0.65 fold change,  $p=0.03$ ), MRPL28 (-0.65 fold change,  $p=0.03$ ) and MRPL38 (-0.64 fold change,  $p=0.01$ ), intermembrane sulphite oxidase SUOX (-0.8 fold change,  $p=0.02$ ), apoptosis-inducing oxidase AIFM2 (-0.63 fold change,  $p=0.01$ ), Thioredoxin TXN2 (-0.76 fold change,  $p=0.04$ ), Haem synthase HMBS (-0.73 fold change,  $p=0.03$ ), Glycine cleavage system components AMT (-0.9 fold change,  $p=0.00$ ) and , Cytochrome C CYC1 (-0.69 fold change,  $p=0.05$ ), TIM23 complex component TIMM17B (-0.67 fold change,  $p=0.04$ ), ATP Synthase component ATP5G1 (-0.65 fold change,  $p=0.05$ ) phospholipid transferase AGPAT5 (-1.37 fold change,  $p=0.04$ ), complement component C1QBP (-0.92 fold change,  $p=0.01$ ), CoA dehydrogenase IVD (-0.6 fold change,  $p=0.00$ ), endosomal sorting complex component VPS25 (-0.83 fold change,  $p=0.02$ ) and ATPase components ATP6V1C2 (-0.59 fold change,  $p=0.02$ ) and ATP6V1B1 (-0.83 fold change,  $p=0.05$ ). Also downregulated were novel transcripts LOC787129 (-1.34 fold change,  $p=0.04$ ), LOC613316 (-0.77 fold change,  $p=0.03$ ) and LOC783502 (-0.69 fold change,  $p=0.03$ ), which have homology to glycine cleavage system components and cytochrome c.

#### 5.4.4.6 Genes involved in the electron transport chain

7 genes involved in generation of precursor metabolites and energy release through the electron transport chain were downregulated in BMA treated embryos. A number of these (ATP6V1C2, TXN2, CYC1, ATP5G1, ATP6V1B1, and LOC613316) are described in the mitochondrial polarisation and morphology section above. Additionally, Glutaredoxin GLRX (-0.67 fold change,  $p=0.05$ ) and glutaredoxin-like protein GLRXL (-0.67 fold change,  $p=0.05$ ) were both downregulated. Novel transcripts similar to glutaredoxin-1 LOC786967 (-0.65 fold change,  $p=0.03$ ) and LOC783653 (-0.63 fold change,  $p=0.03$ ). This might suggest that the embryo consumes more oxygen in an attempt to overcome the resulting reduction in electron transport.

#### 5.4.4.7 Genes involved in regulation of transcription

A total of 8 genes involved in regulation of transcription were differentially expressed following BMA treatment. These included a number of proteins mentioned above; MRPL28, VPS25 and PHB2. 5 additional transcription factor genes were also downregulated following inhibition of  $\beta$ -oxidation with BMA. These included msh homeobox protein MSX2 (-0.59 fold change,  $p=0.04$ ), Nuclear factor NFE2 (-0.64 fold change,  $p=0.04$ ), GATA binding protein GATA3 (-0.8 fold change,  $p=0.04$ ), SAM domain containing factor SPDEF (-0.61 fold change,  $p=0.01$ ), transcription factor activating enhancer binding protein  $\gamma$  TFAP2C (-0.81 fold change,  $p=0.05$ ).

#### 5.4.4.8 Genes involved in post-translational modification

A total of 16 genes involved in post-translational modification of proteins were downregulated following BMA treatment. galactosyltransferase B4GALT1 (-0.96 fold change,  $p=0.01$ ), cathepsin CTSL2 (-0.78 fold change,  $p=0.02$ ), myelin protein MPZ (-0.62 fold change,  $p=0.03$ ), fetuin FETUB (-0.63 fold change,  $p=0.00$ ), scavenger receptor SCARA5 (-0.81 fold change,  $p=0.01$ ), Protein S PROS1 (-0.67 fold change,  $p=0.04$ ), solute carrier SLC2A8 (-0.75 fold change,  $p=0.05$ ), purinergic receptor P2RX4 (-0.68 fold change,  $p=0.01$ ), uroplakin UPK3B (-0.62 fold change,  $p=0.03$ ), LMBR1 domain containing protein LMBRD1 (-0.84 fold change,  $p=0.05$ ), FAM55C (-0.71 fold change,  $p=0.04$ ).

#### 5.4.4.9 Genes involved in stress response.

5 genes involved in response to stress, including the 4 heat shock proteins HSPB8 (1.19 fold increase,  $p=0.03$ ), HSPH1 (1.43 fold increase,  $p=0.00$ ), HSPA1A (1.94 fold increase,  $p=0.01$ ) and HSPA1B (1.94 fold increase,  $p=0.01$ ) and heat shock stimulator DNAJB1, were upregulated following BMA treatment.

#### 5.4.4.10 Genes involved in stimulus response

6 genes involved in the response to stimuli including temperature and antibiotics were upregulated following BMA treatment. These include two heat shock proteins mentioned above, HSPB8 and HSPA1B, as well as CASP3. Additionally, DNA repair receptor XRCC2 (0.64 fold increase,  $p=0.00$ ), Crystallin CRYAB (2.6 fold increase,  $p=0.01$ ) and growth factor receptor NGFR (1.46 fold increase,  $p=0.00$ ) were upregulated. Taken together, these upregulations suggest that the embryo is responding to BMA treatment as a stress

stimulus, with similar effects to exposure to increased temperature or antibiotic compounds, suggesting very deleterious conditions for the embryo.

#### 5.4.4.11 Genes involved in cellular remodelling

16 genes identified to have roles in cellular remodelling and transport were upregulated following inhibition of  $\beta$ -oxidation with BMA. These include Stathmin STMN2 (+0.77 fold change), Kinesin light chain components KLC1 (+0.59 fold change) and KLC2 (+0.62 fold change), which are required for ATP-dependent transport towards the + terminus of microtubules, switch-associated protein SWAP70 (+0.98 fold change), ubiquitin esterase UCHL1 (+1.11 fold change), calcium binding protein S100A11 (+1.78 fold change), Tubulin TUBB6 (+0.85 fold change), Cadherin CDH2 (+1.08 fold change), actin component ACTG2 (+0.65 fold change), phospholipase PNPLA2 (+0.63 fold change), calmodulin-dependent kinase CAMK2N2 (+0.63 fold change), GTP cyclohydrolase GCH1 (+0.78 fold change), apoptosis-related complex component AP1S2 (0.86 fold change), spectrin component SPTBN1 (+0.96 fold change), COPII coat component SEC24D (+1.07 fold change) and CASP3, mentioned above.

### 5.4.5 Epigenetic microarray following L-carnitine treatment

A total of 1414 probe binding regions were differentially methylated between carnitine-treated embryos and controls, with 733 hypermethylated in control and 681 hypermethylated in carnitine-treated embryos. Of these, 65 exon sites were hypermethylated and 42 sites within exons were hypomethylated in carnitine treated embryos compared with controls for a total of 107 differentially methylated exons. 42 DMRs were within 1kbp of the transcription start site, 178 within 5kbp and 7 DMRs in CGIs were within 1kbp of the transcription start site of at least 1 gene, with a further 4 within 50kbp of transcription start sites of multiple genes.



Figure 48: Epigenetic circular plot summarising all significantly different probe binding sites between control and L-carnitine treated blastocysts. Only significantly different ( $p < 0.05$ ) sites are displayed. Layers from top to bottom as follows: epigenetic p-value (0-0.05), epigenetic fold-change (difference in methylation in L-carnitine treated embryos relative to controls), condition mean intensity, fold-changes of 18 known imprinted genes; symbols of the imprinted genes.

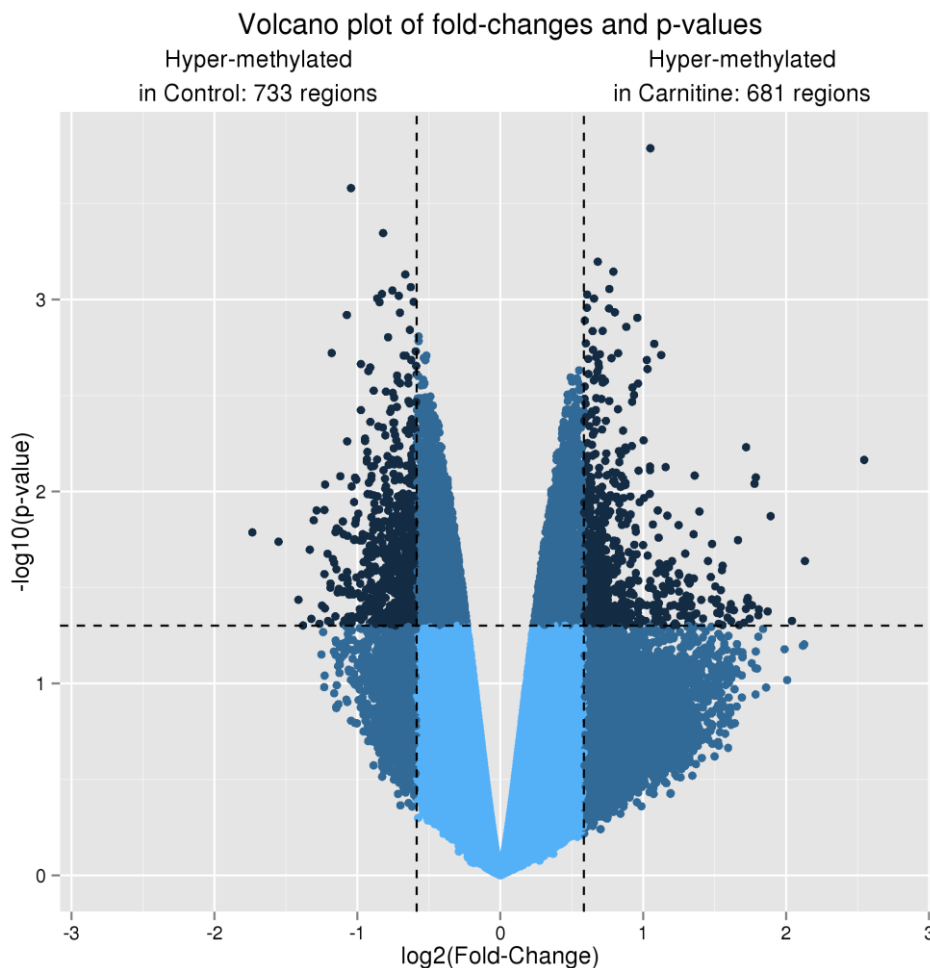


Figure 49: Volcano plot of all probes in methylation microarray between carnitine-treated and control embryos. Hypermethylated regions in carnitine or control treatments were above the threshold of  $\log_2(0.5)$  fold change and  $p < 0.05$ . While high fold-change suggests a greater overall difference in methylation between control and L-carnitine treated embryos, the relationship is not linear.

#### 5.4.5.1 Promoter methylation

Following L-carnitine treatment, 4 CpG Islands within (1kbp) and 1 CGI within 5kbp of a promoter were hypermethylated, while a further 7 regions 5-50kbp from promoter regions regulating a total of 67 genes. These changes are displayed below (Figure 50).

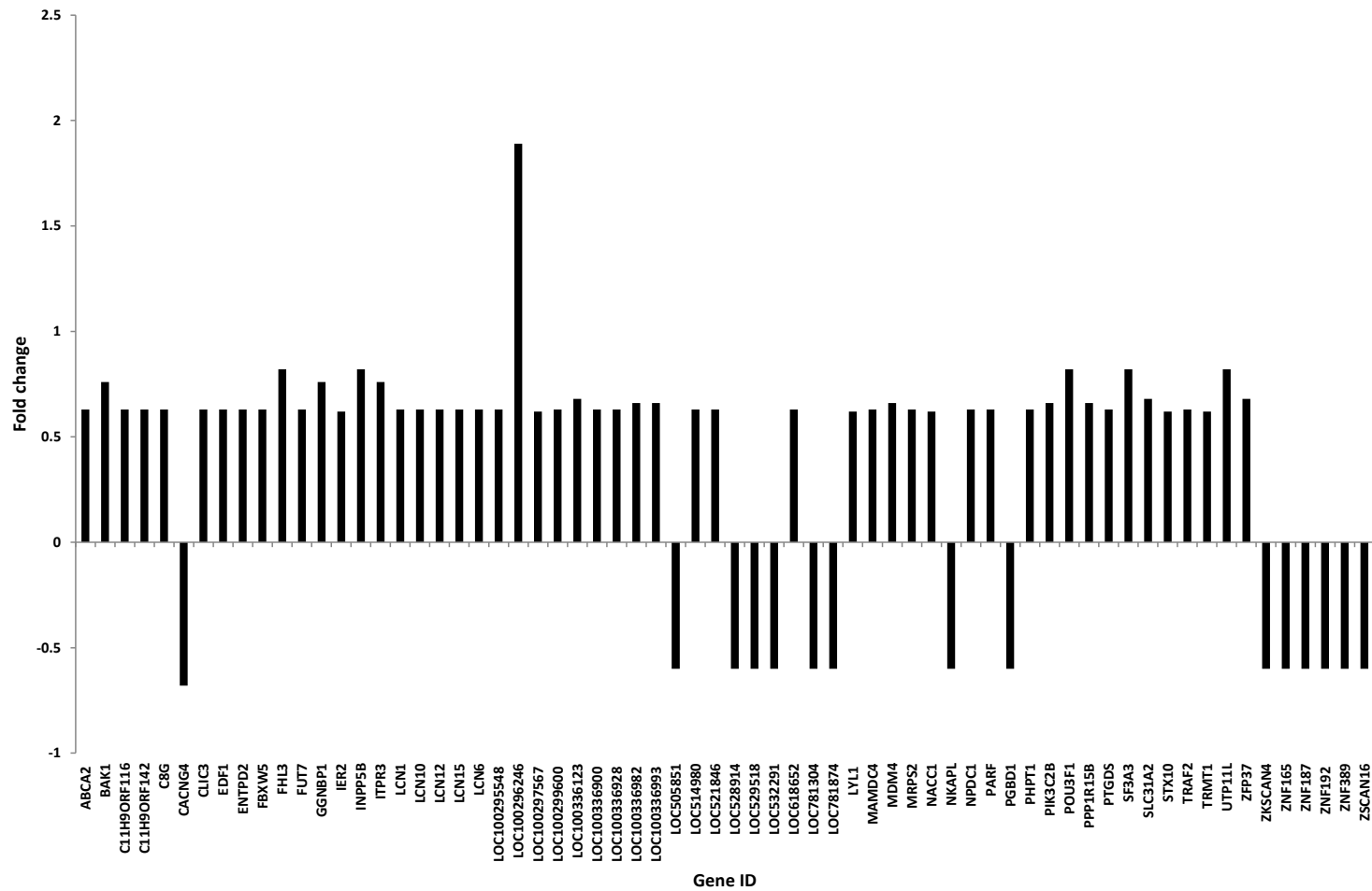


Figure 50: Differential methylation at CGIs within 50kbp of promoter regions in blastocysts produced following culture with L-carnitine.

#### 5.4.5.2 Differential methylation within 5kbp of a promoter region

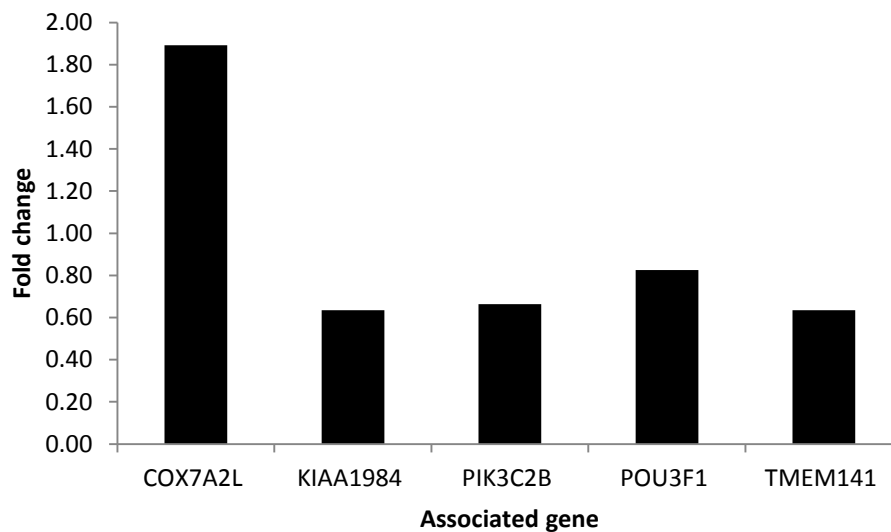


Figure 51: Differential methylation of CpG islands within 1kbp of promoter regions in blastocysts following promotion of  $\beta$ -oxidation with L-carnitine.

Following embryo culture with L-carnitine, 4 CGIs proximal to a gene promoter (within 1kbp) were significantly hypermethylated relative to control embryos. Such modifications are likely to have an inhibitory effect on gene expression. These include COX7A2L, encoding cytochrome c oxidase subunit 7A-related protein (1.89 fold increase,  $p=0.01$ ), KIAA1989 (0.63 fold increase,  $p=0.02$ ), phosphoinositide-3-kinase PIK3CB (0.66 fold increase,  $p=0.04$ ) and the embryonic transcription regulator Oct-6 or POU3F1 (0.82 fold increase,  $p=0.0$ ). A CGI within 50kbp of the promoter controlling expression of transmembrane protein TMEM141 was also hypermethylated (0.63 fold increase,  $p=0.02$ ).

#### 5.4.5.3 Distal promoter methylation

Additionally, a further 7 regions 5-50kbp from promoter regions regulating a total of 67 genes were differentially methylated following promotion of  $\beta$ -oxidation with L-carnitine. It is hard to predict the effect of differential methylation of regions at this distance from a promoter. These are listed in Table 20 below.

Gene ID	Name	Role	Fold change	P value
ABCA2	ATP-Binding Cassette, Sub-Family A (ABC1), Member 2	Thought to export lipid in neural cells.	0.63	0.02
BAK1	BCL2-antagonist/killer 1	Promotes apoptosis by inhibiting the effects of BCL2	0.76	0.03
C11H9ORF116	Chromosome 9 open reading frame 116 ortholog	Encodes protein with unknown function	0.63	0.02
C11H9ORF142	Chromosome 9 open reading frame 142 ortholog	Encodes protein with unknown function	0.63	0.02
C8G	Complement component 8, gamma polypeptide	Component of bactericidal membrane attack complex	0.63	0.02
CACNG4	Calcium channel, voltage-dependent, gamma subunit 4	Regulates trafficking of AMPA-selective glutamate receptors	-0.68	0.04
CLIC3	Chloride intracellular channel 3	Inserts into membranes to form chloride channels	0.63	0.02
EDF1	Endothelial differentiation-related factor 1	Transcriptional coactivator for PPAR $\gamma$ , NR5A1 and NR1H3/LXRA, enhances DNA-binding of ATF1, ATF2, CREB1 and NR5A1	0.63	0.02
ENTPD2	Ectonucleoside triphosphate diphosphohydrolase 2	Hydrolyses nucleotides to regulate purinergic neurotransmission	0.63	0.02
FBXW5	F-box and WD repeat domain containing 5	Substrate recognition component of SCF and DCX ubiquitin-protein ligase complexes.	0.63	0.02
FLH3	Four and a half LIM domains 3	Suppresses tumorigenesis, MyoD and IgE receptor expression.	0.82	0.00
FUT7	Fucosyltransferase 7 (alpha (1,3) fucosyltransferase)	Golgi membrane protein involved in creating sialyl-Lewis X antigens.	0.63	0.02
SGNBP1	Gametogenin binding protein 1	May be involved in spermatogenesis	0.76	0.03
ER2	Immediate early response 2	Promotes tumour cell motility and metastasis	0.62	0.00
INPP5B	Similar to inositol polyphosphate-5-phosphatase, 75kDa	Inactivates IP3 signalling, controlling calcium signalling	0.82	0.00
TPR3	Inositol 1,4,5-triphosphate receptor, type 3	Receptor for IP3, regulates calcium signalling	0.76	0.03
LCN1	Lipocalin 1 (tear prealbumin)	Taste receptor, binds lipids and retinoids.	0.63	0.02
LCN10	Lipocalin 10	Possible retinoid carrier in epididymis with a role in male fertility	0.63	0.02
LCN12	Lipocalin 12	Possible retinoid carrier in epididymis with a role in male fertility	0.63	0.02
LCN15	Lipocalin 15	Protein coding gene, unknown function	0.63	0.02
LCN6	Lipocalin 6	Possible retinoid carrier in epididymis with a role in male fertility	0.63	0.02
LOC100295548	Unassigned	Unknown function	0.63	0.02
LOC100296246	Unassigned	Unknown function	1.89	0.01
LOC100297567	Unassigned	Unknown function	0.62	0.00
LOC100299600	Unassigned	Unknown function	0.63	0.02
LOC100336123	Unassigned	Unknown function	0.68	0.04
LOC100336900	Unassigned	Unknown function	0.63	0.02
LOC100336928	Unassigned	Unknown function	0.63	0.02
LOC100336982	Unassigned	Unknown function	0.66	0.04
LOC100336993	Unassigned	Unknown function	0.66	0.04
LOC505851	Similar to Wilms tumor 1 associated protein	Unknown function	-0.60	0.03
LOC514980	Similar to Epididymal-specific lipocalin-9 precursor	Unknown function	0.63	0.02
LOC521846	Similar to CG15216 CG15216-PA	Unknown function	0.63	0.02
LOC528914	Similar to Olfactory receptor 1F12 (Hs6M1-35P)	Unknown function	-0.60	0.03
LOC529518	Similar to Hcg1805526	Unknown function	-0.60	0.03
LOC532291	Similar to Hcg1805526	Unknown function	-0.60	0.03
LOC618652	Similar to 1A6/DRIM interacting protein	Unknown function	0.63	0.02
LOC781304	Hypothetical LOC781304	Unknown function	-0.60	0.05
LOC781874	Similar to basic helix-loop-helix TF HAND2	Unknown function	-0.60	0.05
LYL1	Lymphoblastic Leukemia Associated Hematopoiesis Regulator 1	Helix-loop-helix transcription factor, roles in regulating haematopoiesis	0.62	0.00
MAMDC4	MAM domain containing 4	Selective transport of receptors and ligands across polarised epithelia	0.63	0.02
MDM4	Mdm4 p53 regulator	Inhibits p53 and p73-mediated apoptosis	0.66	0.04
MRPS2	Mitochondrial ribosomal protein S2	28S mitochondrion subunit	0.63	0.02
NACC1	Nucleus accumbens associated 1, BEN and BTB (POZ) domain containing	Transcriptional corepressor, recruits HDAC3 and HDAC4. Also recruits proteasome to cytoplasm.	0.62	0.00
NKAPL	NFKB activating protein-like	Implicated in schizophrenia	-0.60	0.03
NPDC1	Neural proliferation, differentiation and control, 1	Down-regulates neural proliferation and transformation	0.63	0.02
PARF	Rab-like GTP-binding protein 1A	May enhance proliferation	0.63	0.02
PGBD1	PiggyBac transposable element derived 1	Transposase expressed in brain	-0.60	0.03
PHPT1	Phosphohistidine phosphatase 1	Reversible dephosphorylation of histidine residues in proteins.	0.63	0.02
PIK3C2B	Phosphoinositide-3-kinase, class 2, beta polypeptide	PI3-kinase, involved in EGF and PDGF signalling	0.66	0.04
POU3F1	POU class 3 homeobox 1	Oct-6 octamer-binding transcription factor	0.82	0.00
PPP1R15B	Protein phosphatase 1, regulatory (inhibitor) subunit 15B	Promotes dephosphorylation of transcription factor EIF2 $\alpha$ in unstressed cells	0.66	0.04
PTGDS	Prostaglandin D2 synthase 21kDa (brain)	Maturation and maintenance of CNS and male reproductive system	0.63	0.02
SF3A3	Splicing factor 3a, subunit 3, 60kDa	Required for pre-mRNA splicing	0.82	0.00
SLC31A2	Solute carrier family 31 (copper transporters), member 2	Copper uptake	0.68	0.04
STX10	Syntaxin 10	SNARE involved in transport of vesicles from late endosome to Golgi	0.62	0.00
TRAF2	TNF receptor-associated factor 2	Regulates activation of NF- $\kappa$ B and JNK, promotes ubiquitination of target proteins.	0.63	0.02
TRMT1	TRM1 tRNA methyltransferase 1 homolog (S. cerevisiae)	Demethylates guanine 26 of tRNAs	0.62	0.00
UTP11L	UTP11-like, U3 small nucleolar ribonucleoprotein,	Nuclear processing of pre-18S rRNA	0.82	0.00
ZFP37	Zinc finger protein 37 homolog	Transcriptional regulator	0.68	0.04
ZKSCAN4	Zinc finger with KRAB and SCAN domains 4	Transcriptional regulator, MDM2 and EP300	-0.60	0.03
ZNF165	Zinc finger protein 165	Transcriptional regulator, spermatogenesis	-0.60	0.03
ZNF187	Zinc finger protein 187/ZSCAN26	Transcriptional regulator	-0.60	0.03
ZNF192	Zinc Finger With KRAB And SCAN Domains 8	Transcriptional regulator	-0.60	0.03
ZNF389	Zinc finger protein 389	Pseudogene	-0.60	0.03
ZSCAN16	Zinc finger and SCAN domain containing 16	Transcriptional regulator	-0.60	0.03

Table 20: Differential methylation in CGIs between 5-50kbp of a promoter following promotion of  $\beta$ -oxidation with L-carnitine.

#### 5.4.5.4 Differential methylation at CGI sites within 50kbp of a promoter

Functional annotation analysis of all differentially methylated CGIs within 50kbp of a promoter using DAVID online software revealed 2 functional annotation groups: transcriptional regulators and phosphatidylinositol signalling.

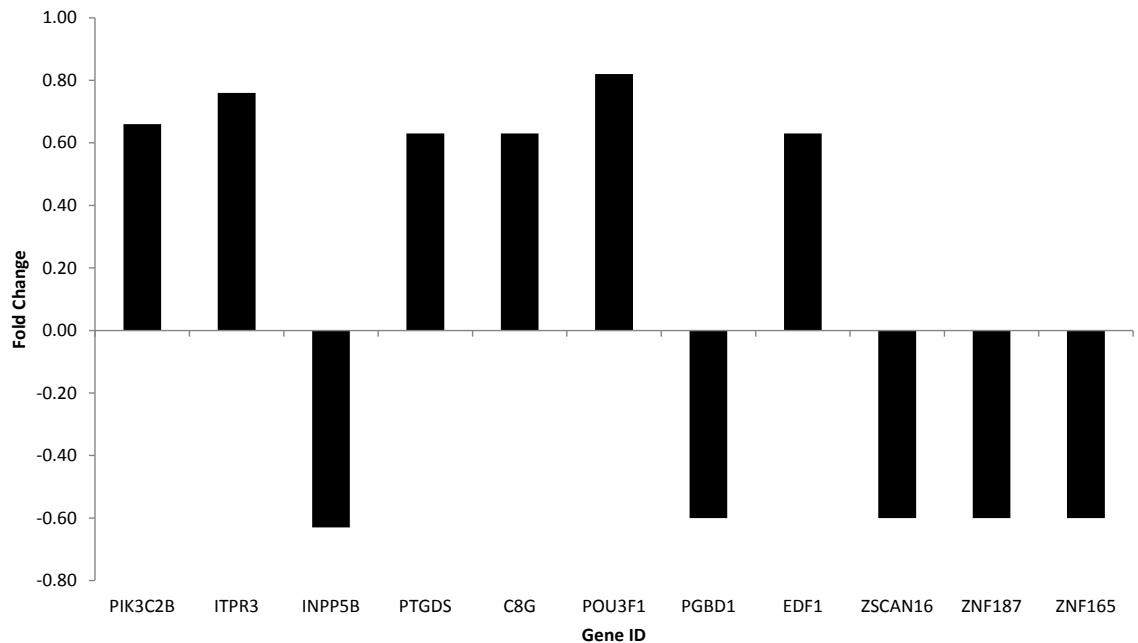


Figure 52: Differential methylation at CGIs within 50kbp of a promoter following L-carnitine treatment.

#### 5.4.5.5 Genes involved in phosphatidylinositol signalling

Several genes involved in phosphatidylinositol signalling were hypermethylated in promoter regions following promotion of  $\beta$ -oxidation with L-carnitine. These included inositol trisphosphate receptor ITPR3 (+0.76 fold change,  $p=0.03$ ), inositol polyphosphate-5-phosphatase INPP5B (+0.82 fold change,  $p=0.03$ ), along with lipocalin family members Prostaglandin D2 synthase PTGDS (+0.63 fold change,  $p=0.02$ ) and complement subunit C8G (+0.63 fold change,  $p=0.02$ ).

#### 5.4.5.6 Genes involved in regulation of transcription

Differentially methylated regions were detected in CGIs within 50kbp of the promoter regions controlling expression of a range of transcription factors. These include POU3F1 (discussed above, +0.82 fold change,  $p=0.00$ ), EDF1 (+0.63 fold change,  $p=0.02$ ), Zinc Finger proteins ZFP37 (+0.68 fold change,  $p=0.04$ ), ZKSCAN4 (-0.6 fold change,  $p=0.03$ ),

ZNF165 (-0.6 fold change, p=0.03), ZNF187 (-0.6 fold change, p=0.03), ZNF192 (-0.6 fold change, p=0.03) and ZSCAN16 (-0.6 fold change, p=0.03). Pseudogene ZNF389 was also hypomethylated (-0.6 fold change, p=0.03).

#### 5.4.5.7 Intragenic CGI methylation following L-carnitine treatment

Table 21 below shows a list of intragenic CGIs which were differentially methylated following L-carnitine treatment. Of these, COX7A2L, KIAA1984, PIK3C2B and POU3F1 were also methylated in promoter regions and are described in more detail above. DAVID functional annotation tools were used to identify the corresponding genes and their functions, with further detail found through literature searches. In general, it is likely that differential methylation of intragenic CGIs will affect expression of the corresponding gene, although the precise effects seem gene-specific. While this is speculative until specific analysis of gene expression and methylation by qPCR is performed, some genes bear discussion in greater detail due to their specific functions and would be prioritised for future study.

#### 5.4.5.8 Intragenic DMRs involved in signalling

A number of genes encoding products with roles in signalling including the wnt and MAP kinase cascades and calcium signal transduction were differentially methylated in intragenic regions following promotion of  $\beta$ -oxidation with L-carnitine throughout embryo culture. These included G protein subunit GNG5 (+0.9 fold change, p=0.03), wnt ligand WNT5B (+0.87 fold change, p=0.05), MAP kinase cascade component MARK3 (-0.66 fold change, p=0.03), Calcium-dependent cell-cell adhesion protein PCDH14 (+0.92 fold change, p=0.00), calcium-activated ion channel Tweety 2 (+0.75 fold change, 0.03).

#### 5.4.5.9 Post-translational modification

Intragenic regions of ubiquitin-binding protein UBAC2 (+0.6 fold change, p=0.02), Histone acetyltransferase component TRRAP (+1.48 fold change, p=0.04) were differentially methylated following embryo culture with L-carnitine.

#### 5.4.5.10 Transcription factors

Transcription factors ZNF462 (-0.72 fold change,  $p=0.00$ ) and ZXDC (+0.69 fold change,  $p=0.04$ ) were differentially methylated following promotion of  $\beta$ -oxidation with L-carnitine.

#### 5.4.5.11 Intragenic CGI methylation

A number of genes encoding protein products involved in intracellular signal transduction were differentially methylated in intragenic regions. These include GNG5, encoding the cell surface linked G-protein coupled chemokine receptor Guanine Nucleotide binding protein, which involved in chemokine signalling transduction. In humans, it co-localises to chromosome 1p22 with lysosomal chitobiase (Ahmad et al. 1995).

WNT5B, encoding Wingless-Type MMTV Integration Site Family, Member 5B, is a key component of the wnt signalling cascade, vital in normal development, regulating cyclin D1 expression and a key component of carcinogenesis (Yang 2003). Interestingly, variation in *wnt5b* is linked to type 2 diabetes (Salpea et al. 2009a). Hypermethylation of WNT5B following L-carnitine treatment could enhance expression of this key protein, potentially allowing accelerated development.

UBAC2, encoding ubiquitin-associated domain-containing protein 2, is potentially involved in ubiquitin-dependent protein degradation. Intronic methylation may enhance transcription of the gene product, potentially increasing protein degradation within the L-carnitine treated embryo. The gene is also associated with a lncRNA (Sawalha et al. 2011).

MARK3 is a protein kinase activated by phosphorylation and activating MAP2 and MAP4 kinases to control cell polarity and cytoskeleton (Drewes et al. 1997). It also phosphorylates HDAC7, regulating localisation and activity of histone deacetylase and potentially leading to further epigenetic regulation of gene expression in the embryo.

Exon	Intron	Name	Role	Fold-change	P-value
CLIP1	CLIP1	Cytoplasmic Linker Protein 1	Links cytoplasmic vesicles to the cytoskeleton	0.83	0.01
COX7A2L	COX7A2L	Cytochrome c oxidase subunit 7All – like protein	Regulatory subunit of complex IV which may increase respiration in response to oestrogen.	1.89	0.01
FRMD1	FRMD1	FERM Domain Containing 1	Associated with smallpox	0.68	0.03
KIAA1984	KIAA1984	Coiled-Coil Domain Containing 183	Unknown function	0.63	0.02
LRRC27	LRRC27	Leucine-Rich Repeat-Containing Protein 27	Unknown function	-1.02	0.03
MARK3	MARK3	MAP/Microtubule Affinity-Regulating Kinase 3	MAP kinase signalling. Phosphorylates MAP2, MAP4 and HDAC7.	-0.66	0.03
PIK3C2B	PIK3C2B	Phosphatidylinositol-Phosphate 3-Kinase C2β	Class II PI3 kinase. Involved in PI3 signalling.	0.66	0.04
POU3F1	POU3F1	POU class 3 homeobox 1	Oct-6. Octamer-binding transcription factor. Roles in embryo development and neurogenesis.	0.82	0.00
SYNRG	SYNRG	Synergyn γ	Interacts with AP1 clathrin-adaptor complex, may have a role in endocytosis/membrane trafficking	0.61	0.01
TTYH2	TTYH2	Tweety family member 2	Ca <sup>2+</sup> -activated chloride channel.	0.75	0.03
VPS33B	VPS33B	Vacuolar Protein Sorting 33 Homolog B	Vesicle mediated protein trafficking, membrane fusion of late endosomes and lysosomes	0.62	0.01
WNT5B	WNT5B	wingless-type MMTV integration site family, member 5B	Ligand in wnt cascade	0.87	0.05
	AATF	Apoptosis Antagonizing Transcription Factor	HDAC1 Inhibitor. Protects against oxidative damage	-0.76	0.02
	ANO4	Anoctamin 4	Associated with Alzheimer's disease	0.75	0.01
	GNG5	Guanine nucleotide binding protein γ5	Heterotrimeric G protein subunit, involved in transmembrane signal transduction	0.90	0.03
	KLC1	Kinesin light chain1	Microtubule-associated protein. May be involved in organelle transport	0.59	0.04
	LOC100336662	Leucine-rich repeat-containing G protein-coupled receptor 5-like	Unknown function	0.68	0.02
	PALLD	Palladin	Cytoskeletal protein, involved in establishing morphology, motility and cell-ECM interactions.	0.71	0.01
	PCDH15	Protocadherin-related 15	Calcium dependent cell adhesion protein	0.92	0.00
	TRRAP	Transformation/Transcription Domain-Associated Protein	Component of histone acetyltransferase complexes. Roles in transcription, DNA repair and epigenetic transcription activation.	1.48	0.04
	UBAC2	UBA Domain Containing 2	Ubiquitin-binding, involved in protein degradation	0.60	0.02
	ZNF462	Zinc Finger 462	Transcription regulation	-0.72	0.00
	ZXDC	ZXD Family Zinc Finger C	Cofactor to promote MHC1 and MHCII transcription	0.69	0.04

Table 21: Intragenic CGI site differential methylation following promotion of β-oxidation with L-carnitine.

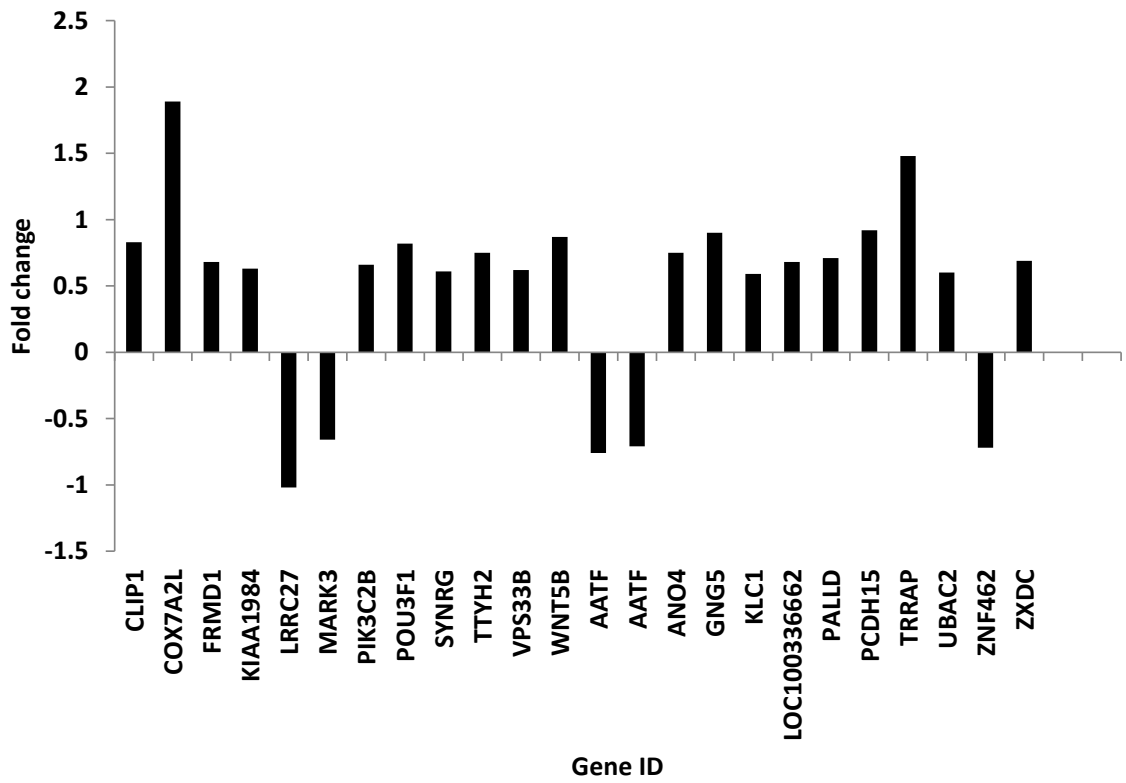


Figure 53: Differential methylation in intragenic regions following promotion of  $\beta$ -oxidation with L-carnitine.

### 5.4.6 Epigenetic microarray following BMA treatment

2,511 probe hybridisation sites were differentially methylated in BMA treatment versus controls. Of these, CpG islands within 49 genic regions and within 50kbp of 17 promoter regions were differentially methylated.

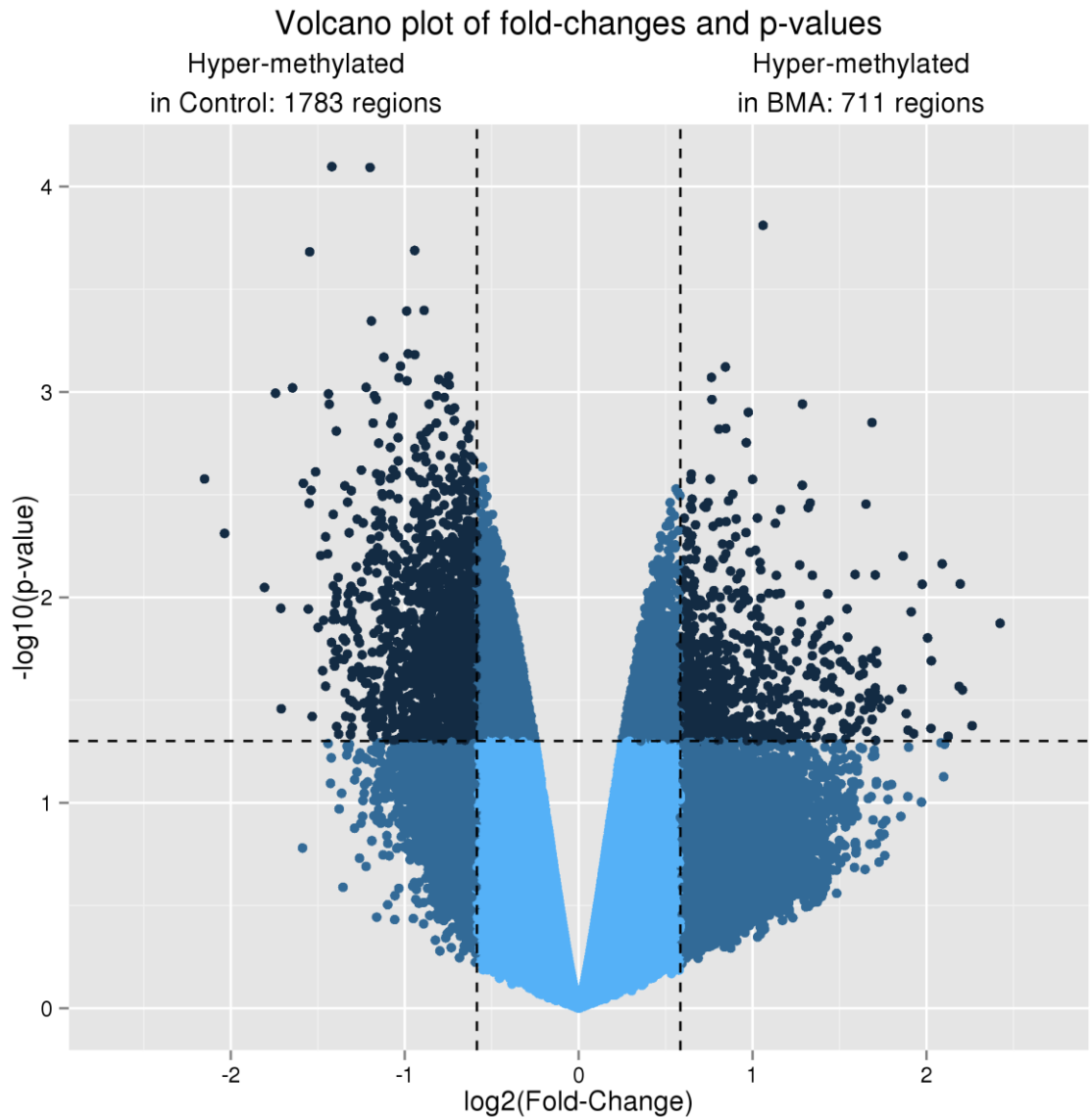


Figure 54: Volcano plot indicating the spread of Differentially Methylated Regions between BMA treated and control embryos. The dark points indicate probes which exceed the thresholds of  $p < 0.05$  and  $\text{fold change} > \log_2(0.5)$ .

### 5.4.6.1 Summary of epigenetic changes following BMA treatment

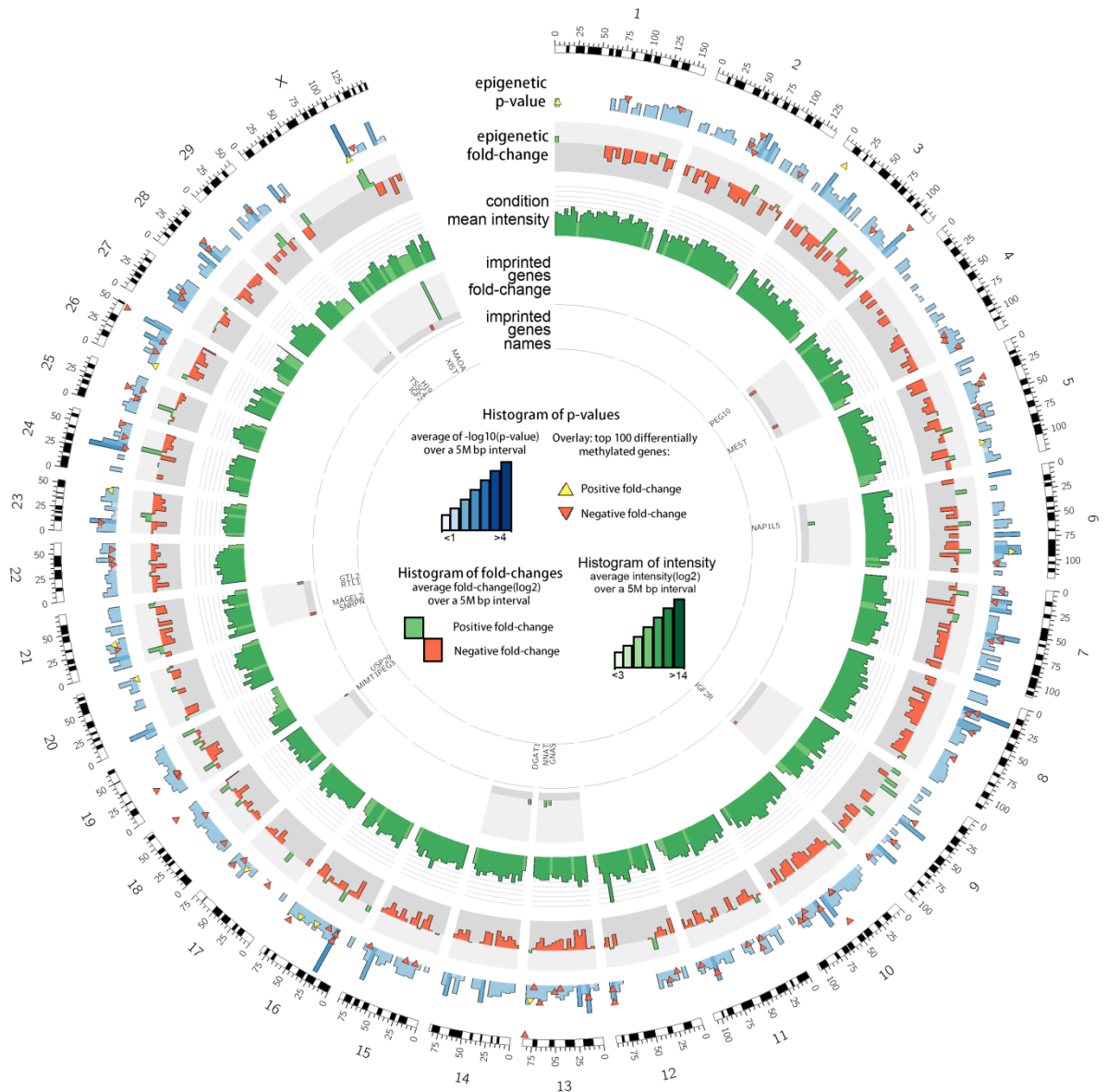


Figure 55: Epigenetic circular plot summarising all significantly different probe binding sites between control and BMA treated blastocysts. Only significantly different ( $p < 0.05$ ) sites are displayed. Layers from top to bottom as follows: epigenetic p-value (0-0.05), epigenetic fold change (difference in methylation in BMA treated embryos relative to controls), condition mean intensity, fold changes of 18 known imprinted genes, symbols of the imprinted genes.

### 5.4.6.2 Promoter methylation in BMA-treated blastocysts

2,511 probe hybridisation sites were differentially methylated in BMA treatment versus controls. Of these, 64 sites were within CpG islands, with 7 of these within (<1kbp) a promoter and a further 4 within 50kbp of a promoter. 30 CGIs overlapped exons and 44 overlapped introns. 8 CGIs did not overlap a genic or promoter region and were not included in this analysis, although they could still have a regulatory role which could be revealed in further investigations.

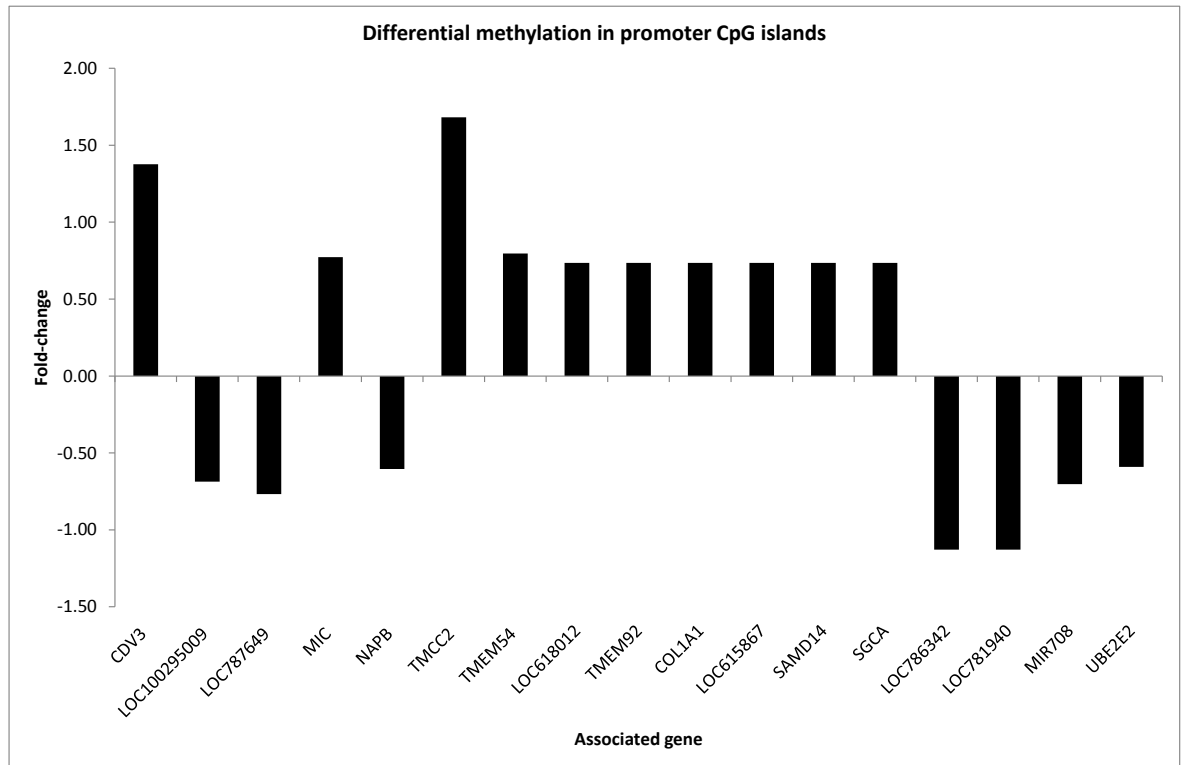


Figure 56: Differential methylation of CpG islands related to promoter regions following BMA treatment of embryos in culture.

Gene ID	Gene name	Product function	Fold change	P value
CDV3	Carnitine-deficiency associated gene expressed in ventricle 3	Expressed with HER-2 in breast cancer cells	1.38	0.04
LOC100295009	Rho guanine nucleotide exchange factor (GEF) 7-like	Now termed ARHGEF7, induces membrane ruffling	-0.69	0.02
LOC787649	Histone H4-like	Pseudogene	-0.77	0.05
MIC	MHC class I-related protein	Stress-induced cell-surface antigen	0.77	0.04
NAPB	N-ethylmaleimide-sensitive factor attachment protein, beta	Involved in vesicular transport between endoplasmic reticulum and Golgi apparatus.	-0.60	0.05
TMCC2	Transmembrane and coiled-coil domain family 2	Involved in genesis of Alzheimer's disease	1.68	0.03
TMEM54	Transmembrane protein 54	Beta-Casein-like, tumour-associated antigen	0.80	0.02
LOC618012	Similar to histone cluster 1	Histone H2B type 1-like	0.73	0.03
TMEM92	Transmembrane Protein 92	Expressed in prostate tumours.	0.73	0.03
COL1A1	Alpha-1 type I collagen	Component of type I collagen is a fibril-forming collagen found in most connective tissues.	0.73	0.03
LOC615867	Similar to Spermatid-specific linker histone H1-like protein	Unknown function	0.73	0.03
SAMD14	Sterile alpha motif domain containing 14	Implicated in adenocarcinoma	0.73	0.03
SGCA	Sarcoglycan, alpha (50kDa dystrophin-associated glycoprotein)	Sarcoglycan complex component, linking F-actin and the ECM	0.73	0.03
LOC786342	Uncharacterised protein	Unknown function	-1.13	0.04
LOC781940	SPACA7: Sperm Acrosome Associated 7	Released following acrosome reaction in sperm.	-1.13	0.04
MIR708	Mir-708 microRNA	Alters gene expression, suppresses wnt signalling.	-0.70	0.01
UBE2E2	Ubiquitin-conjugating enzyme E2E 2 (UBC4/5 homolog, yeast)	Catalyses attachment of ubiquitin to proteins for degradation.	-0.59	0.05

Table 22: Table showing gene name and product function of the data shown above in Figure 56.

#### 5.4.6.3 Differential methylation of intragenic regions

49CGIs in intragenic regions were differentially methylated following BMA treatment. Of these, 29 were exonic and 44 were intronic, with 24 CGIs overlapping exonic and intronic regions of the same gene. These are summarised below in Figure 57.

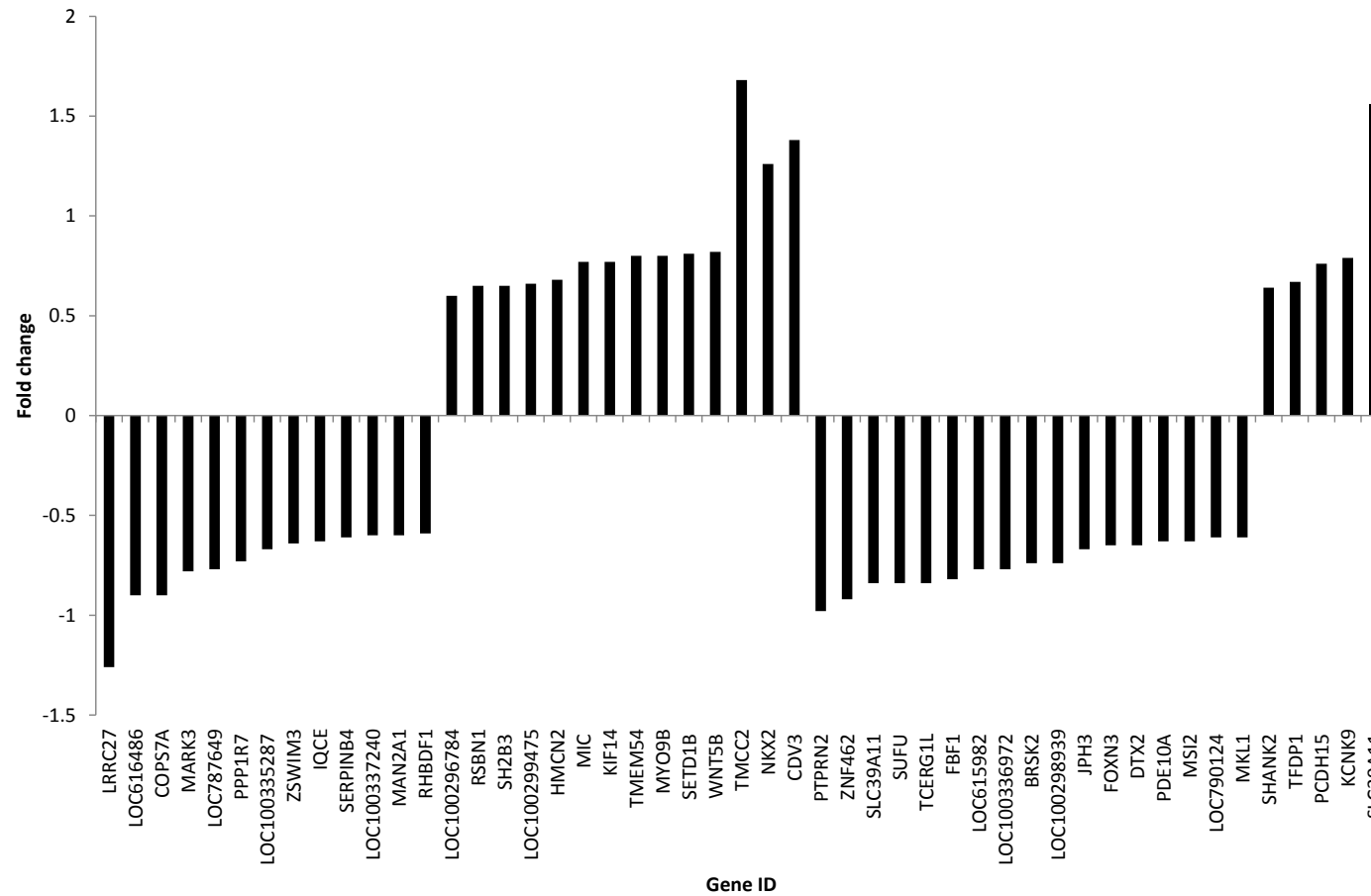


Figure 57: Differential methylation of intragenic CpG island regions following BMA treatment to blastocyst stage. Gene IDs LRR27 to CDV3 were differentially methylated in an exonic CGI, whereas genes from PTPRN2 to SLC29A11 were differentially methylated in an intronic region. All genes displayed exceeded the significance thresholds of fold change  $\log(0.5)$  and  $p < 0.05$ .

Exon	Intron	Gene name	Role	Fold-change	P-value
LRRC27	LRRC27	Leucine rich repeat containing 27	Protein coding, unknown role	-1.26	0.02
LOC616486		Uncharacterised	Similar to uncharacterized protein C17orf47	-0.90	0.03
COP57A	COP57A	COP9 constitutive photomorphogenic homolog subunit 7A	COP9 signalosome complex component. Regulates ubiquitin conjugation	-0.90	0.02
MARK3	MARK3	MAP/microtubule affinity-regulating kinase 3	Phosphorylates tau, MAP2 MAP4 and HDAC7.	-0.78	0.02
LOC787649	LOC787649	Histone H4-like	Similar to Hist1h4c protein	-0.77	0.05
PPP1R7	PPP1R7	Protein phosphatase 1, regulatory (inhibitor) subunit 7	Regulates PP1, required for mitosis and correct localisation of PP1.	-0.73	0.00
LOC100335287		Uncharacterised			
	LRRFIP2	Leucine Rich Repeat (In FLII) Interacting Protein 2	Wnt signalling activator, positively regulates Toll-like receptor signalling.	-0.67	0.01
ZSWIM3		Zinc finger, SWIM-type containing 3	Zinc binding, unknown function	-0.64	0.04
IQCE	IQCE	IQ motif containing E	Implicated in microcephaly	-0.63	0.01
SERPINB4		Serpin peptidase inhibitor, clade B (ovalbumin), member 4	Protease inhibitor, mediate immune response to tumour cells	-0.61	0.03
LOC100337240		Serpin B3-like	Possible protease inhibitor	-0.60	0.01
MAN2A1	MAN2A1	Mannosidase alpha class 2A	Glycosyl hydrolase	-0.60	0.01
RHBDF1	RHBDF1	Rhomboid 5 homolog 1 (Drosophila)	Regulates secretion of EGFR ligands	-0.59	0.04
LOC100296784	LOC100296784	Diabetes related ankyrin repeat protein-like 784	Unknown function.	0.60	0.04
RSBN1	RSBN1	Round spermatid basic protein 1	Transcription regulation in germ cells	0.65	0.01
SH2B3	SH2B3	SH2B adaptor protein 3	Growth factor and cytokine signalling	0.65	0.04
LOC100299475	LOC100299475	Uncharacterised	Unknown function	0.66	0.02
HMCN2	HMCN2	Similar to hemicentin 2	Calcium ion binding	0.68	0.04
MIC	MIC	MHC class I-related protein	Stress-induced cell-surface antigen	0.77	0.04
KIF14	KIF14	Kinesin family member 14	Microtubule-associated motor role in cytokinesis	0.77	0.03
TMEM54	TMEM54	Transmembrane protein 54	Tumour-associated antigen, antisense RNA	0.80	0.02
MYO9B	MYO9B	Myosin IXB	Unconventional myosin, associated with type 1 diabetes	0.80	0.04
SETD1B	SETD1B	SET domain containing 1B	Histone methyltransferase component	0.81	0.00
WNT5B	WNT5B	Wingless-type MMTV integration site family, member 5B	Ligand in wnt cascade	0.82	0.04
TMCC2	TMCC2	Transmembrane and coiled-coil domain family 2	Interacts with amyloid protein precursor and apolipoprotein A.	1.68	0.03
NKX2	NKX2	NK2 homeobox 1	Thyroid-specific transcription regulator	1.26	0.01
CDV3	CDV3	Carnitine-deficiency associated gene expressed in ventricle 3	Expressed with HER-2 in breast cancer cells	1.38	0.04
	PTPRN2	Receptor-type tyrosine-protein phosphatase N2 precursor	Phosphorylates phosphatidylinositol, Autoantigen associated with type II diabetes mellitus	-0.98	0.01
	ZNF462	Zinc finger protein 462	Transcription regulation	-0.92	0.02
	SLC39A11	Solute carrier family 39 (metal ion transporter), member 11	Zinc-influx transporter	-0.84	0.02
	SUFU	Suppressor of fused homolog (Drosophila),	Negative regulator of sonichedgehog/patched signalling	-0.84	0.02
	TCERG1L	Transcription elongation regulator 1-like	Associated with type II diabetes and ADHD	-0.84	0.02
	FBF1	Fas (TNFRSF6) binding factor 1	Apical junction complex assembly in epithelial cells	-0.82	0.03
	LOC615982	Similar to PH domain leucine-rich repeat-containing protein phosphatase	Unknown function	-0.77	0.02
	LOC100336972	Centaurin, gamma 2-like	Unknown function	-0.77	0.02
	BRSK2	BR serine/threonine kinase 2	Key role in axogenesis, cell cycle and insulin secretion.	-0.74	0.04
	LOC100298939	Uncharacterised	Unknown function	-0.74	0.04
	JPH3	Junctophilin 3	Junctional membrane complex component. Brain specific.	-0.67	0.02
	FOXN3	Forkhead box N3	DNA-damage inducible transcription repressor causes cell cycle arrest.	-0.65	0.02
	DTX2	Deltex 2	Ubiquitin E3-ligase, regulator of notch signalling	-0.65	0.01
	PDE10A	Phosphodiesterase 10A	Regulates cAMP and cGMP concentration.	-0.63	0.01
	MSI2	Musashi RNA-binding protein 2	RNA binding protein in neuronal and embryonic stem cells	-0.63	0.04
	LOC790124	Similar to vasoactive intestinal peptide receptor 2	Unknown function	-0.61	0.05
	MKL1	Megakaryoblastic leukemia (translocation) 1	Transcriptional coactivator of serum response factor. Inhibits caspase expression. Embryonic stem cell differentiation	-0.61	0.02
	SHANK2	SH3 and multiple ankyrin repeat domains protein 2	Postsynaptic side of excitatory synapses. Role in autism, also AUTS17	0.64	0.04
	TFDP1	Transcription factor Dp-1	E2F transcription factor, regulates activity of cell cycle promoters	0.67	0.02
	PCDH15	Protocadherin 15	Regulates calcium-dependent cell-cell adhesion	0.76	0.00
	KCNK9	Potassium channel, subfamily K, member 9	pH sensitive K+ channel. Maternally imprinted in brain. Deficiency linked to increased appetite and weight gain in mice	0.79	0.02
	SLC39A11	Solute carrier 39.	Zinc-influx transporter	1.56	0.04

Table 23: Table describing the gene name, product function, fold change and p value of the data shown above in Figure 57.

#### 5.4.6.4 Genes involved in signalling cascades

A number of genes encoding products involved in key signalling cascades were differentially methylated in the blastocyst following inhibition of  $\beta$ -oxidation with BMA. These include frizzled receptor ligand WNT5B (+0.82 fold change,  $p=0.04$ ), Sonichedghehog pathway inhibitor SUFU (-0.84 fold change,  $p=0.02$ ), Rhomboid protease-like protein RHBDF1 (-0.59 fold change,  $p=0.04$ ), adaptor protein SH2B3 (+0.65 fold change,  $p=0.04$ ), MAP kinase cascade component MS12 (-0.63 fold change,  $p=0.04$ ) and wnt signalling regulator LRRFIP2 (-0.67 fold change,  $p=0.01$ ).

#### 5.4.6.5 Genes involved in transcription

Following inhibition of  $\beta$ -oxidation with BMA, transcriptional regulator TFDP (+0.67 fold change,  $p=0.02$ ) and spermatid-specific transcription factor RSB1 (+0.65 fold change,  $p=0.01$ ) were hypermethylated, while FOXN3 (-0.65 fold change,  $p=0.02$ ) was hypomethylated, potentially leading altered expression of these genes and a dysregulated expression of their target genes.

#### 5.4.6.6 Genes involved in post-translational modification

BRSK2 (-0.74 fold change,  $p=0.04$ ), MARK3 (-0.78 fold change,  $p=0.02$ ) and PTPRN2 (-0.98 fold change,  $p=0.01$ ) are all involved in protein phosphorylation and all were hypomethylated following BMA treatment. Mannosidase MAN2A1 (-0.6 fold change,  $p=0.01$ ) and histone methyltransferase component SETD1B (+0.81 fold change,  $p=0.0$ ) were also differentially methylated.

#### 5.4.6.7 Genes related to disease

A number of genes which have been implicated in metabolic diseases were differentially methylated following inhibition of  $\beta$ -oxidation. In addition to BRSK2 and PTPRN2, which are linked to diabetes, MYO9B (+0.8 fold change,  $p=0.04$ ), an unconventional myosin associated with type 1 diabetes (Wirth et al. 1996; Monsuur et al. 2005; Persengiev et al. 2010) and KCNK9 (+0.79 fold change,  $p=0.02$ ), which is linked to increased appetite and weight gain in mice (Pang et al. 2009), were also differentially methylated following inhibition of  $\beta$ -oxidation.

A number of DMRs following BMA treatment were related to neurological disorders, for example JPH3 (-0.67 fold change,  $p=0.02$ ) is associated with Huntington's disease (Sułek-Piatkowska et al. 2008) and SHANK2 (+0.64 fold change,  $p=0.04$ ) with autism (Berkel et al. 2010). TMCC2 (+1.68 fold change,  $p=0.03$ ) interacts with both amyloid protein A and apolipoprotein A and hence is related to Alzheimer's disease (Hopkins et al. 2011; Hopkins 2013).

## 5.4.1 Overview of the L-carnitine treated blastocyst transcriptome and epigenome

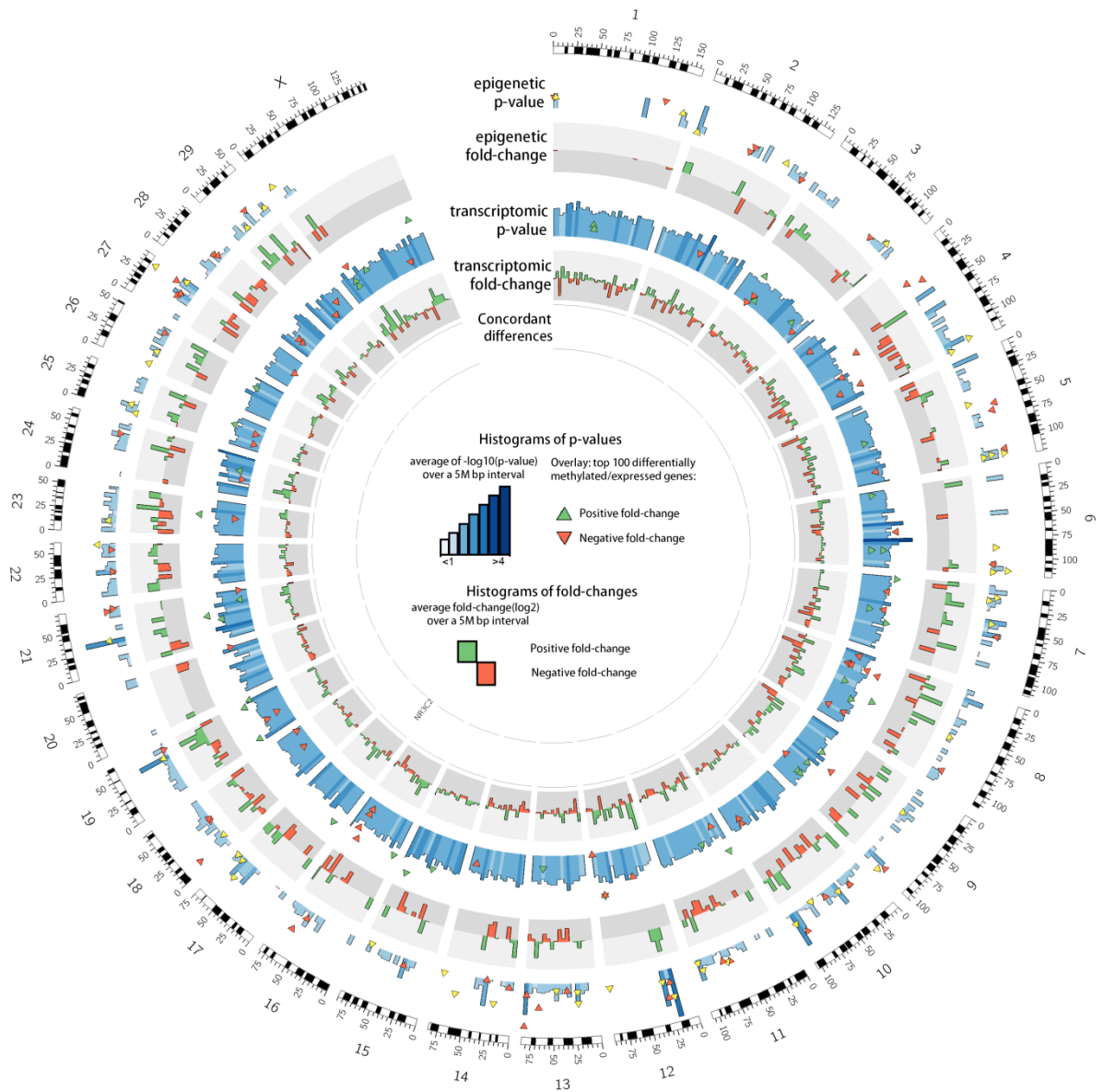


Figure 58: Combined circular plot showing transcriptomic and epigenetic changes following promotion of  $\beta$ -oxidation with L-carnitine. Only genes which were significantly differentially expressed or differentially methylated are displayed.

One gene, encoding the mineralocorticoid and glucocorticoid-dependent transcription factor NR3C2, was upregulated and hypomethylated following L-carnitine treatment. The DMR, however, was in an 'open sea' region and hence located far from the CGI, likely limiting its effect on transcription.

## 5.4.1 Overview of the BMA-treated blastocyst transcriptome and epigenome

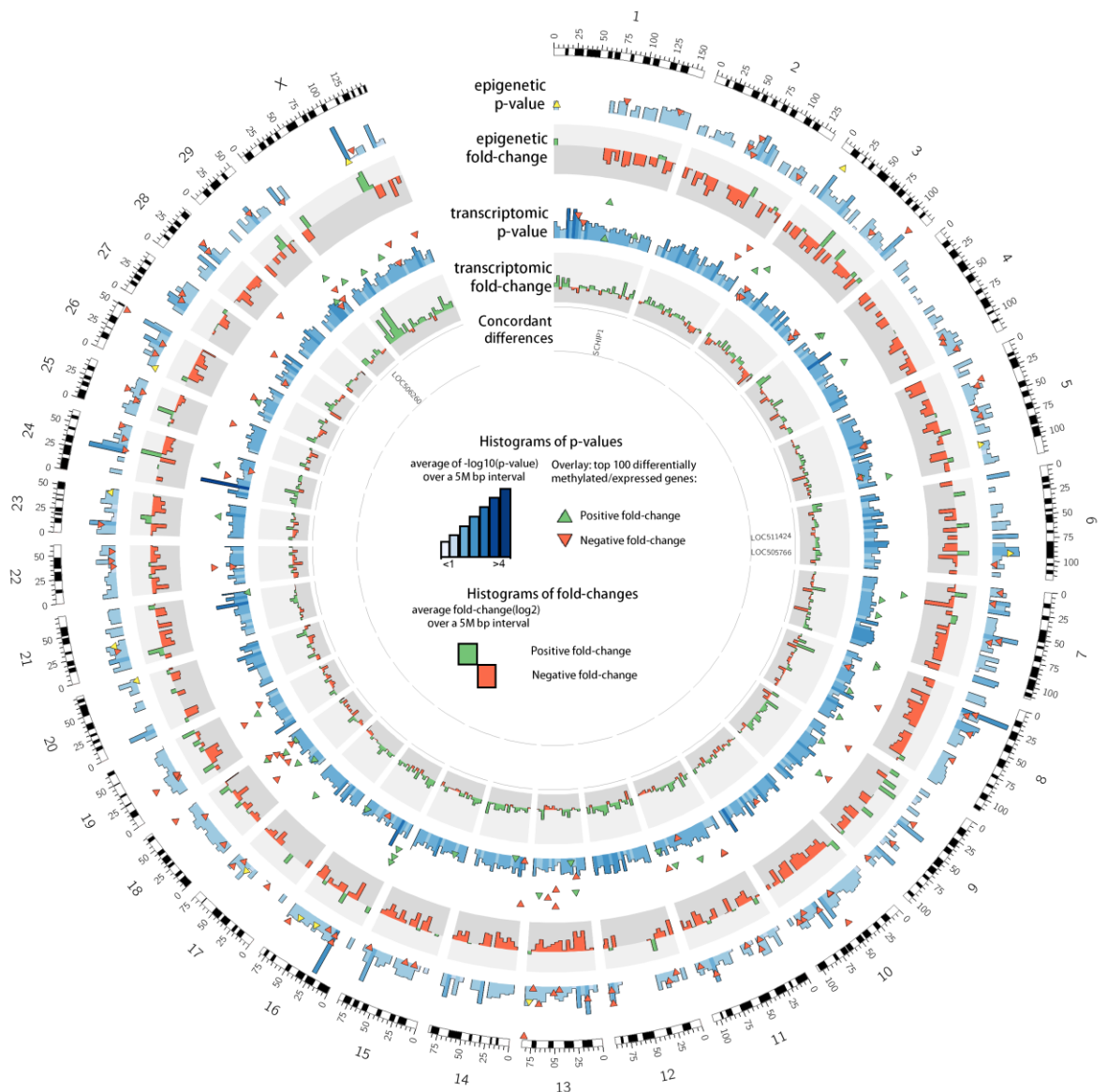


Figure 59: Combined circular plot showing transcriptomic and epigenetic changes following inhibition of  $\beta$ -oxidation with BMA. Only genes which were significantly differentially expressed or differentially methylated are displayed.

Four concordant differences were detected following BMA treatment, LOC506260, LOC511424, LOC505766 and SCHIP1. Encoding Schwannomin-interacting protein 1, SCHIP1 was upregulated and hypomethylated following BMA treatment. SCHIP1 interacts with NF2 or schwannomin, a scaffolding protein and tumour suppressor (Goutebroze et al. 2000).

## 5.5 Discussion

A large number of genes were altered at the level of gene expression or methylation in response to manipulation of fatty acid  $\beta$ -oxidation. While the microarray analysis produces a static impression of the genetic activity of a group of embryos and the fold changes may be minor, differential regulation of gene expression at this early stage of development could have far-reaching consequences for the ongoing development of the embryo. The foetal developmental origin of health and disease (DoHaD) hypothesis was first noted in (Barker 1986), more recently reviewed (Barker 2007) and suggests that minute changes in the oocyte and embryo environment permanently affect the organism's development, metabolism and gene expression, impacting on susceptibility to coronary heart disease and many other conditions. As discussed above, changes in the expression levels of some genes seem to predispose an embryo to a failed implantation or placental development, potentially aborting foetal development. It is equally likely that changes in expression of some genes could generate an apparently normal phenotype, with similar *in vitro* development rates and possibly successful pregnancies, but with far-reaching consequences for the ongoing development of each individual.

It should be noted that the pattern of gene expression differs greatly between *in vivo* derived and *in vitro* produced embryos (Niemann and Wrenzycki 2000; Bertolini et al. 2002; Lonergan et al. 2003). Moreover, comparison of gene expression between embryos produced by IVF had substantial differences in gene expression profile compared to embryos generated by ICSI (Bridges et al. 2011), even between constitutively expressed or so-called 'housekeeping genes' (Luchsinger et al. 2013).

### 5.5.1 Metabolic differences

L-carnitine treated blastocysts had significantly lower OCR and pyruvate consumption rates than control or BMA treated embryos (Figure 42). This is in agreement with the previous OCR data in this thesis (Figure 31). In contrast to previous data (Figure 30, Figure 31), BMA-treated embryos did not have significantly increased OCR compared to control embryos. This may be due to the removal of outliers exceeding mean pyruvate or oxygen consumption  $\pm 2s.d.$  as more metabolically active blastocysts e.g. expanding blastocysts

may have dramatically higher consumption rates than a group of similar stages of early blastocysts.

## 5.5.2 Differential expression following promotion of $\beta$ -oxidation

Promotion of fatty acid  $\beta$ -oxidation with L-carnitine led to a total of 152 changes in gene expression at the blastocyst stage, a shift related to an overall decrease in oxygen and pyruvate consumption (Figure 42). A relatively minor manipulation, providing an increased supply of a physiological compound to manipulate metabolism of an endogenous energy source, can therefore give rise to a wide range of effects at the metabolic and transcript levels. This suggests that fatty acid  $\beta$ -oxidation is linked to overall regulation of metabolism and gene expression and that dysregulated  $\beta$ -oxidation in the earliest stages of preimplantation development can have far-reaching effects.

### 5.5.2.1 Genes involved in successful pregnancy

Several of the genes which were altered at transcript level following promotion of  $\beta$ -oxidation with L-carnitine have previously been reported to be differentially expressed in embryos that failed to give a pregnancy. For example, TNF $\alpha$  is associated with foetal resorption and was upregulated in embryos resulting in no pregnancy (Rekik et al. 2011). In the present study, L-carnitine-treated embryos did not exhibit altered expression of TNF $\alpha$  to controls, but expression of LITAF (lipopolysaccharide-induced TNF factor), encoding a protein which mediates TNF $\alpha$  expression, was downregulated. Also downregulated in the present study were PGTS2 (Cyclooxygenase 2), PLAU (urokinase-type plasminogen activator), and IFN $\tau$ -C1 (interferon tau c), which binds CDX2 in bovine non-trophoblast cells. Transcript abundance of TXNIP (thioredoxin-interacting protein), which inhibits TXN activity or availability, was increased (0.88 fold increase,  $p=0.03$ ). Expression of COX-2, PLAU, TXN and CDX2 was lower in embryos resulting in unsuccessful pregnancy in a study by Rekik et al. (2011), suggesting a potential link between increased  $\beta$ -oxidation and unsuccessful pregnancy.

### 5.5.2.2 Mitochondrial permeability and morphology

The transcription of a number of genes involved in mitochondrial behaviour was altered following carnitine treatment. HEBP2, also known as SOUL, was downregulated at the

transcript level. This gene plays a role in the induction of apoptosis in response to oxidative stress. Normally, mammalian embryos cannot undergo apoptosis prior to the maternal-zygote transition (MZT) and apoptosis is rare in embryos of higher morphological quality before the blastocyst stage (Hardy 1999). However the net effect of reduced HEBP2 expression may allow compromised blastomeres to escape apoptosis. Reduction of HEBP2 may also reduce mitochondrial membrane permeability (Zylka and Reppert 1999; Szigeti et al. 2006; Szigeti et al. 2010; Ambrosi et al. 2011). However, as reported above, L-carnitine-treated embryos did not have significantly different mitochondrial polarisation compared to controls, although mitochondrial polarisation was significantly lower at early cleavage stages (Figure 37, Chapter 4). ALAS2, required for haem biosynthesis, was upregulated following L-carnitine treatment, suggesting that synthesis of hemoproteins could be increased following promotion of  $\beta$ -oxidation. Also upregulated was RAB32, a protein which is required for mitochondrial fission. Perhaps increasing expression of ALAS2 and RAB32 could support or even accelerate mitochondrial development and division. These data suggest that altered expression of genes involved in mitochondrial structure and function could contribute to the metabolic differences observed following promotion of  $\beta$ -oxidation with L-carnitine during preimplantation development.

### 5.5.2.3 Genes involved in metabolism

A number of genes related to fatty acid  $\beta$ -oxidation were modulated at transcript level following L-carnitine treatment. Five genes involved in fatty acid elongation and synthesis of triglyceride were downregulated following carnitine exposure (ELOVL1, ACOT4, ACSL6, THEM4, TPI1), while one transcript required for  $\beta$ -oxidation, CYP422A, was upregulated. It is tempting to speculate that the overall effect of these changes is to reduce the synthesis of triglyceride in an attempt to regulate the rate of  $\beta$ -oxidation to native levels, abating the promoting effect of L-carnitine. CYP422A (cytochrome P450, family 4, subfamily A, polypeptide 22) is required for hydroxylation of laureate and palmitate, two unsaturated fatty acids.

In contrast, only one gene directly related to carbohydrate metabolism was altered. STBD1, starch binding domain 1, may anchor glycogen to intracellular membranes as part of glycogen degradation (Jiang et al. 2011). Interestingly, this transcript was upregulated in L-carnitine-treated blastocysts, suggesting an increased capacity to degrade glycogen.

However, this is the only gene involved in carbohydrate metabolism identified by the transcriptomic platform, suggesting that the reduction in pyruvate consumption in this cohort (Figure 42B) and increased glycolysis by L-carnitine-treated embryos (Figure 32C) are regulated at a metabolic, rather than genetic, level.

#### 5.5.2.4 Genes involved in lipid metabolism

ELOVL1, responsible for elongation of long-chain fatty acids, was downregulated, suggesting a decrease in synthesising longer chain forms for storage and in agreement with the model of increased  $\beta$ -oxidation rather than fat storage. Downregulation of ACSL2, a long-chain fatty acid synthetase, and TPI1, which converts Glyceraldehyde-3-Phosphate (GAP) to Dihydroxyacetone-phosphate (DHA) for TG synthesis, may have a similar effect. A similar gene to ELOVL1, ELOVL5, is differentially expressed in response to serum treatment in the ovine blastocyst and is required for fertility in mice (Moon et al. 2009; Hughes et al. 2011). It is therefore possible that downregulation of ELOVL1 could impact on fertility. ACOT4, which hydrolyses Acyl-CoA, and THEM4, which hydrolyses medium and long-chain fatty acyl-CoA groups, were also downregulated, suggesting a possible regulatory mechanism to limit  $\beta$ -oxidation in spite of increased L-carnitine provision. STBD1, starch binding domain 1, involved in carbohydrate binding and glycogen metabolism, was upregulated in carnitine-treated blastocysts, suggesting a possible increase in glycogen breakdown.

Additionally, MTMR9, linked to obesity and diabetes, along with CLDN23, linked to childhood obesity, were downregulated following treatment with L-carnitine. It is tempting to speculate that such changes might offer a link toward obesity in childhood or adult life following dysregulated embryonic fatty acid metabolism.

#### 5.5.2.5 Genes involved in successful pregnancy

Three transcripts related to successful pregnancy were down-regulated in carnitine-treated blastocysts compared to controls. Interferon- $\tau$  is the primary signal for maternal recognition of pregnancy and low expression, following increased embryonic fatty acid  $\beta$ -oxidation, would likely reduce the chance of successful recognition of pregnancy. Reduced expression of PAG2 has been related to spontaneous abortion, while PAG12 is reportedly involved in implantation and placentogenesis. Taken together, downregulation of PAG genes may have a compounding effect leading to inhibition of successful

implantation and placenta development and an increased likelihood that the embryo will abort. If the carnitine-treated embryos happened to develop more slowly, these changes would be unsurprising, however the carnitine-treated and control embryos were each profiled at around stage B3 (mean=2.7 v 2.6). Therefore, these data suggest that blastocysts with increased  $\beta$ -oxidation have reduced ability to signal to the mother and implant successfully.

Several genes which are altered at transcript level have been reported to have differential expression dependent of the stage of embryo development. In separate experiments, kinetic data collected using the Primovision embryo development tracking system suggested that L-carnitine treated embryos begin blastocoel expansion earlier than control or Etomoxir-treated embryos (Figure 40). However, in this case the metabolic profiles and fixing for microarray analysis were performed on L-carnitine-treated and control blastocysts at similar stages of blastocyst expansion (B3). On average, BMA-treated embryos were at a slightly more advanced stage of development (B4), though this was not a statistically significant difference ( $p=0.8$ ). Where possible, blastocysts of a similar developmental stage were analysed but embryos were primarily selected based on metabolic similarity and blastocyst numbers were dependent on a variable tissue supply. Typically, embryos with slower development rates exhibit lower TNF $\alpha$  expression, but in this case the carnitine-treated embryos were measured at a similar stage of expansion and may have increased development rates (Figure 40). This suggests an even greater discrepancy between the rate of development and TNF $\alpha$  expression in L-carnitine-treated embryos.

#### 5.5.2.6 Genes involved in glutathione metabolism

The gene GSTO1, encoding the cytoplasmic enzyme Glutathione S-transferase omega-1, was downregulated in L-carnitine-treated embryos. L-carnitine treatment has been reported to alter glutathione metabolism, increasing resistance to oxidative stress, in a range of cell types (Gülçin 2006) and this may be part of such a response. GSTO1 is one of a number of enzymes bonding glutathione to a range of reactive moieties (R-X-glutathione). R-X-glutathione is then degraded by GGT1 and GGTL3. This change at the transcript level may lead to an increase in bioavailability of glutathione, but a reduction in glutathione-mediated breakdown of toxic moieties.

### 5.5.2.7 Squalene epoxidase

SQLE, encoding an oxygen-consuming enzyme, may be responsible for some of the non-mitochondrial oxygen consumption reported in Chapter 3 (Figure 19). Interestingly, its expression was downregulated following carnitine treatment, and overall oxygen consumption was correspondingly reduced.

### 5.5.2.8 Genes involved in protein modification

### 5.5.2.9 Genes related to disease

Almost all of the genes discussed above have relevance to disease conditions, including developmental and metabolic disorders related to knockout or overexpression of enzyme-coding genes. However some of the genes identified have hitherto been detected only in association with disease and it is possible that further analysis could elucidate the developmental origins or components of certain conditions. Following L-carnitine treatment, CALB1 is downregulated and is also downregulated in Huntington's disease patients. CLDN23 and MTMR9 are both downregulated and have links to childhood and adult obesity respectively. FSTL1 is upregulated and upregulates other genes involved in the inflammatory component of arthritis. Also upregulated is AUTS2, which has been reported to confer susceptibility to autism.

### 5.5.2.10 Genes involved in prostaglandin synthesis

Prostaglandins are synthesised from arachidonic acid and as L-carnitine treatment promotes increased  $\beta$ -oxidation of fatty acids, it might be expected that bioavailability of arachidonic acid would also be reduced. Indeed, TIA1, encoding a silencer of COX-2, as well as its target gene, PTGS2/COX-2 were both downregulated following L-carnitine supplementation. This suggests a possible mechanism for a reduction in prostaglandin synthesis in embryos with increased  $\beta$ -oxidation. These proteins are mitochondrially localised and their activity may be linked to the changes in mitochondrial polarisation, OCR and potential changes in mitochondrial development following carnitine treatment. Prostaglandin synthesis normally varies with embryo development, so decreased expression of these genes might suggest a reduced ability for L-carnitine-treated embryos to synthesise prostaglandins in comparison with control embryos at the same stage of development.

## 5.5.3 Differential expression following inhibition of $\beta$ -oxidation

### 5.5.3.1 MAP kinase signalling

A number of genes involved in MAP kinase signalling were upregulated following BMA treatment. The MAP kinase pathway typically responds to stimuli including mitogens but also osmotic or heat stress, and regulates proliferation, mitosis, apoptosis and gene expression. An increase in expression of MAP kinase components suggests that the BMA-treated embryo is under stress and may possess altered cell division and apoptosis rates.

It is possible that CACNA1G responds to mitochondrial depolarisation in embryos with dysregulated fatty acid metabolism (Figure 37, Chapter 4). A common mutation of CACNA1G is linked to autism (Strom et al. 2010), adding to a growing evidence base linking calcium signalling, mitochondrial function and autism (Lombard 1998). It is interesting to consider that carnitine-treated embryos have increased lactate production at early cleavage and blastocyst stages, as high blood lactate production is a signature of mitochondrial defects in children with autism (Correia et al. 2006).

TNFRSF1A, an activator of NF- $\kappa$ B, as well as NF- $\kappa$ B itself, were both upregulated following BMA treatment, potentially having a synergistic increase in NF- $\kappa$ B signalling. NF- $\kappa$ B has a wide range of effects and dysregulated activation can cause inflammatory conditions and immunodeficiencies (Piret et al. 1995).

### 5.5.3.2 Genes involved in lipid metabolism

Two genes involved in lipid metabolism were upregulated following BMA treatment. APOA1, the main protein component of high density lipoproteins, is a prostacyclin stabilising factor which promotes fat efflux. Its upregulation following BMA treatment might suggest that the embryo is attempting to remove excess lipid by alternate means, since BMA inhibits  $\beta$ -oxidation. PNPLA2 is a target of PPAR $\gamma$  and its upregulation may increase hydrolysis of lipid in lipid droplets which has been implicated in the response to starvation (Kim et al. 2006; Fischer et al. 2007; Paek et al. 2012).

### 5.5.3.3 Genes involved in amino acid metabolism

A total of 5 genes involved in amino acid degradation were downregulated following BMA treatment. This includes 2 subunits of the glycine cleavage system, polyamine oxidase and

proline dehydrogenase. One interpretation of these results is that the BMA-treated embryo is recovering from reduced  $\beta$ -oxidation by conserving amino acids for use as an energy source, reducing breakdown of amino acids for biosynthetic pathways. PAOX is involved in polyamine back conversion and regulates polyamine intracellular concentration. It is also involved in  $H_2O_2$  generation, so a decrease in expression could reduce ROS generation.

#### 5.5.3.4 WNT signalling

WNT5B, encoding Wingless-Type MMTV Integration Site Family, Member 5B, is a key component of the wnt signalling cascade, vital in normal development, since it regulates cyclin D1 expression and is a key component of carcinogenesis (Yang 2003). Interestingly, variation in wnt5b is linked to type 2 diabetes (Salpea et al. 2009a). Hypermethylation of WNT5B following L-carnitine treatment could enhance expression of this key protein, potentially allowing accelerated development.

#### 5.5.3.5 Genes involved in mitochondrial structure and function

A total of 24 genes involved in mitochondrial structure and function were downregulated following BMA treatment. This is a large number of genes, and likely reflects the decreased mitochondrial polarisation ratio and increased oxygen consumption by BMA-treated embryos (Figure 29 and Figure 36, Chapter 4). Indeed, among the downregulated genes are SLC25A5, SLC25A11, both ADP/ATP carriers involved in ATP synthase activity, along with the ATP synthase component ATP5G1 (F0 subunit) and ATP6VIC2 (ATPase subunit B1), possibly suggesting a decreased capacity to synthesise ATP which might stimulate increased OCR in an attempt to overcome this. Genes encoding subunits of the glycine cleavage system are included in this cluster (loc787129, loc783608). The general functions of loc613316 and loc783502 are generation of precursor metabolites and energy.

PHB2 is involved in regulating mitochondrial respiration (Coates et al. 2001). ENDOG generates RNA primers needed for mtDNA replication and, along with TCF6 and SSBP, is required for mitochondrial biogenesis (Tiranti et al. 1995). MRPL2 encodes the large subunit of the mitoribosome, one of 54 mitoribosomal proteins, all of which are encoded by nuclear DNA (Kenmochi et al. 2001). The homodimeric SUOX localises to the mitochondrial intermembrane space and catalyses the final oxidation in the oxidation of

cysteine and methionine (Kisker et al. 1997). AIFM2 binds ssDNA and mediates caspase-independent apoptosis (Ohiro et al. 2002). SLC25A5 cycles ADP and ATP between the cytoplasm and mitochondrial matrix and its suppression induces apoptosis (Jang et al. 2008). Thioredoxin 2 also has an anti-apoptosis function and regulates mitochondrial membrane potential (Chen et al. 2002). HMBS is involved with heme synthesis and mutations are associated with autosomal dominant disease (Gregor et al. 2002). CYC1 is a component of cytochrome b-c1 complex, which accepts electrons from the Rieske protein and transfers to cytochrome c (Valnot et al. 1999). TIMM17B encodes a component of the TIM23 complex which mediates transport of mitochondrial proteins across the inner mitochondrial membrane (Bauer et al. 1999). ATP5G1 is one of 3 genes encoding subunit c of the proton channel of ATP synthase (Dyer and Walker 1993). IVD catalyses the third step in leucine breakdown and a deficiency leads to a build-up of the toxic isovaleric acid, which can damage the brain and nervous system (Vockley et al. 2000). ATP6V1C2 encodes a subunit of Vacuolar ATPase, which acidifies organelles to regulate protein sorting and receptor-mediator endocytosis (Smith et al. 2002).

#### 5.5.3.6 Post-translational modification

Of these genes, 11 are involved in formation of disulphide bridges (B4GALT1, CTSL2, MPZ, LOC786967, FETUB, LOC783653, SCARA5, PROS1; also TXN2, GLRX, GLRXL, LOC786967 and LOC783653 mentioned above) and 11 with glycoproteins (B4GALT1, SLC2A8, P2RX4, CTSL2, MPZ, FETUB, UPK3B, LMBRD1, FAM55C, SCARA5, PROS1). Concurrent downregulation of these genes is likely to reduce overall protein modification and may have adverse effects on protein turnover.

A number of genes related to ubiquitination were altered during manipulation of  $\beta$ -oxidation. Following BMA treatment, C1QBP expression was downregulated and UBE2E2 was hypomethylated in a promoter region. Abnormalities in ubiquitin-controlled processes has been shown to cause disease including carcinogenesis, so it is possible that these alterations could have a deleterious effect on embryo development aside from dysregulated protein breakdown (El-Sayed et al. 2006).

#### 5.5.3.7 Stress response

5 genes involved in response to stress, including 4 heat shock proteins and DNAJB1, were upregulated following BMA treatment. This suggests that the BMA-treated blastocyst is in

a state of stress reflected by the low mitochondrial polarisation ratio (Figure 36) and altered carbohydrate metabolism (Figure 32). These data suggest that the BMA-treated embryo might be trapped in a hypermetabolic state, forcing the dynamic energy budget, which describes the ability of respiring cells to modulate energy metabolism in response to changing demands and environmental conditions, into a potentially damaging range termed *pejus* (Kooijman 2009; Guerif et al. 2013b). GADD45B is also induced by stressful growth conditions and its upregulation following BMA treatment is another indication that the embryo responds to inhibition of  $\beta$ -oxidation as a stress condition. GADD45B demethylates certain DNA promoter regions, increasing expression of genes involved in neurogenesis in the adult such as brain-derived neurotrophic factor and fibroblast growth factor (Takekawa and Saito 1998; Ma et al. 2009).

#### 5.5.3.8 Stimulus response

Six further genes involved in the response to stimuli including temperature and antibiotics were upregulated following BMA treatment. These include two heat shock proteins mentioned above, HSPB8 and HSPA1B, as well as CASP3. Additionally, DNA repair receptor XRCC2 (0.64 fold increase,  $p=0.00$ ), Crystallin CRYAB (2.6 fold increase,  $p=0.01$ ) and growth factor receptor NGFR (1.46 fold increase,  $p=0.00$ ) were upregulated. Taken together, these upregulations suggest that the embryo is responding to BMA treatment by invoking a stress response, with similar effects as exposure to increased temperature or antibiotic compounds.

#### 5.5.3.9 Cellular remodelling

Of the genes in this category, 8 normally have roles in cell projection, such as cilia, filopodia or axons (STMN2, KLC1, SWAP70, UCHL1, S100A11, TUBB6, CDH2, KLC2) 8 have cytosolic roles (ACTG2, CASP3, KLC1, UCHL1, PNPLA2, KLC2, CAMK2N2, GCH1) and 6 are required for intracellular transport (AP1S2, KLC1, UCHL1, SPTBN1, KLC2, SEC24D). This group of genes cover intracellular structure and trafficking of proteins as well as overall cellular movement into the extracellular space. Typically, in the adult, a number of the genes are associated with axon growth and other cellular extrusions. It might be considered unusual to see such genes significantly upregulated in blastocyst/embryo development but this may be connected with the relative higher stage of expansion compared to the control embryos. However, it seems likely that increased cellular

remodelling would place a greater demand on energy production, possibly explaining the increased oxygen consumption of BMA treated embryos compared to controls.

#### 5.5.4 Differential methylation following promotion of $\beta$ -oxidation

Manipulating fatty acid  $\beta$ -oxidation in the early embryo causes a wide range of metabolic, transcriptomic and now epigenetic effects. These data, along with recently published reports, suggest that the metabolic legacy of dysregulated  $\beta$ -oxidation is complex, potentially interfering with successful recognition of pregnancy and embryo development, programming altered metabolism and genetic susceptibilities to disease.

##### 5.5.4.1 Differential methylation at CGI sites within 5kbp of a promoter

Following embryo culture with L-carnitine, CGIs within 1kbp of the gene promoters controlling expression of COX7A2L, KIAA1989, PIK3CB and POU3F1, along with one further CGI within 5kbp of a promoter (TMEM141), were significantly hypermethylated relative to control embryos. COX7A2L encodes a protein which may bind to electron transport chain complex IV to regulate oxygen consumption following stimulation by oestrogen (Watanabe et al. 1998). Also hypermethylated was a CGI within 1kbp of the promoter controlling expression of phosphoinositide-3-kinase 2 $\beta$  PIK3C2B, which phosphorylates phosphatidylinositol and phosphatidylinositol-4-phosphate and is involved in PI signalling and metabolism (Arcaro 1998; Arcaro et al. 2000). A transcription regulator thought to be involved with key embryonic development events, POU3F1 or Oct-6, was also hypermethylated within 1kbp of its promoter region. This might suggest a potential suppression of expression, which is usually linked to completion of stem cell differentiation (Kawasaki et al. 2003; Patodia and Raivich 2012).

##### 5.5.4.2 Differential methylation at CGI sites within 50kbp of a promoter

Functional annotation analysis of all differentially methylated CGIs within 50kbp of a promoter using DAVID online software revealed 2 functional annotation groups: transcriptional regulators and phosphatidylinositol signalling. Additionally, a number of genes were relevant to metabolic and developmental disease.

#### 5.5.4.3 Genes involved in phosphatidylinositol signalling

Several genes involved in phosphatidylinositol signalling were differentially methylated in promoter regions following promotion of  $\beta$ -oxidation. ITPR3 is an I3P receptor which mediates intracellular calcium release (Bánsághi et al. 2014). I3P receptors are also associated with calmodulin and are phosphorylated by PKA, PKB, PKG and CaMKII. Knockout studies in mice recently suggested that ITPR3 as well as ITPR2 are involved in energy metabolism and growth (Futatsugi et al. 2005). Promoter hypermethylation could cause suppression of ITPR3 expression, restricting aspects of energy metabolism.

INPP5B was hypomethylated in a promoter region. This is a membrane-associated protein which activates phosphatidylinositol 4,5-bisphosphate by hydrolysis and localises to the endocytic and secretory pathways (Williams et al. 2007).

#### 5.5.4.4 Genes involved in prostaglandin metabolism

A CGI within 50kbp of the promoter PTDGS was hypomethylated. This gene encodes Prostaglandin D2 synthase, which converts PGH2 to PGD2, a prostaglandin with a wide variety of roles including maintenance of the male reproductive system and the central nervous system (Ross et al. 1991). Interestingly, increased provision of lipid in the bovine diet has been reported to reduce prostaglandin secretion (Petit et al. 2002). Hypermethylation of this gene in response to promotion of  $\beta$ -oxidation could have a similar effect.

PTDGS and C8G are part of the lipocalin superfamily, along with alpha-1-microglobulin, although PTDGS has diverged in structure and function (Nagata et al. 1991). C8G is a lipocalin family member, the human variant encoding one of three components of the Complement membrane attack complex (Dewald et al. 1996). Lipocalins transport hydrophobic molecules and are associated with innate immunity, prostaglandin synthesis and transport of retinoids and pheromones and are allergens to many mammals.

#### 5.5.4.5 Genes involved in regulation of transcription

Differentially methylated regions were detected in CGIs within 50kbp of the promoter regions controlling expression of a range of transcription factors. These include POU3F1, discussed above, which is a transcription factor binding the octamer motif likely involved in embryo development (Kawasaki et al. 2003; Patodia and Raivich 2012). POU3F1 is

clustered with a long non-coding RNA gene. LncRNAs also have regulatory roles, with some acting as co-activators alongside transcription factor proteins, such as the ncRNA Evf-2 and homeobox TF Dlx2 (Panganiban and Rubenstein 2002; Feng et al. 2006). Hypermethylation of this CGI may affect expression of both Oct-6 and the lncRNA, potentially dysregulating aspects of embryo development.

EDF1 is a transcription co-activator, functioning with TAT-element binding protein and other specific activator proteins to regulate PPAR $\gamma$ , CREB1 and NR5A1 signals. It may therefore have a diverse range of effects in lipid metabolism, cell differentiation and nitric oxide synthesis (Dragoni et al. 1998; Mariotti et al. 2000; Ballabio et al. 2004). A CGI within 50kbp of the EDF1 promoter site was hypermethylated following L-carnitine treatment and a resulting change in Edf-1 expression could dysregulate PPAR $\gamma$  signalling. A lack of PPAR $\gamma$  would decrease lipid storage and increase  $\beta$ -oxidation, supporting the high  $\beta$ -oxidation metabolism of L-carnitine treated embryos.

Zinc Finger and SCAN Domain Containing transcriptional regulators ZFP37, ZKSCAN4, ZNF165, ZNF187 (also known as ZNF25), ZNF192 and ZSCAN16 were differentially methylated in CGIs related to promoter regions following promotion of  $\beta$ -oxidation with L-carnitine. ZNF165 is specific to sperm and testis and may play a role in spermatogenesis (Tirosvoutis et al. 1995; Dong et al. 2004), while ZKSCAN4 regulates expression of the ubiquitin ligase MDM2 and the histone acetyltransferase EP300 (Li et al. 2007). Differential methylation of these transcription factor genes could allow differential expression and a resulting dysregulation in transcription of myriad associated genes.

#### 5.5.4.6 Genes related to disease

PGBD1 encodes a piggyback transposase which is specifically expressed in the brain and implicated in neural disorders including Alzheimer's disease and schizophrenia (Belbin et al. 2011; Ohnuma et al. 2012). Hypomethylation due to dysregulated  $\beta$ -oxidation could allow altered expression, potentially disrupting neural development.

#### 5.5.4.7 Intragenic DMRs involved in signalling

A number of genes encoding protein products involved in intracellular signal transduction were differentially methylated in intragenic regions. These include GNG5, Guanine

nucleotide binding protein 5, encodes a cell surface linked G-protein coupled chemokine receptor involved in chemokine signalling transduction (Ahmad et al. 1995).

WNT5B, encoding Wingless-Type MMTV Integration Site Family, Member 5B, is a key component of the wnt signalling cascade, vital in normal development, regulating cyclin D1 expression and a key component of carcinogenesis (Yang 2003). Interestingly, variation in *wnt5b* is linked to type 2 diabetes (Salpea et al. 2009a). Hypermethylation of WNT5B in an intergenic CGI following L-carnitine treatment could alter expression of this key protein, potentially allowing accelerated development. MARK3 is a protein kinase activated by phosphorylation which activates MAP2 and MAP4 kinases to control cell polarity and cytoskeleton (Drewes et al. 1997). It also phosphorylates HDAC7, regulating localisation and activity of histone deacetylase and potentially leading to further epigenetic regulation of gene expression in the embryo. These relatively minor changes in methylation state of the embryonic genome could have far-reaching effects on ongoing development.

## 5.5.5 Differential methylation following inhibition of $\beta$ -oxidation

### 5.5.5.1 Genes involved in ubiquitination

UBE2E2 transfers ubiquitin from the E1 complex to lysine residues of proteins designated for degradation (Kimura et al. 1997; Ito et al. 1999). Hypomethylation may result in an increase of UBE2E2 expression.

### 5.5.5.2 Genes involved in signalling

Promoter regions of several genes involved in cell signalling pathways were hypomethylated following promotion of  $\beta$ -oxidation. LOC100295009, known as ARHGEF7 or  $\beta$ -Pix is a Rho GTPase which activates Rho proteins, recruiting Rac1 and inducing membrane ruffling and apoptosis. ARHGEF7 also interacts with SHANK genes, which have reported association with autism spectrum disorders (Audebert et al. 2004; Valdes et al. 2011). MIC is similar to human variants MICA and MICB, which act as stress-induced self-antigens recognized by  $\gamma\delta$ T, leading to cell lysis. MIC A and B are associated with a number of diseases including type 1 diabetes (López-Arbesu et al. 2007; Field et al. 2008). NAPB Beta-soluble NSF attachment protein is a component of the intracellular membrane fusion apparatus, which is controlled by SNAP (soluble NSF attachment proteins) receptors (Whiteheart et al. 1993). The micro RNA MIR-708 was also hypomethylated following BMA treatment. Overexpression causes increased cell proliferation, migration and invasion in lung cancer and negatively regulates wnt signalling (Jang et al. 2012; Robin et al. 2012), it is possible that altered expression due to promoter hypomethylation may also affect these pathways.

### 5.5.5.3 Genes related to disease

TMCC2 (Hopkins et al. 2011) is involved in pathogenesis of Alzheimer's disease. It increases production of  $\beta$ -amyloid peptide by interacting with APP (Amyloid precursor protein) and APOE4, the major known cause of Alzheimer's disease (Huang 2011) and increases be specific to presenilin-mediated  $\gamma$ -cleavage (Tharp and Sarkar 2013). Hypermethylation during earlier development could lead to altered production of these proteins.

CDV3 encodes a homolog to the mouse gene: Carnitine Deficiency-Associated Gene Expressed in Ventricle 3. It is highly expressed in the ventricles of carnitine-deficient juvenile visceral steatosis (JVS) mice, a model of cardiac hypertrophy, but this upregulation is reduced when the mice are supplied with L-carnitine within 6h (Fukumaru et al. 2002). In the present study, CDV3 was hypermethylated following inhibition of  $\beta$ -oxidation with BMA. It is tempting to speculate that this would allow an increase in CDV3 expression, causing cardiac hypertrophy in the adult.

SAMD14 was also hypermethylated in the promoter region, an epigenetic alteration previously reported to suppress expression, with involvement in the carcinogenesis of pulmonary adenocarcinoma (Sun et al. 2008).

SGCA is expressed in myotomes during muscle formation and mutations result in autosomal recessive lamb-girdle muscle dystrophy (Fougerousse et al. 1998). Unlike SGCB, which is expressed ubiquitously by the developing post-implantation embryo, SGCA is usually specific to striated muscle.

Now identified as sperm acrosome associated 7 or SPACA7, LOC781940 was hypomethylated in blastocysts following inhibition of  $\beta$ -oxidation with BMA. SPACA7 is expressed in testis in the mouse from postnatal day 21 and is released from spermatozoa following the acrosome reaction, suggesting a role in cumulus dispersal and fertilisation (Nguyen et al. 2014).

#### 5.5.5.4 Differential methylation of intragenic regions

#### 5.5.5.5 Genes involved in signalling cascades

WNT5B and SUFU are both involved in the hedgehog signalling pathway, as well as generation of basal cell carcinoma. LOC790124 may also be involved in signal transduction. WNT5B is a ligand for the frizzled family of receptors as a part of the wnt signalling cascade, involved in development and carcinogenesis (Saitoh and Katoh 2001; Salpea et al. 2009b). LRRFIP2 was also hypomethylated and encodes an enzyme which positively regulates wnt and Toll-like receptor signalling (Jin et al. 2013) (-0.67 fold change,  $p=0.01$ ).

Hypermethylation of WNT5B and hypomethylation of its regulator LRRFIP2 may affect developmental patterning, while hypomethylation of SUFU, a corepressor complex in

sonichedgehog/patch signalling (Chi et al. 2012), and LOC790124 potentially affect hedgehog signalling. The hedgehog cascade is also involved in embryo development, particularly organogenesis, as well as in stem cell renewal.

RHBDF1 is a Rhomboid protease-like protein, but does not have protease activity. Instead it localises to the ER and regulates secretion of ligands for the epidermal growth factor receptor, potentially regulating sleep, cell survival, proliferation and migration (Nakagawa et al. 2005; Yan et al. 2008; Zou et al. 2009). SH2B3 is an adaptor protein involved in negative regulation of cytokine signal transduction and haematopoiesis, mutations are implicated in coeliac disease type 13 and susceptibility to type 2 diabetes (Plagnol et al. 2011). This gene product also has roles in Notch signalling (Yamamoto et al. 2001; Takeyama et al. 2003). Musashi 2, which is involved in embryonic stem cell development and differentiation (Wuebben et al. 2012) as well as Mitogen Activated Phosphorylase Kinase signalling (Zhang et al. 2014) was hypomethylated following L-carnitine treatment (-0.63 fold change,  $p=0.04$ ). Differential methylation of these genes could disrupt several key cell signalling pathways.

#### 5.5.5.6 Genes involved in transcription

Following inhibition of  $\beta$ -oxidation with BMA, transcriptional regulator TFDP was hypermethylated while FOXN3 was hypomethylated, potentially leading to altered expression of these genes and a dysregulated expression of their target genes. TFDP1 is a downstream target of TGF- $\beta$  signalling, and causes arrest at the G1 phase of the cell cycle, while FOXN3 may also be involved in DNA-damage dependent cell cycle arrest and a decrease in its expression could lead to propagation of cells with DNA damage. RSBN1 is expressed in round spermatids, interacts with protein kinase A and as it contains a homeobox motif, is likely to play a role in haploid germ cell transcription regulation (Takahashi et al. 2004). It is also associated with hypothyroidism and type 1 diabetes.

#### 5.5.5.7 Post-translational modification

BRSK2, MARK3, PTPRN2 are all involved in protein phosphorylation and all were hypomethylated following BMA treatment. This could lead to an overall decrease in the phosphorylation of proteins involved in downstream events leading to neuron development, insulin secretion, and histone deacetylation. Both BRSK2 and PTPRN2 are linked to diabetes, as BRSK2 inhibits insulin secretion when phosphorylated, while

PTPRN2 is an auto-antigen in type 1 diabetes. MAN2A1 localises to the Golgi and catalyses the final hydrolysis of the asparagine-linked oligosaccharide maturation pathway. It also has roles in lipid and carbohydrate metabolism and is potentially linked to obesity (Shenfield et al. 2001). SETD1B specifically methylates lysine-4 of histone 3, dependent on demethylation of neighbouring lys-9 (Lee et al. 2007).

#### 5.5.5.8 Genes related to disease

A number of genes which have been implicated in metabolic diseases were differentially methylated following inhibition of  $\beta$ -oxidation. BRSK2 regulates insulin secretion in response to elevated glucose levels via phosphorylation of CDK16 and PAK1. It also regulates cytoskeleton reorganization and may be involved in ER stress-induced apoptosis. PTPRN2 is implicated in insulin-independent diabetes (Li et al. 1997; Caromile et al. 2010). MYO9B is an unconventional myosin associated with type 1 diabetes (Wirth et al. 1996; Monsuur et al. 2005; Persengiev et al. 2010). KCNK9 is maternally imprinted and expressed in the brain (Barel et al. 2008). Deficiency in KCNK9 expression is linked to increased appetite and weight gain in mice (Pang et al. 2009).

A number of DMRs were related to neurological disorders, for example JPH3 is associated with Huntington's disease (Sułek-Piatkowska et al. 2008) and SHANK2 with autism (Berkel et al. 2010). TMCC2 interacts with both amyloid protein A and apolipoprotein A and hence is related to Alzheimer's disease (Hopkins et al. 2011; Hopkins 2013).

Several of the differentially methylated genes are stress-response elements, such as stress-induced cell surface antigen MIC (Collins 2004), while KIF 14 is a microtubule-associated motor with roles in cytokinesis (Gruneberg et al. 2006; Madhavan et al. 2007)

#### 5.5.6 Patterns in the transcriptome and epigenome

Only one concordant difference was identified following L-carnitine treatment, encoding the mineralocorticoid and glucocorticoid-dependent transcription factor NR3C2.

Activation of NR3C2 stimulates expression of transporters including the  $\text{Na}^+$ ,  $\text{K}^+$ ATPase vital to blastocoel development (Fuller and Young 2005). Defects in NR3C2 are associated with early onset hypertension which is severely exacerbated during pregnancy. The transcript is upregulated and hypomethylated following L-carnitine treatment, potentially

allowing an increased bioavailability of the gene product. This could have a protective effect.

Four concordant differences were detected following BMA treatment including four uncharacterised transcripts (LOC506260, LOC511424, LOC505766) and SCHIP1, Schwannomin-interacting protein 1 (Figure 59). SCHIP1, which co-localises with schwannomin adjacent to the plasma membrane (Goutebroze et al. 2000), was upregulated and hypomethylated following BMA treatment. Hypomethylation could enhance expression of SCHIP1, potentially leading to increased interactions with schwannomin. Schwannomin is a scaffolding protein and tumour suppressor, so increased expression of SCHIP1 may affect cell-cell adhesion, or have a protective effect by binding schwannomin to prevent schwannoma tumour formation.

As the present study marks the first report to combine the EmbryoGENE transcriptomic and methylomic platforms, it is not yet possible to compare the current levels of congruence to published data using the same method in the preimplantation embryo. Some studies have combined genome-wide analysis of transcription and methylation status in other tissues. For example, Bock et al. (2012) reported similar hierarchical clustering of differentially methylated and differentially expressed genes in murine blood stem cells, forming a distinct profile to that of murine skin stem cells. However, current understanding suggests that in the mammalian embryo, there is a disconnect between methylation levels and gene expression. Recent studies suggest that most methylation in the human oocyte and embryo occurs in the gene body, rather than promoter regions (Guo et al. 2014; Okae et al. 2014). Therefore it appears that the lack of congruence between methylation status and gene expression in the present study may be typical to preimplantation tissues.

### 5.5.7 Strengths and limitations

Chapter 5 describes and discusses the myriad changes to gene expression and epigenetic status in the bovine blastocyst following manipulation of fatty acid  $\beta$ -oxidation. While many significant alterations were found between each treatment group and controls, unfortunately time was not available to validate these data by qPCR analysis. Data collected using the EmbryoGENE platforms in other studies have been successfully validated (Robert et al. 2011; Plourde et al. 2012; Cagnone and Sirard 2013; Cagnone and

Sirard 2014), but without validation of the key genes discussed in this chapter, interpretation of the data is limited. As the present study marks the first use of the EmbryoGENE methylation microarray, it is not possible to refer to published data using a similar method.

In order to provide enough genetic material for microarray analysis, blastocysts were combined into small groups. As each blastocyst has a unique genome, this introduces heterogeneity. However metabolic profiling of pyruvate and oxygen consumption allowed selection of matched embryos, reducing variation within sample groups.

### 5.5.8 General conclusions

The data presented in this chapter reinforce the causal relationship between preimplantation embryo metabolism and gene expression, potentially extending to lifetime effects through modification of embryo methylation status. Promotion of  $\beta$ -oxidation with L-carnitine, or inhibition of  $\beta$ -oxidation with BMA, each have a wide range of effects on metabolism, gene expression and DNA methylation, despite no change in developmental competence, at least to the blastocyst stage.

Promotion of  $\beta$ -oxidation led to changes in expression of genes involved in mitochondrial structure and function, metabolism, metabolic disease such as obesity, transcription and protein modification. Differential methylation affected genes involved in cell signalling, transcription and post-translational modification.

Inhibition of  $\beta$ -oxidation led to changes in expression of genes involved in mitochondrial structure and function, metabolism of lipid and amino acids, transcription, protein modification, wnt and MAP signalling cascades and stress response, overall suggesting a response to stress conditions and dysregulation of metabolism. Differential methylation again affected genes involved in cell signalling, transcription and post-translational modification.

Changes in gene expression indicate a potentially transient response to the metabolic manipulations, but altered expression can have lasting ramifications in terms of development, metabolism and the successful recognition of pregnancy. Furthermore, expression of stress response genes is also associated with embryo loss or loss of pregnancy (Cagnone and Sirard 2013). In addition, changes in CpG methylation indicate a

heritable regulatory level potentially affecting gene expression throughout a hypothetical organism's lifespan. These data suggest that dysregulated  $\beta$ -oxidation in the preimplantation mammalian embryo can have long-term effects on gene expression through control of epigenetic modification.

## 5.6 Future studies

Analysis of blastocyst DNA and mRNA using the EmbryoGENE platforms has revealed a number of genes involved in embryo metabolism and development which were altered following L-carnitine and BMA treatment. Of these, several groups of genes could be investigated in more detail using a combination of metabolomics and qPCR techniques with individual embryos. Analysis of individual blastocyst expression of genes involved in mitochondrial function and energy metabolism could be compared with oxygen and carbohydrate metabolism to further investigate the mechanisms of dysregulated metabolism following disruption of  $\beta$ -oxidation. Blastocyst biopsy analysis of genes which have been identified to have a role in successful implantation or pregnancy in tandem with metabolomics could verify the apparent link between  $\beta$ -oxidation and post-implantation embryo viability. While pre-implantation embryo viability and cell counts were not altered during L-carnitine or BMA treatment, expression and methylation of many genes involved in proliferation, differentiation and apoptosis were altered. Assays of apoptosis could reveal dysregulated proliferation and apoptosis in BMA-treated embryos suggested by the differential expression of genes involved in these processes.

## 6 General discussion

The basic aspects of mammalian embryo energy metabolism are understood following a programme of research reporting turnover of energy substrates including glucose, pyruvate, lactate, amino acids and oxygen (Leese 2012), although this is limited to *in vitro* studies due to technical challenges and ethical limitations. Oxygen consumption rate (OCR) is an excellent marker of overall metabolic activity, increasing during blastocyst development with a concurrent increase in oxidative phosphorylation to meet high energy demand (Trimarchi et al. 2000b). However relatively few studies have undertaken a detailed examination of the bioenergetics of preimplantation embryo development. In one of the few studies to detail components of oxygen consumption, Manes and Lai (1995) found that 49% of rabbit blastocyst oxygen consumption rate (OCR) was non-mitochondrial, while in another, Trimarchi et al. (2000b) reported that 30% of bovine blastocyst OCR was non-mitochondrial. Lopes et al. (2005) validated the nanorespirometer system, a sensitive, accurate and non-invasive assay of embryo OCR and linked individual morphological blastocyst quality to differences in basal OCR. However, to my knowledge, this thesis represents the first report to measure the components of OCR in the mammalian preimplantation embryo.

Metabolism of fatty acids by  $\beta$ -oxidation in mammalian embryos represents one area of metabolic research which, historically, has been relatively neglected. An exciting and growing body of research has established that  $\beta$ -oxidation of endogenous triglyceride stores provides a vital energy source to mammalian embryo development. Indeed, promotion of  $\beta$ -oxidation with exogenous L-carnitine during *in vitro* oocyte maturation has positive effects on maturation, embryo development and cryopreservation (Downs et al. 2009; Dunning et al. 2010; Sutton-McDowall et al. 2012; Valsangkar and Downs 2013), while supplementation of oocytes *in vitro* with Non-Esterified Fatty Acids (NEFA) has numerous detrimental effects to embryo development, metabolism and gene expression (Van Hoeck et al. 2011; Van Hoeck et al. 2013). One of the aims of this thesis has been to investigate the potential effects of promoting  $\beta$ -oxidation alongside potential negative effects of inhibiting  $\beta$ -oxidation negative on bovine embryo development, energy metabolism and gene expression.

## 6.1 Summary

### 6.1.1 Bioenergetic profiling of bovine embryos.

Chapter 3 describes the optimisation of 2 methods used to produce a detailed breakdown of the components of OCR in bovine blastocysts. The mean coupled OCR was 66%, similar to most somatic cell types (Birket et al. 2011). The mean spare capacity was +89%, potentially allowing the embryo to alter its OCR and ATP production dynamically in response to high-energy demand independently of the number of mitochondria. Non-mitochondrial OCR was lower than values previously reported in rabbit (Manes and Lai 1995) and mouse (Trimarchi, et al. 2000b) at around 12% and may be due to NADPH oxidase activity or non-mitochondrial ROS production. The majority of coupled OCR, 57% was due to electron flow from NADH to complex I, while a smaller portion was due to electron transfer from FADH<sub>2</sub> to complex II. FADH<sub>2</sub> is a lower-energy substrate than NADH and typically supports a lower P/O<sub>max</sub> (Nobes et al. 1990). Around 12% of OCR was unaccounted for and could be part of mitochondrial ROS production, which may be regulated or spontaneous. Individual variation between blastocysts suggests that this profile is dynamic and may provide a useful marker of embryo response to nutritional or pharmacological challenges, such as those described in chapter 4.

### 6.1.2 $\beta$ -oxidation and metabolism

Chapter 4 describes the effects of promoting or inhibiting  $\beta$ -oxidation of endogenous TG stores on oxygen, carbohydrate and lipid metabolism. The effect of increasing exogenous supply of NEFA by serum supplementation was also investigated. To summarise, promoting  $\beta$ -oxidation with exogenous L-carnitine decreased oxygen and pyruvate consumption, increased rates of TG consumption and lactate production, and led to mitochondrial inner membrane depolarisation. Blastocyst development and cell count were unaffected. Dysregulated carbohydrate metabolism and mitochondrial dysfunction are likely to be deleterious effects (Grindler and Moley 2013; Guerif et al. 2013).

Preimplantation embryos show some plasticity by adapting to changing metabolic conditions, allowing culture systems to adopt a 'let the embryo choose' approach (Biggers and Racowsky 2002). For example, bovine embryos increase glucose and oxygen

consumption at blastocyst stage to provide increased ATP for blastocyst expansion and protein synthesis. Embryos can be cultured to the morula stage with only lactate or pyruvate as sole exogenous energy source (Brown and Whittingham 1991).

In contrast to the reported beneficial effects of L-carnitine supply during *in vitro* oocyte maturation (Downs et al. 2009; Wu et al. 2010; Sutton-McDowall et al. 2012), these data suggest that increased  $\beta$ -oxidation during preimplantation development could impact ongoing development. On the other hand, competitive inhibition of  $\beta$ -oxidation with BMA increased oxygen and pyruvate consumption, depolarised mitochondria and decreased the rates of TG consumption and lactate output. Furthermore, inhibiting fatty acid transport upstream of  $\beta$ -oxidation with Etomoxir increased pyruvate consumption and decreased lactate production. Again, cell count and blastocyst development were unaffected but dysregulated carbohydrate metabolism and mitochondrial dysfunction could affect postimplantation development. Furthermore, without any recognisable morphological change, embryos with dysregulated  $\beta$ -oxidation due to diet, disease or environmental effects may potentially lead to downstream problems by mechanisms such as altered gene expression and permanent epigenetic modification.

However, the successful development of embryos to blastocyst stage despite dysregulated  $\beta$ -oxidation suggests an impressive degree of plasticity and adaptability. Even when access to the endogenous energy store of TG is inhibited, the embryo adapts, altering oxygen, carbohydrate and amino acid metabolism to compensate, even if the result is mitochondrial dysfunction and altered gene expression, including upregulation of stress response genes. This might suggest that the embryo is surviving in adverse conditions, rather than thriving, perhaps an indication that the embryo is in a *pejus* state (Kooijman 2009). The ability of the bovine embryo to adapt in this way lends further weight to the 'let the embryo choose' approach to embryo culture.

### 6.1.3 $\beta$ -oxidation and gene expression

Some of the data reported in chapter 4 were suspected to be legacy effects of defective  $\beta$ -oxidation, such as the altered carbohydrate metabolism during early cleavage leading to differences in OCR at blastocyst stages. By contrast, other data pointed to legacy effects in post-implantation development, such as mitochondrial dysfunction and altered lipid consumption. One mechanism for such effects could be alteration of gene

expression by immediate alteration at transcription level or epigenetic modification of DNA. Indeed, changes in expression of genes related to metabolism, development, stress response, metabolic disease and successful pregnancy were identified following manipulation of  $\beta$ -oxidation. Furthermore, differential methylation of genes encoding products involved in metabolism, development and disease were also identified. These data lend weight to the idea that manipulation of metabolism during preimplantation development can lead to permanent impairment.

## 6.2 Further work

Two major research themes were unfortunately not included in the bioenergetic study. One original aim was to continue to define the components of OCR in terms of cellular process, including OCR used for protein synthesis, transcription, DNA replication and signalling using nano respirometry, applying a similar approach to that of Birket et al. (2011). It is well established that transcription and protein synthesis gradually increase during embryo development and profiling the changing oxygen demand from these processes could provide rich information regarding the budgeting of ATP during early development. In addition, this research has focused on blastocyst oxygen metabolism, but ideally the same methods would be applied to cleavage stage embryos. As the number of mitochondria is fixed during embryo development, the maximal OCR may also be fixed, or perhaps regulated by changes in mitochondrial inner membrane polarisation of pH. If so, the spare respiratory capacity would be reduced as an embryo increases OCR in order to undergo blastocoel formation and blastocyst expansion. These studies were not completed due to time constraints and would be a priority for further investigation.

Furthermore, production of Reactive Oxygen Species (ROS) is one fate of uncoupled OCR in most cell types and oxidative damage has a role in embryo development and developmental failure. Multiple methods to detect markers of oxidative damage were trialled, but unfortunately were not sensitive enough for use in individual or small groups of blastocysts. The opportunity for further method development could allow sufficient optimisation to investigate the potential relationship between differences in individual uncoupled OCR and oxidative damage, as well as the effect of manipulating  $\beta$ -oxidation on markers of oxidative damage. These could include techniques previously employed in embryos (Sturmeijer et al. 2009) as well as optimisation of new techniques for use with individual or small groups of embryos such as analysis of Thiobarbituric Acid Reactive Substances (TBARS), a marker of lipid damage (Seljeskog et al. 2006). TBARS have been detected in follicular fluid, albeit at much lower levels than in serum (Jozwik 1999) and may be present in the embryo.

Manipulating  $\beta$ -oxidation was shown to affect basal OCR of embryos. Analysis of mitochondrial polarisation revealed dysfunctional mitochondria in both treatment groups tested; it is therefore likely that the bioenergetic profile of embryos with dysregulated  $\beta$ -

oxidation would be altered; in particular % uncoupled OCR might increase, increasing basal OCR in order to provide enough ATP to meet energy demand and therefore reducing spare respiratory capacity. These factors could be investigated by nanorespirometry to further define the mechanism of altered OCR following manipulation of  $\beta$ -oxidation.

A major consideration of this thesis was the relationship between metabolism during individual embryo development and health and disease during the ongoing development of the organism. Several findings, such as variable coupled OCR and spare capacity, depolarised mitochondria, and epigenetic modification following manipulation of  $\beta$ -oxidation are likely to have far-reaching effects. Uncoupled or dysregulated mitochondrial respiration is implicated in a number of conditions, including late-onset neurological disease such as Alzheimer's disease and Huntington's disease. Dysregulated glucose metabolism is characteristic of metabolic disease including diabetes and metabolic syndrome. Several genes implicated in successful recognition of pregnancy, Autism, diabetes, Alzheimer's and Huntington's diseases, as well as cancers, were differentially expressed or differentially methylated following manipulation of  $\beta$ -oxidation. It can be argued that these discoveries link to developmental origins of health and disease (DoHaD), but without further study, these ideas are speculative. Ideally, metabolically profiled embryos would be transferred to recipient females to investigate the relationship between dysregulated oxygen metabolism or manipulation of  $\beta$ -oxidation and successful pregnancy and live birth. Furthermore, investigation of the relationship between epigenetic alteration and dysregulated metabolism at the blastocyst stage and lifetime health and disease was limited by the lab-based nature of this work.

## 6.3 Concluding remarks

The broad aim of this work, as outlined in Chapter 1, was to investigate the regulation of oxidative metabolism in individual mammalian embryos and the immediate and legacy effects of metabolic dysregulation. To do this, a number of existing methods were employed and optimised, as described in Chapter 2. The data from these studies is summarised in Figure 60. In Chapter 3, the components of oxidative phosphorylation in the bovine blastocyst were reported. Data regarding the coupled OCR and spare respiratory capacity of bovine blastocysts were reported for the first time, providing a new understanding of blastocyst energy metabolism and allowing more accurate calculations of ATP production for future studies.

After a period of neglect in the literature,  $\beta$ -oxidation of endogenous lipid stores is now increasingly regarded as a key component of oocyte and preimplantation embryo metabolism. In Chapter 4, metabolism of endogenous lipid was manipulated using a promoter and inhibitor of  $\beta$ -oxidation. In both cases, blastocyst development was unaffected, however several changes in energy metabolism were reported, including altered OCR, carbohydrate turnover and mitochondrial polarisation. These differences were suspected to have legacy effects and so the relationship between  $\beta$ -oxidation of endogenous fatty acids and gene expression, as well as gene methylation, was investigated in Chapter 5. These studies reveal a number of potentially deleterious effects of dysregulated fatty acid metabolism, but also highlight the plasticity of the mammalian embryo to adapt to sometimes harmful conditions by dynamic metabolic regulation.

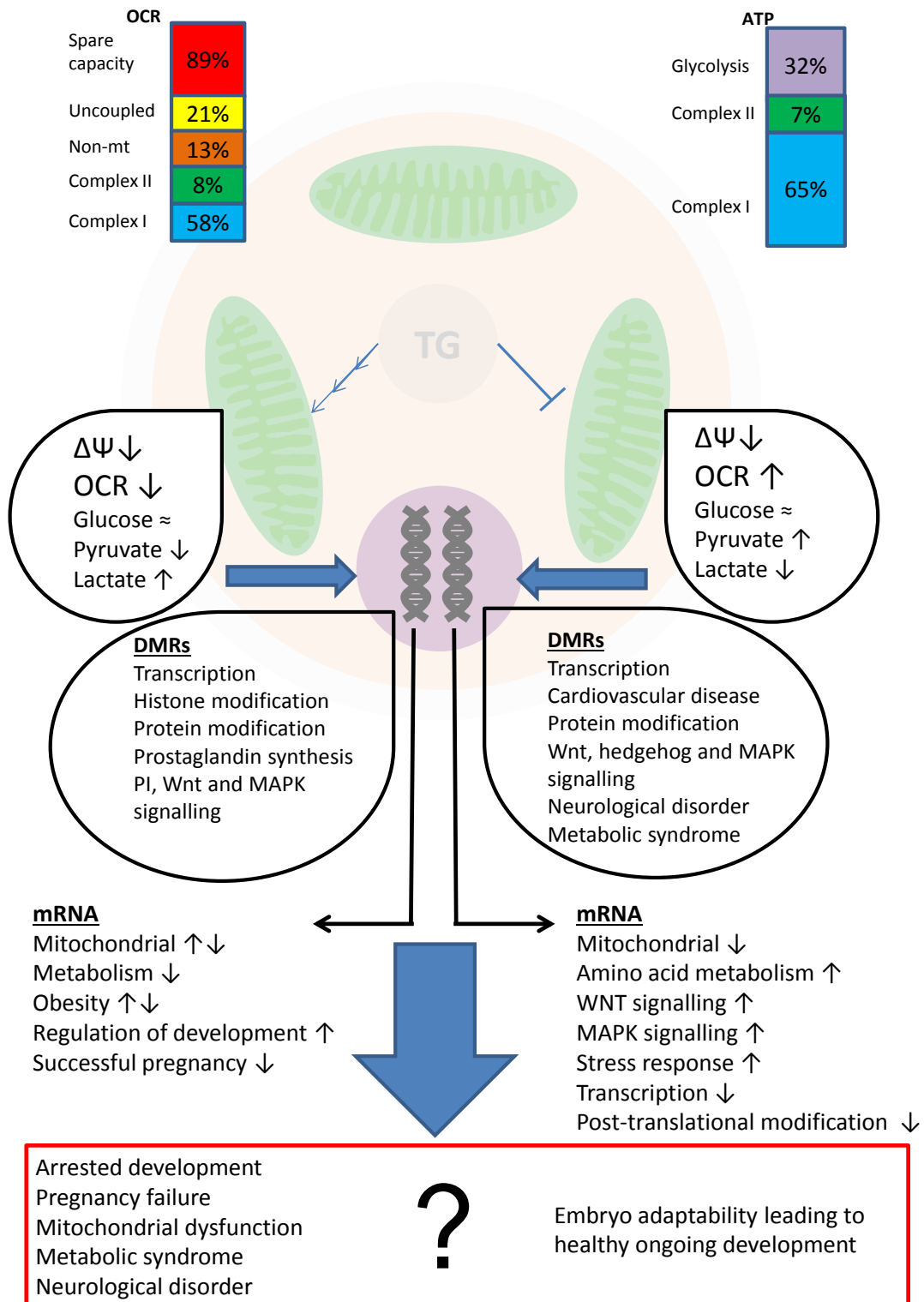


Figure 60: Summary figure combining key data from chapters 3-5. The components of blastocyst oxygen consumption (OCR) were reported (Chapter 3). Promotion of fatty acid transport with **L-carnitine** or inhibition of  $\beta$ -oxidation with  $\beta$ -mercaptoacetate (**BMA**) led to altered mitochondrial energy metabolism during early cleavage and blastocyst stages, including inner mitochondrial membrane polarisation ( $\Delta\Psi$ ), **OCR**, **pyruvate** and **lactate** consumption (Chapter 4). Microarray analysis of blastocysts following L-carnitine or BMA treatment revealed changes in transcription (**mRNA**) and differentially methylated regions (**DMRs**) of genes involved in many key processes (Chapter 5).

## 7 References

- Aardema, H. et al., 2011. Oleic acid prevents detrimental effects of saturated fatty acids on bovine oocyte developmental competence. *Biology of reproduction*, 85(1), pp.62–9. Available at: <http://www.bioreprod.org/content/85/1/62.full> [Accessed August 9, 2014].
- Abbott, B.D., Ebron-mccoy, M. and Andrews, J.E., 1995. Cell death in rat and mouse embryos exposed to methanol in whole embryo culture. *Toxicology*, 97(1-3), pp.159–171. Available at: <http://www.sciencedirect.com/science/article/pii/0300483X9402945Q> [Accessed July 8, 2014].
- Abe, H. et al., 2002. Accumulation of cytoplasmic lipid droplets in bovine embryos and cryotolerance of embryos developed in different culture systems using serum-free or serum-containing media. *Molecular reproduction and development*, 61(1), pp.57–66. Available at: <http://www.ncbi.nlm.nih.gov/pubmed/11774376> [Accessed May 29, 2014].
- Abe, H., 2007. A Non-invasive and Sensitive Method for Measuring Cellular Respiration with a Scanning Electrochemical Microscopy to Evaluate Embryo Quality. *Journal of Mammalian Ova Research*, 24(3), pp.70–78. Available at: <http://dx.doi.org/10.1274/jmor.24.70> [Accessed July 3, 2014].
- Affourtit, C. and Brand, M.D., 2008. Uncoupling protein-2 contributes significantly to high mitochondrial proton leak in INS-1E insulinoma cells and attenuates glucose-stimulated insulin secretion. *The Biochemical journal*, 409, pp.199–204.
- Affourtit, C. and Brand, M.D., 2009. Measuring mitochondrial bioenergetics in INS-1E insulinoma cells. *Methods in enzymology*, 457, pp.405–24. Available at: <http://www.sciencedirect.com/science/article/pii/S007668790905023X> [Accessed July 8, 2014].
- Agung, B. et al., 2005. Relationship between oxygen consumption and sex of bovine in vitro fertilized embryos. *Reproduction in domestic animals = Zuchthygiene*, 40(1), pp.51–6. Available at: <http://www.ncbi.nlm.nih.gov/pubmed/15655001> [Accessed September 1, 2014].
- Ahmad, W. et al., 1995. Lysosomal chitobiase (CTB) and the G-protein  $\gamma 5$  subunit (GNG5) genes co-localize to human chromosome 1p22. *Cytogenetic and Genome Research*, 71(1), pp.44–46. Available at: <http://www.karger.com/Article/FullText/134059> [Accessed June 26, 2014].
- Alikani, M., 2000. Cleavage anomalies in early human embryos and survival after prolonged culture in-vitro. *Human Reproduction*, 15(12), pp.2634–2643. Available at:

<http://humrep.oxfordjournals.org/content/15/12/2634.full> [Accessed August 20, 2014].

- Ambrosi, E. et al., 2011. Structural changes in the BH3 domain of SOUL protein upon interaction with the anti-apoptotic protein Bcl-xL. *The Biochemical journal*, 438(2), pp.291–301. Available at: <http://www.biochemj.org/bj/438/0291/bj4380291.htm> [Accessed April 8, 2014].
- Amo, T. et al., 2008. Experimental assessment of bioenergetic differences caused by the common European mitochondrial DNA haplogroups H and T. *Gene*, 411, pp.69–76.
- Andrews, J.E. et al., 1993. Developmental toxicity of methanol in whole embryo culture: a comparative study with mouse and rat embryos. *Toxicology*, 81(3), pp.205–215. Available at: <http://www.sciencedirect.com/science/article/pii/0300483X9390013I> [Accessed July 8, 2014].
- Aran, D. et al., 2011. Replication timing-related and gene body-specific methylation of active human genes. *Human molecular genetics*, 20(4), pp.670–80. Available at: <http://www.ncbi.nlm.nih.gov/pubmed/21112978> [Accessed July 22, 2014].
- Arcaro, A., 1998. Human Phosphoinositide 3-Kinase C2beta , the Role of Calcium and the C2 Domain in Enzyme Activity. *Journal of Biological Chemistry*, 273(49), pp.33082–33090. Available at: <http://www.jbc.org/content/273/49/33082.long> [Accessed June 25, 2014].
- Arcaro, A. et al., 2000. Class II phosphoinositide 3-kinases are downstream targets of activated polypeptide growth factor receptors. *Molecular and cellular biology*, 20(11), pp.3817–30. Available at: <http://www.pubmedcentral.nih.gov/articlerender.fcgi?artid=85707&tool=pmcentrez&rendertype=abstract> [Accessed June 25, 2014].
- Audebert, S. et al., 2004. Mammalian Scribble forms a tight complex with the betaPIX exchange factor. *Current biology : CB*, 14(11), pp.987–95. Available at: <http://www.cell.com/article/S0960982204003483/fulltext> [Accessed June 24, 2014].
- Austin, E.J., 2001. Alterations in Intrafollicular Regulatory Factors and Apoptosis During Selection of Follicles in the First Follicular Wave of the Bovine Estrous Cycle. *Biology of Reproduction*, 64(3), pp.839–848. Available at: <http://www.biolreprod.org/content/64/3/839.long> [Accessed September 3, 2014].
- Ball, M.P. et al., 2009. Targeted and genome-scale strategies reveal gene-body methylation signatures in human cells. *Nature biotechnology*, 27(4), pp.361–8. Available at: <http://www.pubmedcentral.nih.gov/articlerender.fcgi?artid=3566772&tool=pmcentrez&rendertype=abstract> [Accessed July 10, 2014].
- Ballabio, E. et al., 2004. The dual role of endothelial differentiation-related factor-1 in the cytosol and nucleus: modulation by protein kinase A. *Cellular and molecular life sciences : CMLS*, 61(9), pp.1069–74. Available at: <http://www.ncbi.nlm.nih.gov/pubmed/15112053> [Accessed June 3, 2014].

- Baltz, J.M., 1993. Intracellular pH regulation in the early embryo. *BioEssays : news and reviews in molecular, cellular and developmental biology*, 15(8), pp.523–30. Available at: <http://www.ncbi.nlm.nih.gov/pubmed/8135765> [Accessed September 1, 2014].
- Baltz, J.M., 2001. Osmoregulation and cell volume regulation in the preimplantation embryo. *Current topics in developmental biology*, 52, pp.55–106. Available at: <http://www.ncbi.nlm.nih.gov/pubmed/11529430> [Accessed September 1, 2014].
- Bánsághi, S. et al., 2014. Isoform- and Species-specific Control of Inositol 1,4,5-Trisphosphate (IP3) Receptors by Reactive Oxygen Species. *Journal of Biological Chemistry*, 289 (12 ), pp.8170–8181. Available at: <http://www.jbc.org/content/289/12/8170.abstract>.
- Barel, O. et al., 2008. Maternally inherited Birk Barel mental retardation dysmorphism syndrome caused by a mutation in the genomically imprinted potassium channel KCNK9. *American journal of human genetics*, 83(2), pp.193–9. Available at: <http://www.pubmedcentral.nih.gov/articlerender.fcgi?artid=2495061andtool=pmc.ncbi.nlm.nih.gov/articles/PMC2495061/abstract> [Accessed August 4, 2014].
- Barja, G., 2007. Mitochondrial oxygen consumption and reactive oxygen species production are independently modulated: implications for aging studies. *Rejuvenation research*, 10(2), pp.215–24. Available at: <http://www.ncbi.nlm.nih.gov/pubmed/17523876> [Accessed January 10, 2015].
- Barker, D.J.P., 1986. Infant mortality, childhood nutrition, and ischaemic heart disease in England and Wales. *The Lancet*, 327(8489), pp.1077–1081. Available at: [http://www.thelancet.com/journals/a/article/PIIS0140-6736\(86\)91340-1/fulltext](http://www.thelancet.com/journals/a/article/PIIS0140-6736(86)91340-1/fulltext) [Accessed August 7, 2014].
- Barker, D.J.P., 2007. The origins of the developmental origins theory. *Journal of internal medicine*, 261(5), pp.412–7. Available at: <http://www.ncbi.nlm.nih.gov/pubmed/17444880> [Accessed July 23, 2014].
- Barnett, D.K., Kimura, J. and Bavister, B.D., 1996. Translocation of active mitochondria during hamster preimplantation embryo development studied by confocal laser scanning microscopy. *Developmental dynamics : an official publication of the American Association of Anatomists*, 205(1), pp.64–72. Available at: <http://www.ncbi.nlm.nih.gov/pubmed/8770552> [Accessed August 20, 2014].
- Barres, R. and Zierath, J.R., 2011. DNA methylation in metabolic disorders. *The American journal of clinical nutrition*, 93(4), p.897S–900. Available at: <http://ajcn.nutrition.org/content/early/2011/02/02/ajcn.110.001933> [Accessed August 12, 2014].
- Bauer, M.F. et al., 1999. Genetic and structural characterization of the human mitochondrial inner membrane translocase. *Journal of molecular biology*, 289(1), pp.69–82. Available at: <http://www.sciencedirect.com/science/article/pii/S0022283699927511> [Accessed June 23, 2014].

- Bausenwein, J. et al., 2010. Elevated levels of oxidized low-density lipoprotein and of catalase activity in follicular fluid of obese women. *Molecular human reproduction*, 16(2), pp.117–24. Available at: <http://molehr.oxfordjournals.org/content/16/2/117.long> [Accessed August 9, 2014].
- Beard, C., Li, E. and Jaenisch, R., 1995. Loss of methylation activates Xist in somatic but not in embryonic cells. *Genes and Development*, 9(19), pp.2325–2334. Available at: <http://genesdev.cshlp.org/content/9/19/2325.short> [Accessed August 21, 2014].
- Beaujean, N. et al., 2004. Non-conservation of mammalian preimplantation methylation dynamics. *Current biology : CB*, 14(7), pp.R266–7. Available at: <http://www.cell.com/article/S0960982204001861/fulltext> [Accessed August 21, 2014].
- Belbin, O. et al., 2011. Investigation of 15 of the top candidate genes for late-onset Alzheimer's disease. *Human genetics*, 129(3), pp.273–82. Available at: <http://www.pubmedcentral.nih.gov/articlerender.fcgi?artid=3036835andtool=pmcentrezandrendertype=abstract> [Accessed June 26, 2014].
- Berg, J.M., Tymoczko, J.L. and Stryer, L., 2002. *Biochemistry* 5th ed., New York: W H Freeman. Available at: <http://www.ncbi.nlm.nih.gov/books/NBK21154/> [Accessed July 3, 2014].
- Berkel, S. et al., 2010. Mutations in the SHANK2 synaptic scaffolding gene in autism spectrum disorder and mental retardation. *Nature genetics*, 42(6), pp.489–91. Available at: <http://dx.doi.org/10.1038/ng.589> [Accessed July 13, 2014].
- Bertolini, M. et al., 2002. Growth, development, and gene expression by in vivo- and in vitro-produced day 7 and 16 bovine embryos. *Molecular reproduction and development*, 63(3), pp.318–28. Available at: <http://www.ncbi.nlm.nih.gov/pubmed/12237947> [Accessed July 2, 2014].
- Biggers, J.D. and Racowsky, C., 2002. The development of fertilized human ova to the blastocyst stage in KSOM(AA) medium: is a two-step protocol necessary? *Reproductive biomedicine online*, 5(2), pp.133–40. Available at: <http://www.ncbi.nlm.nih.gov/pubmed/12419037> [Accessed January 11, 2015].
- Birket, M.J. et al., 2011. A reduction in ATP demand and mitochondrial activity with neural differentiation of human embryonic stem cells. *Journal of cell science*, 124(Pt 3), pp.348–58. Available at: <http://www.pubmedcentral.nih.gov/articlerender.fcgi?artid=3021997andtool=pmcentrezandrendertype=abstract> [Accessed November 12, 2013].
- Van Blerkom, J., 2004. Mitochondria in human oogenesis and preimplantation embryogenesis: engines of metabolism, ionic regulation and developmental competence. *Reproduction (Cambridge, England)*, 128(3), pp.269–80. Available at: <http://www.reproduction-online.org/content/128/3/269.long> [Accessed June 29, 2014].

- Van Blerkom, J., 2008. Mitochondria as regulatory forces in oocytes, preimplantation embryos and stem cells. *Reproductive biomedicine online*, 16(4), pp.553–69. Available at: <http://www.ncbi.nlm.nih.gov/pubmed/18413065> [Accessed August 20, 2014].
- Van Blerkom, J., 2011. Mitochondrial function in the human oocyte and embryo and their role in developmental competence. *Mitochondrion*, 11(5), pp.797–813. Available at: <http://www.ncbi.nlm.nih.gov/pubmed/20933103> [Accessed December 2, 2013].
- Bock, C. et al., 2012. DNA methylation dynamics during in vivo differentiation of blood and skin stem cells. *Molecular cell*, 47(4), pp.633–47. Available at: <http://www.pubmedcentral.nih.gov/articlerender.fcgi?artid=3428428andtool=pmc.ncbi.nlm.nih.gov/articles/PMC3428428/> [Accessed April 26, 2015].
- Borst, P. et al., 1962. Uncoupling activity of long-chain fatty acids. *Biochimica et Biophysica Acta*, 62(3), pp.509–518. Available at: <http://www.sciencedirect.com/science/article/pii/0006300262902329> [Accessed August 14, 2014].
- Boveris, A., Cadenas, E. and Stoppani, A.O.M., 1976. Role of ubiquinone in the mitochondrial generation of hydrogen peroxide. *Biochemical Journal*, 156(2), pp.435–444. Available at: <http://www.scopus.com/inward/record.url?eid=2-s2.0-0017154414andpartnerID=40andmd5=5e2fe02c5ffb83d385c8752f97151608>.
- Boveris, A. and Chance, B., 1973. The mitochondrial generation of hydrogen peroxide. General properties and effect of hyperbaric oxygen. *Biochemical Journal*, 134(3), pp.707–716. Available at: <http://www.scopus.com/inward/record.url?eid=2-s2.0-0015882341andpartnerID=40andmd5=58239f4b405fe3468128e5ca1e6fdaa5>.
- Boyer, P.D., Cross, R.L. and Momsen, W., 1973. A new concept for energy coupling in oxidative phosphorylation based on a molecular explanation of the oxygen exchange reactions. *Proceedings of the National Academy of Sciences of the United States of America*, 70(10), pp.2837–9. Available at: <http://www.pubmedcentral.nih.gov/articlerender.fcgi?artid=427120andtool=pmc.ncbi.nlm.nih.gov/articles/PMC427120/> [Accessed November 1, 2014].
- Brand, M.D., 1994. The stoichiometry of proton pumping and ATP synthesis in mitochondria. *The Biochemist*. Available at: <http://scholar.google.com/scholar?q=The+stoichiometry+of+proton+pumping+and+ATP+synthesis+in+mitochondria&lr=#0> [Accessed September 3, 2014].
- Brand, M.D., 2000. Uncoupling to survive? The role of mitochondrial inefficiency in ageing. *Experimental Gerontology*, 35(6-7), pp.811–820. Available at: <http://www.sciencedirect.com/science/article/pii/S0531556500001352> [Accessed July 8, 2014].
- Brand, M.D. et al., 2005. The efficiency and plasticity of mitochondrial energy transduction. *Nutrition, Human*, pp.897–904.

- Brand, M.D. and Nicholls, D.G., 2011. Assessing mitochondrial dysfunction in cells. *The Biochemical journal*, 435(2), pp.297–312. Available at: <http://www.pubmedcentral.nih.gov/articlerender.fcgi?artid=3076726&tool=pmcentrez&rendertype=abstract> [Accessed November 7, 2013].
- Braude, P., Bolton, V. and Moore, S., 1988. Human gene expression first occurs between the four- and eight-cell stages of preimplantation development. *Nature*, 332(6163), pp.459–61. Available at: <http://dx.doi.org/10.1038/332459a0> [Accessed November 1, 2014].
- Bremer, J., 1983. Carnitine--metabolism and functions. *Physiological reviews*, 63(4), pp.1420–80. Available at: <http://classic.physrev.physiology.org/content/63/4/1420.abstract> [Accessed August 18, 2014].
- Bridges, P.J. et al., 2011. Methodology matters: IVF versus ICSI and embryonic gene expression. *Reproductive biomedicine online*, 23(2), pp.234–44. Available at: <http://www.rbmojournal.com/article/S1472648311002331/fulltext> [Accessed July 2, 2014].
- Brown, J.J. and Whittingham, D.G., 1991. The roles of pyruvate, lactate and glucose during preimplantation development of embryos from F1 hybrid mice in vitro. *Development (Cambridge, England)*, 112(1), pp.99–105. Available at: <http://www.ncbi.nlm.nih.gov/pubmed/1769345> [Accessed January 11, 2015].
- Burdge, G.C. et al., 2009. Folic Acid Supplementation during the Juvenile-Pubertal Period in Rats Modifies the Phenotype and Epigenotype Induced by Prenatal Nutrition. *The Journal of Nutrition*, 139 (6), pp.1054–1060. Available at: <http://jn.nutrition.org/content/139/6/1054.abstract>.
- Burkitt, M.J. and Mason, R.P., 1991. Direct evidence for in vivo hydroxyl-radical generation in experimental iron overload: an ESR spin-trapping investigation. *Proceedings of the National Academy of Sciences of the United States of America*, 88(19), pp.8440–4. Available at: <http://www.pubmedcentral.nih.gov/articlerender.fcgi?artid=52524&tool=pmcentrez&rendertype=abstract> [Accessed December 12, 2014].
- Butcher, L. et al., 1998. Metabolism of pyruvate by the early human embryo. *Biology of Reproduction*, 58 (4), pp.1054–1056. Available at: <http://www.biolreprod.org/content/58/4/1054.abstract>.
- Buttgereit, F. and Brand, M.D., 1995. A hierarchy of ATP-consuming processes in mammalian cells. Available at: <http://www.biochemj.org/bj/312/bj3120163.htm> [Accessed August 26, 2014].
- Cagnone, G. and Sirard, M.-A., 2014. The impact of exposure to serum lipids during in vitro culture on the transcriptome of bovine blastocysts. *Theriogenology*, 81(5), pp.712–722.e3. Available at: <http://www.scopus.com/inward/record.url?eid=2-s2.0-84893831031&partnerID=tZOTx3y1> [Accessed March 17, 2014].



*chemistry*, 277(36), pp.33242–8. Available at:  
<http://www.jbc.org/content/277/36/33242.long> [Accessed June 23, 2014].

- Chi, S. et al., 2012. Rab23 negatively regulates Gli1 transcriptional factor in a Su(Fu)-dependent manner. *Cellular signalling*, 24(6), pp.1222–8. Available at:  
<http://www.pubmedcentral.nih.gov/articlerender.fcgi?artid=3319238&tool=pmcentrez&rendertype=abstract> [Accessed August 4, 2014].
- Choi, S.W., Gerencser, A. a and Nicholls, D.G., 2009. Bioenergetic analysis of isolated cerebrocortical nerve terminals on a microgram scale: spare respiratory capacity and stochastic mitochondrial failure. *Journal of neurochemistry*, 109(4), pp.1179–91. Available at:  
<http://www.pubmedcentral.nih.gov/articlerender.fcgi?artid=2696043&tool=pmcentrez&rendertype=abstract> [Accessed December 2, 2013].
- Ciccone, D.N. et al., 2009. KDM1B is a histone H3K4 demethylase required to establish maternal genomic imprints. *Nature*, 461(7262), pp.415–8. Available at:  
<http://www.ncbi.nlm.nih.gov/pubmed/19727073> [Accessed August 5, 2014].
- Coates, P.J. et al., 2001. Mammalian prohibitin proteins respond to mitochondrial stress and decrease during cellular senescence. *Experimental cell research*, 265(2), pp.262–73. Available at:  
<http://www.sciencedirect.com/science/article/pii/S0014482701951663> [Accessed June 23, 2014].
- Coffman, J.A. and Denegre, J.M., 2007. Mitochondria, redox signaling and axis specification in metazoan embryos. *Developmental biology*, 308(2), pp.266–80. Available at: <http://www.sciencedirect.com/science/article/pii/S0012160607011128> [Accessed May 31, 2014].
- Collins, R.W.M., 2004. Human MHC class I chain related (MIC) genes: their biological function and relevance to disease and transplantation. *European journal of immunogenetics : official journal of the British Society for Histocompatibility and Immunogenetics*, 31(3), pp.105–14. Available at:  
<http://www.ncbi.nlm.nih.gov/pubmed/15182323> [Accessed August 4, 2014].
- Conaghan, J. et al., 1993. Selection criteria for human embryo transfer: a comparison of pyruvate uptake and morphology. *Journal of assisted ...*, 10(1), pp.21–30. Available at: <http://link.springer.com/article/10.1007/BF01204436> [Accessed August 26, 2014].
- Cooper, W.N. et al., 2012. DNA methylation profiling at imprinted loci after periconceptional micronutrient supplementation in humans: Results of a pilot randomized controlled trial. *FASEB Journal*, 26(5), pp.1782–1790. Available at:  
<http://www.scopus.com/inward/record.url?eid=2-s2.0-84860909449&partnerID=40&md5=45f34dce83720ee2e44e1464a6af9c91>.
- Correia, C. et al., 2006. Brief report: High frequency of biochemical markers for mitochondrial dysfunction in autism: no association with the mitochondrial aspartate/glutamate carrier SLC25A12 gene. *Journal of autism and developmental*

- disorders*, 36(8), pp.1137–40. Available at:  
<http://www.ncbi.nlm.nih.gov/pubmed/17151801> [Accessed July 1, 2014].
- Cran, D.G., 1985. Qualitative and quantitative structural changes during pig oocyte maturation. *Reproduction*, 74(1), pp.237–245. Available at:  
<http://www.reproduction-online.org/content/74/1/237.short> [Accessed August 9, 2014].
- Crosier, A.E., 2001. Ultrastructural Morphometry of Bovine Blastocysts Produced In Vivo or In Vitro. *Biology of Reproduction*, 64(5), pp.1375–1385. Available at:  
<http://www.biolreprod.org/content/64/5/1375.long> [Accessed August 12, 2014].
- Cummins, J., 1998. Mitochondrial DNA in mammalian reproduction. *Reviews of Reproduction*, 3(3), pp.172–182. Available at: <http://ror.reproduction-online.org/cgi/content/abstract/3/3/172>.
- Cummins, J., 2000. Fertilization and elimination of the paternal mitochondrial genome. *Human Reproduction*, 15(suppl 2), pp.92–101. Available at:  
[http://humrep.oxfordjournals.org/content/15/suppl\\_2/92.abstract](http://humrep.oxfordjournals.org/content/15/suppl_2/92.abstract) [Accessed July 2, 2014].
- Cummins, J., 2002. The role of maternal mitochondria during oogenesis, fertilization and embryogenesis. *Reproductive BioMedicine Online*, 4(2), pp.176–182. Available at:  
<http://www.sciencedirect.com/science/article/pii/S1472648310619372> [Accessed July 4, 2014].
- Darvey, I.G., 2006. How does the ratio of ATP yield from the complete oxidation of palmitic acid to that of glucose compare with the relative energy contents of fat and carbohydrate ? *Biochemical Education*, 26(1998), pp.22–23.
- David, R.M. et al., 2012. Interference with xenobiotic metabolic activity by the commonly used vehicle solvents dimethylsulfoxide and methanol in zebrafish (*Danio rerio*) larvae but not *Daphnia magna*. *Chemosphere*, 88(8), pp.912–917. Available at:  
<http://www.sciencedirect.com/science/article/pii/S0045653512003323>.
- Davuluri, R. V, Grosse, I. and Zhang, M.Q., 2001. Computational identification of promoters and first exons in the human genome. *Nature genetics*, 29(4), pp.412–7. Available at: <http://dx.doi.org/10.1038/ng780> [Accessed June 19, 2014].
- Deaton, A.M. and Bird, A., 2011. CpG islands and the regulation of transcription. *Genes and development*, 25(10), pp.1010–22. Available at:  
<http://genesdev.cshlp.org/content/25/10/1010.full> [Accessed April 29, 2014].
- Dekel, N., 1979. Maturation Effects of Gonadotropins on the Cumulus-Oocyte Complex of the Rat. *Biology of Reproduction*, 20(2), pp.191–197. Available at:  
<http://www.biolreprod.org/content/20/2/191> [Accessed November 1, 2014].
- Dewald, G. et al., 1996. The human complement C8G gene, a member of the lipocalin gene family: polymorphisms and mapping to chromosome 9q34.3. *Annals of Human*

*Genetics*, 60(4), pp.281–291. Available at: <http://doi.wiley.com/10.1111/j.1469-1809.1996.tb01192.x> [Accessed June 26, 2014].

- Dierich, A. et al., 1998. Impairing follicle-stimulating hormone (FSH) signaling in vivo: targeted disruption of the FSH receptor leads to aberrant gametogenesis and hormonal imbalance. *Proceedings of the National Academy of Sciences of the United States of America*, 95(23), pp.13612–7. Available at: <http://www.pubmedcentral.nih.gov/articlerender.fcgi?artid=24867&tool=pmcentrez&rendertype=abstract> [Accessed November 16, 2014].
- Diskin, M.G., Murphy, J.J. and Sreenan, J.M., 2006. Embryo survival in dairy cows managed under pastoral conditions. *Animal reproduction science*, 96(3-4), pp.297–311. Available at: <http://www.ncbi.nlm.nih.gov/pubmed/16963203> [Accessed August 9, 2014].
- Divakaruni, A.S. and Brand, M.D., 2011. The regulation and physiology of mitochondrial proton leak. *Physiology (Bethesda, Md.)*, 26(3), pp.192–205. Available at: <http://www.ncbi.nlm.nih.gov/pubmed/21670165> [Accessed November 10, 2013].
- Dokras, A., Sargent, I.L. and Barlow, D.H., 1993. Fertilization and early embryology: Human blastocyst grading: an indicator of developmental potential? *Hum. Reprod.*, 8(12), pp.2119–2127. Available at: <http://humrep.oxfordjournals.org/content/8/12/2119> [Accessed September 1, 2014].
- Dong, X.-Y. et al., 2004. Zinc-finger protein ZNF165 is a novel cancer-testis antigen capable of eliciting antibody response in hepatocellular carcinoma patients. *British journal of cancer*, 91(8), pp.1566–70. Available at: <http://dx.doi.org/10.1038/sj.bjc.6602138> [Accessed June 26, 2014].
- Donnay, I. et al., 2002. Impact of adding 5.5 mM glucose to SOF medium on the development, metabolism and quality of in vitro produced bovine embryos from the morula to the blastocyst stage. *Zygote*, 10(03), pp.189–199. Available at: [http://journals.cambridge.org/abstract\\_S0967199402002253](http://journals.cambridge.org/abstract_S0967199402002253) [Accessed July 2, 2014].
- Donnay, I. and Leese, H.J., 1999. Embryo metabolism during the expansion of the bovine blastocyst. *Molecular Reproduction and Development*, 53(2), pp.171–178. Available at: [http://dx.doi.org/10.1002/\(SICI\)1098-2795\(199906\)53:2<171::AID-MRD6>3.0.CO](http://dx.doi.org/10.1002/(SICI)1098-2795(199906)53:2<171::AID-MRD6>3.0.CO).
- Downs, S.M. and Hudson, E.D., 2000. Energy substrates and the completion of spontaneous meiotic maturation. *Zygote (Cambridge, England)*, 8(4), pp.339–51. Available at: <http://www.ncbi.nlm.nih.gov/pubmed/11108555> [Accessed September 3, 2014].
- Downs, S.M., Mosey, J.L. and Klinger, J., 2009. Fatty acid oxidation and meiotic resumption in mouse oocytes. *Molecular reproduction and development*, 76(9), pp.844–53. Available at: <http://www.pubmedcentral.nih.gov/articlerender.fcgi?artid=3995453&tool=pmcentrez&rendertype=abstract> [Accessed August 9, 2014].

- Dragoni, I. et al., 1998. EDF-1, a Novel Gene Product Down-regulated in Human Endothelial Cell Differentiation. *Journal of Biological Chemistry*, 273(47), pp.31119–31124. Available at: <http://www.jbc.org/content/273/47/31119.long> [Accessed June 26, 2014].
- Drewes, G. et al., 1997. MARK, a Novel Family of Protein Kinases That Phosphorylate Microtubule-Associated Proteins and Trigger Microtubule Disruption. *Cell*, 89(2), pp.297–308. Available at: <http://www.sciencedirect.com/science/article/pii/S0092867400802081> [Accessed June 26, 2014].
- Dudkina, N. V et al., 2010. Structure and function of mitochondrial supercomplexes. *Biochimica et biophysica acta*, 1797(6-7), pp.664–70. Available at: <http://www.sciencedirect.com/science/article/pii/S0005272809003089> [Accessed June 12, 2014].
- Dudkina, N. V et al., 2011. Interaction of complexes I, III, and IV within the bovine respirasome by single particle cryoelectron tomography. *Proceedings of the National Academy of Sciences of the United States of America*, 108(37), pp.15196–200. Available at: <http://www.pnas.org/content/108/37/15196.short> [Accessed June 2, 2014].
- Dumollard, R., Duchen, M. and Carroll, J., 2007. The role of mitochondrial function in the oocyte and embryo. *Current topics in developmental biology*, 77, pp.21–49. Available at: <http://www.sciencedirect.com/science/article/pii/S0070215306770028> [Accessed June 24, 2014].
- Dunning, K.R. et al., 2010. Beta-oxidation is essential for mouse oocyte developmental competence and early embryo development. *Biology of reproduction*, 83(6), pp.909–18. Available at: <http://www.ncbi.nlm.nih.gov/pubmed/20686180> [Accessed November 22, 2013].
- Dunning, K.R. et al., 2011. Increased beta-oxidation and improved oocyte developmental competence in response to l-carnitine during ovarian in vitro follicle development in mice. *Biology of reproduction*, 85(3), pp.548–55. Available at: <http://www.biolreprod.org/content/85/3/548.short> [Accessed November 29, 2014].
- Dyer, M.R. and Walker, J.E., 1993. Sequences of members of the human gene family for the c subunit of mitochondrial ATP synthase. *The Biochemical journal*, 293 ( Pt 1), pp.51–64. Available at: <http://www.pubmedcentral.nih.gov/articlerender.fcgi?artid=1134319andtool=pmc.ncbi.nlm.nih.gov/articles/PMC1134319/abstract> [Accessed June 23, 2014].
- Edwards, J.R. et al., 2010. Chromatin and sequence features that define the fine and gross structure of genomic methylation patterns. *Genome research*, 20(7), pp.972–80. Available at: <http://www.pubmedcentral.nih.gov/articlerender.fcgi?artid=2892098andtool=pmc.ncbi.nlm.nih.gov/articles/PMC2892098/abstract> [Accessed June 9, 2014].

- Ekstrand, M.I. et al., 2004. Mitochondrial transcription factor A regulates mtDNA copy number in mammals. *Human molecular genetics*, 13(9), pp.935–44. Available at: <http://www.ncbi.nlm.nih.gov/pubmed/15016765> [Accessed January 26, 2014].
- El-Sayed, A. et al., 2006. Large-scale transcriptional analysis of bovine embryo biopsies in relation to pregnancy success after transfer to recipients. *Physiological genomics*, 28(1), pp.84–96. Available at: <http://physiolgenomics.physiology.org/content/28/1/84.long> [Accessed April 28, 2014].
- Eppig, J.J., 1980. Regulation of Cumulus Oophorus Expansion by Gonadotropins in vivo and in vitro. *Biology of Reproduction*, 23(3), pp.545–552. Available at: <http://www.biolreprod.org/content/23/3/545> [Accessed November 1, 2014].
- Eppig, J.J., 2001. Review Oocyte control of ovarian follicular development and function in mammals. *Reproduction*, 122, pp.829–838.
- Fedorenko, A., Lishko, P. V and Kirichok, Y., 2012. Mechanism of fatty-acid-dependent UCP1 uncoupling in brown fat mitochondria. *Cell*, 151(2), pp.400–13. Available at: <http://www.pubmedcentral.nih.gov/articlerender.fcgi?artid=3782081andtool=pmcentrezandrendertype=abstract> [Accessed August 19, 2014].
- Feng, J. et al., 2006. The Evf-2 noncoding RNA is transcribed from the Dlx-5/6 ultraconserved region and functions as a Dlx-2 transcriptional coactivator. *Genes and development*, 20(11), pp.1470–84. Available at: <http://www.pubmedcentral.nih.gov/articlerender.fcgi?artid=1475760andtool=pmcentrezandrendertype=abstract> [Accessed June 3, 2014].
- Ferguson, E.M. and Leese, H.J., 1999. Triglyceride content of bovine oocytes and early embryos. *Reproduction*, 116(2), pp.373–378. Available at: <http://www.reproduction-online.org/content/116/2/373.short> [Accessed August 9, 2014].
- Ferguson, E.M. and Leese, H.J., 2006. A potential role for triglyceride as an energy source during bovine oocyte maturation and early embryo development. *Molecular reproduction and development*, 73(9), pp.1195–201. Available at: <http://www.ncbi.nlm.nih.gov/pubmed/16804881> [Accessed September 3, 2014].
- Field, S.F. et al., 2008. Sequencing-based genotyping and association analysis of the MICA and MICB genes in type 1 diabetes. *Diabetes*, 57(6), pp.1753–6. Available at: <http://diabetes.diabetesjournals.org/content/57/6/1753.long> [Accessed June 24, 2014].
- Fischer, B. and Bavister, B.D., 1993. Oxygen tension in the oviduct and uterus of rhesus monkeys, hamsters and rabbits. *Journal of reproduction and fertility*, 99(2), pp.673–9. Available at: <http://www.ncbi.nlm.nih.gov/pubmed/8107053> [Accessed September 1, 2014].
- Fischer, J. et al., 2007. The gene encoding adipose triglyceride lipase (PNPLA2) is mutated in neutral lipid storage disease with myopathy. *Nature genetics*, 39(1), pp.28–30. Available at: <http://dx.doi.org/10.1038/ng1951> [Accessed June 14, 2014].

- Fleming, T.P. et al., 2011. Adaptive responses of the embryo to maternal diet and consequences for post-implantation development. *Reproduction, fertility, and development*, 24(1), pp.35–44. Available at: <http://www.ncbi.nlm.nih.gov/pubmed/22394716>.
- Flynn, J.M. et al., 2011. Impaired spare respiratory capacity in cortical synaptosomes from Sod2 null mice. *Free Radical Biology and Medicine*, 50, pp.866–873.
- Forsey, K.E. et al., 2013. Expression and localization of creatine kinase in the preimplantation embryo. *Molecular reproduction and development*, 80(3), pp.185–92. Available at: <http://www.ncbi.nlm.nih.gov/pubmed/23280606> [Accessed July 8, 2014].
- Fortune, J.E., 1994. Ovarian follicular growth and development in mammals. *Biology of reproduction*, 50(2), pp.225–32. Available at: <http://www.ncbi.nlm.nih.gov/pubmed/8142540> [Accessed September 3, 2014].
- Fougerousse, F. et al., 1998. Expression of genes (CAPN3, SGCA, SGCB, and TTN) involved in progressive muscular dystrophies during early human development. *Genomics*, 48(2), pp.145–56. Available at: <http://www.sciencedirect.com/science/article/pii/S0888754397951600> [Accessed June 24, 2014].
- Fraker, C. et al., 2006. The Use of the BD Oxygen Biosensor System to Assess Isolated Human Islets of Langerhans: Oxygen Consumption as a Potential Measure of Islet Potency. *Cell Transplantation*, 15(8), pp.745–758. Available at: <http://www.ingentaconnect.com/content/cog/ct/2006/00000015/F0020008/art00007?token=00551b68ef751e8312d7e442f20672123763c702c497b467b4025687627502b333e3568263c2b53c769ca> [Accessed March 13, 2014].
- Fridhandler, L., Hafez, E.S.E. and Pincus, G., 1956. Respiratory Metabolism of Mammalian Eggs. *Experimental Biology and Medicine*, 92(1), pp.127–129. Available at: <http://ebm.sagepub.com/content/92/1/127.abstract> [Accessed July 3, 2014].
- Fridhandler, L., Hafez, E.S.E. and Pincus, G., 1957. Developmental changes in the respiratory activity of rabbit ova. *Experimental Cell Research*, 13(1), pp.132–139. Available at: <http://www.sciencedirect.com/science/article/pii/001448275790054X> [Accessed July 3, 2014].
- Fry, M. and Green, D.E., 1980a. Energized cation transport by Complex III (ubiquinone-cytochrome reductase). *Biochemical and Biophysical Research Communications*, 97(3), pp.852–859. Available at: <http://www.sciencedirect.com/science/article/pii/0006291X80914552> [Accessed November 1, 2014].
- Fry, M. and Green, D.E., 1980b. Ion-transport chain of cytochrome oxidase: the two chain-direct coupling principle of energy coupling. *Proceedings of the National Academy of Sciences of the United States of America*, 77(11), pp.6391–5. Available at: <http://www.pubmedcentral.nih.gov/articlerender.fcgi?artid=350290andtool=pmcentrezandrendertype=abstract> [Accessed November 1, 2014].

- Fry, M. and Green, D.E., 1981. Cardiolipin requirement for electron transfer in complex I and III of the mitochondrial respiratory chain. *J. Biol. Chem.*, 256(4), pp.1874–1880. Available at: <http://www.jbc.org/content/256/4/1874.short> [Accessed November 1, 2014].
- Fuks, F., 2005. DNA methylation and histone modifications: teaming up to silence genes. *Current opinion in genetics and development*, 15(5), pp.490–5. Available at: <http://www.sciencedirect.com/science/article/pii/S0959437X05001322> [Accessed May 29, 2014].
- Fukumaru, S. et al., 2002. Novel mRNA molecules are induced in hypertrophied ventricles of carnitine-deficient mice and belong to a family of up-regulated gene in cells overexpressing c-erbB-2. *Biochimica et Biophysica Acta (BBA) - Gene Structure and Expression*, 1577(3), pp.437–444. Available at: <http://www.sciencedirect.com/science/article/pii/S0167478102004475> [Accessed June 24, 2014].
- Fulka, H. et al., 2004. DNA methylation pattern in human zygotes and developing embryos. *Reproduction (Cambridge, England)*, 128(6), pp.703–8. Available at: <http://www.reproduction-online.org/content/128/6/703> [Accessed August 21, 2014].
- Fuller, P.J. and Young, M.J., 2005. Mechanisms of mineralocorticoid action. *Hypertension*, 46(6), pp.1227–35. Available at: <http://hyper.ahajournals.org/content/46/6/1227.long> [Accessed April 26, 2015].
- Futatsugi, A. et al., 2005. IP3 receptor types 2 and 3 mediate exocrine secretion underlying energy metabolism. *Science (New York, N.Y.)*, 309(5744), pp.2232–4. Available at: <http://www.sciencemag.org/content/309/5744/2232.abstract> [Accessed May 26, 2014].
- Gad, A. et al., 2012. Molecular mechanisms and pathways involved in bovine embryonic genome activation and their regulation by alternative in vivo and in vitro culture conditions. *Biology of reproduction*, 87(4), p.100. Available at: <http://www.biolreprod.org/content/87/4/100.long> [Accessed August 10, 2014].
- Gandhi, A.P. et al., 2001. Substrate utilization in porcine embryos cultured in NCSU23 and G1.2/G2.2 sequential culture media. *Molecular reproduction and development*, 58(3), pp.269–75. Available at: <http://www.ncbi.nlm.nih.gov/pubmed/11170267> [Accessed September 10, 2014].
- Gardner, D.K. et al., 2004. Single blastocyst transfer: a prospective randomized trial. *Fertility and sterility*, 81(3), pp.551–5. Available at: <http://www.ncbi.nlm.nih.gov/pubmed/15037401> [Accessed September 1, 2014].
- Gardner, D.K. and Sakkas, D., 1993. Mouse embryo cleavage, metabolism and viability: role of medium composition. *Human Reproduction*, 8 (2), pp.288–295. Available at: <http://humrep.oxfordjournals.org/content/8/2/288.abstract>.

- Garrett, L.J. a, Revell, S.G. and Leese, H.J., 2008. Adenosine triphosphate production by bovine spermatozoa and its relationship to semen fertilizing ability. *Journal of andrology*, 29(4), pp.449–58. Available at: <http://www.ncbi.nlm.nih.gov/pubmed/18046050> [Accessed December 2, 2013].
- Ge, H. et al., 2012. The importance of mitochondrial metabolic activity and mitochondrial DNA replication during oocyte maturation in vitro on oocyte quality and subsequent embryo developmental competence. *Molecular reproduction and development*, 79(6), pp.392–401. Available at: <http://www.ncbi.nlm.nih.gov/pubmed/22467220> [Accessed December 2, 2013].
- Ghanem, N. et al., 2014. Differential expression of selected candidate genes in bovine embryos produced in vitro and cultured with chemicals modulating lipid metabolism. *Theriogenology*, 82(2), pp.238–50. Available at: <http://www.sciencedirect.com/science/article/pii/S0093691X14001654> [Accessed August 23, 2014].
- Gopichandran, N. and Leese, H.J., 2003. Metabolic characterization of the bovine blastocyst, inner cell mass, trophoctoderm and blastocoel fluid. *Reproduction*, 126(3), pp.299–308. Available at: <http://www.reproduction-online.org/content/126/3/299.abstract> [Accessed July 3, 2014].
- Gopichandran, N. and Leese, H.J., 2006. The effect of paracrine/autocrine interactions on the in vitro culture of bovine preimplantation embryos. *Reproduction (Cambridge, England)*, 131(2), pp.269–77. Available at: <http://www.ncbi.nlm.nih.gov/pubmed/16452720> [Accessed December 2, 2013].
- Goutebroze, L. et al., 2000. Cloning and characterization of SCHIP-1, a novel protein interacting specifically with spliced isoforms and naturally occurring mutant NF2 proteins. *Molecular and cellular biology*, 20(5), pp.1699–712. Available at: <http://www.pubmedcentral.nih.gov/articlerender.fcgi?artid=85353andtool=pmcentrezandrendertype=abstract> [Accessed July 1, 2014].
- Gowher, H. et al., 2005. Mechanism of stimulation of catalytic activity of Dnmt3A and Dnmt3B DNA-(cytosine-C5)-methyltransferases by Dnmt3L. *The Journal of biological chemistry*, 280(14), pp.13341–8. Available at: <http://www.jbc.org/content/280/14/13341> [Accessed June 20, 2014].
- Gregor, A. et al., 2002. Molecular study of the hydroxymethylbilane synthase gene (HMBS) among Polish patients with acute intermittent porphyria. *Human mutation*, 19(3), p.310. Available at: <http://www.ncbi.nlm.nih.gov/pubmed/11857754> [Accessed June 23, 2014].
- Gresser, M.J., Myers, J.A. and Boyer, P.D., 1982. Catalytic site cooperativity of beef heart mitochondrial F1 adenosine triphosphatase. Correlations of initial velocity, bound intermediate, and oxygen exchange measurements with an alternating three-site model. *The Journal of biological chemistry*, 257(20), pp.12030–8. Available at: <http://www.ncbi.nlm.nih.gov/pubmed/6214554> [Accessed November 1, 2014].

- Grindler, N.M. and Moley, K.H., 2013. Maternal obesity, infertility and mitochondrial dysfunction: potential mechanisms emerging from mouse model systems. *Molecular human reproduction*, 19(8), pp.486–94. Available at: <http://www.pubmedcentral.nih.gov/articlerender.fcgi?artid=3712655&tool=pmcentrez&rendertype=abstract> [Accessed August 17, 2014].
- Gruneberg, U. et al., 2006. KIF14 and citron kinase act together to promote efficient cytokinesis. *The Journal of cell biology*, 172(3), pp.363–72. Available at: <http://www.pubmedcentral.nih.gov/articlerender.fcgi?artid=2063646&tool=pmcentrez&rendertype=abstract> [Accessed July 15, 2014].
- Guarino, R.D. et al., 2004. Method for determining oxygen consumption rates of static cultures from microplate measurements of pericellular dissolved oxygen concentration. *Biotechnology and bioengineering*, 86(7), pp.775–87. Available at: <http://www.ncbi.nlm.nih.gov/pubmed/15162453> [Accessed March 13, 2014].
- Guerif, F. et al., 2013. A simple approach for CO<sub>2</sub> consumption and RElease (CORE) analysis of metabolic activity in single mammalian embryos. *PloS one*, 8(8), p.e67834. Available at: <http://www.pubmedcentral.nih.gov/articlerender.fcgi?artid=3744531&tool=pmcentrez&rendertype=abstract> [Accessed December 2, 2013].
- Gülçin, I., 2006. Antioxidant and antiradical activities of L-carnitine. *Life sciences*, 78(8), pp.803–11. Available at: <http://www.ncbi.nlm.nih.gov/pubmed/16253281> [Accessed March 18, 2014].
- Guo, H. et al., 2014. The DNA methylation landscape of human early embryos. *Nature*, 511(7511), pp.606–610. Available at: <http://dx.doi.org/10.1038/nature13544>.
- Guraya, S.S., 1965. A histochemical analysis of lipid yolk deposition in the oocytes of cat and dog. *The Journal of experimental zoology*, 160(1), pp.123–35. Available at: <http://www.ncbi.nlm.nih.gov/pubmed/5894324>.
- Gutiérrez-Adán, A. et al., 2001. Influence of glucose on the sex ratio of bovine IVM/IVF embryos cultured in vitro. *Reproduction, fertility, and development*, 13(5-6), pp.361–5. Available at: <http://www.ncbi.nlm.nih.gov/pubmed/11833931> [Accessed September 1, 2014].
- Hackett, J.A. and Surani, M.A., 2013. DNA methylation dynamics during the mammalian life cycle. *Philosophical transactions of the Royal Society of London. Series B, Biological sciences*, 368(1609), p.20110328. Available at: <http://www.scopus.com/inward/record.url?eid=2-s2.0-84876517882&partnerID=40&md5=8b5c41d32965261d9f6714c3f261684a>.
- Harding, H.P. et al., 2003. An Integrated Stress Response Regulates Amino Acid Metabolism and Resistance to Oxidative Stress. *Molecular Cell*, 11(3), pp.619–633. Available at: <http://www.sciencedirect.com/science/article/pii/S1097276503001059> [Accessed September 1, 2014].

- Hardy, K. et al., 1989. Non-invasive measurement of glucose and pyruvate uptake by individual human oocytes and preimplantation embryos. *Human Reproduction*, 4(2), pp.188–191. Available at: <http://humrep.oxfordjournals.org/content/4/2/188.abstract>.
- Hardy, K., 1999. Apoptosis in the human embryo. *Reviews of Reproduction*, 4(3), pp.125–134. Available at: <http://ror.reproduction-online.org/cgi/content/abstract/4/3/125>.
- Harper, J. a, Dickinson, K. and Brand, M.D., 2001. Mitochondrial uncoupling as a target for drug development for the treatment of obesity. *Obesity reviews : an official journal of the International Association for the Study of Obesity*, 2(4), pp.255–65. Available at: <http://www.ncbi.nlm.nih.gov/pubmed/12119996>.
- Harris, S.E. et al., 2007. Carbohydrate metabolism by murine ovarian follicles and oocytes grown in vitro. *Reproduction (Cambridge, England)*, 134(3), pp.415–24. Available at: <http://www.reproduction-online.org/content/134/3/415.short> [Accessed August 29, 2014].
- Harrison, K.L. et al., 1990. Embryotoxicity of micropore filters used in liquid sterilization. *Journal of in vitro fertilization and embryo transfer : IVF*, 7(6), pp.347–50. Available at: <http://www.ncbi.nlm.nih.gov/pubmed/2077089>.
- Harvey, A.J., Kind, K.L. and Thompson, J.G., 2004. Effect of the oxidative phosphorylation uncoupler 2,4-dinitrophenol on hypoxia-inducible factor-regulated gene expression in bovine blastocysts. *Reproduction, Fertility and Development*, 16(7), p.665. Available at: [http://www.publish.csiro.au/view/journals/dsp\\_journal\\_fulltext.cfm?nid=44andf=RD04027](http://www.publish.csiro.au/view/journals/dsp_journal_fulltext.cfm?nid=44andf=RD04027) [Accessed July 3, 2014].
- Hawk, H.W. and Wall, R.J., 1994. Improved yields of bovine blastocysts from in vitro-produced oocytes. I. Selection of oocytes and zygotes. *Theriogenology*, 41(8), pp.1571–1583. Available at: <http://www.sciencedirect.com/science/article/pii/0093691X9490822Z> [Accessed September 1, 2014].
- Hellman, A. and Chess, A., 2007. Gene body-specific methylation on the active X chromosome. *Science (New York, N.Y.)*, 315(5815), pp.1141–3. Available at: <http://www.ncbi.nlm.nih.gov/pubmed/17322062> [Accessed August 21, 2014].
- Hewitson, L.C. and Leese, H.J., 1993. Energy metabolism of the trophectoderm and inner cell mass of the mouse blastocyst. *The Journal of experimental zoology*, 267(3), pp.337–43. Available at: <http://www.ncbi.nlm.nih.gov/pubmed/8228868> [Accessed August 20, 2014].
- Hewitson, L.C., Martin, K.L. and Leese, H.J., 1996. Effects of metabolic inhibitors on mouse preimplantation embryo development and the energy metabolism of isolated inner cell masses. *Molecular reproduction and development*, 43(3), pp.323–30. Available at: <http://www.ncbi.nlm.nih.gov/pubmed/8868245> [Accessed August 19, 2014].

- Hinkle, P.C. et al., 1991. Mechanistic stoichiometry of mitochondrial oxidative phosphorylation. *Biochemistry*, 30(14), pp.3576–3582. Available at: <http://dx.doi.org/10.1021/bi00228a031> [Accessed September 3, 2014].
- Ho, Y. et al., 1995. Preimplantation development of mouse embryos in KSOM: augmentation by amino acids and analysis of gene expression. *Molecular reproduction and development*, 41(2), pp.232–8. Available at: <http://www.ncbi.nlm.nih.gov/pubmed/7654376> [Accessed September 1, 2014].
- Van Hoeck, V. et al., 2011. Elevated non-esterified fatty acid concentrations during bovine oocyte maturation compromise early embryo physiology. *PloS one*, 6(8), p.e23183. Available at: <http://www.pubmedcentral.nih.gov/articlerender.fcgi?artid=3157355andtool=pmcentrezandrendertype=abstract> [Accessed December 2, 2013].
- Van Hoeck, V. et al., 2013. Oocyte developmental failure in response to elevated nonesterified fatty acid concentrations: mechanistic insights. *Reproduction (Cambridge, England)*, 145(1), pp.33–44. Available at: <http://www.reproduction-online.org/content/145/1/33.short> [Accessed August 20, 2014].
- Holm, P., Booth, P.J. and Callesen, H., 2002. Kinetics of early in vitro development of bovine in vivo- and in vitro-derived zygotes produced and/or cultured in chemically defined or serum-containing media. *Reproduction (Cambridge, England)*, 123(4), pp.553–65. Available at: <http://www.ncbi.nlm.nih.gov/pubmed/11914118> [Accessed September 1, 2014].
- Hooper, M.A.K. and Leese, H.J., 1989. Activity of hexokinase in mouse oocytes and preimplantation embryos. In *Biochemical Society Transactions*. PORTLAND PRESS 59 PORTLAND PLACE, LONDON, ENGLAND W1N 3AJ, pp. 546–547.
- Hopkins, P.C.R., 2013. Neurodegeneration in a Drosophila model for the function of TMCC2, an amyloid protein precursor-interacting and apolipoprotein E-binding protein. D. Kretschmar, ed. *PloS one*, 8(2), p.e55810. Available at: <http://dx.plos.org/10.1371/journal.pone.0055810> [Accessed June 2, 2014].
- Hopkins, P.C.R., Sainz-Fuertes, R. and Lovestone, S., 2011. The Impact of a Novel Apolipoprotein E and Amyloid-beta Protein Precursor-Interacting Protein on the Production of Amyloid-beta. *JOURNAL OF ALZHEIMERS DISEASE*, 26(2), pp.239–253.
- Houghton, F.D. et al., 1996. Oxygen consumption and energy metabolism of the early mouse embryo. *Molecular reproduction and development*, 44(4), pp.476–85. Available at: <http://www.ncbi.nlm.nih.gov/pubmed/8844690>.
- Houghton, F.D. et al., 2002. Non-invasive amino acid turnover predicts human embryo developmental capacity. *Human reproduction (Oxford, England)*, 17(4), pp.999–1005. Available at: <http://www.ncbi.nlm.nih.gov/pubmed/11925397> [Accessed September 1, 2014].
- Houghton, F.D., 2006. Energy metabolism of the inner cell mass and trophoblast of the mouse blastocyst. *Differentiation; research in biological diversity*, 74(1), pp.11–8.

Available at: <http://www.sciencedirect.com/science/article/pii/S0301468109601924> [Accessed August 8, 2014].

- Huang, D.W., Sherman, B.T. and Lempicki, R.A., 2009. Systematic and integrative analysis of large gene lists using DAVID bioinformatics resources. *Nature protocols*, 4(1), pp.44–57. Available at: <http://dx.doi.org/10.1038/nprot.2008.211> [Accessed April 28, 2014].
- Huang, Y., 2011. Roles of apolipoprotein E4 (ApoE4) in the pathogenesis of Alzheimer's disease: lessons from ApoE mouse models. *Biochemical Society transactions*, 39(4), pp.924–32. Available at: <http://www.biochemsoctrans.org/bst/039/0924/bst0390924.htm> [Accessed June 16, 2014].
- Hue, L. and Taegtmeier, H., 2009. The Randle cycle revisited: a new head for an old hat. *American journal of physiology. Endocrinology and metabolism*, 297(3), pp.E578–91. Available at: <http://www.pubmedcentral.nih.gov/articlerender.fcgi?artid=2739696&tool=pmcentrez&rendertype=abstract> [Accessed July 23, 2014].
- Hughes, J. et al., 2011. Effects of omega-3 and -6 polyunsaturated fatty acids on ovine follicular cell steroidogenesis, embryo development and molecular markers of fatty acid metabolism. *Reproduction (Cambridge, England)*, 141(1), pp.105–18. Available at: <http://www.reproduction-online.org/content/141/1/105.short> [Accessed July 29, 2014].
- Humpherson, P.G., Leese, H.J. and Sturmeier, R.G., 2005. Amino acid metabolism of the porcine blastocyst. *Theriogenology*, 64(8), pp.1852–1866. Available at: <http://www.sciencedirect.com/science/article/pii/S0093691X05001433>.
- Huntriss, J.D. et al., 2013. Variable imprinting of the MEST gene in human preimplantation embryos. *European journal of human genetics : EJHG*, 21(1), pp.40–7. Available at: <http://www.pubmedcentral.nih.gov/articlerender.fcgi?artid=3522198&tool=pmcentrez&rendertype=abstract> [Accessed June 19, 2014].
- Igosheva, N. et al., 2010. Maternal diet-induced obesity alters mitochondrial activity and redox status in mouse oocytes and zygotes. *PloS one*, 5(4), p.e10074. Available at: <http://www.pubmedcentral.nih.gov/articlerender.fcgi?artid=2852405&tool=pmcentrez&rendertype=abstract> [Accessed July 17, 2014].
- Illingworth, R.S. et al., 2010. Orphan CpG islands identify numerous conserved promoters in the mammalian genome. W. Reik, ed. *PLoS genetics*, 6(9), p.e1001134. Available at: <http://dx.plos.org/10.1371/journal.pgen.1001134> [Accessed May 29, 2014].
- Ito, K. et al., 1999. cDNA cloning, characterization, and chromosome mapping of UBE2E3 (alias UbcH9), encoding an N-terminally extended human ubiquitin-conjugating enzyme. *Cytogenetic and Genome Research*, 84(1-2), pp.99–104. Available at: <http://www.karger.com/DOI/10.1159/000015229>.

- Jaenisch, R., 1997. DNA methylation and imprinting: why bother? *Trends in Genetics*, 13(8), pp.323–329. Available at: [http://www.cell.com/trends/genetics/abstract/S0168-9525\(97\)01180-3](http://www.cell.com/trends/genetics/abstract/S0168-9525(97)01180-3).
- Jang, J.S. et al., 2012. Increased miR-708 expression in NSCLC and its association with poor survival in lung adenocarcinoma from never smokers. *Clinical cancer research : an official journal of the American Association for Cancer Research*, 18(13), pp.3658–67. Available at: <http://clincancerres.aacrjournals.org/content/18/13/3658.long> [Accessed June 24, 2014].
- Jang, J.-Y. et al., 2008. Suppression of adenine nucleotide translocase-2 by vector-based siRNA in human breast cancer cells induces apoptosis and inhibits tumor growth in vitro and in vivo. *Breast cancer research : BCR*, 10(1), p.R11. Available at: <http://breast-cancer-research.com/content/10/1/R11> [Accessed June 23, 2014].
- Javed, M.H. and Wright, R.W., 1991. Determination of pentose phosphate and Embden-Meyerhof pathway activities in bovine embryos. *Theriogenology*, 35(5), pp.1029–1037. Available at: <http://www.sciencedirect.com/science/article/pii/0093691X91903122> [Accessed September 1, 2014].
- Jiang, S., Wells, C.D. and Roach, P.J., 2011. Starch-binding domain-containing protein 1 (Stbd1) and glycogen metabolism: Identification of the Atg8 family interacting motif (AIM) in Stbd1 required for interaction with GABARAPL1. *Biochemical and biophysical research communications*, 413(3), pp.420–5. Available at: <http://www.pubmedcentral.nih.gov/articlerender.fcgi?artid=3411280&tool=pmc.ncbi&rendertype=abstract> [Accessed April 9, 2014].
- Jiménez, A. et al., 2003. Hyperglycemia-induced apoptosis affects sex ratio of bovine and murine preimplantation embryos. *Molecular reproduction and development*, 65(2), pp.180–7. Available at: <http://www.ncbi.nlm.nih.gov/pubmed/12704729> [Accessed November 7, 2013].
- Jin, J. et al., 2013. LRRFIP2 negatively regulates NLRP3 inflammasome activation in macrophages by promoting Flightless-I-mediated caspase-1 inhibition. *Nature communications*, 4, p.2075. Available at: <http://www.nature.com/ncomms/2013/130814/ncomms3075/full/ncomms3075.html> [Accessed August 4, 2014].
- Johnson, J. et al., 2004. Germline stem cells and follicular renewal in the postnatal mammalian ovary. *Nature*, 428(6979), pp.145–50. Available at: <http://www.ncbi.nlm.nih.gov/pubmed/15014492>.
- Johnson, M.H., 2012. *Essential Reproduction*, John Wiley and Sons. Available at: <http://books.google.com/books?id=qXpBst5hJs0C&pgis=1> [Accessed August 29, 2014].
- Johnson, M.H. and Nasr-Esfahani, M.H., 1994. Radical solutions and cultural problems: could free oxygen radicals be responsible for the impaired development of preimplantation mammalian embryos in vitro? *BioEssays : news and reviews in*

*molecular, cellular and developmental biology*, 16(1), pp.31–8. Available at: <http://www.ncbi.nlm.nih.gov/pubmed/8141805> [Accessed August 29, 2014].

Jones, P.A., 2012. Functions of DNA methylation: islands, start sites, gene bodies and beyond. *Nat Rev Genet*, 13(7), pp.484–492. Available at: <http://dx.doi.org/10.1038/nrg3230>.

Jozwik, M., 1999. Oxidative stress markers in preovulatory follicular fluid in humans. *Molecular Human Reproduction*, 5(5), pp.409–413. Available at: <http://molehr.oxfordjournals.org/content/5/5/409.long> [Accessed September 3, 2014].

Jungheim, E.S. et al., 2011. Elevated serum alpha-linolenic acid levels are associated with decreased chance of pregnancy after in vitro fertilization. *Fertility and Sterility*, 96(4), pp.880–883. Available at: [http://www.fertstert.org/article/S0015-0282\(11\)02231-X/abstract](http://www.fertstert.org/article/S0015-0282(11)02231-X/abstract).

Kaelin, W.G. and McKnight, S.L., 2013. Influence of metabolism on epigenetics and disease. *Cell*, 153(1), pp.56–69. Available at: <http://www.pubmedcentral.nih.gov/articlerender.fcgi?artid=3775362andtool=pmcentrezandrendertype=abstract> [Accessed July 9, 2014].

Kaipia, A. and Hsueh, A.J., 1997. Regulation of ovarian follicle atresia. *Annual review of physiology*, 59, pp.349–63. Available at: [http://www.annualreviews.org/doi/abs/10.1146/annurev.physiol.59.1.349?url\\_ver=Z39.88-2003andrfr\\_dat=cr\\_pub=pubmedandrfr\\_id=ori:rid:crossref.organdjournalCode=physiol](http://www.annualreviews.org/doi/abs/10.1146/annurev.physiol.59.1.349?url_ver=Z39.88-2003andrfr_dat=cr_pub=pubmedandrfr_id=ori:rid:crossref.organdjournalCode=physiol) [Accessed August 27, 2014].

Kane, M.T., 1979. Fatty Acids as Energy Rabbit for Culture Morulae of One-Cell Ova to Viable essential acting. *BIOLOGY OF REPRODUCTION*, 20, pp.323–332.

Kawasaki, T. et al., 2003. Oct6, a transcription factor controlling myelination, is a marker for active nerve regeneration in peripheral neuropathies. *Acta neuropathologica*, 105(3), pp.203–8. Available at: <http://www.ncbi.nlm.nih.gov/pubmed/12557005> [Accessed June 7, 2014].

Kenmochi, N. et al., 2001. The human mitochondrial ribosomal protein genes: mapping of 54 genes to the chromosomes and implications for human disorders. *Genomics*, 77(1-2), pp.65–70. Available at: <http://www.sciencedirect.com/science/article/pii/S0888754301966224> [Accessed June 23, 2014].

Kenney, M.C. et al., 2014. Molecular and bioenergetic differences between cells with African versus European inherited mitochondrial DNA haplogroups: Implications for population susceptibility to diseases. *Biochimica et Biophysica Acta - Molecular Basis of Disease*, 1842, pp.208–219.

Kim, J.H. et al., 1993. Effects of phosphate, energy substrates, and amino acids on development of in vitro-matured, in vitro-fertilized bovine oocytes in a chemically

- defined, protein-free culture medium. *Biology of Reproduction* , 48 (6 ), pp.1320–1325. Available at: <http://www.biolreprod.org/content/48/6/1320.abstract>.
- Kim, J.Y. et al., 2006. The adipose tissue triglyceride lipase ATGL/PNPLA2 is downregulated by insulin and TNF-alpha in 3T3-L1 adipocytes and is a target for transactivation by PPARgamma. *American journal of physiology. Endocrinology and metabolism*, 291(1), pp.E115–27. Available at: <http://ajpendo.physiology.org/content/291/1/E115.short> [Accessed July 1, 2014].
- Kimura, M. et al., 1997. cDNA cloning, characterization, and chromosome mapping of UBE2E2 encoding a human ubiquitin-conjugating E2 enzyme. *Cytogenetic and Genome Research*, 78(2), pp.107–111. Available at: <http://www.karger.com/DOI/10.1159/000134639>.
- King, W.A. et al., 1988. Nucleolus organizer regions and nucleoli in preattachment bovine embryos. *Journal of Reproduction and Fertility* , 82 (1 ), pp.87–95. Available at: <http://www.reproduction-online.org/content/82/1/87.abstract>.
- Kirkegaard, K., Agerholm, I.E. and Ingerslev, H.J., 2012. Time-lapse monitoring as a tool for clinical embryo assessment. *Human reproduction (Oxford, England)*, 27(5), pp.1277–85. Available at: <http://humrep.oxfordjournals.org/content/early/2012/03/14/humrep.des079.full> [Accessed November 14, 2014].
- Kisker, C. et al., 1997. Molecular Basis of Sulfite Oxidase Deficiency from the Structure of Sulfite Oxidase. *Cell*, 91(7), pp.973–983. Available at: <http://www.sciencedirect.com/science/article/pii/S0092867400804882> [Accessed June 23, 2014].
- Kobayashi, H. et al., 2012. Contribution of Intragenic DNA Methylation in Mouse Gametic DNA Methylomes to Establish Oocyte-Specific Heritable Marks. *PLoS Genet*, 8(1), p.e1002440. Available at: <http://dx.doi.org/10.1371/journal.pgen.1002440>.
- Kooijman, S.A.L.M., 2009. *Dynamic energy budget theory for metabolic organisation*, Cambridge university press.
- Kruip, T.A.M. et al., 1983. Structural Changes in Bovine Oocytes During Final Maturation In Vivo. *Gamete Research*, 8, pp.29–47.
- Kumar, T.R., 2009. FSHbeta knockout mouse model: a decade ago and into the future. *Endocrine*, 36(1), pp.1–5. Available at: <http://www.pubmedcentral.nih.gov/articlerender.fcgi?artid=4074305andtool=pmc.ncbiandrendertype=abstract> [Accessed November 16, 2014].
- Lamb, V.K. and Leese, H.J., 1994. Uptake of a mixture of amino acids by mouse blastocysts. *Journal of reproduction and fertility*, 102(1), pp.169–75. Available at: <http://www.ncbi.nlm.nih.gov/pubmed/7799310> [Accessed September 1, 2014].
- Lan, F., Nottke, A.C. and Shi, Y., 2008. Mechanisms involved in the regulation of histone lysine demethylases. *Current opinion in cell biology*, 20(3), pp.316–25. Available at:

<http://www.pubmedcentral.nih.gov/articlerender.fcgi?artid=2674377&tool=pmcentrez&rendertype=abstract> [Accessed July 21, 2014].

Larsson, N.G. et al., 1998. Mitochondrial transcription factor A is necessary for mtDNA maintenance and embryogenesis in mice. *Nature genetics*, 18(3), pp.231–6. Available at: <http://dx.doi.org/10.1038/ng0398-231> [Accessed May 23, 2014].

Leary, C., Leese, H.J. and Sturme, R.G., 2014. Human embryos from overweight and obese women display phenotypic and metabolic abnormalities. *Human reproduction (Oxford, England)*, p.deu276–. Available at: <http://humrep.oxfordjournals.org/content/early/2014/11/04/humrep.deu276.short?rss=1> [Accessed November 16, 2014].

Lee, J.-H. et al., 2007. Identification and characterization of the human Set1B histone H3-Lys4 methyltransferase complex. *The Journal of biological chemistry*, 282(18), pp.13419–28. Available at: <http://www.jbc.org/content/282/18/13419.long> [Accessed July 14, 2014].

Lee, J.T., Davidow, L.S. and Warshawsky, D., 1999. Tsix, a gene antisense to Xist at the X-inactivation centre. *Nature genetics*, 21(4), pp.400–4. Available at: <http://www.ncbi.nlm.nih.gov/pubmed/10192391> [Accessed August 21, 2014].

Lee, K.K. and Workman, J.L., 2007. Histone acetyltransferase complexes: one size doesn't fit all. *Nat Rev Mol Cell Biol*, 8(4), pp.284–295. Available at: <http://dx.doi.org/10.1038/nrm2145>.

Lee, M.-J. et al., 2012. Cleavage speed and implantation potential of early-cleavage embryos in IVF or ICSI cycles. *Journal of assisted reproduction and genetics*, 29(8), pp.745–50. Available at: <http://www.pubmedcentral.nih.gov/articlerender.fcgi?artid=3430780&tool=pmcentrez&rendertype=abstract> [Accessed August 20, 2014].

Leese, H.J. et al., 1986. Uptake of pyruvate by early human embryos determined by a non-invasive technique. *Hum. Reprod.*, 1(3), pp.181–182. Available at: <http://humrep.oxfordjournals.org/content/1/3/181.short> [Accessed September 1, 2014].

Leese, H.J., 1995. Metabolic control during preimplantation mammalian development. *Human Reproduction Update*, 1(1), pp.63–72. Available at: <http://humupd.oxfordjournals.org/content/1/1/63.abstract>.

Leese, H.J., 2002. Quiet please, do not disturb: a hypothesis of embryo metabolism and viability. *Bioessays*. Available at: <http://onlinelibrary.wiley.com/doi/10.1002/bies.10137/abstract> [Accessed August 26, 2014].

Leese, H.J. et al., 2007. Female reproductive tract fluids: composition, mechanism of formation and potential role in the developmental origins of health and disease. *Reproduction, Fertility and Development*, 20(1), pp.1–8. Available at: <http://www.publish.csiro.au/paper/RD07153>.

- Leese, H.J. et al., 2008. Metabolism of the viable mammalian embryo: quietness revisited. *Molecular Human Reproduction*, 14(12), pp.667–672. Available at: <http://molehr.oxfordjournals.org/content/14/12/667.abstract>.
- Leese, H.J., 2012. Metabolism of the preimplantation embryo: 40 years on. *Reproduction*, 143(4), pp.417–427. Available at: <http://www.reproduction-online.org/content/143/4/417.abstract>.
- Leese, H.J. and Barton, A., 1985. Production of pyruvate by isolated mouse cumulus cells. *Journal of Experimental Zoology*. Available at: <http://onlinelibrary.wiley.com/doi/10.1002/jez.1402340208/abstract> [Accessed August 26, 2014].
- Leese, H.J. and Barton, A.M., 1984. Pyruvate and glucose uptake by mouse ova and preimplantation embryos. *Reproduction*, 72(1), pp.9–13. Available at: <http://www.reproduction-online.org/content/72/1/9.abstract> [Accessed January 10, 2015].
- Leese, H.J., Donnay, I. and Thompson, J.G., 1998. Human assisted conception: a cautionary tale. Lessons from domestic animals. *Human Reproduction*, 13(suppl 4), pp.184–202. Available at: [http://humrep.oxfordjournals.org/content/13/suppl\\_4/184.short](http://humrep.oxfordjournals.org/content/13/suppl_4/184.short) [Accessed September 1, 2014].
- Lei, H. et al., 1996. De novo DNA cytosine methyltransferase activities in mouse embryonic stem cells. *Development (Cambridge, England)*, 122(10), pp.3195–205. Available at: <http://www.ncbi.nlm.nih.gov/pubmed/8898232>.
- Leroy, J.L.M.R. et al., 2005. Short Communication Evaluation of the Lipid Content in Bovine Oocytes and Embryos with Nile Red : a Practical Approach. *Reprod Dom Anim*, 40, pp.76–78.
- Leroy, J.L.M.R., Opsomer, G., et al., 2008a. Reduced fertility in high-yielding dairy cows: are the oocyte and embryo in danger? Part I. The importance of negative energy balance and altered corpus luteum function to the reduction of oocyte and embryo quality in high-yielding dairy cows. *Reproduction in domestic animals = Zuchthygiene*, 43(5), pp.612–22. Available at: <http://www.ncbi.nlm.nih.gov/pubmed/18384499> [Accessed August 8, 2014].
- Leroy, J.L.M.R., Van Soom, A., et al., 2008b. Reduced fertility in high-yielding dairy cows: are the oocyte and embryo in danger? Part II. Mechanisms linking nutrition and reduced oocyte and embryo quality in high-yielding dairy cows. *Reproduction in domestic animals = Zuchthygiene*, 43(5), pp.623–32. Available at: <http://www.ncbi.nlm.nih.gov/pubmed/18384498> [Accessed August 26, 2014].
- Leroy, J.L.M.R. et al., 2011. Intrafollicular conditions as a major link between maternal metabolism and oocyte quality: a focus on dairy cow fertility. *Reproduction, fertility, and development*, 24(1), pp.1–12. Available at: <http://www.ncbi.nlm.nih.gov/pubmed/22394712>.

- Leroy, J.L.M.R. et al., 2013. Dietary lipid supplementation on cow reproductive performance and oocyte and embryo viability : a real benefit ?
- Leunda-Casi, A. et al., 2002. Increased cell death in mouse blastocysts exposed to high D-glucose in vitro: implications of an oxidative stress and alterations in glucose metabolism. *Diabetologia*, 45(4), pp.571–9. Available at: <http://www.ncbi.nlm.nih.gov/pubmed/12032635> [Accessed July 2, 2014].
- Leverve, X. et al., 1998. Oxidative phosphorylation in intact hepatocytes: Quantitative characterization of the mechanisms of change in efficiency and cellular consequences. In V. Saks et al., eds. *Bioenergetics of the Cell: Quantitative Aspects SE - 5*. Developments in Molecular and Cellular Biochemistry. Springer US, pp. 53–65. Available at: [http://dx.doi.org/10.1007/978-1-4615-5653-4\\_5](http://dx.doi.org/10.1007/978-1-4615-5653-4_5).
- Lewin, B., 2004. *Genes 8*, Pearson Prentice Hall. Available at: <http://books.google.co.uk/books?id=M1BqAAAAMAAJ>.
- Li, E., Beard, C. and Jaenisch, R., 1993. Role for DNA methylation in genomic imprinting. *Nature*, 366(6453), pp.362–5. Available at: <http://dx.doi.org/10.1038/366362a0> [Accessed August 21, 2014].
- Li, E., Bestor, T.H. and Jaenisch, R., 1992. Targeted mutation of the DNA methyltransferase gene results in embryonic lethality. *Cell*, 69(6), pp.915–926. Available at: <http://www.cell.com/article/009286749290611F/fulltext> [Accessed August 2, 2014].
- Li, J. et al., 2007. ZNF307, a novel zinc finger gene suppresses p53 and p21 pathway. *Biochemical and biophysical research communications*, 363(4), pp.895–900. Available at: <http://www.sciencedirect.com/science/article/pii/S0006291X07019055> [Accessed August 7, 2014].
- Li, Q. et al., 1997. Autoantigens in insulin-dependent diabetes mellitus: molecular cloning and characterization of human IA-2 beta. *Proceedings of the Association of American Physicians*, 109(4), pp.429–39. Available at: <http://europepmc.org/abstract/med/9220540> [Accessed August 4, 2014].
- Lillycrop, K.A. et al., 2005. Dietary Protein Restriction of Pregnant Rats Induces and Folic Acid Supplementation Prevents Epigenetic Modification of Hepatic Gene Expression in the Offspring. *J. Nutr.*, 135(6), pp.1382–1386. Available at: <http://jn.nutrition.org/content/135/6/1382.abstract> [Accessed August 21, 2014].
- Lin, Y. et al., 1994. A hyaluronidase activity of the sperm plasma membrane protein PH-20 enables sperm to penetrate the cumulus cell layer surrounding the egg. *The Journal of Cell Biology*, 125(5), pp.1157–1163. Available at: <http://jcb.rupress.org/content/125/5/1157.abstract> [Accessed August 27, 2014].
- Lobo, R.A., 2003. Early ovarian ageing: a hypothesis: What is early ovarian ageing? *Human Reproduction*, 18(9), pp.1762–1764. Available at: <http://humrep.oxfordjournals.org/content/18/9/1762.full> [Accessed August 28, 2014].

- Lombard, J., 1998. Autism: a mitochondrial disorder? *Medical Hypotheses*, 50(6), pp.497–500. Available at: <http://www.medical-hypotheses.com/article/S0306987798902705/fulltext> [Accessed July 1, 2014].
- Lonergan, P. et al., 1999. Effect of time interval from insemination to first cleavage on the developmental characteristics, sex ratio and pregnancy rate after transfer of bovine embryos. *Journal of reproduction and fertility*, 117(1), pp.159–67. Available at: <http://www.ncbi.nlm.nih.gov/pubmed/10645257> [Accessed August 20, 2014].
- Lonergan, P. et al., 2000. Relationship between time of first cleavage and the expression of IGF-I growth factor, its receptor, and two housekeeping genes in bovine two-cell embryos and blastocysts produced in vitro. *Molecular reproduction and development*, 57(2), pp.146–52. Available at: <http://www.ncbi.nlm.nih.gov/pubmed/10984414> [Accessed August 20, 2014].
- Lonergan, P. et al., 2003. Relative messenger RNA abundance in bovine oocytes collected in vitro or in vivo before and 20 hr after the preovulatory luteinizing hormone surge. *Molecular reproduction and development*, 66(3), pp.297–305. Available at: <http://www.ncbi.nlm.nih.gov/pubmed/14502609> [Accessed November 21, 2013].
- Lopes, A.S. et al., 2005. Respiration rates of individual bovine in vitro-produced embryos measured with a novel, non-invasive and highly sensitive microsensor system. *Reproduction (Cambridge, England)*, 130(5), pp.669–79. Available at: <http://www.ncbi.nlm.nih.gov/pubmed/16264096> [Accessed December 2, 2013].
- Lopes, A.S. et al., 2007. Investigation of respiration of individual bovine embryos produced in vivo and in vitro and correlation with viability following transfer. *Human reproduction (Oxford, England)*, 22(2), pp.558–66. Available at: <http://humrep.oxfordjournals.org/content/22/2/558.long> [Accessed June 23, 2014].
- Lopes, A.S., Lane, M. and Thompson, J.G., 2010. Oxygen consumption and ROS production are increased at the time of fertilization and cell cleavage in bovine zygotes. *Human reproduction (Oxford, England)*, 25(11), pp.2762–73. Available at: <http://humrep.oxfordjournals.org/content/early/2010/09/07/humrep.deq221.abstract> [Accessed June 6, 2014].
- López-Arbesu, R. et al., 2007. MHC class I chain-related gene B (MICB) is associated with rheumatoid arthritis susceptibility. *Rheumatology (Oxford, England)*, 46(3), pp.426–30. Available at: <http://rheumatology.oxfordjournals.org/content/46/3/426.long> [Accessed June 24, 2014].
- Lorincz, M.C. et al., 2004. Intragenic DNA methylation alters chromatin structure and elongation efficiency in mammalian cells. *Nature structural and molecular biology*, 11(11), pp.1068–75. Available at: <http://dx.doi.org/10.1038/nsmb840> [Accessed May 29, 2014].
- Lucas, E.S., 2013. Epigenetic effects on the embryo as a result of periconceptual environment and assisted reproduction technology. *Reproductive biomedicine online*, 27(5), pp.477–85. Available at: <http://www.ncbi.nlm.nih.gov/pubmed/23933034> [Accessed August 11, 2014].

- Luchsinger, C. et al., 2013. Stability of reference genes for normalization of reverse transcription quantitative real-time PCR (RT-qPCR) data in bovine blastocysts produced by IVF, ICSI and SCNT. *Zygote (Cambridge, England)*, pp.1–8. Available at: [http://journals.cambridge.org/abstract\\_S0967199413000099](http://journals.cambridge.org/abstract_S0967199413000099) [Accessed July 2, 2014].
- Luisetto, S. et al., 1990. On the nature of the uncoupling effect of fatty acids. *Journal of bioenergetics and biomembranes*, 22(5), pp.635–43. Available at: <http://www.ncbi.nlm.nih.gov/pubmed/2249976> [Accessed January 8, 2015].
- Luisetto, S., Pietrobon, D. and Azzone, G.F., 1987. Uncoupling of oxidative phosphorylation. 1. Protonophoric effects account only partially for uncoupling. *Biochemistry*, 26(23), pp.7332–8. Available at: <http://www.ncbi.nlm.nih.gov/pubmed/2827753> [Accessed January 8, 2015].
- Luzzo, K.M. et al., 2012. High fat diet induced developmental defects in the mouse: oocyte meiotic aneuploidy and fetal growth retardation/brain defects. *PloS one*, 7(11), p.e49217. Available at: <http://www.pubmedcentral.nih.gov/articlerender.fcgi?artid=3495769andtool=pmcentrezandrendertype=abstract> [Accessed July 17, 2014].
- Ma, D.K. et al., 2009. Neuronal activity-induced Gadd45b promotes epigenetic DNA demethylation and adult neurogenesis. *Science (New York, N.Y.)*, 323(5917), pp.1074–7. Available at: <http://www.pubmedcentral.nih.gov/articlerender.fcgi?artid=2726986andtool=pmcentrezandrendertype=abstract> [Accessed May 28, 2014].
- Ma, J.-Y. et al., 2012. Active DNA demethylation in mammalian preimplantation embryos: new insights and new perspectives. *Molecular human reproduction*, 18(7), pp.333–40. Available at: <http://molehr.oxfordjournals.org/content/18/7/333.abstract> [Accessed August 21, 2014].
- Macháty, Z. et al., 2001. Inhibitors of mitochondrial ATP production at the time of compaction improve development of in vitro produced porcine embryos. *Molecular reproduction and development*, 58(1), pp.39–44. Available at: <http://www.ncbi.nlm.nih.gov/pubmed/11144218> [Accessed July 3, 2014].
- Madhavan, J. et al., 2007. High expression of KIF14 in retinoblastoma: association with older age at diagnosis. *Investigative ophthalmology and visual science*, 48(11), pp.4901–6. Available at: <http://www.iovs.org/content/48/11/4901.long> [Accessed August 4, 2014].
- Magli, M.C. et al., 2014. Embryo morphology and development are dependent on the chromosomal complement. *Fertility and Sterility*, 87(3), pp.534–541. Available at: [http://www.fertstert.org/article/S0015-0282\(06\)04024-6/abstract](http://www.fertstert.org/article/S0015-0282(06)04024-6/abstract).
- Magnusson, C. et al., 1986. Oxygen consumption by human oocytes and blastocysts grown in vitro. *Hum. Reprod.*, 1(3), pp.183–184. Available at: <http://humrep.oxfordjournals.org/content/1/3/183.short> [Accessed July 3, 2014].

- Mak, W. et al., 2004. Reactivation of the paternal X chromosome in early mouse embryos. *Science (New York, N.Y.)*, 303(5658), pp.666–9. Available at: <http://www.ncbi.nlm.nih.gov/pubmed/14752160> [Accessed August 21, 2014].
- Mandelbaum, J., 2000. Oocytes. *Human reproduction (Oxford, England)*, 15 Suppl 4, pp.11–8. Available at: <http://www.ncbi.nlm.nih.gov/pubmed/19682941>.
- Manes, C. and Lai, N.C., 1995. Nonmitochondrial oxygen utilization by rabbit blastocysts and surface production of superoxide radicals. *Journal of reproduction and fertility*, 104(1), pp.69–75. Available at: <http://www.ncbi.nlm.nih.gov/pubmed/7636807>.
- Mariotti, M. et al., 2000. Interaction between endothelial differentiation-related factor-1 and calmodulin in vitro and in vivo. *The Journal of biological chemistry*, 275(31), pp.24047–51. Available at: <http://www.jbc.org/content/275/31/24047.long> [Accessed June 26, 2014].
- Market Velker, B.A., Denomme, M.M. and Mann, M.R.W., 2012. Loss of genomic imprinting in mouse embryos with fast rates of preimplantation development in culture. *Biology of reproduction*, 86(5), pp.143, 1–16. Available at: <http://www.ncbi.nlm.nih.gov/pubmed/22278980> [Accessed August 20, 2014].
- Martin, K.L. et al., 1993. Activity of enzymes of energy metabolism in single human preimplantation embryos. *Reproduction*, 99(1), pp.259–266. Available at: <http://www.reproduction-online.org/content/99/1/259.short> [Accessed September 1, 2014].
- Martin, K.L. and Leese, H.J., 1999. Role of developmental factors in the switch from pyruvate to glucose as the major exogenous energy substrate in the preimplantation mouse embryo. *Reproduction, Fertility and Development*, 11(8), p.425. Available at: [http://www.publish.csiro.au/view/journals/dsp\\_journal\\_fulltext.cfm?nid=44andf=RD97071](http://www.publish.csiro.au/view/journals/dsp_journal_fulltext.cfm?nid=44andf=RD97071) [Accessed September 1, 2014].
- Maunakea, A.K. et al., 2010. Conserved role of intragenic DNA methylation in regulating alternative promoters. *Nature*, 466(7303), pp.253–7. Available at: <http://dx.doi.org/10.1038/nature09165> [Accessed May 29, 2014].
- Max, B., 1992. This and that: hair pigments, the hypoxic basis of life and the Virgilian journey of the spermatozoon. *Trends in pharmacological sciences*, 13(7), pp.272–6. Available at: <http://www.ncbi.nlm.nih.gov/pubmed/1324539> [Accessed April 7, 2015].
- May-Panloup, P. et al., 2003. Increased sperm mitochondrial DNA content in male infertility. *Human Reproduction*, 18(3), pp.550–556. Available at: <http://humrep.oxfordjournals.org/content/18/3/550.short> [Accessed August 27, 2014].
- McKeegan, P.J. and Sturmeay, R.G., 2011. The role of fatty acids in oocyte and early embryo development. *Reproduction, fertility, and development*, 24(1), pp.59–67. Available at: <http://www.ncbi.nlm.nih.gov/pubmed/22394718>.

- Meisenberg, G. and Simmons, W.H., 2011. *Principles of Medical Biochemistry*, Elsevier Health Sciences. Available at: <http://books.google.com/books?id=6ktlaxWorm4Candpgis=1> [Accessed September 3, 2014].
- Migeon, B.R. et al., 2001. Identification of TSIX, encoding an RNA antisense to human XIST, reveals differences from its murine counterpart: implications for X inactivation. *American journal of human genetics*, 69(5), pp.951–60. Available at: <http://www.pubmedcentral.nih.gov/articlerender.fcgi?artid=1274371andtool=pmcentrezandrendertype=abstract> [Accessed August 21, 2014].
- Milagro, F.I. et al., 2012. CLOCK, PER2 and BMAL1 DNA methylation: association with obesity and metabolic syndrome characteristics and monounsaturated fat intake. *Chronobiology international*, 29(9), pp.1180–94. Available at: <http://informahealthcare.com/doi/abs/10.3109/07420528.2012.719967> [Accessed August 8, 2014].
- Mills, R.M. and Brinster, R.L., 1967. Oxygen consumption of preimplantation mouse embryos. *Experimental Cell Research*, 47(1-2), pp.337–344. Available at: <http://www.sciencedirect.com/science/article/pii/0014482767902364> [Accessed July 3, 2014].
- Miyamura, M. et al., 1996. Total number of follicles in the ovaries of Japanese black cattle. M. Miyamura, M. Kuwayama, A. Hamawaki, Y. Eguchi. 1996. *Total number of follicles in the ovaries of Japanese black cattle. Theriogenology* 45 (1): 300., 1(45), p.300. Available at: <https://www.infona.pl/resource/bwmeta1.element.elsevier-f497a6ac-1606-3696-9971-5a473883f4cf> [Accessed January 10, 2015].
- Monsur, A.J. et al., 2005. Myosin IXB variant increases the risk of celiac disease and points toward a primary intestinal barrier defect. *Nature genetics*, 37(12), pp.1341–4. Available at: <http://dx.doi.org/10.1038/ng1680> [Accessed August 4, 2014].
- De Montera, B. et al., 2013. Combined methylation mapping of 5mC and 5hmC during early embryonic stages in bovine. *BMC genomics*, 14, p.406. Available at: <http://www.pubmedcentral.nih.gov/articlerender.fcgi?artid=3689598andtool=pmcentrezandrendertype=abstract> [Accessed January 21, 2015].
- Van Montfoort, A.P.A. et al., 2004. Early cleavage is a valuable addition to existing embryo selection parameters: a study using single embryo transfers. *Human Reproduction*, 19(9), pp.2103–2108. Available at: <http://humrep.oxfordjournals.org/content/19/9/2103.abstract>.
- Moon, Y.-A., Hammer, R.E. and Horton, J.D., 2009. Deletion of ELOVL5 leads to fatty liver through activation of SREBP-1c in mice. *Journal of lipid research*, 50(3), pp.412–23. Available at: <http://www.pubmedcentral.nih.gov/articlerender.fcgi?artid=2638104andtool=pmcentrezandrendertype=abstract> [Accessed July 29, 2014].
- Moor, R.M. et al., 1990. Maturation of pig oocytes in vivo and in vitro. In *Control of pig reproduction III. Proceedings of the Third International Conference on Pig*

*Reproduction, held at Sutton Bonington, UK, Apr. 1989.* The Journals of Reproduction and Fertility Ltd, pp. 197–210. Available at: <http://www.cabdirect.org/abstracts/19900178843.html#> [Accessed August 28, 2014].

Motlik, J., Fulka, J. and Flechon, J.-E., 1986. Changes in intercellular coupling between pig oocytes and cumulus cells during maturation in vivo and in vitro. *Reproduction*, 76(1), pp.31–37. Available at: <http://www.reproduction-online.org/content/76/1/31> [Accessed November 1, 2014].

Nagashima, H. et al., 1994. Recent advances in cryopreservation of porcine embryos. *Theriogenology*, 41(1), pp.113–118. Available at: <http://www.sciencedirect.com/science/article/pii/S0093691X05800561>.

Nagata, A. et al., 1991. Human brain prostaglandin D synthase has been evolutionarily differentiated from lipophilic-ligand carrier proteins. *Proceedings of the National Academy of Sciences of the United States of America*, 88(9), pp.4020–4. Available at: <http://www.pubmedcentral.nih.gov/articlerender.fcgi?artid=51585andtool=pmcentrezandrendertype=abstract> [Accessed June 26, 2014].

Nagyova, E., 2012. Regulation of cumulus expansion and hyaluronan synthesis in porcine oocyte-cumulus complexes during in vitro maturation. *Endocrine regulations*, 46(4), pp.225–35. Available at: <http://www.ncbi.nlm.nih.gov/pubmed/23127506> [Accessed October 29, 2014].

Nakagawa, T. et al., 2005. Characterization of a human rhomboid homolog, p100hRho/RHBDF1, which interacts with TGF- $\alpha$  family ligands. *Developmental dynamics : an official publication of the American Association of Anatomists*, 233(4), pp.1315–31. Available at: <http://www.ncbi.nlm.nih.gov/pubmed/15965977> [Accessed July 18, 2014].

Newsholme, E.A., Crabtree, B. and Ardawi, M.S., 1985. The role of high rates of glycolysis and glutamine utilization in rapidly dividing cells. *Bioscience reports*, 5(5), pp.393–400. Available at: <http://www.ncbi.nlm.nih.gov/pubmed/3896338> [Accessed September 1, 2014].

Nguyen, E.B., Westmuckett, A.D. and Moore, K.L., 2014. SPACA7 Is a Novel Male Germ Cell-Specific Protein Localized to the Sperm Acrosome That Is Involved in Fertilization in Mice. *Biology of Reproduction*, 90(1), p.16. Available at: <http://www.biolreprod.org/content/90/1/16.abstract>.

Niakan, K.K. et al., 2012. Human pre-implantation embryo development. *Development (Cambridge, England)*, 139(5), pp.829–41. Available at: <http://dev.biologists.org/content/139/5/829.full> [Accessed July 22, 2014].

Nicol, C.J. et al., 2000. An embryoprotective role for glucose-6-phosphate dehydrogenase in developmental oxidative stress and chemical teratogenesis. *FASEB journal : official publication of the Federation of American Societies for Experimental Biology*, 14(1), pp.111–27. Available at: <http://www.ncbi.nlm.nih.gov/pubmed/10627286>.

- Niemann, H. and Wrenzycki, C., 2000. Alterations of expression of developmentally important genes in preimplantation bovine embryos by in vitro culture conditions: Implications for subsequent development. *Theriogenology*, 53(1), pp.21–34. Available at: <http://www.sciencedirect.com/science/article/pii/S0093691X9900237X> [Accessed July 2, 2014].
- Nilsson, B.O. et al., 1982. Correlation between blastocyst oxygen consumption and trophoblast cytochrome oxidase reaction at initiation of implantation of delayed mouse blastocysts. *J Embryol Exp Morphol*, 71(1), pp.75–82. Available at: <http://dev.biologists.org/content/71/1/75.short> [Accessed July 3, 2014].
- Nobes, C.D., Hay, W.W. and Brand, M.D., 1990. The mechanism of stimulation of respiration by fatty acids in isolated hepatocytes. *Journal of Biological Chemistry*, 265(22), pp.12910–12915. Available at: <http://www.jbc.org/content/265/22/12910.abstract>.
- Norris, D.P. et al., 1994. Evidence that random and imprinted Xist expression is controlled by preemptive methylation. *Cell*, 77(1), pp.41–51. Available at: <http://www.ncbi.nlm.nih.gov/pubmed/8156596> [Accessed August 21, 2014].
- Ohiro, Y. et al., 2002. A novel p53-inducible apoptogenic gene, PRG3, encodes a homologue of the apoptosis-inducing factor (AIF). *FEBS Letters*, 524(1-3), pp.163–171. Available at: <http://www.sciencedirect.com/science/article/pii/S0014579302030491> [Accessed June 5, 2014].
- Ohnuma, T. et al., 2012. No Associations Found between PGBD1 and the Age of Onset in Japanese Patients Diagnosed with Sporadic Alzheimer’s Disease. *Dementia and geriatric cognitive disorders extra*, 2(1), pp.496–502. Available at: <http://www.karger.com/Article/FullText/345085> [Accessed June 26, 2014].
- Okoe, H. et al., 2014. Genome-Wide Analysis of DNA Methylation Dynamics during Early Human Development. *PLoS Genetics*, 10(12), pp.1–12.
- Okamoto, I. et al., 2004. Epigenetic dynamics of imprinted X inactivation during early mouse development. *Science (New York, N.Y.)*, 303(5658), pp.644–9. Available at: <http://www.ncbi.nlm.nih.gov/pubmed/14671313> [Accessed August 21, 2014].
- Olson, S.E. and Seidel, G.E.J., 2000. Culture of In Vitro-Produced Bovine Embryos with Vitamin E Improves Development In Vitro and After Transfer to Recipients. *Biology of Reproduction*, 62(2), pp.248–252. Available at: <http://www.biolreprod.org/content/62/2/248.long> [Accessed September 1, 2014].
- Orsi, N.M. and Leese, H.J., 2004. Amino acid metabolism of preimplantation bovine embryos cultured with bovine serum albumin or polyvinyl alcohol. *Theriogenology*, 61(2-3), pp.561–72. Available at: <http://www.ncbi.nlm.nih.gov/pubmed/14662152> [Accessed September 1, 2014].
- Ottosen, L.D.M. et al., 2007. Murine pre-embryo oxygen consumption and developmental competence. *Journal of assisted reproduction and genetics*, 24(8), pp.359–65.

Available at:

<http://www.pubmedcentral.nih.gov/articlerender.fcgi?artid=3454938&tool=pmcentrez&rendertype=abstract> [Accessed December 2, 2013].

Overström, E., 1996. In vitro assessment of embryo viability. *Theriogenology*, (95).

Available at: <http://www.sciencedirect.com/science/article/pii/S0093691X96846255> [Accessed January 8, 2014].

Overstrom, E.W. et al., 1992. Viability and oxidative metabolism of the bovine blastocyst. , 37(1), p.1992.

Paczkowski, M. et al., 2013. Comparative importance of fatty acid beta-oxidation to nuclear maturation, gene expression, and glucose metabolism in mouse, bovine, and porcine cumulus oocyte complexes. *Biology of reproduction*, 88(5), p.111. Available at: <http://www.ncbi.nlm.nih.gov/pubmed/23536372> [Accessed December 2, 2013].

Paek, J. et al., 2012. Mitochondrial SKN-1/Nrf mediates a conserved starvation response. *Cell metabolism*, 16(4), pp.526–37. Available at: <http://www.cell.com/article/S1550413112003671/fulltext> [Accessed July 1, 2014].

Pang, D.S.J. et al., 2009. An unexpected role for TASK-3 potassium channels in network oscillations with implications for sleep mechanisms and anesthetic action. *Proceedings of the National Academy of Sciences of the United States of America*, 106(41), pp.17546–51. Available at: <http://www.pubmedcentral.nih.gov/articlerender.fcgi?artid=2751655&tool=pmcentrez&rendertype=abstract> [Accessed August 2, 2014].

Panganiban, G. and Rubenstein, J.L.R., 2002. Developmental functions of the Distal-less/Dlx homeobox genes. *Development*, 129(19), pp.4371–4386. Available at: <http://dev.biologists.org/content/129/19/4371.long> [Accessed June 26, 2014].

Pantaleon, M. et al., 1997. Glucose transporter GLUT3: Ontogeny, targeting, and role in the mouse blastocyst. *Proceedings of the National Academy of Sciences*, 94(8), pp.3795–3800. Available at: <http://www.pnas.org/content/94/8/3795.short> [Accessed September 1, 2014].

Partridge, R.J. and Leese, H.J., 1996. Consumption of amino acids by bovine preimplantation embryos. *Reproduction, fertility, and development*, 8(6), pp.945–50. Available at: <http://www.ncbi.nlm.nih.gov/pubmed/8896028> [Accessed September 1, 2014].

Patodia, S. and Raivich, G., 2012. Role of transcription factors in peripheral nerve regeneration. *Frontiers in molecular neuroscience*, 5, p.8. Available at: <http://journal.frontiersin.org/Journal/10.3389/fnmol.2012.00008/abstract> [Accessed May 30, 2014].

Persengiev, S. et al., 2010. Association analysis of myosin IXB and type 1 diabetes. *Human immunology*, 71(6), pp.598–601. Available at: <http://www.sciencedirect.com/science/article/pii/S0198885910000741> [Accessed August 4, 2014].

- Petit, H. V et al., 2002. Milk production and composition, ovarian function, and prostaglandin secretion of dairy cows fed omega-3 fats. *Journal of dairy science*, 85(4), pp.889–99. Available at: <http://www.sciencedirect.com/science/article/pii/S0022030202741477> [Accessed June 25, 2014].
- Phillips, T., 2008. The Role of Methylation in Gene Expression. *Nature Education*, 1(1), p.116. Available at: <http://www.nature.com/scitable/topicpage/the-role-of-methylation-in-gene-expression-1070> [Accessed August 5, 2014].
- Pietrobon, D., Luvisetto, S. and Azzone, G.F., 1987. Uncoupling of oxidative phosphorylation. 2. Alternative mechanisms: intrinsic uncoupling or decoupling. *Biochemistry*, 26(23), pp.7339–7347. Available at: <http://dx.doi.org/10.1021/bi00397a022> [Accessed August 14, 2014].
- Piret, B. et al., 1995. NF-kappa B Transcription Factor and Human Immunodeficiency Virus Type 1 (HIV-1) Activation by Methylene Blue Photosensitization. *European Journal of Biochemistry*, 228(2), pp.447–455. Available at: <http://doi.wiley.com/10.1111/j.1432-1033.1995.0447n.x> [Accessed July 1, 2014].
- Plagnol, V. et al., 2011. Genome-wide association analysis of autoantibody positivity in type 1 diabetes cases. *PLoS genetics*, 7(8), p.e1002216. Available at: <http://www.pubmedcentral.nih.gov/articlerender.fcgi?artid=3150451andtool=pmcentrezandrendertype=abstract> [Accessed August 4, 2014].
- Plante, L. and King, W.A., 1994. Light and electron microscopic analysis of bovine embryos derived by in Vitro and in Vivo fertilization. *Journal of Assisted Reproduction and Genetics*, 11(10), pp.515–529. Available at: <http://link.springer.com/10.1007/BF02216032> [Accessed August 8, 2014].
- Plourde, D. et al., 2012. Contribution of oocyte source and culture conditions to phenotypic and transcriptomic variation in commercially produced bovine blastocysts. *Theriogenology*, 78(1), pp.116–31.e1–3. Available at: [http://www.theriojournal.com/article/S0093-691X\(12\)00062-3/abstract](http://www.theriojournal.com/article/S0093-691X(12)00062-3/abstract) [Accessed July 23, 2014].
- Porter, R.K. and Brand, M.D., 1995. Causes of differences in respiration rate of hepatocytes from mammals of different body mass. *The American journal of physiology*, 269, pp.R1213–R1224.
- Puumala, S.E. et al., 2012. Similar DNA methylation levels in specific imprinting control regions in children conceived with and without assisted reproductive technology: a cross-sectional study. *BMC pediatrics*, 12(1), p.33. Available at: <http://www.biomedcentral.com/1471-2431/12/33> [Accessed August 21, 2014].
- Quinn, P. and Wales, R.G., 1973. THE RELATIONSHIPS BETWEEN THE ATP CONTENT OF PREIMPLANTATION MOUSE EMBRYOS AND THEIR DEVELOPMENT IN VITRO DURING CULTURE. *Reproduction*, 35(2), pp.301–309. Available at: <http://www.reproduction-online.org/content/35/2/301.short> [Accessed August 30, 2014].

- Radford, E.J. et al., 2012. An unbiased assessment of the role of imprinted genes in an intergenerational model of developmental programming. M. Bartolomei, ed. *PLoS genetics*, 8(4), p.e1002605. Available at: <http://dx.plos.org/10.1371/journal.pgen.1002605> [Accessed August 21, 2014].
- Randle, P.J. et al., 1963. The glucose fatty-acid cycle Its role in insulin sensitivity and the metabolic disturbance of diabetes mellitus. *The Lancet*, 281(7285), pp.785–789. Available at: [http://www.thelancet.com/journals/a/article/PIIS0140-6736\(63\)91500-9/fulltext](http://www.thelancet.com/journals/a/article/PIIS0140-6736(63)91500-9/fulltext) [Accessed August 18, 2014].
- Randle, P.J., 1998. Regulatory interactions between lipids and carbohydrates: the glucose fatty acid cycle after 35 years. *Diabetes/metabolism reviews*, 14(4), pp.263–83. Available at: <http://www.ncbi.nlm.nih.gov/pubmed/10095997> [Accessed August 12, 2014].
- Al Rawi, S. et al., 2011. Postfertilization autophagy of sperm organelles prevents paternal mitochondrial DNA transmission. *Science (New York, N.Y.)*, 334(6059), pp.1144–7. Available at: <http://www.sciencemag.org/content/334/6059/1144.abstract> [Accessed August 27, 2014].
- Rekik, W., Dufort, I. and Sirard, M.-A., 2011. Analysis of the gene expression pattern of bovine blastocysts at three stages of development. *Molecular reproduction and development*, 78(4), pp.226–40. Available at: <http://www.ncbi.nlm.nih.gov/pubmed/21509852> [Accessed April 8, 2014].
- Restall, B. and Wales, R., 1966. The Fallopian Tube of the Sheep III. The Chemical Composition of the Fluid from the Fallopian Tube. *Australian Journal of Biological Sciences*, 19(4), pp.687–698. Available at: [http://www.publish.csiro.au/view/journals/dsp\\_journal\\_fulltext.cfm?nid=280andf=B19660687](http://www.publish.csiro.au/view/journals/dsp_journal_fulltext.cfm?nid=280andf=B19660687) [Accessed January 11, 2015].
- Rieger, D. and Guay, P., 1988. Measurement of the metabolism of energy substrates in individual bovine blastocysts. *Reproduction*, 83(2), pp.585–591. Available at: <http://www.reproduction-online.org/content/83/2/585.short> [Accessed September 1, 2014].
- Rieger, D., Loskutoff, N.M. and Betteridge, K.J., 1992. Developmentally related changes in the metabolism of glucose and glutamine by cattle embryos produced and co-cultured in vitro. *Journal of Reproduction and Fertility*, 95(2), pp.585–595. Available at: <http://www.reproduction-online.org/content/95/2/585.abstract>.
- Rigoulet, M. et al., 1998. Quantitative analysis of some mechanisms affecting the yield of oxidative phosphorylation: Dependence upon both fluxes and forces. In V. Saks et al., eds. *Bioenergetics of the Cell: Quantitative Aspects SE - 4*. Developments in Molecular and Cellular Biochemistry. Springer US, pp. 35–52. Available at: [http://dx.doi.org/10.1007/978-1-4615-5653-4\\_4](http://dx.doi.org/10.1007/978-1-4615-5653-4_4).
- Robert, C. et al., 2011. Combining resources to obtain a comprehensive survey of the bovine embryo transcriptome through deep sequencing and microarrays. *Molecular*

- reproduction and development*, 78(9), pp.651–64. Available at: <http://www.ncbi.nlm.nih.gov/pubmed/21812063> [Accessed August 10, 2014].
- Robin, T.P. et al., 2012. EWS/FLI1 regulates EYA3 in Ewing sarcoma via modulation of miRNA-708, resulting in increased cell survival and chemoresistance. *Molecular cancer research : MCR*, 10(8), pp.1098–108. Available at: <http://mcr.aacrjournals.org/content/10/8/1098.long> [Accessed June 24, 2014].
- Robker, R.L. et al., 2009. Obese women exhibit differences in ovarian metabolites, hormones, and gene expression compared with moderate-weight women. *The Journal of clinical endocrinology and metabolism*, 94(5), pp.1533–40. Available at: <http://press.endocrine.org/doi/abs/10.1210/jc.2008-2648> [Accessed August 9, 2014].
- Rodgers, R.J. and Irving-Rodgers, H.F., 2010. Formation of the ovarian follicular antrum and follicular fluid. *Biology of reproduction*, 82(6), pp.1021–9. Available at: <http://www.biolreprod.org/content/82/6/1021.short> [Accessed August 26, 2014].
- Rose, G. et al., 2011. Further support to the uncoupling-to-survive theory: the genetic variation of human UCP genes is associated with longevity. J. Vina, ed. *PLoS one*, 6(12), p.e29650. Available at: <http://dx.plos.org/10.1371/journal.pone.0029650> [Accessed June 1, 2014].
- Ross, T.S. et al., 1991. Cloning and expression of human 75-kDa inositol polyphosphate-5-phosphatase. *J. Biol. Chem.*, 266(30), pp.20283–20289. Available at: <http://www.jbc.org/content/266/30/20283.abstract> [Accessed June 25, 2014].
- Rottenberg, H. and Hashimoto, K., 1986. Fatty acid uncoupling of oxidative phosphorylation in rat liver mitochondria. *Biochemistry*, 25(7), pp.1747–1755. Available at: <http://dx.doi.org/10.1021/bi00355a045> [Accessed January 8, 2015].
- Rousset, S. et al., 2004. The biology of mitochondrial uncoupling proteins. *Diabetes*, 53 Suppl 1(February), pp.S130–5. Available at: <http://www.ncbi.nlm.nih.gov/pubmed/14749278>.
- Sado, T. et al., 2000. X inactivation in the mouse embryo deficient for Dnmt1: distinct effect of hypomethylation on imprinted and random X inactivation. *Developmental biology*, 225(2), pp.294–303. Available at: <http://www.ncbi.nlm.nih.gov/pubmed/10985851> [Accessed August 21, 2014].
- Sado, T. and Sakaguchi, T., 2013. Species-specific differences in X chromosome inactivation in mammals. *Reproduction (Cambridge, England)*, 146(4), pp.R131–9. Available at: <http://www.reproduction-online.org/content/146/4/R131.long> [Accessed August 12, 2014].
- Saitoh, T. and Katoh, M., 2001. Molecular cloning and characterization of human WNT5B on chromosome 12p13.3 region. *International Journal of Oncology*, 19(2), pp.347–351. Available at: <http://www.spandidos-publications.com/ijo/19/2/347/abstract> [Accessed August 4, 2014].

- Salpea, K.D. et al., 2009a. The effect of WNT5B IVS3C>G on the susceptibility to type 2 diabetes in UK Caucasian subjects. *Nutrition, metabolism, and cardiovascular diseases : NMCD*, 19(2), pp.140–5. Available at: [http://www.nmcd-journal.com/article/S0939-4753\(08\)00058-6/abstract](http://www.nmcd-journal.com/article/S0939-4753(08)00058-6/abstract) [Accessed June 26, 2014].
- Salpea, K.D. et al., 2009b. The effect of WNT5B IVS3C>G on the susceptibility to type 2 diabetes in UK Caucasian subjects. *Nutrition, metabolism, and cardiovascular diseases : NMCD*, 19(2), pp.140–5. Available at: <http://www.nmcd-journal.com/article/S0939475308000586/fulltext> [Accessed August 4, 2014].
- Santos, T.A., El Shourbagy, S. and St John, J.C., 2006. Mitochondrial content reflects oocyte variability and fertilization outcome. *Fertility and sterility*, 85(3), pp.584–91. Available at: <http://www.ncbi.nlm.nih.gov/pubmed/16500323> [Accessed August 20, 2014].
- Sata, R. et al., 1999. Fatty Acid Composition of Bovine Embryos Cultured in Serum-Free and Serum-Containing Medium during Early Embryonic Development. *Journal of Reproduction and Development*, 45(1), pp.97–103. Available at: [https://www.jstage.jst.go.jp/article/jrd/45/1/45\\_1\\_97/\\_article](https://www.jstage.jst.go.jp/article/jrd/45/1/45_1_97/_article) [Accessed August 9, 2014].
- Sathananthan, A.H. and Trounson, A.O., 2000. Mitochondrial morphology during preimplantational human embryogenesis. *Human Reproduction*, 15(suppl 2), pp.148–159. Available at: [http://humrep.oxfordjournals.org/content/15/suppl\\_2/148.short](http://humrep.oxfordjournals.org/content/15/suppl_2/148.short) [Accessed July 2, 2014].
- Sawalha, A.H. et al., 2011. A putative functional variant within the UBAC2 gene is associated with increased risk of Behçet’s disease. *Arthritis and rheumatism*, 63(11), pp.3607–12. Available at: <http://www.pubmedcentral.nih.gov/articlerender.fcgi?artid=3205238andtool=pmc.ncbi.nlm.nih.gov/pubmed/21511111> [Accessed June 26, 2014].
- Scott, L. et al., 2008. Human oocyte respiration-rate measurement – potential to improve oocyte and embryo selection? *Reproductive BioMedicine Online*, 17(4), pp.461–469. Available at: <http://europepmc.org/abstract/MED/18854099> [Accessed July 3, 2014].
- Seljeskog, E., Hervig, T. and Mansoor, M.A., 2006. A novel HPLC method for the measurement of thiobarbituric acid reactive substances (TBARS). A comparison with a commercially available kit. *Clinical biochemistry*, 39(9), pp.947–54. Available at: <http://www.ncbi.nlm.nih.gov/pubmed/16781699> [Accessed November 28, 2013].
- Seshagiri, P.B. and Bavister, B.D., 1991. Glucose and phosphate inhibit respiration and oxidative metabolism in cultured hamster eight-cell embryos: evidence for the “crabtree effect”. *Molecular reproduction and development*, 30(2), pp.105–11. Available at: <http://www.ncbi.nlm.nih.gov/pubmed/1954025> [Accessed September 1, 2014].

- Shahbazian, M.D. and Grunstein, M., 2007. Functions of site-specific histone acetylation and deacetylation. *Annual review of biochemistry*, 76, pp.75–100. Available at: <http://www.ncbi.nlm.nih.gov/pubmed/17362198> [Accessed July 15, 2014].
- Shehab-El-Deen, M.A. et al., 2009. Cryotolerance of bovine blastocysts is affected by oocyte maturation in media containing palmitic or stearic acid. *Reproduction in domestic animals = Zuchthygiene*, 44(1), pp.140–2. Available at: <http://www.ncbi.nlm.nih.gov/pubmed/18992093> [Accessed August 9, 2014].
- Shenfield, F. et al., 2001. I . The moral status of the pre-implantation embryo ESHRE Task Force on Ethics and Law In this first statement of the ESHRE Task Force on Ethics and Law , the focus is on the pre-implantation embryo . *Human Reproduction*, 16(5), pp.1046–1048. Available at: <http://humrep.oxfordjournals.org/content/16/5/1046.abstract>.
- Shi, Y. et al., 2004. Histone demethylation mediated by the nuclear amine oxidase homolog LSD1. *Cell*, 119(7), pp.941–53. Available at: <http://www.ncbi.nlm.nih.gov/pubmed/15620353> [Accessed July 12, 2014].
- Shiku, H. et al., 2001. Oxygen consumption of single bovine embryos probed by scanning electrochemical microscopy. *Analytical chemistry*, 73(15), pp.3751–8. Available at: <http://www.ncbi.nlm.nih.gov/pubmed/11510844>.
- Saadi, H.A.S. et al., 2014. An integrated platform for bovine DNA methylome analysis suitable for small samples. *BMC Genomics*, 15(1), p.451. Available at: <http://www.pubmedcentral.nih.gov/articlerender.fcgi?artid=4092217andtool=pmcentrezandrendertype=abstract> [Accessed March 17, 2015].
- Shukla, S. et al., 2011. CTCF-promoted RNA polymerase II pausing links DNA methylation to splicing. *Nature*, 479(7371), pp.74–9. Available at: <http://dx.doi.org/10.1038/nature10442> [Accessed May 25, 2014].
- Si, Y., Shi, H. and Lee, K., 2009. Metabolic flux analysis of mitochondrial uncoupling in 3T3-L1 adipocytes. J. Peccoud, ed. *PLoS one*, 4(9), p.e7000. Available at: <http://dx.plos.org/10.1371/journal.pone.0007000> [Accessed May 23, 2014].
- Simerly, C.R. et al., 1993. Tracing the incorporation of the sperm tail in the mouse zygote and early embryo using an anti-testicular alpha-tubulin antibody. *Developmental biology*, 158(2), pp.536–48. Available at: <http://www.sciencedirect.com/science/article/pii/S001216068371211X> [Accessed August 27, 2014].
- Sinclair, K.D. et al., 2007. DNA methylation, insulin resistance, and blood pressure in offspring determined by maternal periconceptional B vitamin and methionine status. *Proceedings of the National Academy of Sciences* , 104 (49 ) , pp.19351–19356. Available at: <http://www.pnas.org/content/104/49/19351.abstract>.
- Sinclair, K.D. and Singh, R., 2007. Modelling the developmental origins of health and disease in the early embryo. *Theriogenology*, 67(1), pp.43–53. Available at:

<http://www.sciencedirect.com/science/article/pii/S0093691X06005139> [Accessed September 3, 2014].

Smallwood, S.A. et al., 2011. Dynamic CpG island methylation landscape in oocytes and preimplantation embryos. *Nature genetics*, 43(8), pp.811–4. Available at: <http://dx.doi.org/10.1038/ng.864> [Accessed July 30, 2014].

Smith, A.N., Borthwick, K.J. and Karet, F.E., 2002. Molecular cloning and characterization of novel tissue-specific isoforms of the human vacuolar H<sup>+</sup>-ATPase C, G and d subunits, and their evaluation in autosomal recessive distal renal tubular acidosis. *Gene*, 297(1-2), pp.169–177. Available at: <http://www.sciencedirect.com/science/article/pii/S0378111902008843> [Accessed June 23, 2014].

Smith, Z.D. et al., 2012. A unique regulatory phase of DNA methylation in the early mammalian embryo. *Nature*, 484(7394), pp.339–44. Available at: <http://dx.doi.org/10.1038/nature10960> [Accessed July 15, 2014].

Smiths, M.F., McIntush, E.W. and Smith, G.W., 1994. Mechanisms Associated with Corpus Luteum Development. *J Anim Sci*, (72), pp.1857–1872.

Van Soom, A. and de Kruif, A., 1992. A comparative study of in vivo and in vitro derived bovine embryos. *Proceedings of the International Congress on Animal Reproduction and Artificial Insemination, vol. 3*, pp. 1365-1367. Available at: <https://biblio.ugent.be/record/238735> [Accessed September 1, 2014].

Spindler, R.E., Pukazhenthil, B.S. and Wildt, D.E., 2000. Oocyte metabolism predicts the development of cat embryos to blastocyst in vitro. *Molecular reproduction and development*, 56(2), pp.163–71. Available at: <http://www.ncbi.nlm.nih.gov/pubmed/10813848>.

St John, J. et al., 2000. Failure of elimination of paternal mitochondrial DNA in abnormal embryos. *The Lancet*, 355(9199), p.200. Available at: <http://www.sciencedirect.com/science/article/pii/S0140673699038428> [Accessed July 2, 2014].

Stegers-Theunissen, R.P.M. et al., 2013. The periconceptual period, reproduction and long-term health of offspring: the importance of one-carbon metabolism. *Human reproduction update*, 19(6), pp.640–55. Available at: <http://humupd.oxfordjournals.org/content/early/2013/08/18/humupd.dmt041.short> [Accessed August 27, 2014].

Stitt, D.T. et al., 2002. DRUG DISCOVERY Determination of Growth Rate of Microorganisms in Broth from Oxygen-Sensitive. , 32(3).

Stöger, R. et al., 1993. Maternal-specific methylation of the imprinted mouse Igf2r locus identifies the expressed locus as carrying the imprinting signal. *Cell*, 73(1), pp.61–71. Available at: <http://www.ncbi.nlm.nih.gov/pubmed/8462104> [Accessed August 21, 2014].

- Stojkovic, M. et al., 2001. Mitochondrial distribution and adenosine triphosphate content of bovine oocytes before and after in vitro maturation: correlation with morphological criteria and developmental capacity after in vitro fertilization and culture. *Biology of reproduction*, 64(3), pp.904–9. Available at: <http://www.ncbi.nlm.nih.gov/pubmed/11207207> [Accessed August 20, 2014].
- Stokes, P.J., Abeydeera, L.R. and Leese, H.J., 2005. Development of porcine embryos in vivo and in vitro; evidence for embryo “cross talk” in vitro. *Developmental biology*, 284(1), pp.62–71. Available at: <http://www.sciencedirect.com/science/article/pii/S0012160605002721> [Accessed July 24, 2014].
- Strom, S.P. et al., 2010. High-density SNP association study of the 17q21 chromosomal region linked to autism identifies CACNA1G as a novel candidate gene. *Molecular psychiatry*, 15(10), pp.996–1005. Available at: <http://www.pubmedcentral.nih.gov/articlerender.fcgi?artid=2889141&tool=pmcentrez&rendertype=abstract> [Accessed July 1, 2014].
- Sturmey, R.G., Hawkhead, J.A., et al., 2009a. DNA damage and metabolic activity in the preimplantation embryo. *Human Reproduction*, 24(1), pp.81–91. Available at: <http://humrep.oxfordjournals.org/content/24/1/81.abstract>.
- Sturmey, R.G., Reis, a, et al., 2009b. Role of fatty acids in energy provision during oocyte maturation and early embryo development. *Reproduction in domestic animals = Zuchthygiene*, 44 Suppl 3, pp.50–8. Available at: <http://www.ncbi.nlm.nih.gov/pubmed/19660080> [Accessed December 2, 2013].
- Sturmey, R.G. et al., 2010. Amino acid metabolism of bovine blastocysts: a biomarker of sex and viability. *Molecular Reproduction and Development*, 77(3), pp.285–296. Available at: <http://dx.doi.org/10.1002/mrd.21145>.
- Sturmey, R.G. and Leese, H.J., 2003. Energy metabolism in pig oocytes and early embryos. *Reproduction*, 126(2), pp.197–204. Available at: <http://www.reproduction-online.org/content/126/2/197.abstract>.
- Sturmey, R.G., O’Toole, P.J. and Leese, H.J., 2006. Fluorescence resonance energy transfer analysis of mitochondrial:lipid association in the porcine oocyte. *Reproduction (Cambridge, England)*, 132(6), pp.829–37. Available at: <http://www.reproduction-online.org/content/132/6/829.full> [Accessed August 9, 2014].
- Sułek-Piatkowska, A. et al., 2008. Searching for mutation in the JPH3, ATN1 and TBP genes in Polish patients suspected of Huntington’s disease and without mutation in the IT15 gene. *Neurologia i neurochirurgia polska*, 42(3), pp.203–9. Available at: <http://europepmc.org/abstract/MED/18651325> [Accessed August 4, 2014].
- Sun, W. et al., 2008. Frequent aberrant methylation of the promoter region of sterile alpha motif domain 14 in pulmonary adenocarcinoma. *Cancer science*, 99(11), pp.2177–84. Available at: <http://www.ncbi.nlm.nih.gov/pubmed/18823374> [Accessed June 24, 2014].

- Sutovsky, P. et al., 1999. Ubiquitin tag for sperm mitochondria. *Nature*, 402(6760), pp.371–2. Available at: <http://dx.doi.org/10.1038/46466> [Accessed July 2, 2014].
- Sutton-McDowall, M.L. et al., 2012. Utilization of endogenous fatty acid stores for energy production in bovine preimplantation embryos. *Theriogenology*, (0). Available at: <http://www.sciencedirect.com/science/article/pii/S0093691X11006558>.
- Sutton-McDowall, M.L., Gilchrist, R.B. and Thompson, J.G., 2004. Cumulus expansion and glucose utilisation by bovine cumulus-oocyte complexes during in vitro maturation: the influence of glucosamine and follicle-stimulating hormone. *Reproduction (Cambridge, England)*, 128(3), pp.313–9. Available at: <http://www.ncbi.nlm.nih.gov/pubmed/15333782> [Accessed December 2, 2013].
- Sweetlove, L.J. et al., 2006. Mitochondrial uncoupling protein is required for efficient photosynthesis. *Proceedings of the National Academy of Sciences of the United States of America*, 103(51), pp.19587–92. Available at: <http://www.pubmedcentral.nih.gov/articlerender.fcgi?artid=1748269andtool=pmcentrezandrendertype=abstract> [Accessed May 29, 2014].
- Szigeti, A. et al., 2006. Induction of necrotic cell death and mitochondrial permeabilization by heme binding protein 2/SOUL. *FEBS letters*, 580(27), pp.6447–54. Available at: <http://www.sciencedirect.com/science/article/pii/S0014579306012956> [Accessed April 8, 2014].
- Szigeti, A. et al., 2010. Facilitation of mitochondrial outer and inner membrane permeabilization and cell death in oxidative stress by a novel Bcl-2 homology 3 domain protein. *The Journal of biological chemistry*, 285(3), pp.2140–51. Available at: <http://www.jbc.org/content/285/3/2140.long> [Accessed April 7, 2014].
- Takagi, N. and Sasaki, M., 1975. Preferential inactivation of the paternally derived X chromosome in the extraembryonic membranes of the mouse. *Nature*, 256(5519), pp.640–2. Available at: <http://www.ncbi.nlm.nih.gov/pubmed/1152998> [Accessed August 21, 2014].
- Takahashi, T. et al., 2004. Rosbin: a novel homeobox-like protein gene expressed exclusively in round spermatids. *Biology of reproduction*, 70(5), pp.1485–92. Available at: <http://www.bioreprod.org/content/70/5/1485.long> [Accessed August 4, 2014].
- Takahashi, Y. and First, N.L., 1992. In vitro development of bovine one-cell embryos: Influence of glucose, lactate, pyruvate, amino acids and vitamins. *Theriogenology*, 37(5), pp.963–978. Available at: <http://www.sciencedirect.com/science/article/pii/0093691X9290096A> [Accessed September 1, 2014].
- Takai, D. and Jones, P.A., 2002. Comprehensive analysis of CpG islands in human chromosomes 21 and 22. *Proceedings of the National Academy of Sciences of the United States of America*, 99(6), pp.3740–5. Available at: <http://www.pubmedcentral.nih.gov/articlerender.fcgi?artid=122594andtool=pmcentrezandrendertype=abstract> [Accessed June 19, 2014].

- Takekawa, M. and Saito, H., 1998. A Family of Stress-Inducible GADD45-like Proteins Mediate Activation of the Stress-Responsive MTK1/MEKK4 MAPKKK. *Cell*, 95(4), pp.521–530. Available at: <http://www.cell.com/article/S0092867400816190/fulltext> [Accessed July 1, 2014].
- Takeyama, K. et al., 2003. The BAL-binding protein BBAP and related Deltex family members exhibit ubiquitin-protein isopeptide ligase activity. *The Journal of biological chemistry*, 278(24), pp.21930–7. Available at: <http://www.jbc.org/content/278/24/21930.long> [Accessed August 4, 2014].
- Tanphaichitr, V. and Broquist, H.P., 1974. Site of Carnitine Biosynthesis in the Rat. *The Journal of Nutrition*, 104(12), pp.1669–1673. Available at: <http://jn.nutrition.org/content/104/12/1669.short>.
- Tay, J.I. et al., 1997. Human tubal fluid: production, nutrient composition and response to adrenergic agents. *Human reproduction (Oxford, England)*, 12(11), pp.2451–6. Available at: <http://www.ncbi.nlm.nih.gov/pubmed/9436683> [Accessed November 16, 2014].
- Tejera, A. et al., 2011. Oxygen consumption is a quality marker for human oocyte competence conditioned by ovarian stimulation regimens. *Fertility and sterility*, 96(3), pp.618–623.e2. Available at: <http://www.fertstert.org/article/S0015028211010363/fulltext> [Accessed June 19, 2014].
- Tejera, A. et al., 2012. Time-dependent O<sub>2</sub> consumption patterns determined optimal time ranges for selecting viable human embryos. *Fertility and sterility*, 98(4), pp.849–857.e3. Available at: <http://linkinghub.elsevier.com/retrieve/pii/S0015028212006930?showall=true> [Accessed July 2, 2014].
- Telford, N.A., Watson, A.J. and Schultz, G.A., 1990. Transition from maternal to embryonic control in early mammalian development: A comparison of several species. *Molecular Reproduction and Development*, 26(1), pp.90–100. Available at: <http://dx.doi.org/10.1002/mrd.1080260113>.
- Tervit, H.R., Whittingham, D. and Rowson, L.E., 1972. Successful culture in vitro of sheep and cattle ova. *Reproduction*, 30(3), pp.493–497. Available at: <http://www.reproduction-online.org/content/30/3/493.short> [Accessed January 11, 2015].
- Tharp, W.G. and Sarkar, I.N., 2013. Origins of amyloid- $\beta$ . *BMC genomics*, 14(1), p.290. Available at: <http://www.biomedcentral.com/1471-2164/14/290> [Accessed June 24, 2014].
- Thompson, J.G. et al., 1996. Oxygen uptake and carbohydrate metabolism by in vitro derived bovine embryos. *Reproduction*, 106(2), pp.299–306. Available at: <http://www.reproduction-online.org/content/106/2/299.short> [Accessed July 3, 2014].

- Thompson, J.G. and Peterson, A.J., 2000. Bovine embryo culture in vitro: new developments and post-transfer consequences. *Human Reproduction*, 15(suppl 5), pp.59–67. Available at: [http://humrep.oxfordjournals.org/content/15/suppl\\_5/59.short](http://humrep.oxfordjournals.org/content/15/suppl_5/59.short) [Accessed July 3, 2014].
- Thouas, G. et al., 2001. Simplified technique for differential staining of inner cell mass and trophectoderm cells of mouse and bovine blastocysts. *Reproductive BioMedicine Online*, 3(1), pp.25–29. Available at: <http://www.sciencedirect.com/science/article/pii/S1472648310619608> [Accessed July 30, 2014].
- Tiranti, V. et al., 1995. Chromosomal localization of mitochondrial transcription factor A (TCF6), single-stranded DNA-binding protein (SSBP), and Endonuclease G (ENDOG), three human housekeeping genes involved in mitochondrial biogenesis. *Genomics*, 25(2), pp.559–564. Available at: <http://www.sciencedirect.com/science/article/pii/088875439580058T> [Accessed June 23, 2014].
- Tirosvoutis, K.N. et al., 1995. Characterization of a novel zinc finger gene (ZNF165) mapping to 6p21 that is expressed specifically in testis. *Genomics*, 28(3), pp.485–90. Available at: <http://europepmc.org/abstract/MED/7490084> [Accessed June 26, 2014].
- Toshima, S. et al., 2000. Circulating Oxidized Low Density Lipoprotein Levels: A Biochemical Risk Marker for Coronary Heart Disease. *Arteriosclerosis, Thrombosis, and Vascular Biology*, 20(10), pp.2243–2247. Available at: <http://atvb.ahajournals.org/content/20/10/2243.abstract>.
- Tremblay, K.D. et al., 1995. A paternal-specific methylation imprint marks the alleles of the mouse H19 gene. *Nature genetics*, 9(4), pp.407–13. Available at: <http://dx.doi.org/10.1038/ng0495-407> [Accessed August 21, 2014].
- Trimarchi, J.R., Liu, L., et al., 2000a. A non-invasive method for measuring preimplantation embryo physiology. *Zygote (Cambridge, England)*, 8(1), pp.15–24. Available at: <http://www.ncbi.nlm.nih.gov/pubmed/10840870>.
- Trimarchi, J.R., Liu, L., et al., 2000b. Oxidative phosphorylation-dependent and -independent oxygen consumption by individual preimplantation mouse embryos. *Biology of reproduction*, 62(6), pp.1866–74. Available at: <http://www.ncbi.nlm.nih.gov/pubmed/10819794>.
- Tripathi, A., Kumar, K.V.P. and Chaube, S.K., 2010. Meiotic cell cycle arrest in mammalian oocytes. *Journal of Cellular Physiology*, 223(3), pp.592–600. Available at: <http://dx.doi.org/10.1002/jcp.22108>.
- Trounson, A. and Gardner, D.K., 2000. Handbook of in vitro fertilization. Available at: <http://agris.fao.org/agris-search/search.do?recordID=US201300040859> [Accessed March 16, 2015].

- Valckx, S.D.M. et al., 2012. BMI-related metabolic composition of the follicular fluid of women undergoing assisted reproductive treatment and the consequences for oocyte and embryo quality. *Human reproduction (Oxford, England)*, 27(12), pp.3531–9. Available at: <http://humrep.oxfordjournals.org/content/27/12/3531> [Accessed July 31, 2014].
- Valdes, J.L. et al., 2011. Sorting nexin 27 protein regulates trafficking of a p21-activated kinase (PAK) interacting exchange factor ( $\beta$ -Pix)-G protein-coupled receptor kinase interacting protein (GIT) complex via a PDZ domain interaction. *The Journal of biological chemistry*, 286(45), pp.39403–16. Available at: <http://www.jbc.org/content/286/45/39403.long> [Accessed June 2, 2014].
- Vallot, C. et al., 2013. XACT, a long noncoding transcript coating the active X chromosome in human pluripotent cells. *Nature genetics*, 45(3), pp.239–41. Available at: <http://www.ncbi.nlm.nih.gov/pubmed/23334669> [Accessed August 21, 2014].
- Valnot, I. et al., 1999. A mitochondrial cytochrome b mutation but no mutations of nuclearly encoded subunits in ubiquinol cytochrome c reductase (complex III) deficiency. *Human genetics*, 104(6), pp.460–6. Available at: <http://www.ncbi.nlm.nih.gov/pubmed/10453733>.
- Valsangkar, D. and Downs, S.M., 2013. A requirement for fatty acid oxidation in the hormone-induced meiotic maturation of mouse oocytes. *Biology of reproduction*, 89(2), p.43. Available at: <http://www.biolreprod.org/content/early/2013/07/11/biolreprod.113.109058.short> [Accessed August 18, 2014].
- Vaz, F.M. and Wanders, R.J.A., 2002. Carnitine biosynthesis in mammals. *The Biochemical journal*, 361(Pt 3), pp.417–29. Available at: <http://www.pubmedcentral.nih.gov/articlerender.fcgi?artid=1222323&tool=pmcentrez&rendertype=abstract> [Accessed September 3, 2014].
- Vockley, J. et al., 2000. Exon skipping in IVD RNA processing in isovaleric acidemia caused by point mutations in the coding region of the IVD gene. *American journal of human genetics*, 66(2), pp.356–67. Available at: <http://www.pubmedcentral.nih.gov/articlerender.fcgi?artid=1288088&tool=pmcentrez&rendertype=abstract> [Accessed June 23, 2014].
- Wales, R.G. and Brinster, R.L., 1968. THE UPTAKE OF HEXOSES BY PRE-IMPLANTATION MOUSE EMBRYOS IN VITRO. *Reproduction*, 15(3), pp.415–422. Available at: <http://www.reproduction-online.org/content/15/3/415.short> [Accessed August 30, 2014].
- Wang, J. et al., 2009. The lysine demethylase LSD1 (KDM1) is required for maintenance of global DNA methylation. *Nature genetics*, 41(1), pp.125–9. Available at: <http://www.ncbi.nlm.nih.gov/pubmed/19098913> [Accessed August 20, 2014].
- Watanabe, T. et al., 1998. Isolation of Estrogen-Responsive Genes with a CpG Island Library. *Mol. Cell. Biol.*, 18(1), pp.442–449. Available at: <http://mcb.asm.org/content/18/1/442.long> [Accessed June 24, 2014].

- Wettemann, R.P. et al., 1972. Estradiol and progesterone in blood serum during the bovine estrous cycle. *Journal of animal science*, 34(6), pp.1020–4. Available at: <http://www.ncbi.nlm.nih.gov/pubmed/5063646> [Accessed September 3, 2014].
- White, Y.A.R. et al., 2012. Oocyte formation by mitotically active germ cells purified from ovaries of reproductive-age women. *Nat Med*, advance on. Available at: <http://dx.doi.org/10.1038/nm.2669>.
- Whitewar, S.L. and Leese, H.J., 2008. Amino acid transporter expression in bovine oviduct epithelial cells. *Reproduction, Fertility and Development*, 20(1), p.175. Available at: [http://www.publish.csiro.au/view/journals/dsp\\_journal\\_fulltext.cfm?nid=44andf=RDv20n1Ab192](http://www.publish.csiro.au/view/journals/dsp_journal_fulltext.cfm?nid=44andf=RDv20n1Ab192) [Accessed September 1, 2014].
- Whiteheart, S.W. et al., 1993. SNAP family of NSF attachment proteins includes a brain-specific isoform. *Nature*, 362(6418), pp.353–5. Available at: <http://dx.doi.org/10.1038/362353a0> [Accessed June 24, 2014].
- Williams, C. et al., 2007. Targeting of the type II inositol polyphosphate 5-phosphatase INPP5B to the early secretory pathway. *Journal of cell science*, 120(Pt 22), pp.3941–51. Available at: <http://jcs.biologists.org/content/120/22/3941.long> [Accessed May 27, 2014].
- Winge, D.R., 2012. Sealing the mitochondrial respirasome. *Molecular and cellular biology*, 32(14), pp.2647–52. Available at: <http://mcb.asm.org/content/32/14/2647.short> [Accessed June 13, 2014].
- Van Winkle, L.J., 2001. Amino acid transport regulation and early embryo development. *Biology of reproduction*, 64(1), pp.1–12. Available at: <http://www.ncbi.nlm.nih.gov/pubmed/11133652> [Accessed September 1, 2014].
- Wirth, J. et al., 1996. Human myosin-IXb, an unconventional myosin with a chimerin-like rho/rac GTPase-activating protein domain in its tail. *J. Cell Sci.*, 109(3), pp.653–661. Available at: <http://jcs.biologists.org/content/109/3/653.abstract> [Accessed August 4, 2014].
- Wittkopp, P.J. and Kalay, G., 2012. Cis-regulatory elements: molecular mechanisms and evolutionary processes underlying divergence. *Nature reviews. Genetics*, 13(1), pp.59–69. Available at: <http://dx.doi.org/10.1038/nrg3095> [Accessed May 27, 2014].
- Wodnicka, M., 2000. Novel Fluorescent Technology Platform for High Throughput Cytotoxicity and Proliferation Assays. *Journal of Biomolecular Screening*, 5(3), pp.141–152. Available at: <http://jbx.sagepub.com/cgi/doi/10.1177/108705710000500306> [Accessed March 13, 2014].
- Wrenzycki, C. et al., 2004. Messenger RNA expression patterns in bovine embryos derived from in vitro procedures and their implications for development. *Reproduction, Fertility and Development*, 17(2), pp.23–35. Available at: <http://dx.doi.org/10.1071/RD04109>.

- Wrenzycki, C. and Niemann, H., 2003. Epigenetic reprogramming in early embryonic development: effects of in-vitro production and somatic nuclear transfer. *Reproductive BioMedicine Online*, 7(6), pp.649–656. Available at: <http://linkinghub.elsevier.com/retrieve/pii/S1472648310620871> [Accessed September 11, 2014].
- Wu, G.Q. et al., 2011. L-carnitine enhances oocyte maturation and development of parthenogenetic embryos in pigs. *Theriogenology*. Available at: <http://linkinghub.elsevier.com/retrieve/pii/S0093691X11001853?showall=true>.
- Wu, L.L.-Y. et al., 2010. High-fat diet causes lipotoxicity responses in cumulus-oocyte complexes and decreased fertilization rates. *Endocrinology*, 151(11), pp.5438–45. Available at: <http://press.endocrine.org/doi/abs/10.1210/en.2010-0551> [Accessed August 9, 2014].
- Wu, M. et al., 2007. Multiparameter metabolic analysis reveals a close link between attenuated mitochondrial bioenergetic function and enhanced glycolysis dependency in human tumor cells. *American journal of physiology. Cell physiology*, 292, pp.C125–C136.
- Wuebben, E.L. et al., 2012. Musashi2 is required for the self-renewal and pluripotency of embryonic stem cells. Z. Zhou, ed. *PloS one*, 7(4), p.e34827. Available at: <http://dx.plos.org/10.1371/journal.pone.0034827> [Accessed August 4, 2014].
- Yadav, B.R., King, W.A. and Betteridge, K.J., 1993. Relationships between the completion of first cleavage and the chromosomal complement, sex, and developmental rates of bovine embryos generated in vitro. *Molecular reproduction and development*, 36(4), pp.434–9. Available at: <http://www.ncbi.nlm.nih.gov/pubmed/8305205> [Accessed August 20, 2014].
- Yadava, N. and Nicholls, D.G., 2007. Spare respiratory capacity rather than oxidative stress regulates glutamate excitotoxicity after partial respiratory inhibition of mitochondrial complex I with rotenone. *The Journal of neuroscience : the official journal of the Society for Neuroscience*, 27(27), pp.7310–7. Available at: <http://www.jneurosci.org/content/27/27/7310.long> [Accessed June 11, 2014].
- Yamamoto, N. et al., 2001. Role of Deltex-1 as a transcriptional regulator downstream of the Notch receptor. *The Journal of biological chemistry*, 276(48), pp.45031–40. Available at: <http://www.jbc.org/content/276/48/45031.long> [Accessed August 4, 2014].
- Yan, Z. et al., 2008. Human rhomboid family-1 gene silencing causes apoptosis or autophagy to epithelial cancer cells and inhibits xenograft tumor growth. *Molecular cancer therapeutics*, 7(6), pp.1355–64. Available at: <http://www.pubmedcentral.nih.gov/articlerender.fcgi?artid=3426753&tool=pmcentrez&rendertype=abstract> [Accessed August 4, 2014].
- Yang, Y., 2003. Wnt5a and Wnt5b exhibit distinct activities in coordinating chondrocyte proliferation and differentiation. *Development*, 130(5), pp.1003–1015. Available at: <http://dev.biologists.org/content/130/5/1003.short> [Accessed June 5, 2014].

- Yoshizawa, Y. et al., 2010. Impaired active demethylation of the paternal genome in pronuclear-stage rat zygotes produced by in vitro fertilization or intracytoplasmic sperm injection. *Molecular reproduction and development*, 77(1), pp.69–75. Available at: <http://www.ncbi.nlm.nih.gov/pubmed/19743475> [Accessed August 21, 2014].
- Zeleznik, A., 2004. The physiology of follicle selection. *Reprod Biol Endocrinol*. Available at: <http://www.biomedcentral.com/content/pdf/1477-7827-2-31.pdf> [Accessed January 10, 2015].
- Zhang, F.P. et al., 2001. Normal prenatal but arrested postnatal sexual development of luteinizing hormone receptor knockout (LuRKO) mice. *Molecular endocrinology (Baltimore, Md.)*, 15(1), pp.172–83. Available at: <http://www.ncbi.nlm.nih.gov/pubmed/11145748> [Accessed November 16, 2014].
- Zhang, H. et al., 2014. Musashi2 modulates K562 leukemic cell proliferation and apoptosis involving the MAPK pathway. *Experimental cell research*, 320(1), pp.119–27. Available at: <http://www.sciencedirect.com/science/article/pii/S0014482713003911> [Accessed August 4, 2014].
- Zou, H. et al., 2009. Human rhomboid family-1 gene RHBDF1 participates in GPCR-mediated transactivation of EGFR growth signals in head and neck squamous cancer cells. *FASEB journal : official publication of the Federation of American Societies for Experimental Biology*, 23(2), pp.425–32. Available at: <http://www.pubmedcentral.nih.gov/articlerender.fcgi?artid=2638965andtool=pmcentrezandrendertype=abstract> [Accessed August 4, 2014].
- Zylka, M.J. and Reppert, S.M., 1999. Discovery of a putative heme-binding protein family (SOUL/HBP) by two-tissue suppression subtractive hybridization and database searches. *Molecular Brain Research*, 74(1-2), pp.175–181. Available at: <http://www.sciencedirect.com/science/article/pii/S0169328X99002776> [Accessed April 8, 2014].

## 8 Appendix: suppliers and materials

## 8.1 Suppliers

Alpha Laboratories Ltd  
40 Parham Drive  
Eastleigh  
Hampshire  
SO50 4NU  
United Kingdom

Analox Instruments  
Unit 22  
Acton Park Estate  
The Vale  
London W3 7QE  
United Kingdom

BOC LIMITED  
P O BOX 12  
Priestly Road  
Lancashire  
M28 2UT  
United Kingdom

Camlab House  
Norman Way Industrial Estate  
Over  
Cambridge  
CB24 5WE (formerly CB4 5WE)  
United Kingdom

Crawford Scientific™ Ltd  
Holm Street  
Strathaven  
Lanarkshire  
ML10 6NB  
United Kingdom

Ferring Pharmaceuticals Ltd  
Drayton Hall  
Church Road  
West Drayton  
UB7 7PS  
United Kingdom

Fisher Scientific UK Ltd  
Bishop Meadow Road  
Loughborough  
LE11 5RG  
United Kingdom

Fresenius Kabi  
Cestrian Court  
Eastgate Way  
Manor Park  
Runcorn  
Cheshire  
WA7 1NT  
United Kingdom

Life Technologies Ltd  
3 Fountain Drive  
Inchinnan Business Park  
Paisley  
PA4 9RF  
United Kingdom

Sarstedt Ltd.  
68 Boston Road  
Beaumont Leys  
Leicester LE4 1AW  
United Kingdom

Scientific Laboratory Supplies Limited  
Wilford Industrial Estate  
Ruddington Lane  
Wilford  
Nottingham  
NG11 7EP  
United Kingdom

Sigma-Aldrich Company Ltd.  
The Old Brickyard  
New Road  
Gillingham  
Dorset  
SP8 4XT  
United Kingdom

## 8.2 Materials

Chemical	Supplier	Cat No.	Amount
(+)-Etomoxir sodium salt hydrate	Sigma-Aldrich	E1905-5MG	5mg
2,4-Dinitrophenol	Sigma-Aldrich	<i>D198501</i>	5g
Antibiotic/Antimycotic (Gibco, 100X)	Fisher	11580486	20ml
Antimycin A	Sigma-Aldrich	A8674- 25MG	25mg
BME 50x	Sigma-Aldrich	B6766	100ml
BSA FAF	Sigma-Aldrich	A6003	25g
BSA Fr V	Sigma-Aldrich	A9418	50g
Calcium Chloride Dihydrate (CaCl <sub>2</sub> .2H <sub>2</sub> O)	Sigma-Aldrich	C7902	500g
Decon 90 Detergent	SLS	CLE1020	1L
Di-Sodium Hydrogen Orthophosphate Dihydrate (Na <sub>2</sub> HPO <sub>4</sub> .2H <sub>2</sub> O)	Sigma-Aldrich	71638	500g
EGF (bovine)	Sigma-Aldrich	E4127	1mg
Ethanol (Mol.Bio grade)	Sigma-Aldrich	51976- 500ML-F	500ml
FCS	Sigma-Aldrich	F9665	50ml
FGF (bovine)	Sigma-Aldrich	F3133	10µg
FSH (ovine)	Sigma-Aldrich	F8174-1VL	1 vial
Gentamycin Solution	Sigma-Aldrich	G1272	10ml
Glucose	Sigma-Aldrich	G6152	100g
Glucose standard, 5.0mmol/L, 30ml	Analox	GMRD-010	30ml
Heparin (bovine)	Sigma-Aldrich	H0777	100kU
Heparin (porcine)	Sigma-Aldrich	H3149	25kU
HEPES free acid	Sigma-Aldrich	H4034	100g
HEPES sodium salt	Sigma-Aldrich	H7006	100g
Hypotaurine	Sigma-Aldrich	H1384	10mg
JC-1	Molecular Probes	T-3168	5mg

Kanamycin Sulphate	Sigma-Aldrich	K1377	5g
Lactate standard, 5.0mmol/L, 25ml	Analox	GMRD-079	25ml
L-Carnitine inner salt	Sigma-Aldrich	C0158	5g
L-Glutamine	Sigma-Aldrich	G8540	25g
LH (ovine)	Sigma-Aldrich	L5269-1VL	1 vial
LONG® R3 IGF-I (human)	Sigma-Aldrich	I1271-.1MG	1mg
M199 liquid	Sigma-Aldrich	M4530	100ml
M199 liquid 10x	Sigma-Aldrich	M0650	100ml
Magnesium Sulphate Heptahydrate (MgCl <sub>2</sub> .7H <sub>2</sub> O)	Sigma-Aldrich	M2643	500g
MEM 100x	Sigma-Aldrich	M7145	100ml
Mineral Oil	Sigma-Aldrich	M8410	1l
Myxothiazol	Sigma-Aldrich	T5580	1mg
Nile Red	Molecular Probes	N-1142	25mg
Oligomycin	Sigma-Aldrich	O4876-5MG	5mg
PBS Tablets	Sigma-Aldrich	P4417- 100TAB	100x
Penicillamine	Sigma-Aldrich	P4875	1g
Penicillin/Streptomycin	Sigma-Aldrich	P0781	100ml
Penicillin/Streptomycin 10mg/ml	Sigma-Aldrich	P4333- 100ML	100ml
Percoll®	SLS	17089102	250ml
Phenol Red Solution	Sigma-Aldrich	P0290	100ml
Phosphate Buffered Saline	Sigma-Aldrich	P4417- 100TAB	100 tablets
Potassium Chloride (KCl)	Sigma-Aldrich	P5405	250g
Potassium Di-Hydrogen Orthophosphate (KH <sub>2</sub> PO <sub>4</sub> )	Sigma-Aldrich	P5655	100g
Pyruvate reagent kit, 30 tests, incl. std	Analox	GMRD-140	5ml
Sodium Bicarbonate (NaHCO <sub>3</sub> )	Sigma-Aldrich	S4772	500g
Sodium Chloride (NaCl)	Sigma-Aldrich	S5886	500g
Sodium Di-Hydrogen Orthophosphate	Sigma-Aldrich	71500	250g

Dihydrate (NaH <sub>2</sub> PO <sub>4</sub> ·2H <sub>2</sub> O)			
Sodium Lactate Syrup	Sigma-Aldrich	L1375	100ml
Sodium Pyruvate	Sigma-Aldrich	P2256	5g
β-mercaptoacetate	Sigma-Aldrich	108995	5g